AD-A230 239

RADC-TR-90-100
Final Technical Report
November 1990

EXTERNAL CAVITY COHERENT TRANSMITTER MODULES

University of Rhode Island

Dr. Harish Sunak

DTIC
ELECTE
DEC 20 1990
S D
D

BEST
AVAILABLE COPY

Rome Air Development Center
Air Force Systems Command
Griffiss Air Force Base, NY 13441-5700

90 12 19 143

This report has been reviewed by the RADC Public Affairs Division (PA) and is releasable to the National Technical Information Services (NTIS) At NTIS it will be releasable to the general public, including foreign nations.

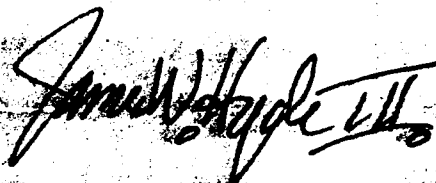RADC-TR-90-100 has been reviewed and is approved for publication.

APPROVED: *Paul Sierak*

PAUL SIERAK
Project Engineer

APPROVED: *John A. Graniero*

JOHN A. GRANIERO
Technical Director
Directorate of Communications

FOR THE COMMANDER: *James W. Hyde III*

JAMES W. HYDE III
Directorate of Plans & Programs

If your address has changed or if you wish to be removed from the RADC mailing list, or if the addressee is no longer employed by your organization, please notify RADC (DCLW) Griffiss AFB NY 13441-5700. This will assist us in maintaining a current mailing list.

Do not return copies of this report unless contractual obligations or notices on a specific document require that it be returned.

REPORT DOCUMENTATION PAGE

Public reporting burden for this collection of information is estimated to average 1 hour per response, including the time for reviewing instructions, searching existing data sources, gathering and maintaining the data needed, and completing and reviewing the collection of information. Send comments regarding this burden estimate or any other aspect of this collection of information, including suggestions for reducing this burden, to Washington Headquarters Services, Directorate for Information Operations and Reports, 1215 Jefferson Davis Highway, Suite 1204, Arlington, VA 22202-4302, and to the Office of Management and Budget, Paperwork Reduction Project (0704-0188), Washington, DC 20503.

1. AGENCY USE ONLY (Leave Blank)	2. REPORT DATE November 1990	3. REPORT TYPE AND DATES COVERED Final Oct 87 - Sep 88

4. TITLE AND SUBTITLE
EXTERNAL CAVITY COHERENT TRANSMITTER MODULES

5. FUNDING NUMBERS
C - F30602-81-C-0193
PE - 63726F
PR - 2863
TA - 92
WU - PA

6. AUTHOR(S)
Dr. Harish Sunak

7. PERFORMING ORGANIZATION NAME(S) AND ADDRESS(ES)
University of Rhode Island
Department of Electrical Engineering
Kingston RI 02881

8. PERFORMING ORGANIZATION REPORT NUMBER

9. SPONSORING/MONITORING AGENCY NAME(S) AND ADDRESS(ES)
Rome Air Development Center (DCLW)
Griffiss AFB NY 13441-5700

10. SPONSORING/MONITORING AGENCY REPORT NUMBER
RADC-TR-90-100

11. SUPPLEMENTARY NOTES
RADC Project Engineer: Paul Sierak/DCLW/(315) 330-4092

12a. DISTRIBUTION/AVAILABILITY STATEMENT
Approved for public release; distribution unlimited

12b. DISTRIBUTION CODE

13. ABSTRACT (Maximum 200 words)

This report covers work done with a Fabry-Perot semiconductor laser based external cavity structure, for use with coherent fiber optical communications systems. A novel structure was developed which uses a single-mode fiber as part of the external cavity, together with a graded-index rod lens and a diffraction grating end reflector. The advantages of choosing this structure are highlighted, the principal being that it can be used with any modulation format, at any bit rate and also as the transmitter laser or the local oscillator laser. The latter has to have wide tunability so that the coherent receiver can select closely packed optical channels, and the structure selected is the only one that offers very wide tunability of over 100nm or 12,000 GHz. Various measurements done with this structure are included in this report. Extensive theoretical work on spectral linewidth and tunability is also reported and detailed comparison of the above structure is made with those based on distributed feedback lasers and also having external cavities.

14. SUBJECT TERMS
Fiber Optics, Narrow linewidth sources, Optical Sources, Coherent fiber optic links

15. NUMBER OF PAGES
224

16. PRICE CODE

17. SECURITY CLASSIFICATION OF REPORT UNCLASSIFIED	18. SECURITY CLASSIFICATION OF THIS PAGE UNCLASSIFIED	19. SECURITY CLASSIFICATION OF ABSTRACT UNCLASSIFIED	20. LIMITATION OF ABSTRACT UL

CONTENTS

Introduction

This final report is for the Contract F30602-81-C-0193, with Task Title and Description "External Cavity Coherent Transmitter Module" and funded through RADC/DCLW, Griffiss Air Force Base. The objective of this effort was to study, design and test an external cavity based coherent optical transmitter module for use in coherent fiber optic systems. The approach specified in the contract was as follows: Conduct theoretical and detailed implementation analysis of the various architectures of external cavity based coherent optical transmitters. Perform sensitivity and comparative analysis for the various architectures of external cavity based coherent optical transmitters. Provide detailed design recommendations for the external cavity coherent transmitter modules appropriate to the various coherent modulation schemes. Fabricate and test one coherent transmitter module.

There were 14 specific tasks that were specified in the contract and these are listed below so that convenient reference can be made to them while studying the report:

Task 1.

Conduct tasks 2 through 8 below for distributed feedback lasers (DFB) and separately for Fabry-Perot (FP) lasers.

Task 2.

Analyze performance of external cavity based coherent optical transmitters with strong frequency selective feedback.

Task 3.

Characterize linewidth and tunability aspects of external cavity based coherent optical transmitters.

Task 4.

Identify and characterize critical parameters upon which the linewidth and tunability depends. such as: facet reflectivity, feedback ratio, detuning angle, and external cavity length.

3

Task 5.

Investigate the comparative performance of bulk and fiber diffraction gratings.

Task 6.

Identify design features of the best coherent transmitter module based upon the results of task 5.

Task 7.

Based on the above tasks, identify critical parameter combinations of the coherent transmitter modules that can support the various coherent modulation schemes.

Task 8.

Develop theoretical models to characterize the stability of linewidth and output frequency of the coherent transmitter modules as a function of environmental parameters such as temperature and pressure.

Task 9.

Develop detailed comparisons between the results of tasks 2-8 for distributed feedback lasers and Fabry-Perot lasers.

Task 10.

Identify detailed designs of distributed feedback or Fabry-Perot laser based external cavity coherent transmitter modules most appropriate for use with the various coherent modulation schemes. Provide rationale for design selection.

Task 11.

Evaluate the impact of the use of high power Fabry-Perot lasers on coherent transmitter linewidth and integrate results into tasks 8, 9 and 10.

Task 12.

Identify and perform key parameter experimental evaluations towards substantiating the basis for the rationale for the detailed designs identified in task 10.

Task 13.

Based on the above tasks, recommend, fabricate and test one model of a external cavity based coherent transmitter module.
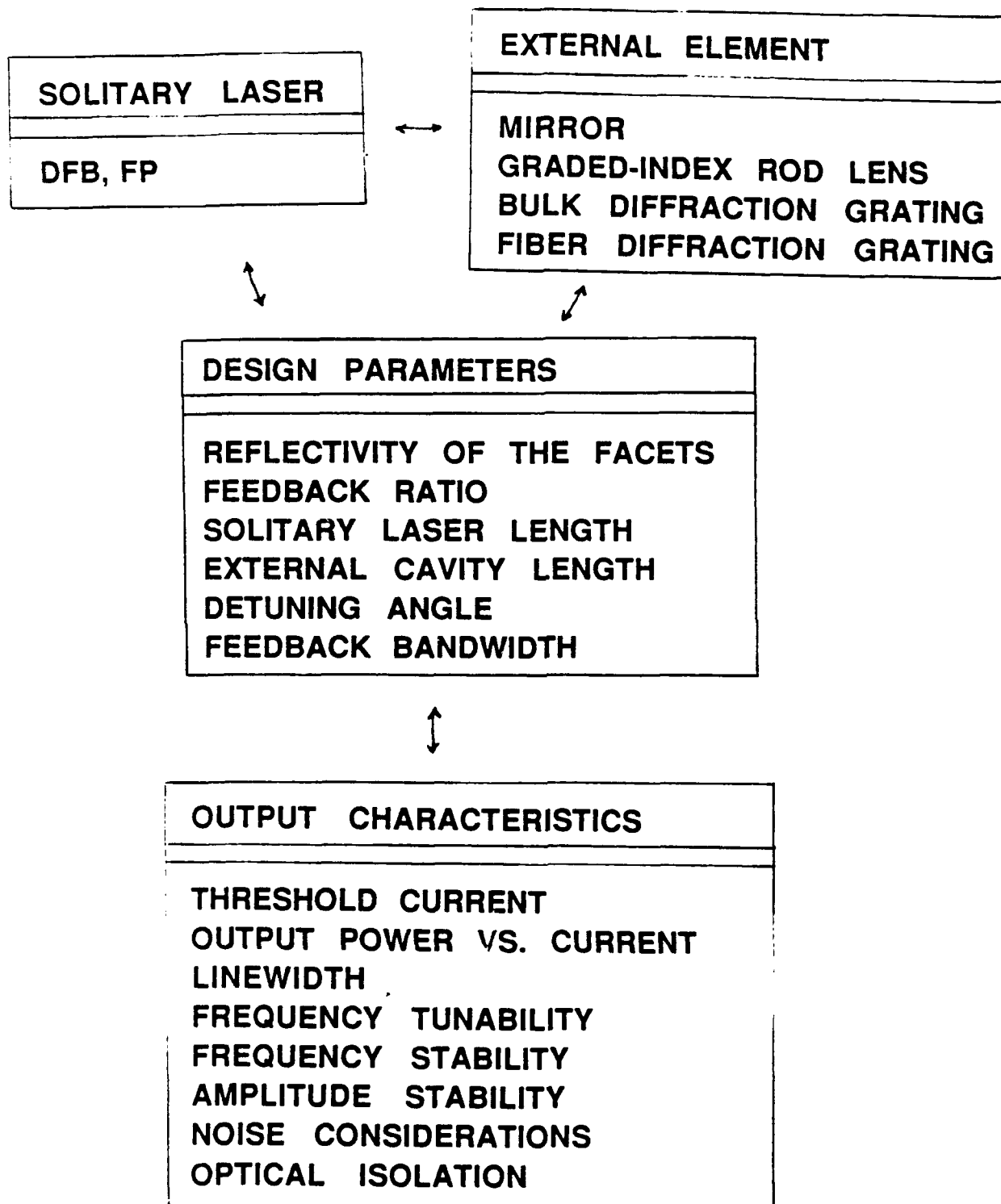
Task 14.

Compare test results for the module developed under task 13 to the projected results of earlier tasks.

We shall report on each task in sequence as specified above. Tasks 2 through 8 for DFB lasers will be reported on first, and these are labelled as Tasks 2A through 8A. Similarly Tasks 2B to 8B are labelled for FP lasers, and are dealt with next; finally Tasks 9-14 are reported on . The contents pages contain the exact page numbers where each of these Tasks can be found. The references are at the end of the report, after Task 14. Following the references are five manuscripts which contain the many relevant details of the work that was performed in this contract. These will be sent for publication in appropriate journals in the lightwave technology area. Following this is a small appendix. The importance of external cavity lasers for coherent lightwave systems is discussed in considerable detail in the introduction of these manuscripts, and hence will not be repeated here. Each individual task will commence on a new page so that it is easy to identify it.

Before getting into the details of each task, we give an overview of external cavity semiconductor lasers for COherent Fiber Optical Communication Systems, which has been abbreviated to COFOCS throughout·this report. The two solitary active laser structures considered are distributed feedback (DFB) and Fabry-Perot (FP). To build an external cavity, these are combined with one or more of the following external elements: a highly reflective mirror, a graded-index (GRIN) rod lens, a bulk diffraction grating or a fiber diffraction grating. Various design parameters of this external cavity can be varied so that the desired output characteristics from the coherent module can be obtained. The design parameters are as follows: reflectivity of the two facets of the solitary laser, the feedback ratio from the external cavity, the solitary laser length, the external cavity length, the detuning angle which determines the shift of

the laser modes from the external cavity modes, and the spectral bandwidth of the light that is fed back into the solitary laser. The spectral bandwidth of the light depends on the external element and for the bulk diffraction grating, it decreases as the number of lines per mm increases. Various output characteristics are of importance and the study of these give insight into the performance of the coherent external cavity semiconductor laser. These are: the threshold current; the output power at a current above threshold; the spectral linewidth and its stability; fine, medium and coarse frequency tunability and the stability of the center frequency, amplitude stability, noise considerations, optical isolation etc. A summary of these above comments is provided in fig. 1, which is a block diagram showing the interplay of the solitary laser, external element, design parameters and the output characteristics.

SOLITARY LASER		EXTERNAL ELEMENT
DFB, FP	↔	MIRROR GRADED-INDEX ROD LENS BULK DIFFRACTION GRATING FIBER DIFFRACTION GRATING

DESIGN PARAMETERS

REFLECTIVITY OF THE FACETS
FEEDBACK RATIO
SOLITARY LASER LENGTH
EXTERNAL CAVITY LENGTH
DETUNING ANGLE
FEEDBACK BANDWIDTH

OUTPUT CHARACTERISTICS

THRESHOLD CURRENT
OUTPUT POWER VS. CURRENT
LINEWIDTH
FREQUENCY TUNABILITY
FREQUENCY STABILITY
AMPLITUDE STABILITY
NOISE CONSIDERATIONS
OPTICAL ISOLATION

Fig 1:   Block diagram to show the interplay of the solitary laser, the external element, the design parameters and the output characteristics.

7

Task 2A:

(DFB Lasers) Analyze the performance of external cavity based coherent optical transmitter with strong frequency selective feedback.

For this analysis we performed a literature search and references 1 through 14 were studied. We have only considered strong feedback as in the task stipulation (Some work has also been done with weak feedback.) Frequency selective feedback is not relevant for DFB-ECSL (Distributed Feedback-External Cavity Semiconductor Lasers) as the single longitudinal mode frequency is determined by the diffraction grating which is etched into the solitary DFB structure during fabrication. Frequency selective feedback is more relevant with FP lasers as will be shown in Task 2B.

There are three basic external cavity structures which have been built with DFB solitary laser. They are:

1.   DFB Laser + External Mirror Cavity (MC)

2.   DFB Laser + Graded-index (GRIN) Rod Lens (GRECC)

3.   DFB Laser + External Cavity with a single-mode optical fiber i.e. a fiber external cavity.

We now analyze the performance of each of the above three DFB-ECSL. This will be done by considering the following:

(i)   Optical Schematic Diagram

(ii)   Advantages and Disadvantages

(iii)   The Design Features

(iv)   The Output Characteristics

I.   DFB Laser and External Mirror Cavity

The optical schematic diagram of this first external cavity is shown in fig. 2. The advantages of this structure are as follows:

(i)   No intracavity mode selection elements are used and the cavity is very simple;

DFB LASER AND EXTERNAL MIRROR CAVITY

40×0.65 N A
microscope
objective

DFB laser

output

R_1

L_s

AR coating(R_2)

mirror
(F_2)

L_{ex}
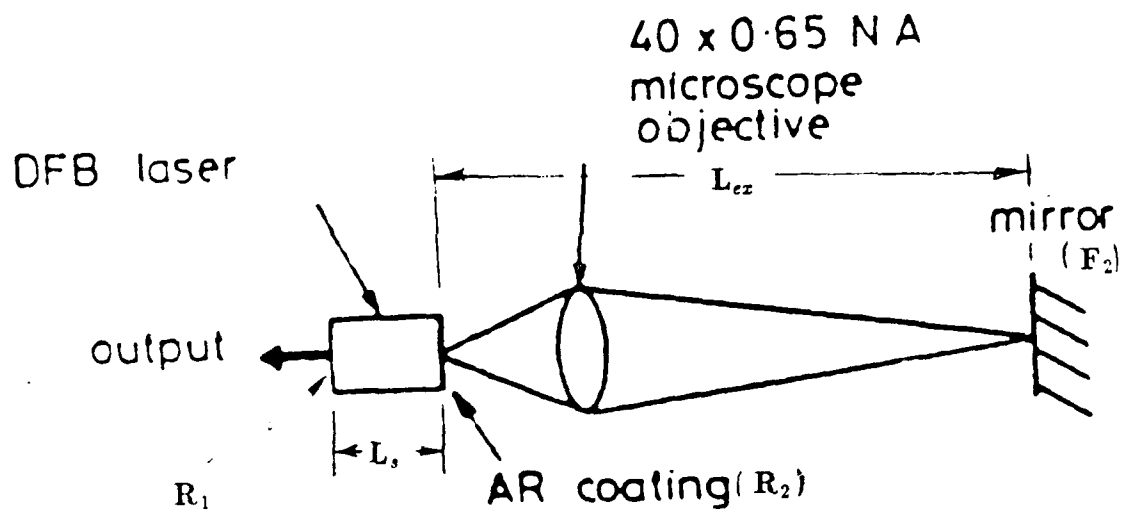
Fig. 2:   DFB Laser and External Mirror Cavity

L_S: Solitary Laser Length

L_{ex}:   External Cavity Length

R_1:   Output facet reflectivity

R_2:   AR coated facet

F_2:   Reflectivity of Mirror

9

(ii)   Wavelength and single-frequency selection is determined by the grating in the solitary DFB laser;

(iii)   Tunability characteristics are similar to the solitary DFB laser;

(iv)   The laser is immune to external optical pertubations as the feedback is strong.

The disadvantages of this structure are:

(i)   One laser facet needs anti-reflection coating;

(ii)   Air path does not give a compact cavity and can cause changes in external cavity length;

(iii)   Microscope objective coupling lens is bulky.

The design features of two DFB-ECSL with external mirror cavities are summarized in Table I, and the output characteristics of one of them (first one) is summarized in Table II. From these tables it is clear that the external cavities are fairly long, 10-18 cm, and hence not very compact. The linewidths are fairly narrow, 40 kHz, due to the long cavity lengths and the output power is 2.2 mW but this is not coupled into a single-mode fiber. Also, the side mode supression ratio of the satellite longitudinal mode is only -26 dB (30-40 dB is desirable for COFOCS). Due to its disadvantages, this structure has not been widely researched; the two DFB-ECSL to be described below have been.

II   DFB Laser and GRIN Rod External Cavity

The schematic diagram, not to scale, for this structure is shown in fig. 3. The components are mounted on a Peltier thermo-electric cooler to control the temperature of the laser. This is important for frequency stability; indeed changing the temperature and current are means of tuning the frequency of the laser. From Table IV, it can be seen that tuning of up to 2 GHz can be obtained for every mA of current.

The advantages of the DFB-ECSL with GRIN rod external cavity are as follows:

(i)   Compact size of ~4 mm as the length of the rod lens is very small;

**Table I:** Design features of two DFB-ECSL with external mirror cavities

Design Parameter	AT & T Labs.	AT & T Labs
LASER STRUCTURE	VAPOR PHASE TRANSPORT (VPT)	DOUBLE-CHANNEL PLANAR BURIED-HETERO-STRUCTURE (DCPBH)
SOLITARY LENGTH	250 μm	250 μm
DFB GRATINGS	SECOND ORDER	SECOND ORDER
R_2 REFLECTIVITY	3-5%	1%
POWER* FEEDBACK INTO LASER (R_3)	16%	4%
EXTERNAL CAVITY LENGTH	18 CM	10 CM

* FROM FACET F-2, THROUGH LENS, REFLECTED OFF MIRROR, THROUGH LENS AND COUPLED BACK INTO FACET F2.

Table II: Output characteristics of DFB-ECSL with external mirror cavity

OUTPUT PARAMETER	AT & T LABS
POWER LINEWIDTH PRODUCT	88 kHz. mW
OUTPUT POWER	2.2 mW
LINEWIDTH	40 kHz
SIDE MODE SUPRESSION RATIO	-26dB (x400)
TUNABILITY (DFB LASER)	1.7 GHz/mA, 20 GHz/$^\circ$C

DFB LASER & GRIN ROD EXTERNAL CAVITY
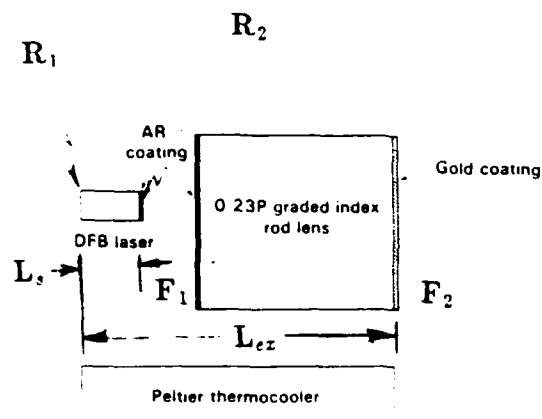
Fig 3: DFB Laser and Grin Rod External Cavity

R_1:   Reflectivity of output facet (32%)

R_2:   AR Coated facet of laser

L_s: Solitary laser length

L_{ex}:   External cavity length

F_1:   AR coated facet of GRIN Rod lens

F_2:   High reflectivity facet of GRIN Rod lens

13

(ii)   Linewidth is reduced by x 20 from the solitary DFB laser linewidth and a few MHz
is easily possible;

(iii)   Wavelength and single frequency selection are determined by the DFB solitary
laser;

(iv)   Tunability is similar to the solitary DFB laser as the external cavity has no
frequency selective component;

(v)   Laser is immune to external optical pertubations as we have strong feedback.

The disadvantages of this structure are:

(i)   the grin-rod lens needs anti-reflection coating on the facet nearer to the laser and a
high-reflectivity coating on the other facet;

(ii)   We must use a high quality DFB laser to be of practical use; prefer spectral
linewidth of the solitary laser to be < 35 MHz;

(iii)   Precision longitudinal movement of lens is needed to be tune the cavity length for
phase-matched condition.

From the design features of this DFB-ECSL in Table III, it can be seen that the solitary
laser lengths are relatively long (400 mm and 500 mm) so that spectral linewidths of < 35 MHz can
be obtained. Due to the short external cavity of ~ 4 mm, the output linewidth, as seen in Table IV
is a few MHz for a few mW of output power. The normalized power.linewidth product is ~ 2-4
MHz.mW. This is abundantly adequate for many COFOCS as will be discussed in later tasks.
From Table IV, we can also notice that the side-mode supression ratio is very good indeed, ~ 38.5
dB.

A compact module having this structure was designed and built by Bellcore and is
illustrated in fig. 4. It's principal features are summarized below:

(i)   DFB laser source;

(ii)   2 graded-index rod lenses used, one for collimating and the other for refecting;

(iii)   piezo-electric crystal for fine longitudinal movements to obtain in-phase feedback
condition;

14

Table III

Design features of two DFB laser and GRIN rod
external cavities (Reported by Bell Core)

DESIGN PARAMETER	BELL CORE	BELL CORE
LASER STRUCTURE	BH	BH
SOLITARY LASER LENGTH	400 μm	550 μm
DFB GRATING	FIRST ORDER	FIRST ORDER
R_2	(*)	(*)
POWER FEEDBACK INTO LASER (R_3)	4% (-13.9dB)	10% (-10dB)
EXTERNAL CAVITY LENGTH	4 mm	4 mm

(*) Not specified; has to be <5% for good coupling and side mode rejection ratio.

Table IV

Output Characteristics of the two DFB Lasers and GRIN Rod External Cavities Specified in Table III

OUTPUT PARAMETERS	BELL CORE	BELL CORE
POWER LINEWIDTH PRODUCT	3.75 MHz·mW	2 MHz·mW
OUTPUT POWER	2.5 mW	1 mW
LINEWIDTH	1.5 MHz	2 MHz
SIDE MODE SUPRESSION RATIO	38.5dB (x7000)*	?
TUNABILITY	2 GHz/mA	200 MHz/mA (at 1.2 GHz modulation)

* quoted for solitary DFB laser

COHERENT TRANSMITTER PACKAGED MODULE

(DFB + GRIN ROD)
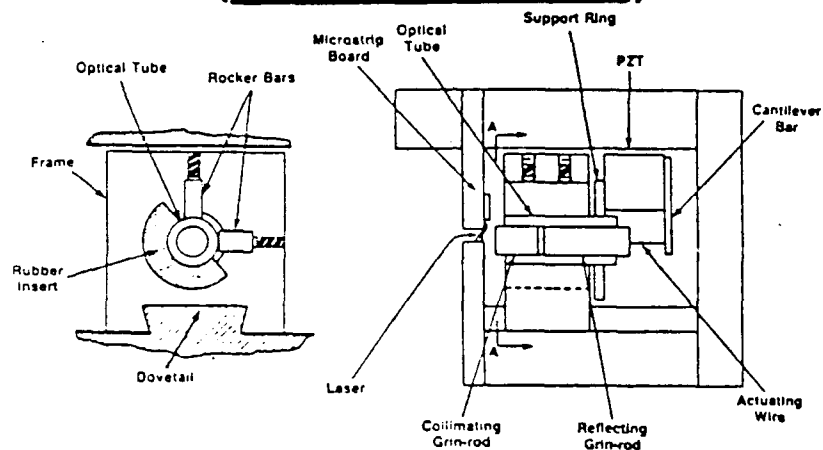
Fig 4: Commercial DFB-ECSL module built by **Bellcore** (Ref. 4) using GRIN-ROD lens.

(iv)   milli-Kelvin temperature control element

(v)   microwave bias board

(vi)   all the components are enclosed in 1 cubic inch enclosure, which is thermally insulated.

This module was used in 565 Mbit/s FSK system, and has a linewidth minimum of 1.3 MHz. The short term frequency stability is ± 10 MHz. There is a 20-50 times linewidth reduction compared to theoretical value of 100. A flat frequency response (modulated by current) of ~1.1 GHz was obtained.

III   DFB Laser and Single-mode Fiber External Cavity

The schematic diagram, not to scale, for this structure is shown in fig. 5. The components are again mounted on a Peltier thermo-electric cooler to control the temperature of the laser. The reasons for this have already been discussed in structure II above.

The advantages of this DFB-ECSL with single-mode fiber external cavity are as follows:

(i)   a simple cavity extended with an optical fiber;

(ii)   wavelength and single frequency selection are determined by the DFB solitary laser selection;

(iii)   tunability characteristics are similar to the solitary DFB laser;

(iv)   the laser is immune to external optical pertubations due to strong feedback;

(v)   ~ 1000-fold reduction in linewidth, from the solitary DFB laser, is possible.

The disadvantages of this structure are as follows:

(i)   the fiber feedback facet (F2) must be perpendicular to the fiber axis to within 1%;

(ii)   R2 facet reflectivity of < 1% is needed for the best results.

From the design features of this DFB-ECSL in Table V, it can be seen that the solitary laser length is relatively short, 250 mm and the external cavity length is 5.5 cm, or an order of magnitude greater than the DFB-ECSL with GRIN rod lens discussed in II above. This is why the

DFB LASER & FIBER EXTERNAL CAVITY
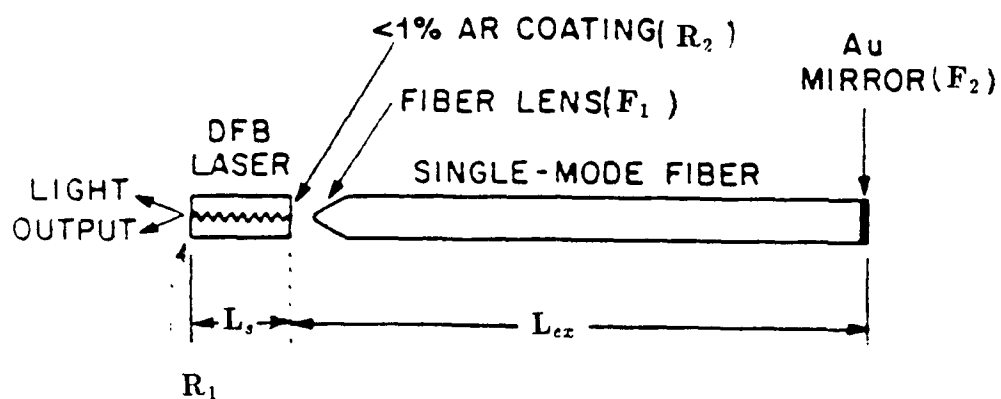
Fig 5: DFB Laser and Single-mode Fiber External Cavity

R_1:   Reflectivity of output facet (32%)

R_2:   AR coated facet (<1% reflectivity)

L_S: Solitary laser length

L_{ex}:   External cavity length

F_1:   Tapered facet of single-mode fiber

F_2:   Feedback facet of single-mode fiber with high reflectivity

Table V: Design features of a DFB-ECSL with Single-Mode Fiber External Cavity (Reported by AT & T Bell Labs.)

DESIGN PARAMETER	AT & T
LASER STRUCTURE	DOUBLE-CHANNEL PLANAR BURIED HETEROSTRUCTURE (DCPBH)
SOLITARY LASER LENGTH	$250\mu m$
DFB GRATING	SECOND ORDER
R_2	< 1%
POWER FEEDBACK INTO LASER (R_3)	-9 dB
EXTERNAL CAVITY LENGTH	5.5 cm

spectral linewidth obtained is ~ 70 kHz, as summarized in Table VI, in the output characteristics. Hence this structure can be used, as the transmitter laser, with any modulation format in a COFOCS, and at any bit rate. The side-mode supression ratio is also acceptable at ~ 31 dB.

A compact module having this structure was designed and built by Fujitsu Labs., and is illustrated in fig. 6. It's principal features are summarized below:

(i)   1.55 µm InGaAsP DFB laser source was used;

(ii)   two optical isolators were used to ensure good stability ;

(iii)   5 cm long single-mode fiber was used; with one end hemispherically tapered and the other end having a high reflective coating;

(iv)   Piezoelectric translator (PZT) was used for in-phase condition;

(v)   Peltier thermo cooler and temperature controller were used for frequency stability;

(vi)   the module size was 26 mm x 29 mm x 95 mm including the thermal insulator.

The module was used in a 1.2 G bit/s DPSK system over 190 km. A 70 kHz linewidth for in-phase condition was obtained. The frequency stability, between 2 modules was 50 MHz in an office environment.

Table VI: Output characteristics of DFB-ECSL with Fiber External Cavity

OUTPUT PARAMETER	AT & T LABS
POWER LINEWIDTH PRODUCT	70 kHz·m W
OUTPUT POWER	1 m W
LINEWIDTH	70 kHz
SIDE MODE SUPRESSION RATIO	-31dB (x1000)
TUNABILITY	SAME AS ORIGINAL DFB LASER

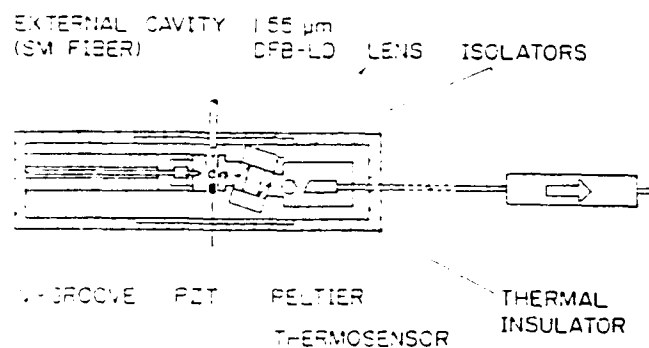# COHERENT TRANSMITTER PACKAGED MODULE

(DFB + FIBER CAVITY)

EXTERNAL CAVITY 1 55 μm
(SM FIBER)   DFB-LD   LENS   ISOLATORS

V GROOVE   PZT   PELTIER   THERMAL
                THERMOSENSOR   INSULATOR

Fig. 6: Commerical DFB-ECSL module built by
Fujitsu Labs. (Ref. 7) using single-mode
fiber external cavity

<u>Task 3A:</u>   Characterize linewidth and tunability aspects of DFB laser based external cavity coherent optical modules.

<u>Task 4A:</u>   Identify and charaterize the critical parameters upon which the linewidth and tunability depends, such as: facet reflectivity, feedback ratio, detuning angle, and external cavity length.

It can be seen that the above two tasks are related to the linewidth and tunability aspects and hence have been lumped together. Some discussion will be provided here. Further details are available in the two manuscripts enclosed at the end of this report.

(i) Manuscript 1 on "Tunability Aspects of DFB External Cavity Lasers"

(ii) Manuscript 2 on "Linewidth Considerations for DFB External Cavity Lasers"

LINEWIDTH CONSIDERATIONS

From a review of the literature and the discussion already made in Task 2A, the linewidth achievable from a DFB solitary laser is in the range 7 to 100 MHz, with output powers in the 1-5 mW range. By incorporating the laser in an external cavity, the linewidth can be reduced substantially, as we have seen in Task 2A, to betweeen 70 kHz and 2 MHz. The dependence of the theoretical linewidth of a solitary DFB laser, on various parameters, is shown in Table VII. To illustrate a typical numerical example, a typical linewidth of 69 MHz is obtained, and is shown in Table VIII. Typical parameters have been used, such as length of laser = 300 μm: output power of 1mW, linewidth enhancement factor of 5.4. The normalized linewidth ·power product is 69 MHz·mW. From Table VII it can be seen that the linewidth is inversely proportional to the output power and cavity length. Confirmation of this can be seen in fig. 7; the results were obtained by

24

TABLE VII

The dependence of the theoretical linewidth ($\Delta\upsilon$) of a solitary DFB laser

$$\Delta\upsilon = \frac{n_{sp} \, V_g^2 \, h\nu \, g}{4\pi P L} \cdot F \cdot (1+\alpha^2)$$

n_{sp} = ratio of spontaneous and stimulated emission = $\left[1 - exp\left\{\frac{(h\nu - eV)}{kT}\right\} \right]^{-1}$

V_g = group velocity

$h\upsilon$ = photon energy

ev = bandgap energy

k = Boltzmann's constant

T = Absolute Temperature

α = linewidth enhancement factor = $\left(\frac{\partial n / \delta Ne}{\partial G / \delta Ne} \right)$

g = gain in active region

F = normalized end loss

P = output power

L = laser cavity length

TABLE VIII

A Numerical example to illustrate the typical linewidth of a DFB solitary laser

$$\Delta \nu = \frac{n_{sp}\, V_g^2\, h\nu\, g}{4\pi P L} \cdot F \cdot (1+\alpha^2)$$

When $KL > 1$, $F = \left(\frac{\pi}{KL}\right)^2$

$$\therefore \quad \Delta \nu = \frac{n_{sp}\, V_g^2\, h\nu\, g}{4\pi P L}\left(\frac{\pi}{KL}\right)^2 \cdot (1+\alpha^2)$$
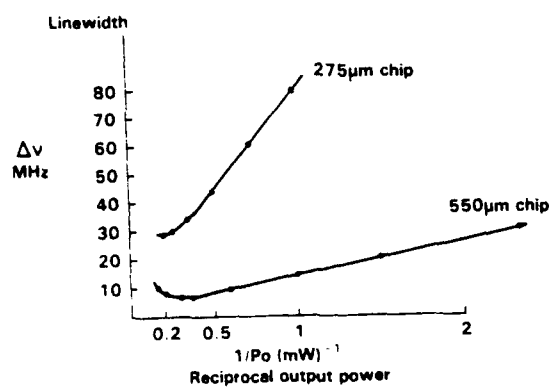
Using $L = 300\ \mu m$; $P = 1\ mW$

$\kappa = 150\ cm^{-1}$; $h\nu = 1.42\ ev$

$V_g = c/4.33$; $g = 61.3\ cm^{-1}$

$n_{sp} = 2.7$; $\alpha = 5.4$ (3-10)

$\underline{\Delta \nu = 69\ MHZ}$

Linewidth-Power Product = 69 MHz·mW

Fig. 7: Variation of the linewidth as a function of reciprocal output power for two different Lengths solitary DFB laser chips (After Ref. 5)

Research Labs. (Ref. 5). In this figure linewidth is plotted versus inverse power for two solitary laser lengths. Further discussion on this figure is as follows:

(i) $\Delta\upsilon$ was measured with a delayed self-heterodyne technique, which is well-known and widely used in the industry;

(ii)   for L = 275 µm, $\Delta\upsilon_{min}$ = 30 MHz;

(iii)   for L = 550 µm, $\Delta\upsilon_{min}$ = 7-10 MHz;

(iv)   output powers of 1-5 mW can be obtained;

(v) $\Delta\upsilon$ rebroadening at higher powers may be due to mode competition between two DFB laser modes.

(vi)   there is a limit on $\Delta\upsilon$ reduction and increase in the coupling coefficient.

The equation for spectral linewidth ($\Delta\upsilon$) in an external cavity DFB laser is given by

$$\Delta\upsilon = \Delta\upsilon_s \Big/ \Big(1 + \tau\ \gamma\sqrt{R_3}\ \Big)^2$$

where $\Delta\upsilon$ is the original linewidth of the solitary laser; τ is the round trip time with the external resonator; γ is the damping constant of the main resonator; R_3 is the power feedback . The round trip time with the external resonator is given by $\tau = (2nL_{ex}/c)$ where n is the refractive index of the external cavity; L_{ex} is the length of the external cavity and c is the speed of light.

From Figs. 8 thru 11 we can see the results of varying the different parameters. The damping constant γ influences the linewidth of the DFB-ECSL structure, inversely by the quantity squared. However, this is misleading, since the original linewidth is also dependent on γ. By providing a better DFB laser source, the linewidth of the DFB-ECSL is superior by a factor greater than γ^{-2}.

The next most important parameter is the effective length of the external cavity. The effective length, which is defined as the index of refraction of the external cavity medium times the length of the medium, reduces the linewidth by a factor of L^{-2}_{eff}. This can be seen by comparing and
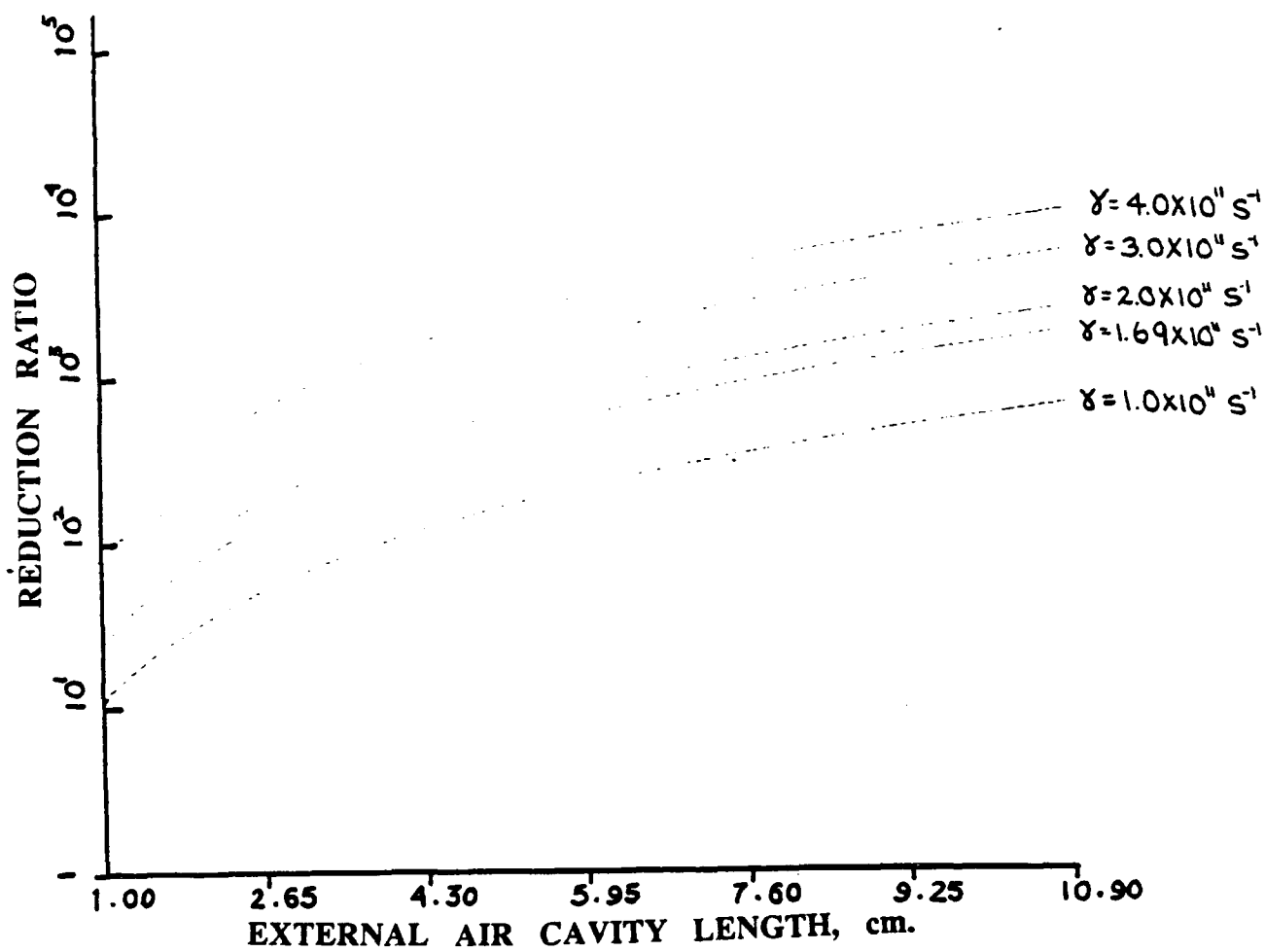
Fig. 8: Linewidth reduction ratio in DFB-ECSL as a function of external
air cavity length for different values of γ, the damping
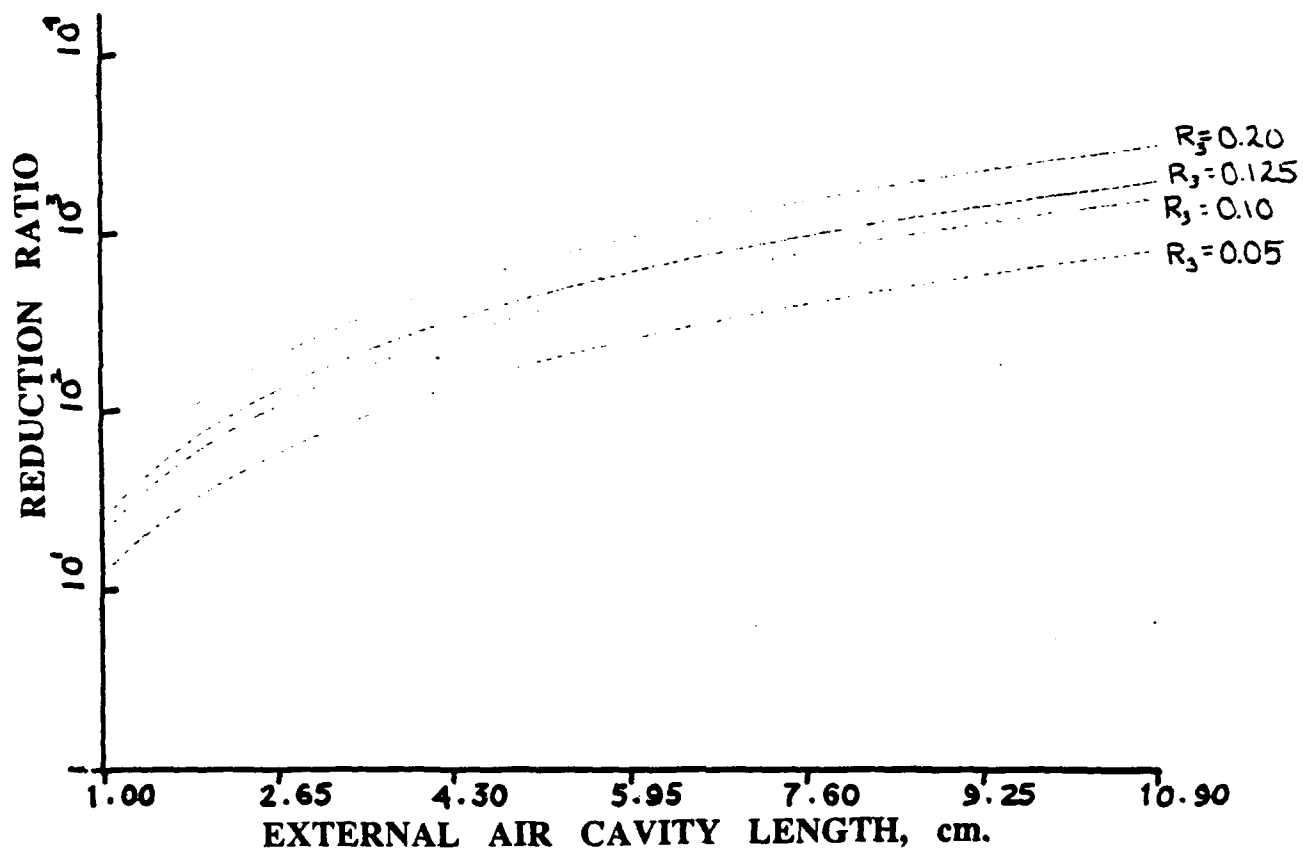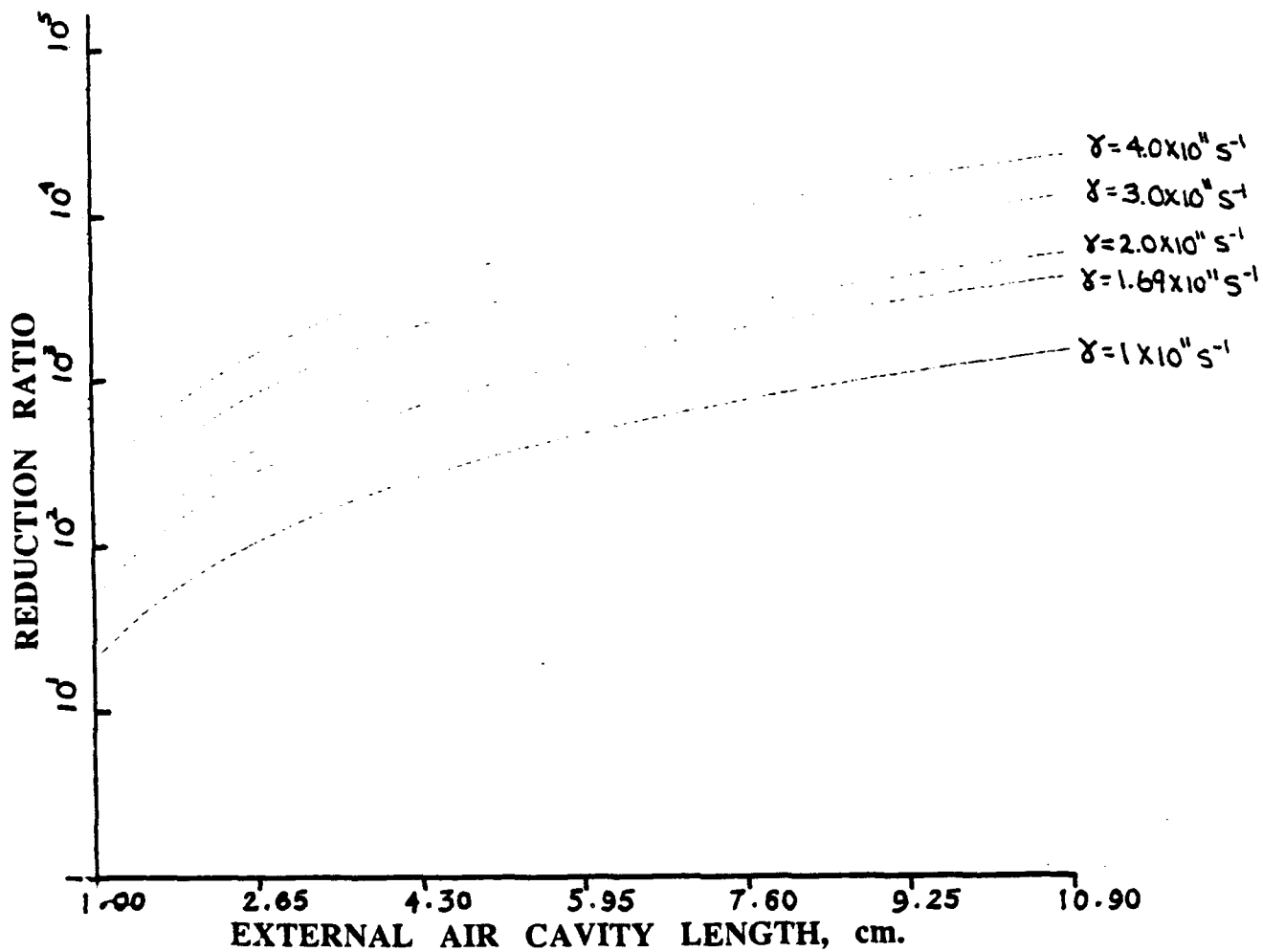constant. (R_3 = 0.125; n = 1.0)

29

Fig. 9: Linewidth reduction ratio in DFB-ECSL as a function of external
air cavity length for different values of R_3, the power
feedback. ($\gamma = 1.69 \times 10^{11}$ S^{-1}; n = 1.0)

Fig. 10: Linewidth reduction ratio in DFB-ECSL as a function of external fiber cavity length for different values of γ, the damping constant. ($R_3 = 0.125$; n = 1.0)
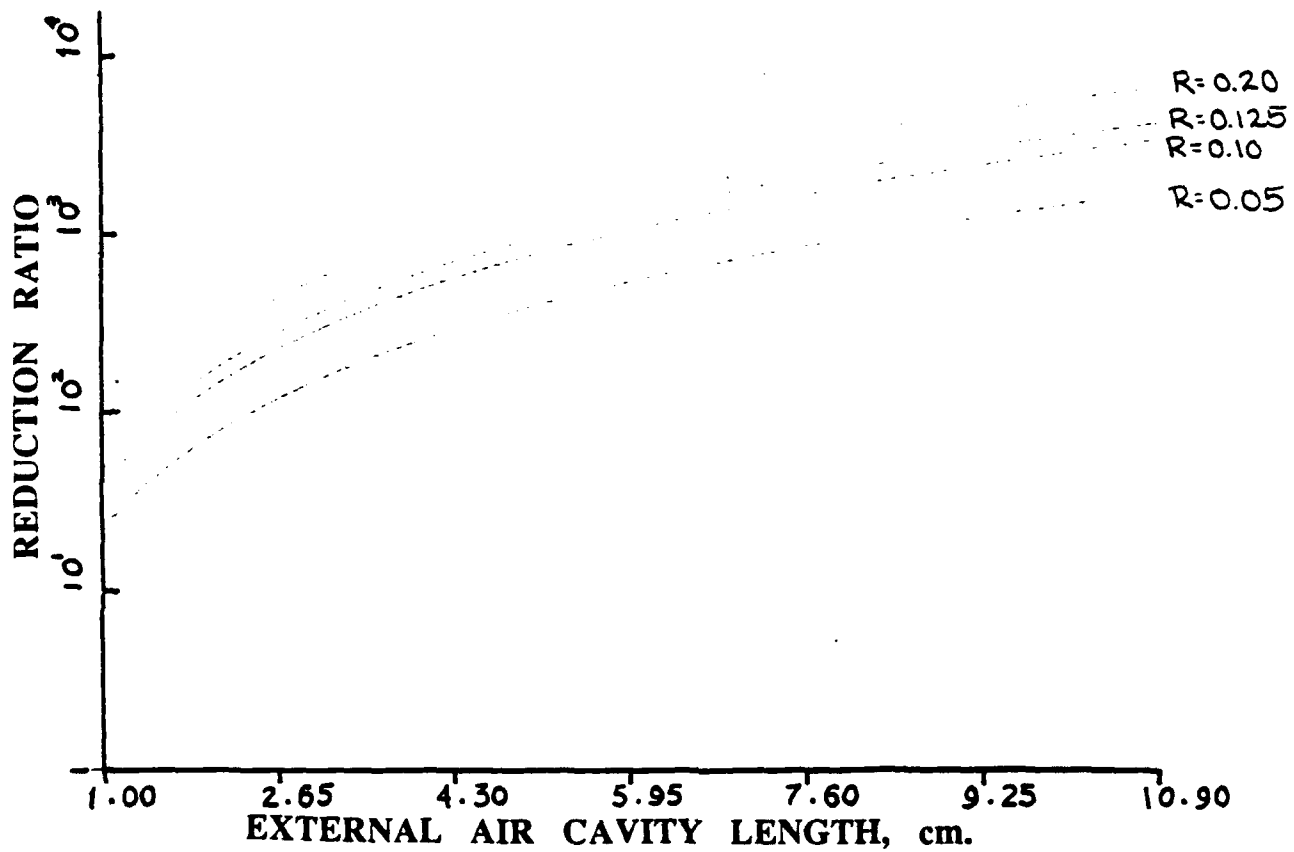
Fig. 11: Linewidth reduction ratio in DFB-ECSL as a function of external fiber cavity length for different values of R_3, the power feedback. ($\gamma = 1.69 \times 10^{11}$ S^{-1}; n = 1.0)

contrasting figures 8 and 9 with figures 10 and 11. The only parameter that is changed in the figures is the refractive index which corresponds to 1.0 and 1.5.

The last and least important parameter which affects the linewidth reduction ratio is the feedback level. The total feedback level is limited by the coupling losses, external cavity losses, and the reflection facet of the extenal cavity. The effect of changing the feedback can be seen in figures 9 and 11. One can see that the higher the feedback ratio the greater is the linewidth reduction.

R_1 is the reflectivity of the output facet and R_2 that of the other facet adjacent to the external cavity. Because of the need for strong coupling, R_2, must have a small value; the requirement that R_1 must remain about 32%, for Fabry-Perot modes to be set-up between the external cavity and the output facet of the DFB laser, then R_2 must be less than 5%. This 5% is the minimum requiremnt for the side mode supression ratio (SMSR) of about 30 dB. Ideally R_2 should be as low as possible for two basic reasons:

(i)   The first is coupling. Coupling between the DFB laser and external cavity should be as high as possible to increase the linewidth reduction ratio.

(ii)   The second reason is from the consideration of the side modes. If R_2 is greater than 5% these side modes become more pronounced. To limit this, and hence to get at least a 30 dB SMSR, it is required that R_2 be as small as possible ($<1\%$).

The tuning characteristics of DFB and DBR lasers continues on the next page.

Tuning Characteristics of DFB and DBR Lasers

To understand the tuning characteristics of DFB and DBR lasers one must first understand losses in these lasers. So effective mirror losses will be presented briefly and will be referred back to when discussing tuning aspects.

Effective Mirror Losses

The lasing wavelength is dependent upon the feedback caused by the grating. By changing the frequency selectivity of the feedback, one can change the threshold condition and cause a change in the lasing wavelength. Therefore, our analysis will start by finding the feedback caused by the grating. To find the effective mirror losses, that is, the losses from the laser through the facets as in a Fabry-Perot laser, a complex, rigorous mathematical derivation is needed. To shorten this report, only the results from such a derivation given in the book by G.P. Agrawal and N.K. Dutta(*Long-Wavelength Semiconductor Lasers*, Van Nostrand Reinhold Company,1986) for a DFB and DBR laser will be used. The threshold condition for a DFB laser is given by,

$$\left(\frac{r_1 - r}{1 - rr_1}\right)\left(\frac{r_2 - r}{1 - rr_2}\right) e^{2i\gamma l} = 1 \tag{1}$$

where,

$r =$ effective DFB reflection coefficient,

r_1, r_2 = reflectivities of the facets,

γ = the propagation factor,

L = the length of the laser cavity.

The value of r is given by,

$$r = -\frac{\kappa}{\gamma + \Delta\beta} \tag{2}$$

where,

κ = coupling coefficient,

$\Delta\beta = \pm(\gamma^2 + \kappa^2)^{1/2} = \delta - i\bar{\alpha}/2.$

δ is the detuning parameter which will be defined later and $\bar{\alpha}$ is the effective mirror loss or mode loss.

If the reflectivities of the facets are not assumed to be zero, then

$$r_j = R_j^{\frac{1}{2}} exp(i\phi) \tag{3}$$

where,

R= facet reflectivity,

ϕ = phase change due to incomplete grating periods.

Ideally the value of ϕ should be known, but due to manufacturing techniques in cleaving, this value will change from device to device. As we will see, this is the physical mechanism which will be used to tune the DFB or DBR lasers in the phase region. The value of ϕ varies from 0 to 2π and is the ratio of the last partial grating period length to a complete period length. Another useful parameter which will be used is the detuning parameter which is equal to,

$$\delta = \beta - \frac{m\pi}{\Lambda} \tag{4}$$

where,

m = order of the period,

Λ = period of the grating.

The detuning parameter measures the frequency difference from the Bragg condition.

By using appropriate parameters particular to the device structure, then equations [1] and [2] will yield a transcendental equation which would have a solution as in figure 12.

To make the solution independent of the length of the laser cavity the parameters are normalized by multipling in the cavity length.
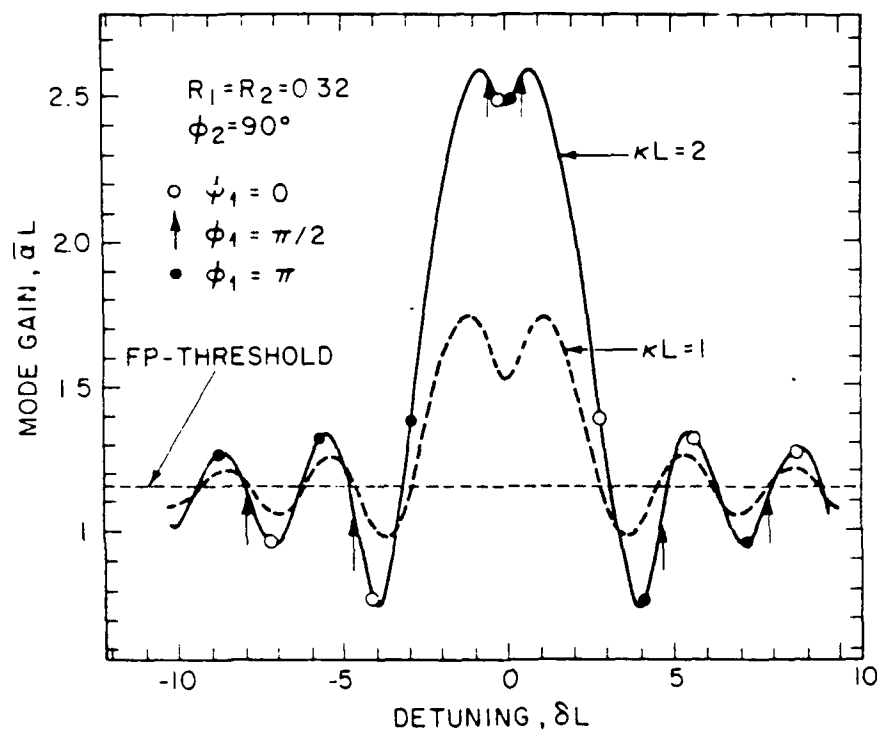
The same analysis can be done with the DBR laser. However,

Fig. 12: The mode gain vs detuning for fixed values of R_1, R_2, ϕ_2.

for DBR lasers, a coupling term from the active waveguide and the passive DBR region must be considered. The power coupling efficiency is given by C_0, which causes the effective reflectivity of the grating to be equal to

$$r_{eff} = C_0 r_g \tag{5}$$

where, r_g = grating reflectivity,and

C_0 = coupling coefficient.

The grating coefficient is given by,

$$r_g = \frac{i\kappa \sin \gamma l}{\gamma \cos \gamma l - i\Delta\beta \sin \gamma l} \tag{6}$$

and, $\Delta\beta = \delta + i\alpha_g/2$.

The α_g takes into account the loss due to absorption in the DBR region and that is why it is positive as opposed to the $\Delta\beta$ given for the DFB laser. Now if we consider the effective reflectivity as a facet reflection at both ends, then the threshold condition becomes

$$C_0^2 |r_g|^2 \exp 2i\beta L = 1 \tag{7}$$

By equating the modulus and the phase of both sides, we can solve for the mode loss and the phase condition. With the DBR mode loss defined as,

$$\alpha_{DBR} = \frac{1}{L} ln \frac{1}{C_0^2 |r_g|^2}, \tag{8}$$

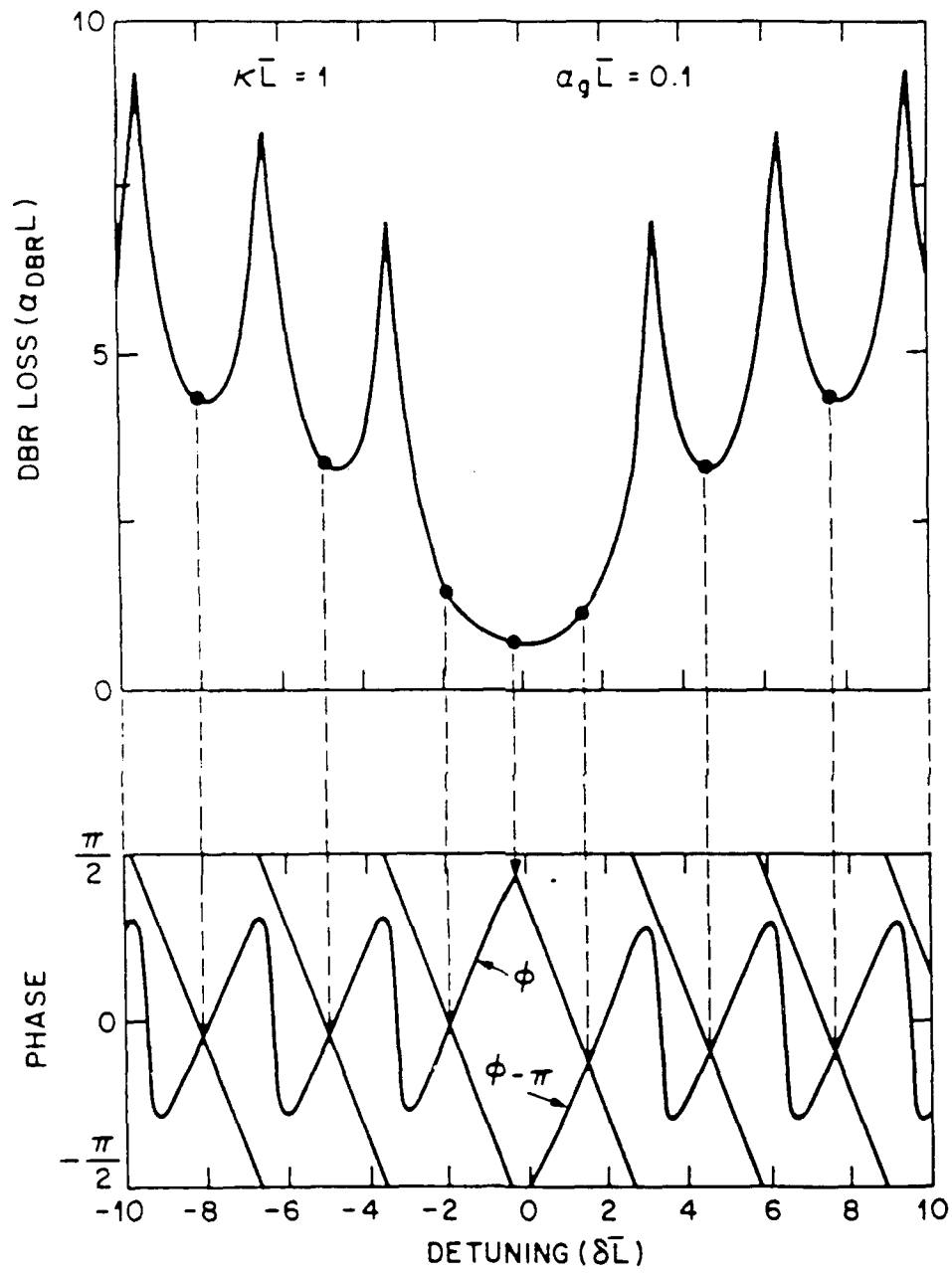the result obtained is plotted in fig. 13, shown on the next page.

38

Fig. 13: DBR mode loss and phase as a function of the detuning.

Tuning

There are basically two mechanisms which change the lasing wavelength of DFB and DBR lasers. Each type is dependant upon the **change of the refractive index associated with the change of injected current.** By changing the index of refraction one either changes the phase condition inside the cavity or changes the Bragg wavelength, as we shall see.

A phase change is introduced between the reflecting facet and active region(DBR) or between the grating region and active region(DBR) by locating a transparent region between these regions. If this region, called the phase region, is electrically isolated from the other regions, then pumping this region with current will not effect the other regions. By injecting current into the phase region causes a decrease in the refractive index of this region. This change causes a change in the effective length of this region and changes the phase conditions for the cavity. The change in the phase caused by this pumping is given by,

$$\Delta\phi = \frac{4\pi l}{\lambda}\Delta n, \tag{9}$$

where,

λ =wavelength of the propagating wave, and

l :=transparent cavity length.

For the DFB laser the new phase would change the operating point on the respective normalized coupling coefficient line in figure

40

13 which was shown previously. From this figure, a different phase would change the power output and linewidth due to a different mode loss. Ideally, the tuning mechanism should be made independent of the power output and linewidth. One can see from fig 13. that the larger the amount of change of the linewidth and power output the greater the value of the normalized coupling coefficient. Therefore, the product of the normalized coupling coefficient should be kept relatively small.

For the DBR laser an increase in the current will cause a continuous change in the wavelength until the operating point gets near the second mode. At this point a further increase in the current will cause an instability which will cause the lasing wavelength to be shifted back to the original mode. This occurs because the phase condition is satisfied by both modes and the original mode has less losses. For a DBR laser this type of tuning also changes the power output because absorption increases with increasing current. The tuning range for both the DFB and DBR lasers are approximately 1.2 nm which is the typical mode separation [ref:S.Murata *et al.*,Electron.Lett., vol.23, pp12-14, 1987].

The other way of changing the lasing wavelength is to pump the grating region which causes a change in the Bragg wavelength. The effect of this is to shift the plots for mode loss to lower wavelengths. For DFB lasers this is impractical because the Bragg condition is held by the active region. However for a DBR laser a large continuous tuning region of 5.8 nm[ref:S.Murata *et al.*,OFC/IOOC '87, paper]

WC3] can be realized. By changing the refractive index, one shifts the Bragg condition by,

$$\Delta\lambda_B = \frac{2\Lambda}{m}\Delta n \tag{10}$$

From fig. 13 we can see that the plot would shift to a lower wavelength with an increase in current, thereby causing a different wavelength to lase. However, this shift is not continuous. The phase of the round trip photon must be a integer multiple of π so that the mode is locked to that wavelength until the phase requirement is satisfied. When satisfied, the mode loss will jump to the next mode that satisfies this condition. This causes the lowest loss mode to move towards lower wavelengths. Since the mode loss is approximately constant except at a mode jump, the linewidth and power output are relatively constant also. The Bragg tuning also inherently has a greater range then phase tuning since it is not limited by the mode separation.

These results above can be seen to explain the typical tuning parameters for a three region DBR [ref:S. Murata *et al.*,OFC/IOOC'87, paper WC3]laser as seen in fig. 14. Fig. 15 shows the lasing wavelength as a function of the phase current. As can be seen, the tuning is continuous until the jump back to the original lasing wavelength. In fig. 16 we see that the output power changes during phase tuning . This mechanism is due to the absorption increase in the phase control region with increasing free carriers. The stepwise tuning with respect to the Bragg tuning can be seen in fig. 17 Notice that the power

42

was also kept approximately constant over the entire tuning range in fig. **16.** By controlling the currents in the active region, phase region, and Bragg region then one can obtain continuous wavelength tuning with constant power output [ref:S. Murata *et al.*,Electron. Lett.,pp. 403-405, 1987].

Conclusions which can be drawn from theory is that the DBR laser inherently has a greater tuning range than the DFB laser. Also one can conclude that the DFB laser can not be tuned without changing the linewidth output. On the other hand the DBR laser can be tuned with a constant output power if both phase and Bragg tuning is used.
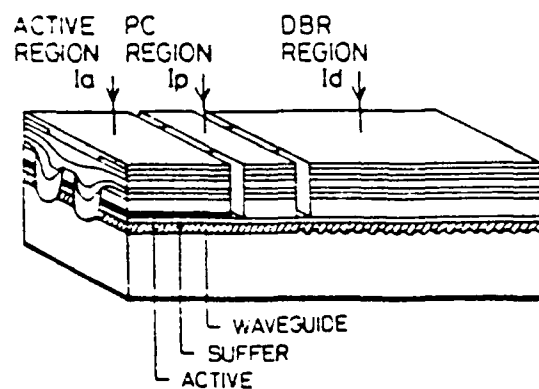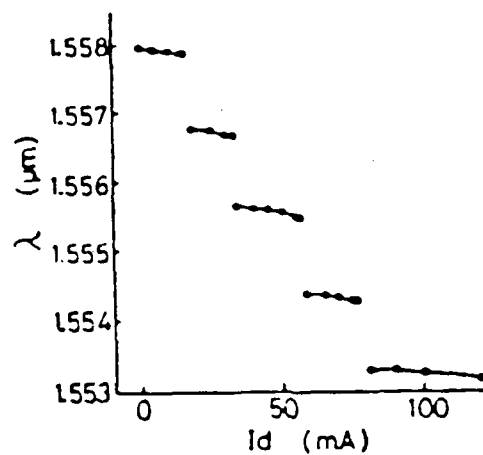
Fig. 14: THREE REGION DBR LASER
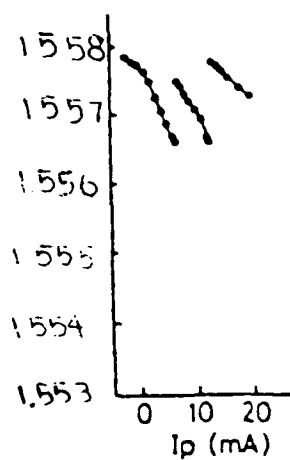
FIG. 15: LASING WAVELENGTH AS A FUNCTION
OF THE PHASE CURRENT
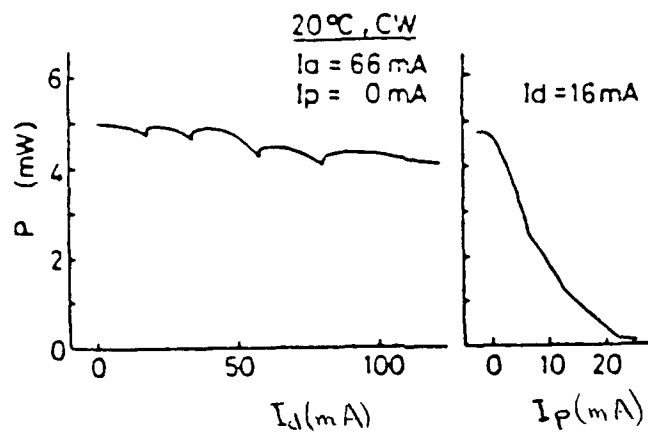
FIG 16: OUTPUT POWER AS A FUNCTION OF DBR REGION CURRENT AND PHASE REGION CURRENT

FIG. 17: LASING WAVELENGTH AS A FUNCTION OF THE DBR REGION CURRENT

Frequency Tunable DFB Lasers: Experimental Results.

From the previous discussion, it is evident that DFB lasers can be tuned by either changing the feedback phase or the Bragg wavelength. This is shown in fig. 18 and 19 respectively. In fig. 18, terminal A supplies the current to the active region and terminal P supplies the current to the tuning region. By changing I_p, the phase of the reflected light will change. This gives the maximum tuning range for a DFB laser. The disadvantage of this tuning mechanism is that the output power and linewidth will also change.

As an example, we quote the results obtained by Murata et al. of NEC Corp. (Ref. 10). These are summarized in Table IX. The advantages of the phase tunable DFB laser are as follows:

(i)   Large continuous tuning region (1.2 nm);

(ii)   Manufacturing is not very complex;

(iii)   FM response is flat up to 100 MHz;

The disadvantages of this structure are:

(i)   Change in the linewidth and the power output while tuning occurs;

(ii)   Linewidth also changes with tuning; minimum linewidth of 20 MHz and maximum of 120 MHz obtained;

(iii)   Phase-tuning is dependent upon reflectivity of the facet.

The Bragg wavelength change to tune DFB lasers is shown in fig. 19. Terminal A1 or A2 could be used for the tuning. Changing the amount of current in one section changes the Bragg wavelength which causes a change in the emitted wavelength. As an example we quote the results obtained by Dutta et al. of AT & T Bell Labs. (Ref. 18). These are summarized in Table X. The advantages of this structure are as follows:
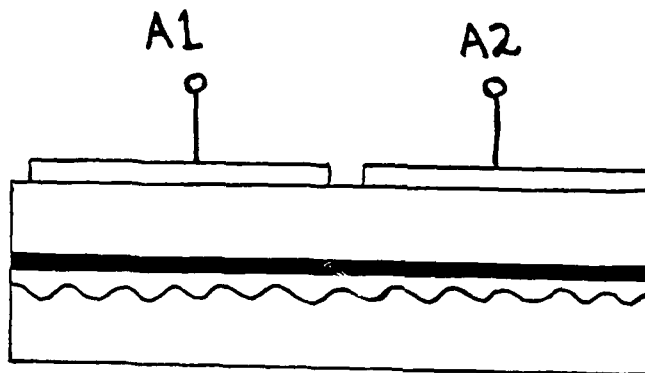
(i)   Either side can be used for tuning;

(ii)   The laser are easily manufacturable;

(iii)   No change in the linewidth is observed; 50 MHz linewidth is obtained for the entire tuning region

The disadvantages of this structure are:

46
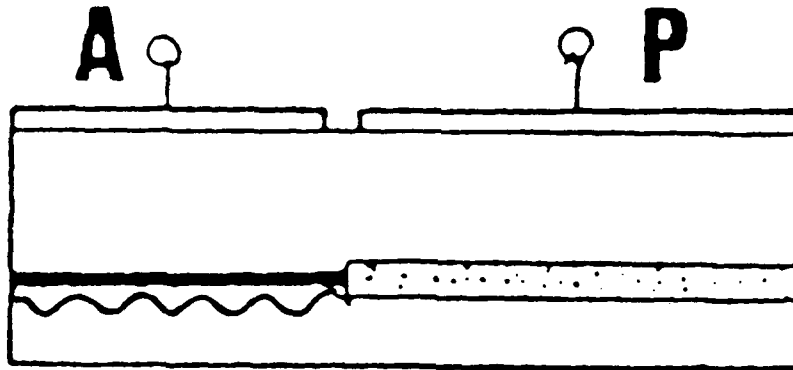
FIG. 18: SCHEMATIC FOR FREQUENCY TUNABLE DFB
LASER WITH PHASE CHANGE.

FIG. 19: SCHEMATIC OF FREQUENCY TUNABLE DFB LASER
WITH CHANGES IN THE BRAGG WAVELENGTH

TABLE IX

RESULTS OBTAINED BY MURATA ET. AL (REF. 10)

WITH PHASE-TUNABLE DFB LASER

PARAMETER	NEC Corp (Murata)
Active Region Length	250 μm
Tuning Region Length	130 μm
Maximum Tuning Range	1.2 nm (150 GHz)
Power Change with Respect to Tuning	Yes
Limitations on Tuning	Multimode oscillation foreseen by coupled mode theory
Isolation Resistance	280 Ω

TABLE X: Results obtained by Dutta et. al. (ref 18) with Bragg-Wavelength tunable DFB laser

PARAMETER	AT & T (Dutta)
Active Region Length	250 μm
Tuning Region Length	250 μm
Maximum Tuning Range	2 Å
Change in Linewidth with Respect to Tuning	None
Power Changes with Respect to Tuning	None
Limitations on Tuning	Tuning region reaches threshold and also leakage current

(i)   Very small tuning range of 2Å

(ii)   Limitation on tuning is caused by the tuning region reaching threshold, at which time the temperature increases and causes the tuning in the opposite direction.

<u>Task 5A</u>: Investigate the comparative performance of bulk and fiber diffraction gratings for DFB-ECSLs.

This above task is not relevant for DFB-ECSL as the frequency selection is accomplished by the grating in the solitary DFB laser. The external cavity in a DFB-ECSL only reduces the linewidth. This section will be relevant for FP-ECSL to be discussed later in Task 5B.

<u>Task 6A:</u> Identify design features of the coherent transmitter modules based on the results of Task 5A.

This task is again not relevant for DFB-ECSL for reasons quoted above in Task 5A.

<u>Task 7A:</u> Identify critical parameter combinations for DFB-ECSL that can support the various coherent modulation schemes.

For the DFB solitary laser, the selected values of the critical parameters and the reasons for their selection is given below. They were chosen because they are typical of readily available devices:

(i)   P[2mW] -Normal operating power of a DFB laser (up to 5 mW have been reported).

(ii) L[275 μm]-Normal length of DFB laser which depends on the manufacturing technique and cost.

(iii) R_1[<5%]-An antireflecting coating on the output facet must be provided to achieve a side mode surpression ration (SMSR) greater than 30 dB.

(iv) R_2[32%]-Since no coating is necessary, this is the reflectivity of the semiconductor/air interface.

(v) κ[160 cm^{-1}] -Typical value of the coupling coefficient for a readily available DFB laser.

(vi) Grating type [2nd order]-Type of grating used by most off-the-shelf DFB lasers.

For the DFB laser used in combination with external cavities, the following parameters are assumed and the rationale for these is as follows:

(i)   P[2 mW]-See above

(ii) L[275 μm]-See above.

(iii) R_1[32%]- No antireflection coating is needed on the output facet because we want a Fabry-Perot reson_tor to be set-up between F_2 and R_1, while using the DFB laser as a frequency selecting device.

(iv) R_2 [<5%]-Antireflection coating is needed to increase the coupling between the laser and the external cavity for strong feedback.

(v) κ[160 cm^{-1}] -see above.

A spectral linewidth of 40 MHz is assumed with the above parameters and agrees well with theoretical calculations.

For the DFB laser and GRIN Rod external cavity, the selected values of the critical param..ers and the reasons for their selection is as follows (see fig. 3);

(i) F_1 [<5%)-Antireflection coating required for strong feedback

(ii) F_2[95%]-Usually a gold coating which gives very high reflectivity.

(iii) η[4%]-Corresponds to the above criterion for F_1 and F_2.

(iv) L_{ex} Fixed at ~ 6 mm with a 0.23 pitch lens of about 4 mm long.

For the DFB laser and single-mode fiber cavity, the following were selected (see fig. 5):

(i) F_1 [fiber lens]-Needed to increase the coupling i..o the fiber. (No coating required)

(ii) F_2 [95%]-Usually a gold coating which gives very high reflectivity

(iii) η [10%]- Corresponds to the above criterion for F_1 and F_2.

(iv) L_{ex}- See design tables, to follow.

For the DFB laser and mirror cavity, the following were selected (see fig. 2):

(i) F_2 [95%]-High reflection coating needed to provide mirror.

(ii) η [12.5%]-Corresponds to the above criterion.

(iii) L_{ex}-See design tables, to follow.

In the above external cavity set-ups, it is assumed that the in-phase external feedback condition is met, by using precise longitudinal movement with a piezoelectric translator.

Note: The GRIN-rod external cavity is more practical than either the fiber or mirror cavity but can only be used for fixed lengths of 6 mm with ~ 0.23 pitch of lens to get the necessary collimation of light from the laser. Hence, linewidths are limited to ~ 1-2 MHz. For narrower linewidths, the fiber cavity is most practical. The mirror cavity is the least practical because the microscopic objective must be aligned and also pertubations in the air path bring on instabilities. The idea of long external cavity lengths, to get reduced linewidths, was tested by using the mirror cavity and practical devices have been built with GRIN rod lens and fiber external cavities, as highlighted in Task 2A.

From the above selection, it can be seen that the only variable parameter is the external cavity length. Tables XI, XII, XIII and XIV show the value of the optimum external cavity length (last column) of the different DFB-ECSLs, at four different bit rates, namely 140 Mbit/s, 565 Mbit/s, 1.2 Gbit/s and 2.4 Gbit/s. Each table has the 4 different modulation formats (ASK, FSK, DPSK and PSK) and the 4 different demodulation formats shown. The linewidth requirements are also shown. The preferred structure is also shown with an (*) and is based on the already cited advantages of this preferred structure.

From the above four Tables of the optimum cavity length and the relative advantages of each of the three DFB-ECSL discussed, we have identified the preferred structure that can be used in a system, clearly again in four Tables, labelled XV, XVI, XVII and XVIII. The variables are similar to the above four Tables. We have also shown the laser linewidth requirement, as a percentage of the bit rate, for each modulation format. It can be seen that the requirements for DPSK and PSK are considerably more stringent than ASK and FSK modulation.

It can be seen that as the bit rate (B) increases, the linewidth requirements become less stringent. The mirror cavity is obviously not preferred and the two DFB-ECSLs preferred are those with the GRIN rod and single-mode fiber. This is why we have compared, in considerable detail these two structures in Table XIX, which stretches over 2 pages. An advantage is denoted with a (+) and a disadvantage by (-). At lower bit rates, the fiber cavity has to be used while at higher bit rates, the grin rod external cavity can be used, as shown in the previous tables.

TABLE XI

DFB-ECSL FOR COFOCS

DESIGN TABLE FOR OPTIMUM EXTERNAL CAVITY LENGTHS

BIT-RATE = 140 MBITS/SEC

MODU-LATION	DEMODU-LATION	LINE-WIDTH	STRUCTURE	OPTIMUM LENGTH
ASK	Heterodyne with envelope	14 MHz to	Solitary DFB(*) GRIN-Rod	L=550μm L=4 mm
FSK	Detection	70 MHz	Solitary DFB (*)	L=275μm
DPSK	Heterodyne with delay time demodulation	420 kHz to 700 kHz	Fiber Cavity(*) Mirror Cavity	L=17-13mm L=18-13mm
PSK	Heterodyne	140 kHz to 700 kHz	Fiber Cavity (*) Mirror Cavity	L=30 -13mm L= 32-13mm
PSK	Homodyne	70 kHz to 140 kHz	Fiber Cavity (*) Mirror Cavity	L=43-30mm L=46-32mm

*Preferred structure

54

TABLE XII

DFB-ECSL FOR COFOCS

DESIGN TABLE FOR OPTIMUM EXTERNAL CAVITY LENGTHS

BIT-RATE = 565 MBITS/SEC

MODU-LATION	DEMODU-LATION	LINE-WIDTH	STRUCTURE	OPTIMUM LENGTH(mm)
ASK	Heterodyne with envelope	56 MHz to	Solitary DFB	L=275 μm
FSK	Detection	282 MHz		
DPSK	Heterodyne with delay time demodulation	1.7 MHz to 2.83 MHz	GRIN Rod(*) Fiber Cavity(*) Mirror Cavity	L=4 L=7.2-5.2 L=9.7-7.0
PSK	Heterodyne	565 kHz to 2.83 MHz	Fiber Cavity (*) Mirror Cavity	L=15-5.2 L= 20-7.0
PSK	Homodyne	282 kHz to 565 kHz	Fiber Cavity (*) Mirror Cavity	L=21-15 L=28-20

*Preferred structure

55

TABLE XIII

DFB-ECSL FOR COFOCS

DESIGN TABLE FOR OPTIMUM EXTERNAL CAVITY LENGTHS

BIT-RATE = 1.2 GBITS/SEC

MODU-LATION	DEMODU-LATION	LINE-WIDTH	STRUCTURE	OPTIMUM LENGTH(mm)
ASK	Heterodyne with envelope	120 MHz to	Solitary DFB	L=275 μm
FSK	Detection	600 MHz		
DPSK	Heterodyne with delay time demodulation	3.6 MHz to 6.0 MHz	GRIN Rod(*) Fiber Cavity(*) Mirror Cavity	L=4 L=4.5-3.0 L=5.8-3.9
PSK	Heterodyne	1.2 MHz to 6.0 MHz	Fiber Cavity (*) Mirror Cavity	L=9.0-3.0 L= 10-3.9
PSK	Homodyne	600 kHz to 1.2 MHz	Fiber Cavity (*) Mirror Cavity	L=14-9.0 L=15-10.0

*Preferred structure

TABLE XIV

DFB-ECSL FOR COFOCS

DESIGN TABLE FOR OPTIMUM EXTERNAL CAVITY LENGTHS

BIT-RATE = 2.4 GBITS/SEC

MODU- LATION	DEMODU- LATION	LINE- WIDTH	STRUCTURE	OPTIMUM LENGTH(mm)
ASK FSK	Heterodyne with envelope Detection	240 MHz to 1.2 GHz	Solitary DFB	L=275 μm
DPSK	Heterodyne with delay time demodulation	7.2 MHz to 12.0 MHz	GRIN Rod(*) Fiber Cavity Mirror Cavity	L=4 L=2.6-1.6 L=3.4-2.1
PSK	Heterodyne	2.4 MHz to 12.0 MHz	GRIN Rod(*) Fiber Cavity Mirror Cavity	L=4 L=5.8-1.6 L= 7.8-2.1
PSK	Homodyne	1.2 MHz to 2.4 MHz	GRIN Rod(*) Fiber Cavity Mirror Cavity	L=4 L=9.9-5.8 L=10-7.8

*Preferred structure

TABLE XV

<u>DFB-ECSL FOR COFOCS</u>

<u>LASER LINEWIDTH REQUIREMENTS</u>
<u>AND</u>
<u>DFB LASER BASED STRUCTURES</u>
(Bit Rate = 140 Mbit/s)

Modu-lation	Demodu-lation	$\Delta v/B$ (%)	Δv	DFB-Laser based Structure
ASK	Heterodyne with	10 to	14 MHz to	ANY STRUCTURE;
FSK	Envelope Detection	50	70 MHz	(SOLITARY DFB LASER PREFERRED)
DPSK (MSK)	Heterodyne with Delay Time Demodu-lation	0.3 to 0.5	420 kHz to 700 kHz	DFB LASER + FIBER CAVITY (PREFERRED STRUCTURE) OR DFB LASER + MIRROR CAVITY
PSK	Heterodyne	0.1 to 0.5	140 kHz to 700 kHz	DFB LASER + FIBER CAVITY (PREFERRED STRUCTURE) OR DFB LASER + MIRROR CAVITY
PSK	Homodyne	0.05 to 0.1	70 kHz to 140 kHz	DFB LASER + FIBER CAVITY (PREFERRED STRUCTURE) OR DFB LASER + MIRROR CAVITY

TABLE XVI

DFB-ECSL FOR COFOCS

LASER LINEWIDTH REQUIREMENTS
AND
DFB LASER BASED STRUCTURES
(Bit Rate = 565 Mbit/s)

Modulation	Demodulation	$\Delta v/B$ (%)	Δv	DFB- Laser based Structure
ASK FSK	Heterodyne with Envelope Detection	10 to 50	56 MHz to 282 MHz	ANY STRUCTURE (SOLITARY DFB LASER PREFERRED)
DPSK (MSK)	Heterodyne with Delay Time Demodulation	0.3 to 0.5	1.7 MHz to 2.83 MHz	DFB LASER + GRIN ROD (PREFERRED CAVITY) OR DFB LASER + FIBER CAVITY; OR DFB LASER + MIRROR
PSK	Heterodyne	0.1 to 0.5	565 kHz to 2.83 MHz	DFB LASER + MIRROR OR DFB LASER + FIBER CAVITY (PREFERRED CAVITY)
PSK	Homodyne	0.05 to 0.1	282 kHz to 565 kHz	DFB LASER + MIRROR OR DFB LASER + FIBER CAVITY (PREFERRED CAVITY)

TABLE XVII

DFB-ECSL FOR COFOCS

LASER LINEWIDTH REQUIREMENTS
AND
DFB LASER BASED STRUCTURES
(Bit Rate = 1.2 Gbit/s)

Modulation	Demodulation	$\Delta\upsilon/B$ (%)	$\Delta\upsilon$	DFB- Laser based Structure
ASK FSK	Heterodyne with Envelope Detection	1 0 to 5 0	120 MHz to 600 MHz	ANY STRUCTURE (SOLITARY DFB LASER PREFERRED)
DPSK (MSK)	Heterodyne with Delay Time Demodulation	0.3 to 0.5	3.6 MHz to 6.0 MHz	DFB LASER + GRIN ROD (PREFERRED CAVITY) OR DFB LASER + FIBER CAVITY; OR DFB LASER + MIRROR CAVITY
PSK	Heterodyne	0.1 to 0.5	1.2 MHz to 6.0 MHz	DFB LASER + MIRROR OR DFB LASER + FIBER CAVITY; OR DFB LASER + GRIN ROD (PREFERRED CAVITY)
PSK	Homodyne	0.05 to 0.1	600 kHz to 1.2 MHz	DFB LASER + MIRROR OR DFB LASER + FIBER CAVITY; (PREFERRED CAVITY)

TABLE XVIII

DFB-ECSL FOR COFOCS

LASER LINEWIDTH REQUIREMENTS
AND
DFB LASER BASED STRUCTURES
(Bit Rate = 2.4 Gbit/s)

Modu-lation	Demodu-lation	$\Delta\upsilon/B$ (%)	$\Delta\upsilon$	DFB- Laser based Structure
ASK FSK	Heterodyne with Envelope Detection	10 to 50	240 MHz to 1.2 GHz	ANY STRUCTURE (SOLITARY DFB LASER PREFERRED)
DPSK (MSK)	Heterodyne with Delay Time Demodu-lation	0.3 to 0.5	7.2 MHz to 12 MHz	ANY STRUCTURE (SOLITARY DFB LASER PREFERRED)
PSK	Heterodyne	0.1 to 0.5	2.4 MHz to 12 MHz	DFB LASER + MIRROR OR DFB LASER + FIBER CAVITY; OR DFB LASER + GRIN ROD (PREFERRED CAVITY)
PSK	Homodyne	0.05 to 0.1	1.2 MHz to 2.4 MHz	DFB LASER + MIRROR OR DFB LASER + FIBER CAVITY; OR DFB LASER + GRIN ROD (PREFERRED CAVITY)

TABLE XIX

<u>DFB-ECSL FOR COFOCS</u>

<u>COMPARISON OF PREFERABLE STRUCTURES</u>

DFB Laser + GRIN rod	DFB Laser + Fiber Cavity
(+) Lens ends do not have to be tapered or cleaved; available commercially in useable form.	(-) End preparation of fiber into taper-with-hemisphere lens is important for good coupling.
(-) A high reflection coating must be applied to the re-flection facet.	(-) Reflection end must be per-pendicular to fiber axis to within 1° and have a high reflection coating.
(-) An anti-reflection coating must be applied to have good coupling.	(+) No further processing of coupling end required.
(-) Linewidth power product limited to 1-2 MHz· mW, due to lens size and cavity length.	(+) Linewidth power product is two orders of magnitude better, 70 kHz·mW.
(+) Because of size, both the GRIN rod and DFB laser can be mounted on a Peltier thermocooler.	(-) Short lengths of SMF are impractical to prepare & handle.
	(-) Entire module must be thermally insulated and temperature controlled be-cause fiber cavity & DFB laser both cannot fit on Peltier thermocooler.

+ signifies an advantage

- signifies a disadvantage

TABLE XIX (CONTINUED)

DFB-ECSL FOR COFOCS

COMPARISON OF PREFERABLE STRUCTURES
(Continued)

DFB Laser + GRIN rod	DFB Laser + Fiber Cavity
(+) Dimensions of a practical module are approximately 20 mm x 20 nm x 40 mm; can be made small and robust.	(-) Dimensions of a typical module are 26 mm x 29 mm x 95 mm; not as compact.
(-) GRIN rod must be very precisely controlled by a piezoelectric translator for the minimum linewidth condition.(~0,3 μm)	(-) Fiber cavity must also be very precisely controlled by piezoelectric translator for the minimum linewidth condition.
(-) DFB solitary laser must be good (~40 MHz linewidth) to give linewidths which can be used in lesser stringent modulation schemes.	(+) DFB laser selection not needed for relatively narrow linewidth for practical use.
(-) Temperature control must be approximately .01° C.	(-) Temperature control must be approximately .01°C.

+ signifies an advantage

- signifies a disadvantage

Task 8A: Develop theoretical models to characterize the stability of linewidth and output frequency of the DFB-ECSLs as a function of environmental parameters such as temperature and pressure.

Environmental parameters such as temperature and pressure are relatively unimportant in a packaged module and no attention has been given to them in the literature on ECSLs. This is because the temperature of the heat sink, of the solitary laser, is controlled to ~0.01°C by using two stages of thermo-electric coolers. This is absolutely necessary to ensure good frequency stability of the laser. Tuning the frequency of the laser, by changing the injected current or the heat sink temperature, is well-known. This is due to a shift of the semiconductor laser gain profile towards higher energy levels when the carrier injection level, which is proportional to the injection current, is changed. Further a commercial package is hermically sealed and environmental pressure changes are eliminated. Analysis of the frequency change with injected current and heat sink temperature are well documented in the literature and hence the theoretical models were not developed in preference to tasks 13 and 14 which were extremely important and vital to this contract.

Tasks 2B through 8B now follow for Fabry-Perot laser based external cavities.

Task 2B: Analyze performance of FP-ECSL coherent optical transmitter with strong frequency selective feedback.

There are four basic external cavity structures which have been built with FP solitary laser. These are

   (i)   FP laser + Bulk diffraction grating

   (ii)   FP laser + Fiber diffraction grating

   (iii) FP laser + Prism diffraction rating

   (iv) FP laser + External waveguide Bragg Reflector

The references, in the literature, which have reported the above structures, referred to as FP-ECSL (Fabry-Perot External Cavity Semiconductor Lasers), are listed as References 19 thru 28. We have only considered strong feedback, as in the task stipulation. Frequency selection is provided by the external diffraction grating.

We now analyze the performance of each of the above FP-ECSL as was done previously for DFB-ECSL.

I   FP Laser with Bulk Diffracting Grating

The optical schematic is shown in Fig. 20. The advantages of this structure are as follows:

   (i)   Very wide tuning capability of ~ 130 nm, which is ~ 14,000 GHz!

   (ii)   Continuous tuning is possible as well as fine, medium and coarse tuning;

   (iii) Easy coarse tuning can be achieved by rotating the bulk diffraction grating;

   (iv) Very narrow spectral linewidths can be obtained, of ~ 10 kHz and less, for every mW of output power.

The disadvantages of this structure is as follows:

   (i)   requires AR coating on one facet;

   (ii)   Degradation of direct frequency modulation capability with the external cavity

   (iii) Low feedback coupling efficiency (~ 10%)

   (iv) Unguided air path and hence acoustic disturbance can disrupt performance

F-P Laser with Bulk Diffraction Grating

Fine tuning   Medium tuning   Coarse tuning

L_o

R_3

θ

R_2

Output

M

L_{ex}

plate   F-P etalon   Diffraction grating
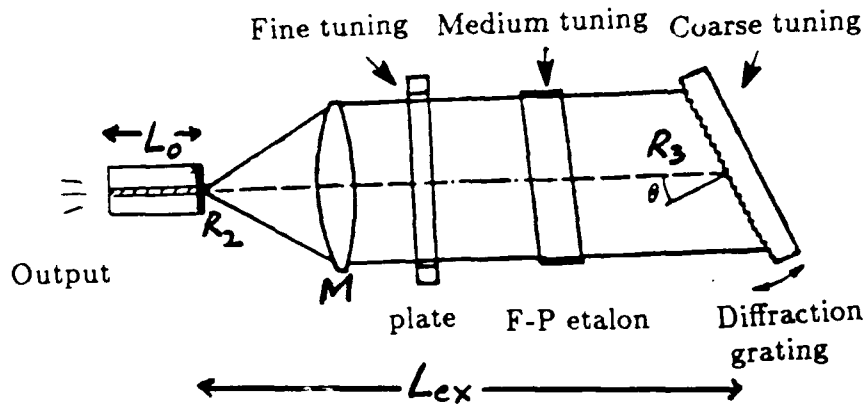
Fig. 20:   Schematic of Fabry-Perot Laser with Bulk Diffraction Grating

L_o = Solitary laser length

L_{ex} = external cavity length

R_2 = Reflectivity of AR coated facet

R_3 = Feedback level

M = collimating maicroscope objective

(v)   Package can be bulky.

(vi)   Frequency stability depends on mechanical design

(vii)   Both laser facets must be available; One for feedback, the other coupling the for output
from the laser, into a single-mode fiber.

The design features of five different FP-ECSL structures built at 1.55 μm are summarized
in Table XX. The key design features include solitary laser length (L_o), AR coated facet reflectivity
(R_2), feedback ratio (R_3), external cavity length (L_{ex}) detuning angle (ϕ), whether on an optical
bench or package and the reference. The solitary structure is also specified. It can be seen that the
external cavity length varies between 5-18 cm. The corresponding output characteristics of these
structures are shown in Table XXI. The key point to notice is that the spectral linewidths are very
narrow (500 Hz -20 kHz) compared to DFB-ECSL. The output powers are in the 1-5 mW range
and are comparable to DFB-ECSL.

II FP Laser with Fiber Diffraction Grating

The schematic of this structure is shown in Fig. 21. The advantages of this structure are as
follows:

(i)   the laser facet, nearer to the fiber, does not require an AR coating, R_2 is left at 32%.

(ii)   the feedback R_3 is as high as 90%

(iii)   the feedback coupling efficiency is very good at 50%

(iv)   Since the feedback path is in an optical fiber, no acoustic or other disturbances affect the
performance of the laser.

(v)   very narrow spectral linewidths can be obtained (~20 kHz · mW.)

(vi)   we can use only one facet of the laser both for feedback and output power.

The disadvantages of this structure are as follows:

(i)   it has limited tuning capability of ~2 nm, or ~240 GHz

(ii)   it is relatively hard to tune by changing the refractive index or the grating period by using a
specially made fan grating.

67

TABLE XX

FP-ECSL FOR COFOCS

F-P Laser Based External Cavity Structures

FP Laser + Bulk Diffraction Grating

1) DESIGN FEATURES:

Wavelength = 1.5 μm				LAB	
PARAMETER		BTRL	BTRL	AT & T	AT & T
SOL. STRUCTURE	CSBC	DCPBH	DCPBH	CSBH	CSBH
LASER $\Delta\upsilon_s$ or L_o	–	–	–	–	$\Delta\upsilon_s=$ 100 MHz·mW
R_2	3.5%	9%	3%	4%	2%
R_3	25%	25%	–	–	–
L_{ex}[cm]	12	10	5	5 ~ 15	18
ϕ	110°	80°	–	–	–
Comments	On Optical Bench		Package	On Optical Bench	On Optical Bench
Ref.	Elec. Lett. Vol 21, p. 658 1985		Elec. Lett. Vol. 21, p. 113, 1985	Appl. Phys. Lett. Vol.48 p. 885 1986	J. Light Tech. LT-5, p 510, 1987

CSBH: Channel Substrate
        buried Hetero-structure

CSBC: Channel Substrate Buried
        Cresent

DCPBH: Double Channel Planar
        Buried Hetero-structure

TABLE XXI

FP-ECSL FOR COFOCS

F-P Laser Based External Cavity Structures

FP Laser + Bulk Diffraction Grating

2) OUTPUT CHARACTERISTICS

		LAB			
PARAMETER	BTRL		BTRL	AT & T	AT & T
$\Delta\upsilon_{ex}$	300 Hz	500 Hz	20 kHz	–	2 kHz
kHz·mW	2	~2	–	18kHz·mW	7.4 kHz·mW
Tunability [nm]	120	–	60	60	90
Output [mW]	1-5	1-5	–	1	1~4
Freq. Drift	--		<150 MHz		<15 MHz
Comment			Fine tuning with silica plate		Fine tuning with external cavity length

F-P Laser with Fiber Diffraction Grating

(a)

(b)
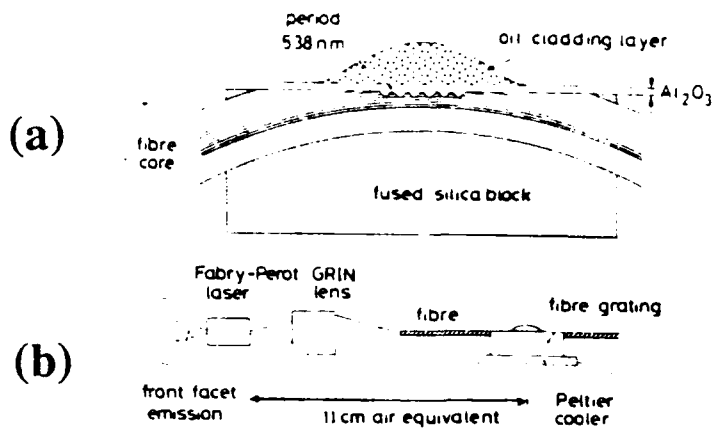
Fig. 21: Schematic of Fabry-Perot laser with Fiber Diffraction Grating

    (a)   Detailed view of fiber diffraction grating

    (b)   Overall set-up of laser

FP- ECSL WITH PRISM GRATING
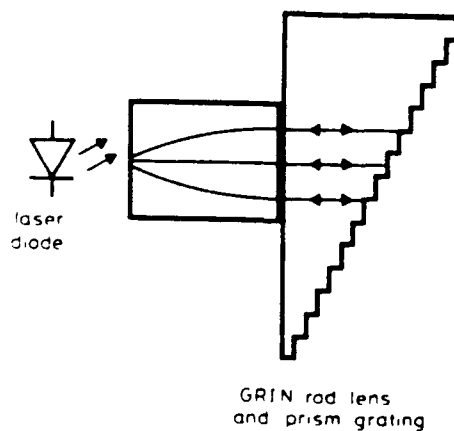
Fig. 22: Schematic of Fabry-Perot laser with Prism Diffraction Grating

(iii)   fairly involved processing is required for producing the grating on the single-mode fiber, as compared to a bulk diffracting grating which can be commercially bought relatively cheaply.

III   FP Laser with Prism Diffraction Grating

The schematic diagram of this structure is shown in fig. 22. The advantages of this structure are:

(i)   compactness, as the external cavity length in only 2 cms.

(ii)   the feedback coupling efficiency is very high (50%)

(iii)   very wide coarse tuning of 40 nm can be obtained.

The disadvantages of this structure are:

(i)   the spectral linewidth is not very narrow, 1 MHz·mW;

(ii)   one laser facet requires an AR coating, as with the bulk diffraction grating.

(iv)   fine tuning is very difficult with extremely small displacement of the prism; for every μm, 16 GHz variation is obtained; hence for 1000 MHz, a displacement of 16 nm would be required.

IV   FP with External Waveguide Bragg Reflector (EWBR)

The schematic diagram of this structure is shown in fig. 23. The advantages of this structure are as follows:

(i)   very compact size, as the total length is 5 mm;

(ii)   substantial chirp reduction can be obtained

(iii)   narrow linewidth of 1 MHz at 3 mW;

(iv)   insenstitive to spurious optical feedback

(v)   strong feedback can be obtain ($R_3 > 60\%$)

(vi)   relatively easy to use 1st order Bragg reflection

The disadvantages of this structure are:

(i)   Low coupling efficiency due to butt coupling (~20%)

FP + EXTERNAL WAVEGUIDE BRAGG REFLECTOR (EWBR)

BRAGG REFLECTOR
CHIP

GRATING

LASER CHIP

FIBER

SiO₂

Si₃N₄

SiO₂

Si
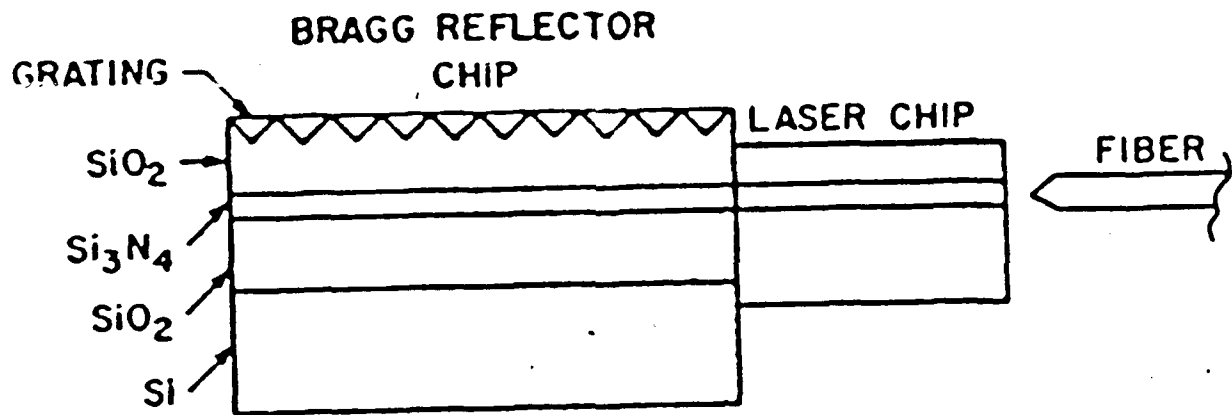
Fig. ___ Schematic of Fabry-Perot laser chip with external waveguide Bragg reflector on the left. The output fiber is also shown.

(ii) Hard to tune, tuning with temperature can be achieved.

(iii) Stability depends on mechanical design. It is mechanically weak to external perturbations.

The design features of this FP-EWBR laser, built by AT & T Bell Labs, is shown in Table XXII and the output characteristics are shown in Table XXIII. All the data is explained well and unambiguously in these tables and will not be repeated here.

TABLE XXII

FP + EXTERNAL WAVEGUIDE BRAGG REFLECTOR (EWBR)

DESIGN FEATURES

Design Parameters	AT and T Lab.
Wavelength	1.5 μm
Laser Diode	CSP (Channel substrate planar)
Facet Reflectivity	$R_1 = R_2 = 0.32$
Bragg Reflector	Silicon substrate ($n_e = 1.46$) 1st order grating FWHM of reflection: 6Å 5 mm single mode ridge waveguide
Feedback	$R_3 > 0.6$
External cavity length	5 mm

TABLE XXIII

FP + EXTERNAL WAVEGUIDE BRAGG REFLECTOR (EWBR)

OUTPUT CHARACTERISTICS

OUTPUT PARAMETER	AT & T LABORATORY
DC Chip reduction	650 MHz/mA (without EWBR) 30 MHz/mA (with EWBR)
AC Chirp reduction (1 GHz modulation)	220 MHz/mA (without EWBR) 15 MHZ/mA (with EWBR)
Output Power	~ 3 mW
Linewidth	1 MHz at 3 mW
Sidemode Suppression	-37 dB (x5000)
Temp. Tuning	Laser 1Å/°C EWBR 0.1 Å/°C

Task 3B: Characterize linewidth and tunability aspects of FP-ECSL external cavity based coherent optical transmitters

Task 4B: Identify and characterize critical parameters upon which the linewidth and tunability depends, such as facet reflectivity, feedback ratio, detuning angle and external cavity length.

The above tasks are related to linewidth and tunability and have been dealt with in considerable detail in three manuscripts enclosed at the end this report. These are:

Manuscripts 3 and 4: "Linewidth calculations in tunable external cavity Fabry-Perot semiconductor lasers with strong frequency-selective feedback for coherent lightwave systems".

Manuscript 5: "Frequency tuning characteristics of external cavity Fabry-Perot semiconductor lasers with strong feedback for coherent lightwave systems,"

Task 5B: Investigate the comparative performance of bulk and fiber diffraction gratings.

This has been done, in considerable detail, and the results are presented in Table XXIV, which extends over 2 pages. The comparison is made on seven parameters, namely, tuning, devices, packaging, linewidth, stability, output power and modulation. An advantage is labelled with a(+) and a disadvantage with a (-). Tasks 6B and 7B as stated below will be discussed together as they are relevant.

TABLE XXIV
FP-ECSL FOR COFOCS

F-P Laser Based External Cavity Structures

	Bulk Diffraction Grating	Fiber Diffraction Grating
T U N I N G	(+) Wide tuning capability (~130 nm) (+) Continuous tuning possible by coarse tuning, Medium tuning Fine tuning. (+) Easy to coarse tune by changing incident angle Θ $\lambda = 2 \Lambda \sin\theta$ where Λ is a grating period	(-) Limited tuning range (~ 2 nm, ~ 240 GHz) (-) Continuous tuning is very limited (-) Relatively hard to tune. Tuning can be achieved by changing n_e or Λ. $\lambda = 2 n_e. \Lambda$ where n_e: refractive index of oil cladding layer Λ: Grating period
D E V I C E	(-) Need R_2 small ($\leq 5\%$) (-) R_3 moderate (~ 25%) (-) Low feedback coupling efficiency to laser (~10%) (-) Unguided air path (Acoustic disturbances)	(+) R_2 can be uncoated (~32%) (+) R_3 high (~90%) (+) High feedback coupling efficiency to laser (~50%) (+) Guided path in optical fiber (no disturbance)
P A C K A G E	(+) Relatively cheap grating; commercially available (-) Package is bulky (-) Both laser facets must be available; one for feedback, the other for output from laser	(-) Fairly involved processing (Research Device) (+) Package can be small (+) Can use one laser facet for feedback and output ($R_1 = 1$)

TABLE XXIV (CONTINUED)

FP-ECSL FOR COFOCS

F-P Laser Based External Cavity Structures
(Continued)

	Bulk Diffraction Grating	Fiber Diffraction Grating
Line-width $\Delta\upsilon$	$\Delta\upsilon \geq 2$ kHz or $\Delta\upsilon \cdot P = 7.4$ kHz· mW(+) (N.A. Olsson et al.)	$\Delta\upsilon \geq 3$ kHz or $\Delta\upsilon \cdot P = 18$ kHz· mW(+) (C.A. Park et al.)
Sta-bility	• 1/f type amplitude noise. (Modulation freq. need to be greater than 200 MHz.) •Frequency stability is determined by mechanical design. i.e. Freq. drift ≤ 15 MHz (without enclosure) Freq. drift ≤ 1 MHz (with enclosure)	unknown
Output Power	~ 3 mW (depends on bias current)	~ 6 mW (depends on bias current)
Modu-lation	(-) Degradation of direct frequency modulation Capability $\left(\dfrac{\Delta f}{\Delta i}\right)$	unknown

+ signifies an advantage

- signifies a disadvantage

78

Task 6B: Identify design features of the FP-ECSL coherent transmitter module based upon the results of Task 5.

Task 7B: Based on the above tasks, identify critical parameter combinations of the FP-ECSL coherent transmitter modules that can support the various coherent modulation schemes.

The critical parameters selected for the solitary FP laser are shown below and are typical of readily available devices:

(i) $P = 3$ mW; normal operating power of FP laser and easily obtained.

(ii) $L_o = 150$ μm normal length of solitary laser.

(iii) $R_1 = R_2 = 32\%$; normal cleaved facet reflectivities.

(iv) $\lambda = 1.55$ μm; InGaAsP device at the lowest fiber attenuation wavelength.

(v) $\Delta \upsilon_{sol} \approx 322$ MHz; solitary laser linewidth, assuming typical parameters as shown below:

$$\Delta \upsilon_{sol} = \{ V_g^2 \ h \upsilon g_{th} \ \alpha_m \ n_{sp} \} \times (1 + \alpha^2)\Big/ [8 \pi \ P]$$

where $\alpha_l = 50$ cm^{-1}, $\alpha_m = 45$, $\alpha = -6$,

$n_{sp} = 5$, $P = 3$ mW, $\Upsilon = 0.2$ (mode confinement factor)

For the FP laser and the bulk diffraction grating (BDG) the selection of ϕ, R_2 and R_3 are as follows:

(i) $\phi = 2 \pi$; feedback is tuned to FP modes

(ii) $R_2 \leq 3\%$; AR coating must be provided to achieve strong feedback and broad tuning range; this value is easily obtained by present-day technology.

(iii) $R_3 \geq 20\%$: Typical feedback ratio including coupling loss; this value is easily obtained with a bulk diffraction grating.

For the FP laser and the fiber diffraction grating (FDG) the selection of ϕ, R_2, R_3 and n are as follows:

(i) $\phi = 2\pi$; feedback is tuned to FP modes,

(ii) $R_2 = 32\%$; uncoated laser facet is specified as R_3 is fairly high in this arrangement;

(iii) $R_3 \geq 45\%$; including coupling efficiency; this value is easily obtained with this structure;

(iv)   n = 1.45; refractive index of optical fiber;

Determination of the optimum length of the external cavity, for various modulation schemes at various bit rates, can be found from the two graphs, fig. 24 and fig. 25. From these two figures, and the linewidth requirements, for different modulation formats at different bit rates, specific values of the external cavity can be determined and this is shown in Tables XXV, XXVI, XXVII and XXVIII. The minimum workable external cavity length for a practical design is taken to be 40 mm. The preferred FP-ECSL structure is also indicated in each table for each modulation format. This is based on the previous discussions of the advantages of the structure preferred. It can be seen that for bit rates higher than 1 Gbps the FP-EWPR is preferred as it is an integrated structure and can be made very compact. At lower bit rates (<1 Gbit/s), FP-BDG is required, especially for PSK systems.
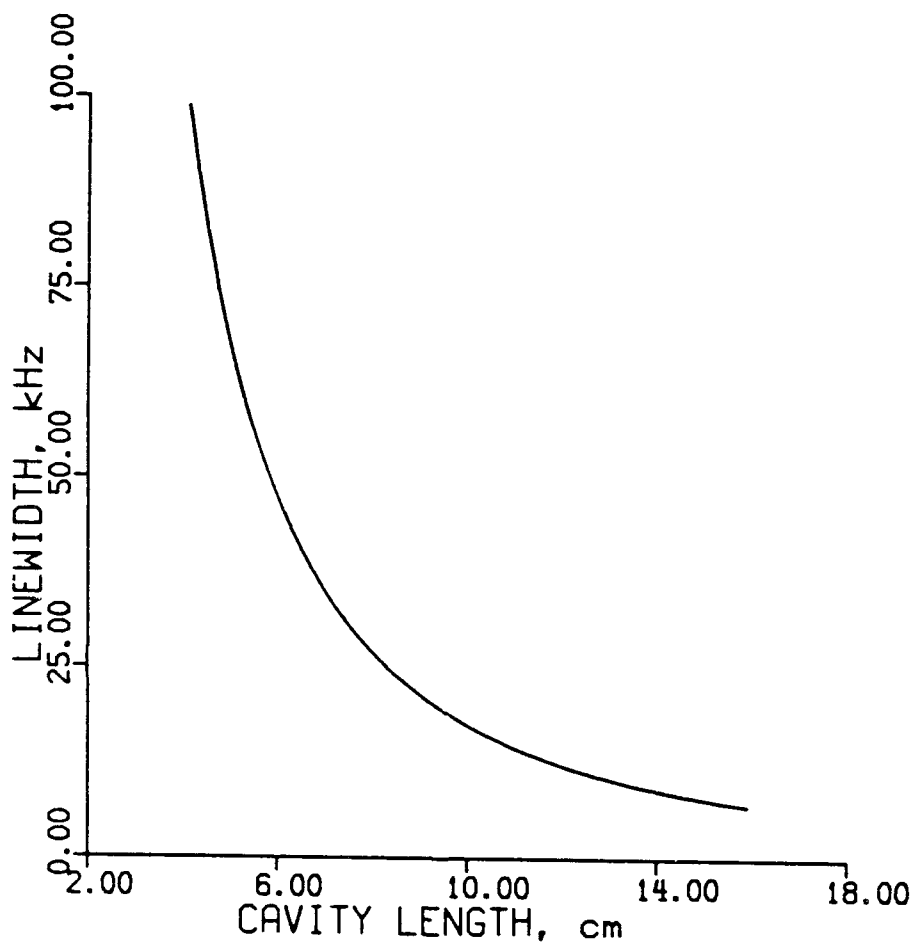
Fig. 24: Linewidth vs. cavity length of FP laser with bulk diffraction grating
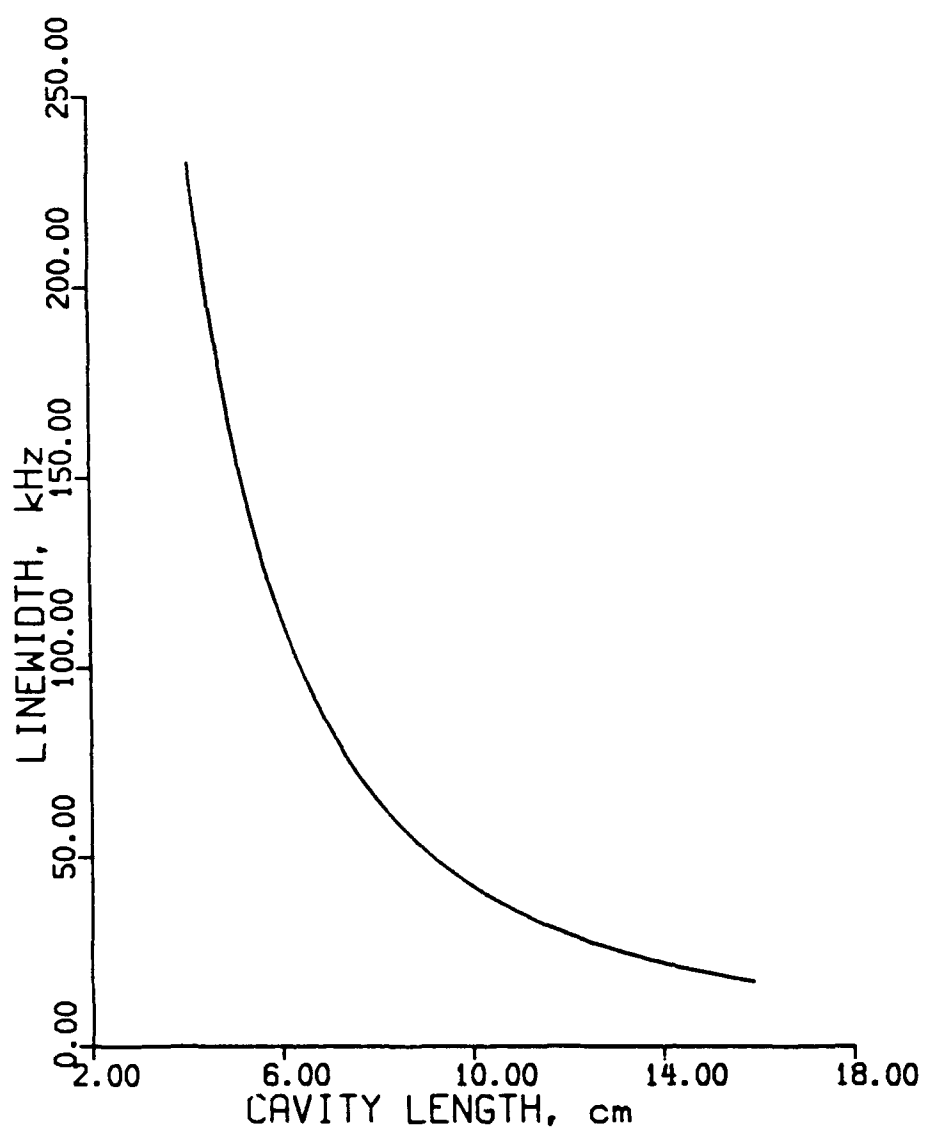
Fig. 25: Linewidth vs cavity length for FP laser with fiber diffraction grating

TABLE XXV

FP - ECSL FOR COFOCS

DESIGN TABLE FOR OPTIMUM EXTERNAL CAVITY LENGTHS

BIT-RATE = 140 MBITS/SEC

MODU-LATION	DEMODU-LATION	LINE-WIDTH	STRUCTURE	OPTIMUM LENGTH (mm)
ASK	Heterodyne with envelope	14 MHz to	FP + EWBR*	5
			FP + PG	20
FSK	Detection	70 MHz	FP + FDG	40 (+) (1-3)**
			FP + BDG	40 (+) (1-2)
DPSK	Heterodyne with delay time demodulation	420 kHz to 700 kHz	FP + PG*	20
			FP + FDG	40 (+) (23-31)
			FP + BDG	40 (+) (13-19)
PSK	Heterodyne	140 kHz to 700 kHz	FP + FDG	54-40 (+) (23)
			FP + BDG*	40 (+) (15-35)
PSK	Homodyne	70 kHz to 140 kHz	FP + FDG	78-52
			FP + BDG*	50-40 (33)

*preferred structure

FP-PG = Fabry Perot Laser + Prism Grating

+ - Minimum Practical Design

** - Figures in brackets are calculated theoretical values

FP - ECSL FOR COFOCS

TABLE XXVI

DESIGN TABLE FOR OPTIMUM EXTERNAL CAVITY LENGTHS

BIT-RATE = 565 MBITS/SEC

MODU-LATION	DEMODU-LATION	LINE-WIDTH	STRUCTURE	OPTIMUM LENGTH (mm)
ASK	Heterodyne	56 MHz	FP + EWBR*	5
	with envelope	to	FP + PG	20
FSK	Detection	282 MHz	FP + FDG	40 (+) (1-2)**
			FP + BDG	40 (+) (1-2)
DPSK	Heterodyne	1.7 MHz	FP + EWBR*	5
	with delay time	to	FP + PG	20 (+)
	demodulation	2.83 MHz	FP + FDG	40 (+) (11-14)
			FP + BDG	40 (+) (6-9)
PSK	Heterodyne	565 kHz	FP + PG*	20
		to	FP +FDG	40 (+) (11-25)
		2.83 MHz	FP + BDG	40 (+) (6-15)
PSK	Homodyne	282 kHz	FP + FDG	40 (+) (25-37)
		to		
		565 kHz	FP + BDG*	40 (+) (15-25)

*preferred structure

(+) -Minimum Practical Design

** - Figure in brackets are calculated theoretical values

FP - ECSL FOR COFOCS

TABLE XXVII

DESIGN TABLE FOR OPTIMUM EXTERNAL CAVITY LENGTHS

BIT-RATE = 1.2 MBITS/SEC

MODU-LATION	DEMODU-LATION	LINE-WIDTH	STRUCTURE	OPTIMUM LENGTH (mm)
ASK	Heterodyne with envelope	120 MHz to	FP + EWBR*	5
			FP + PG	20
FSK	Detection	600 MHz	FP + FDG	40 (+) (1)**
			FP + BDG	40 (+) (1)
DPSK	Heterodyne with delay time demodulation	3.6 MHz to 6.0 MHz	FP + EWBR*	5
			FP + PG	20
			FP + FDG	40 (+) (5-9)**
			FP + BDG	40 (+) (3-7)
PSK	Heterodyne	1.2 MHz to 6.0 MHz	FP + EWBR*	5
			FP + PG	20
			FP + FDG	40 (+) (5-17)
			FP + BDG	40 (+) (3-9)
PSK	Homodyne	600 kHz to 1.2 MHz	FP + PG	20
			FP + FDG	40 (+) (17-25)
			FP + BDG*	40 (+) (9-17)

*preferred structure

+ -Minimum Practical Design

** - Figures in brackets are calculated theoretical values

FP - ECSL FOR COFOCS

TABLE XXVIII

DESIGN TABLE FOR OPTIMUM EXTERNAL CAVITY LENGTHS

BIT-RATE = 2.4 GBITS/SEC

MODU-LATION	DEMODU-LATION	LINE-WIDTH	STRUCTURE	OPTIMUM LENGTH (mm)
ASK FSK	Heterodyne with envelope Detection	240 MHz to 1.2 GHz	ANY STRUCTURE (SOLITARY SINGLE MODE LASER* PREFERRED)	
DPSK	Heterodyne with delay time demodulation	7.2 MHz to 12.0 MHz	FP + EWBR* FP + PG FP + FDG FP + BDG	5 20 40 (+) (2-6)** (40 (+) (1-5)
PSK	Heterodyne	2.4 MHz to 12.0 MHz	FP + EWBR* FP +PG FP + FDG FP + BDG	5 20 40 (+) (4-11) 40 (+) (1-7)
PSK	Homodyne	1.2 MHz to 2.4 MHz	FP + EWBR* FP + PG FP + FDG FP + BDG	5 20 40 (+) (11-17) 40 (+) (7-11)

*preferred structure

+ - Minimum Practical Design
** - Figures in brackets are calculated theoretical values

Task 8B: Develop theoretical models to characterize the stability of linewidth and output frequency of the FP-ECSL coherent transmitter modules as a function of environmental parameters such as temperature and pressure.

As justified in Task 8A, this task was not persued. Environmental parameters such as temperature and pressure are unimportant in a package which is (i) hermetically sealed and (ii) the temperature of the heat sink of the laser can be controlled to 0.01°C with two levels of Peltier Thermoelectric Coolers.

Task 9: Develop detailed comparisons between the results of Tasks 2-8 for DFB and FP laser based ECSL.

We shall do this in tabular form. First, the performance of the various FP-ECSL discussed above are summarized in Table XXIX, and the parameters considered are quoted in the extreme left column and are: output power, linewidth x power product, external cavity length, AR coating requirments, coarse tuning, fine tuning, package consideration and comments. Next, in Table XXX, we do the same comparison for three DFB-ECSL considered in Task 2A. The parameters are the same. Finally, the comparison between FP-ECSL and DFB-ECSL is made with the comments in Table XXXI. These are quite unambiguous and hence no repetition will be made here.

SUMMARY OF FP LASER BASED
EXTERNAL CAVITY STRUCTURES

TABLE XXIX

	Bulk Diffraction Grating	Fiber Diffraction Grating	Prism Diffraction Grating	External Waveguide Bragg Reflector
Output Power [mW]	4	4	2	3
$\Delta v \cdot mW$ [KHz·mW]	7 - 18	20	1000	3000
Lex [cm]	5 - 18	10	2	0.5
AR Coating	yes	no	yes	no
Coarse tuning	with rotat- ing grating (130 nm)	--	---	---
Fine Tuning	with silica plate	with refract. index change	with displacement (6 GHz/μm)	with Tempera- ture
Pack- age	Bulky	Semi- Compact	Compact	Compact
Com- ments	See Task 5	See Task 5	at Siemens	Can utilize ROR

88

TABLE XXX

<u>SUMMARY OF DFB LASER BASED EXTERNAL CAVITY STRUCTURES</u>

	GRIN ROD CAVITY	MIRROR CAVITY	FIBER CAVITY
Output Power [mW]	2.5	2.2	1
$\Delta\upsilon\cdot$mW [kHz·mW}	3750	88	70
Lex [cm]	0.4	10-18	5.5
AR Coating	yes	yes	yes
Tuning (Coarse)	not possible	not possible	not possible
Fine Tuning	Electrical (1.2nm cont.) Temp (1.8nm)	Electrical (1.2nm cont.) Temp (1.8nm)	Electrical (1.2nm cont.) (Temp. 1.8nm)
Package	Compact	Impractical	Semicompact
Comments	See Task 2	See Task 2	See Task 2

TABLE XXXI

COMMENTS ON COMPARISON BETWEEN DFB & FP LASERS WITH EXTERNAL CAVITIES

1. Output Power: Approximately the same, the FP shows a slightly greater power output.

2. Absolute Linewidth: The absolute linewidth is an order of magnitude smaller for the best FP structure (FP-BDG) over the best DFB based structure (DFB-FC)

3. Linewidth Power Product: The FP-BDG structure is 7 times better than the DFB-FC structure, which represents best structure in each laser type.

4. S.M.S.R.: In general DFB structure are better; however the best (lowest linewidth power output) of both structures are equal.

5. Coarse Tuning: FP based structures are much superior, since DFB based structures can not be tuned over a large wavelength range.

6. Fine Tuning: DFBs are superior since they can be tuned electrically.

7. Packaging: DFB structures are generally more compact and easier to work with since there are less components to align.

Task 10: Identify detailed designs of distributed feedback or Fabry-Perot laser based external cavity coherent transmitter modules most appropriate for use with the various coherent modulation schemes. Provide rationale for design selection.

This task has been accomplished in five tables, XXXII, XXXIII, XXXIV, XXXV, and XXXVI. The first four are for the transmitter laser and the fifth one is for the local oscillator laser, in which tunability is of utmost importance and the preferred structure is identified by considering a channel separation of 100 MHz and four different values of the number of channels. For the transmitter laser, tunability is not important and the most appropriate ECSL and the selection rationale is provided in the extreme right column in each table for different bit rates. It can be seen that for higher bit rates (>565 Mbit/s) DFB solitary lasers and DFB-ECSL are most appropriate for the reasons cited. The FP-ECSL with bulk diffraction grating (BDG) is most useful at low bit rates, but more importantly as the local oscillator with 1,000 and 10,000 channels as shown in Table XXXVI.

TABLE XXXII
TRANSMITTER

APPROPRIATE ECSL AND RATIONALE FOR SELECTION

(Bit Rate : 140 Mbit/s)

Modu-lation	Demodu-lation	$\Delta\upsilon/B$ (%)	$\Delta\upsilon$	Most appropriate ECSL & Selection rationale
ASK	heterodyne with	10 to	14 MHz to	Solitary DFB Integrated struc-
FSK	envelope detection	50	70 MHz	ture with all advantages outlined in Task 2
DPSK (MSK)	Heterodyne with	0.3 to	420 kHz to	DFB + FC
	Delay Time Demodu-lation	0.5	700 kHz	Most compact and mechanically stable
PSK	Heterodyne	0.1 to	140 kHz to	FP+BDG
		0.5	700 kHz	Highest power out-put, narrow line-width manufacturable
PSK	Homodyne	0.05 to	70 kHz to	FP + BDG
		0.1	140 kHz	Highest power out-put, narrow line-width, manufacturable

TABLE XXXIII

TRANSMITTER

APPROPRIATE ECSL AND RATIONALE FOR SELECTION

(Bit Rate : 565 Mbit/s)

Modu-lation	Demodu-lation	$\Delta\upsilon/B$ (%)	$\Delta\upsilon$	Most appropriate ECSL & Selection rationale
ASK	heterodyne with	10 to	56 MHz to	Solitary DFB
FSK	envelope detection	50	282 MHz	Least complicated
DPSK (MSK)	Heterodyne with	0.3 to	1.7 MHz to	GRIN-rod
	Delay Time Demodu-lation	0.5	2.83 MHz	Most compact, easily made
PSK	Heterodyne	0.1 to	565 kHz to	DFB + FC
		0.5	2.83 MHz	Compact, mechancially most stable
PSK	Homodyne	0.05 to	282 kHz to	DFB + FC
		0.1	565 kHz	Compact, mechanically most stable

93

TABLE XXXIV

TRANSMITTER

APPROPRIATE ECSL AND RATIONALE FOR SELECTION

(Bit Rate : 1.2 Gbit/s)

Modu-lation	Demodu-lation	$\Delta\upsilon/B$ (%)	$\Delta\upsilon$	Most appropriate ECSL & Selection rationale
ASK	heterodyne with	1.0 to	120 MHz to	Solitary DFB
FSK	envelope detection	50	600 MHz	Least complicated
DPSK (MSK)	Heterodyne with	0.3 to	3.6 MHz to	GRIN-rod
	Delay Time Demodu-lation	0.5	6.0 MHz	Most compact stable easily manufacured
PSK	Heterodyne	0.1 to	1.2 MHz to	DFB + FC
		0.5	6.0 MHz	Most compact, mechanically stable
PSK	Homodyne	0.05 to 0.1	600 kHz to 1.2 MHz	DFB + FC Most compact, mechanically stable

TABLE XXXV

TRANSMITTER

APPROPRIATE ECSL AND RATIONALE FOR SELECTION

(Bit Rate : 2.4 Gbit/s)

Modu-lation	Demodu-lation	$\Delta\upsilon/B$ (%)	$\Delta\upsilon$	Most appropriate ECSL & Selection rationale
ASK	heterodyne with	10 to	240 MHz to	Solitary DFB
FSK	envelope detection	50	1.2 GHz	Least complicated
DPSK (MSK)	Heterodyne with	0.3 to	7.2 MHz to	DFB + GRIN rod
	Delay Time Demodu-lation	0.5	12 MHz	Most compact, mechanically stable, and easily manufactured
PSK	Heterodyne	0.1 to	2.4 MHz to	DFB + GRIN-rod
		0.5	12 MHz	Most compact, mechanically stable, easily manufactured
PSK	Homodyne	0.05 to 0.1	1.2 MHz to 2.4 MHz	DFB + GRIN-rod Most compact, mechancially stable, easily manufactured

TABLE XXXVI

PREFERRED LASER STRUCTURE

LOCAL OSCILLATOR LASER

(100 MHz CHANNEL SEPARATION)

# of Channels	Required Tuning Range[nm]	Preferred Structure
10	0.08	DFB + FC
100	0.8	DFB + FC
1000	8	FP + BDG
10000	80	FP + BDG

TASK 11:

Evaluate the impact of the use of high power Fabry-Perot lasers on coherent transmitter linewidth and integration results into Tasks 8, 9 and 10.

The impact will be minimum as the linewidth is proportional to inverse of power for low output powers only. At higher powers, the linewidth becomes saturated. Hence the conclusions in Tasks 8,9 and 10 are unaltered. As an example, see fig. 26 and some discussion on the three parts of this figure are as follows:

(i)   DFB-DCPBH (Double Channel Planar Buried Heterstructure) solitary laser was used in these experiments.

(ii)   High CW output power of 70 mW was obtained from each facet (Fig. 26a) at 25 $^{\circ}$C and the external differential quantum efficiency was 43%

(iii)   Linewidth reduction due to the high power is less than 0.1 (Fig. 26b) 15 MHz at low power compared to 3 MHz at high power.

(iv)   1/f noise floor is high due to low cavity Q factor (fig. 26c). These results are from conference OFC'87; p. 148, paper WC1.

TASK 12:

Identify and perform key parameter experimental evaluations towards substantiating the basis for the rationale for the detailed designs identified in Task 10.

In order to perform the experimental evaluation of the coherent transmitter module, the equipment & components bought are summarized in Table XXXVII. The measurements done are reported in Task 14.

SOLITARY HIGH POWER LASER
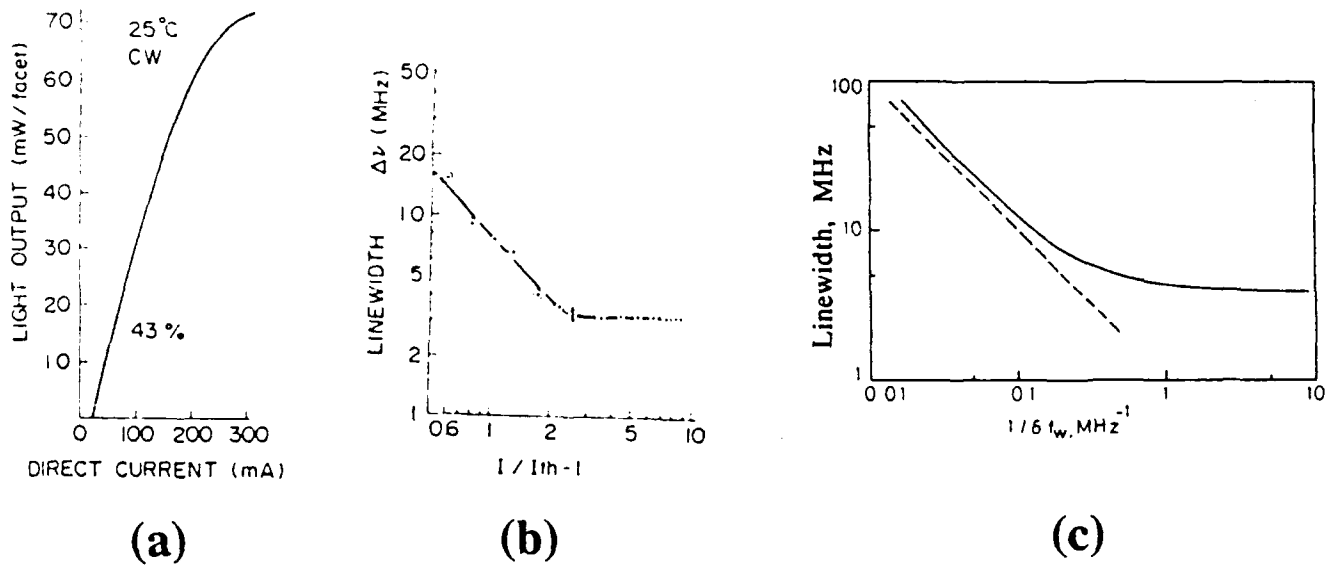
Fig. 26: Characteristics of a solitary high power laser

(a) output power per facet vs. drive current

(b) linewidth as a function of normalized drive current

(c) linewidth as a function of inverse frequency

TABLE XXXVII

Equipment Purchased (quantity in parenthesis)

1. Optical Isolators (2)

2. 1.55 μm Semiconductor Laser (2)

3. TO-8 Package for Lasers in Item #2 (2)

4. Precision Current Source

5. Temperature Controller

6. Precision Translation Stage

7. Low Voltage Amplifier

8. Piezoelectric Pusher

9. Acousto-Optic Modulator

10. RF Driver for Item 9

11. Digital Power Meter

12. Surface Absorbing Calorimeter

13. Isoperibel enclosure for Item 12

14. Precision Diffraction Grating

15. Lenses for use with laser diodes (Anti-reflection coated) (2 off)

16. Fine Focusing Microscope Body

17. Microscope Objective, x7

18. Microscope Objective, x10

19. Eye piece, x10

20. Eye piece, x15

21. Infra-red Sensor Card

22. Fused Silica Etalon

23. Optical Rail (1)
    Adapter Plate (3)
    Sliding Base (6)
    Support Post (5)
    Translating Post Holder (2)
    Tree-axis Translator (2)
    Screw Kit (1)
    Screw Kit (1)
    Universal Optic Holder (2)
    Prism Table (1)
    Translation Stage (1)
    Objective Lens (2)
    High Resolution Mirror Mount (1)
    Tilt/Rotation Stage (1)
    Objective Holder (2)

24. RF Pre-Amplifier

Tasks 13:

Based on the above tasks, recommend, fabricate and test one model of an external cavity based coherent transmitter module.

The external cavity based coherent transmitter module to be built is a Fabry-Perot laser with a bulk diffraction grating. The size of the grating can be miniaturized in a practical package design. We selected the Fabry-Perot laser with bulk diffraction grating (FP-BDG) design for the following reasons:

(i)   Narrowest linewidths (< 100 kHz).

(ii)   Widest tuning range (~ 130 nm).

(iii)   Output powers of up to 5 mW available.

(iv)   Can be used with any modulation scheme at any practical bit rate in the 0.14 to 2.4 GBit/s.

(v)   Can be packaged into usable field modules;

(vi)   Can be finely and coarsely tuned continuously relatively easily.

(vii)   All components are readily readily available commercially at very reasonable prices; especially the bulk diffraction grating.

(viii) Has excellent frequency stability with feedback control.

(ix)   Any variety of Fabry-Perot lasers, with normal lengths of 250 μm can be used and AR coating can be easily applied on one facet. Very low reflectivities (< 0.1%) have been obtained and this increases the continuous tuning range.

(x)   Fabry-Perot lasers at 1.55 μm (lowest loss of silica single-mode fibers) are readily available commercially.

(xi)   It is the only design which can be used as the local oscillator laser to tune and select more than 1000 optical channels separated by 100 MHz from one another.

100

‡

(xii)   Performance of this design has been satisfactorily demonstrated in many systems

          studies in the laboratory.

The design features of the FP-BDG laser to be built are as follows:

(i)   F-P laser at 1.55 μm, AR coated on one facet

(ii)   Diffraction grating, gold coated, 1200 lines/mm.

(iii)   High numerical aperture collimating graded-index rod lens.

(iv)   Tapered single-mode optical fiber (SMF)

(v)   The optical schematic is illustrated in fig. 27. For photographic views, see figs

          56, 57, 58. The features of our novel design and the rationale for its selection are as

          follows:

(i)   Fine tuning of the laser is done by changing the length of the SMF by piezoelectric

          means. With much smaller movements, a much better resolution can be obtained

          compared to changing the length of the cavity with an air-path.

(ii)   The air-path of the light is limited to a minimum and will be < 5 mm.

(iii)   Since the optical path of the light is increased in the SMF, the overall cavity length can

          be small, ~3 cm.

(iv)   The facet F_1 of the SMF is tapered for two reasons: (i) to couple the maximum

          amount of light from the laser facet R_2; (ii) to minimize the amount of light reflected

          back into the laser from the input end of the fiber.

FP-ECSL FOR COFOCS

OUR NOVEL DESIGN
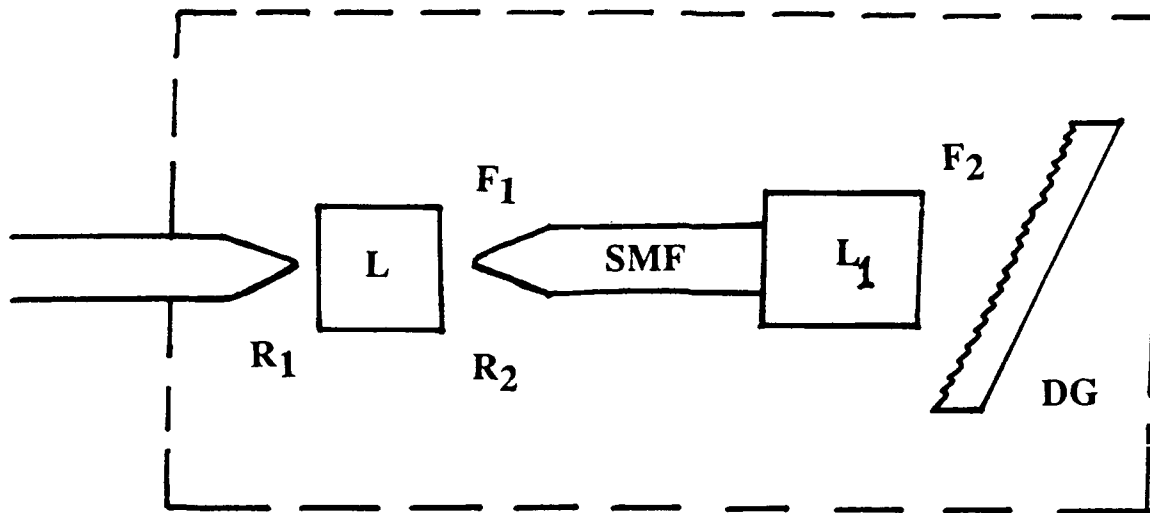
L - Fabry-Perot Semiconductor Laser, $1.56\mu m$.

SMF - Single-mode fiber.

L_1 - Graded-index (GRIN) rod lens; 1/4 Pitch.

DG - Bulk diffraction grating

F_1 - Tapered end facet of SMF

F_2 - AR coated facet of GRIN-rod lens.

Fig. 27:   Schematic of our novel design of a FP-ECSL

Task 14:

Compare test results for the module developed under Task 13 to the projected results of earlier tasks.

First a discussion will be made of the components to be used in our FP-ECSL laser design.

(i)   Two lasers were purchased from the General Optronics Corp. Both facets are accessible as is necessary. The mounting is shown in fig. 28.

(ii)   The light output from the two facets was measured by the manufacturers and is attached. Fig. 29 shows the characteristic for laser W-2808 and Fig. 30 shows the characteristic for the laser W-2809. Facet A, the front facet is AR coated and Facet B is the uncoated facet, and its reflectivity is 32%. Hence it is reasonable to expect more power out from facet A. It can be seen that W-2908 has a better AR coating on facet A as the output power from facet B is smaller. Estimation of the reflectivities of facet A, from the maufacturer, are as follows ~1% for the W-2808 and ~4% for the W-2809.

(iii)   It can be seen that with feedback, 2-3 mW can easily be obtained from FP lasers, as assumed in Task 10.

(iv)   It can also be seen that the wavelength of the lasers are ~1.56 and 1.57 μm. which is the region of interest for the lowest loss in silica fibers.

(v)   From our contacts at the Siemens Research Labs., we also obtained two AR coated lasers at 1.3 μm.

(vi)   The first laser's (LB-195-106-9) characteristics before AR coating is shown in fig. 31. The threshold current is 76 mA and the differential quantum efficiency is 0.288 mW/mA. The output power from the uncoated facet, after AR coating of the other facet is shown in fig. 32. Effectively it doesn't lase any more as a threshold is not reached. Hence the AR coated reflectivity is very good, <1%.
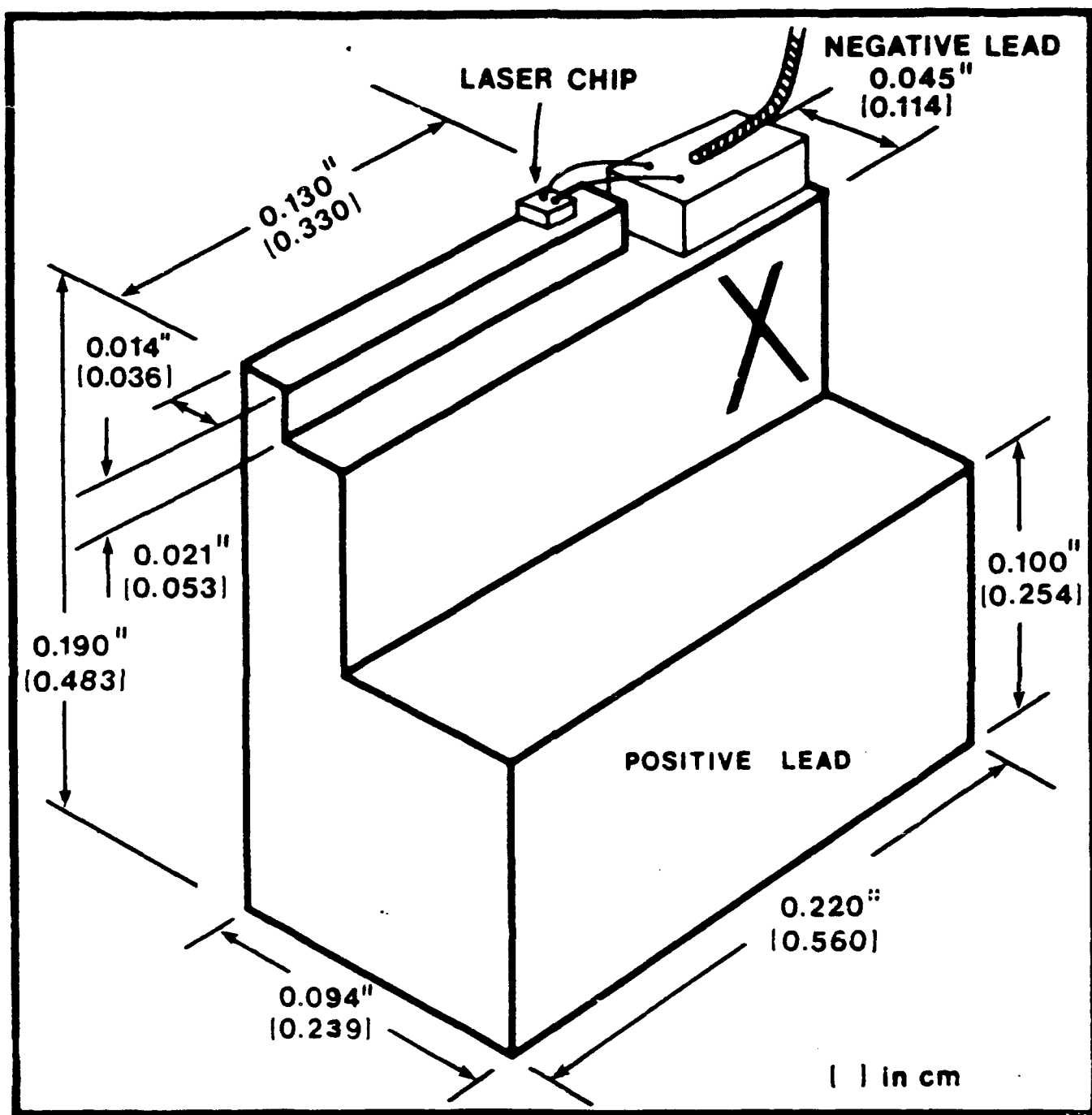
Fig. 28: Mounting arrangement of FP laser on a suitable heat sink
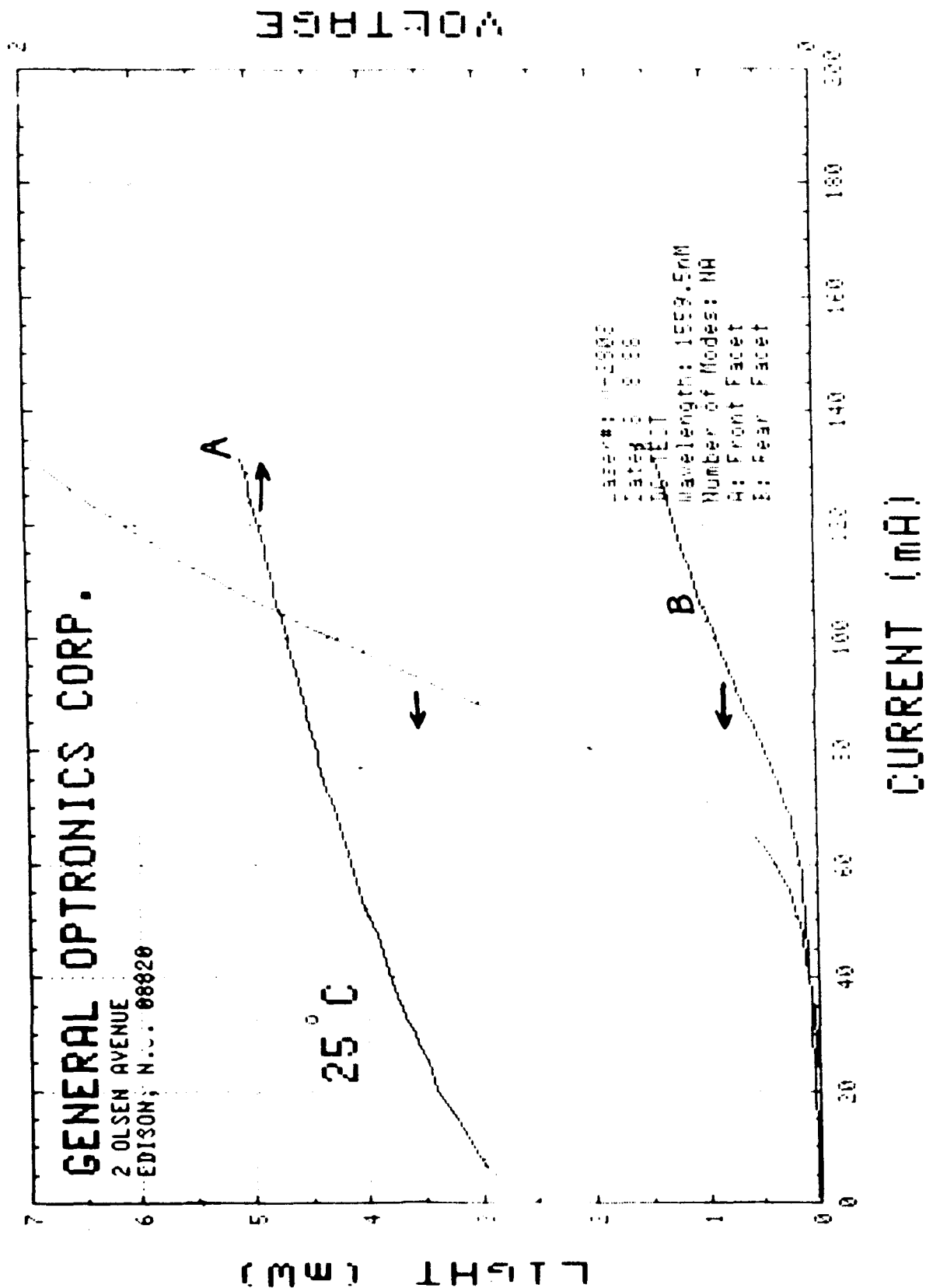
Fig. 29: Light output and device voltage vs. drive current for laser W-2808; A-front AR coated facet; B-rear facet.
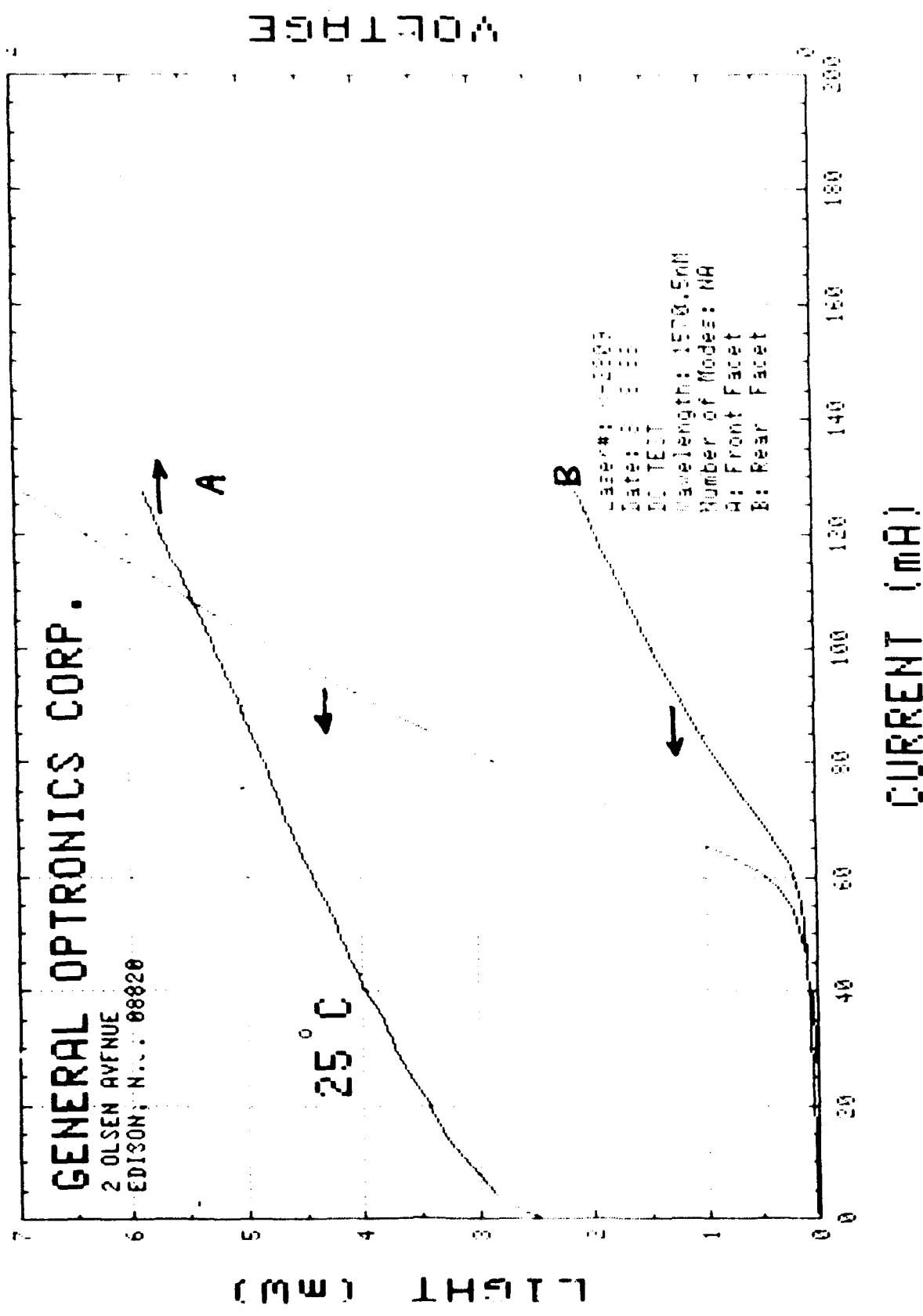
Fig. 30: Light output and device voltage vs. drive current for laser W-2809; A-front AR coated facet; B-rear facet.
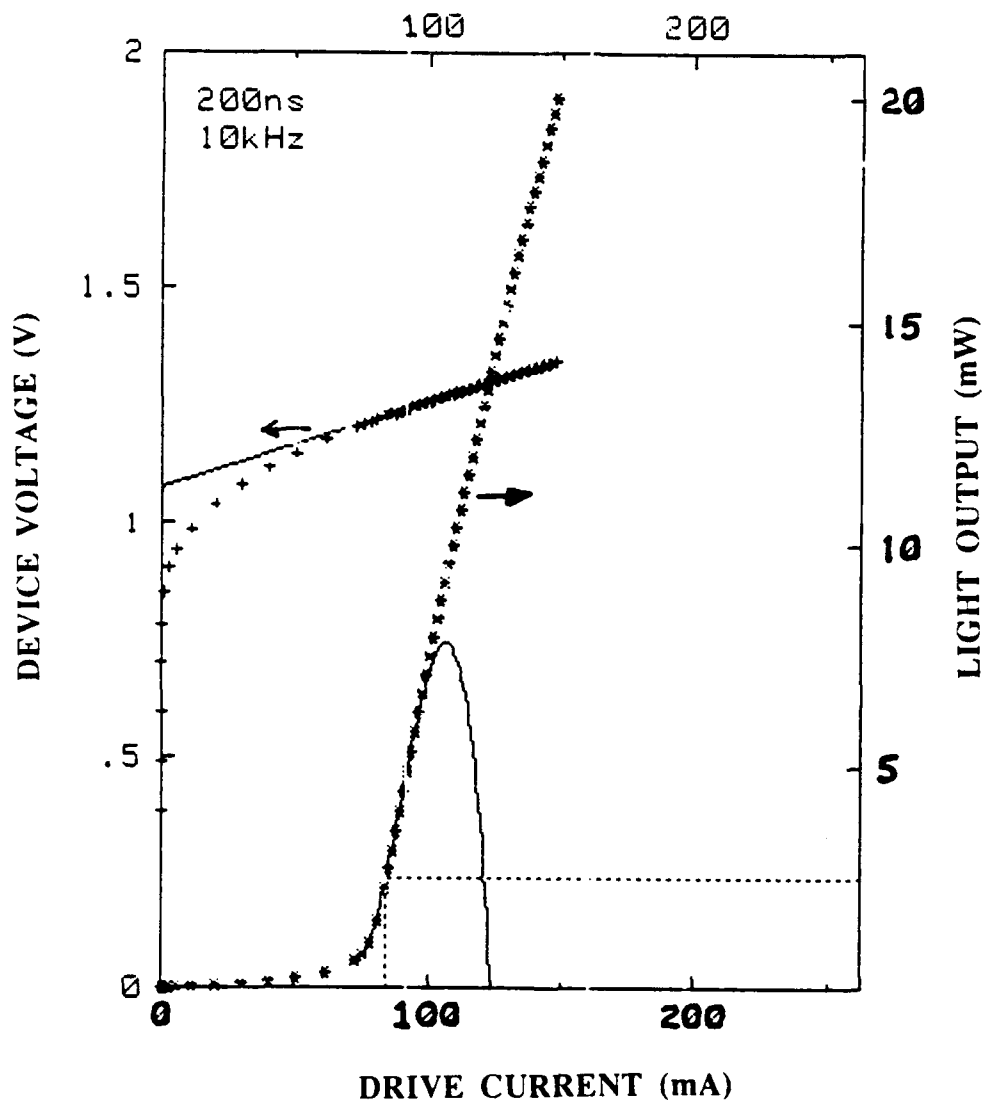
Fig. 31: Device voltage and light output vs. drive current for Siemens laser LB-195-106-9, before AR coating.
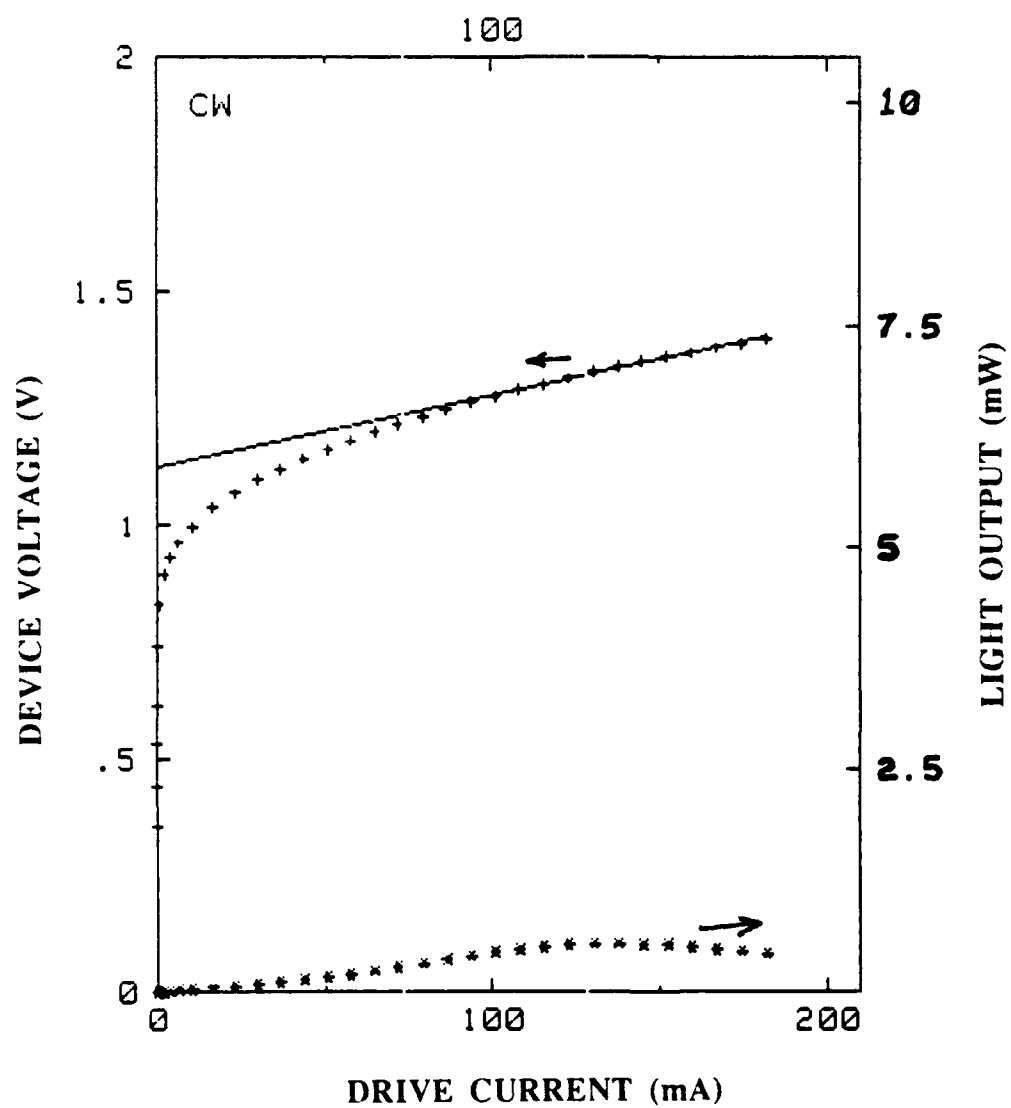
Fig. 32: Device voltage and light output vs. drive current for Siemens laser LB-195-106-9, after AR coating.

(vii)   Similar characteristics for the other Siemen's laser (LB-195-106-10) is shown in figs. 33 and 34 before and after coating.

(viii)   The optical spectrum of our lasers purchased from General Optronics is shown in figs. 35 and 36. Many longitudinal Fabry-Perot modes can be seen, due to gain saturation as the bias current is substantially above threshold. The peak wavelengths are 1.56 and 1.57 μm. The longitudinal mode spacing, as determined from these graphs is 1.21 nm, as each large division is 2 nm. From this measurement, the length of the lasers is estimated to be 285 μm. We varied the temperature and drive current, in our laboratory, to investigate further the mode behavior and the measurements are reported later in this task.

(ix)   In order to control the temperature of the laser accurately, and hence its mode behavior before and after feedback, the laser was mounted in a TO-8 package with a Peltier cooler, by the same company, General Optronics. This is shown in figs. 37 and 38 and its circuit diagram is shown in fig. 39. The laser was mounted vertically and not horizontally as shown in fig. 37. This was to ensure that both facets were accessible. Pins 4 and 5 (fig. 38) were not used as a photodiode was not required in the package. Pin 2 (fig. 38) is a thermistor which senses the temperature and an external temperature controller was used to control the temperature.

(x)   The temperature vs. resistance curve of the thermistor mounted in the TO-8 package is shown in fig. 40 and the cooler current required to maintain a certain temperature is shown in fig. 41. We operated at a temperature of about 23°C.

(xi)   After mounting on the TO-8 package, the output power versus laser current were again verified from the AR coated (front facet A) and are shown in figs. 42 and 43 for the lasers W-2808 and W2809 respectively. These are nearly identical to the curves obtained previously before the lasers were mounted on the TO-8 package.
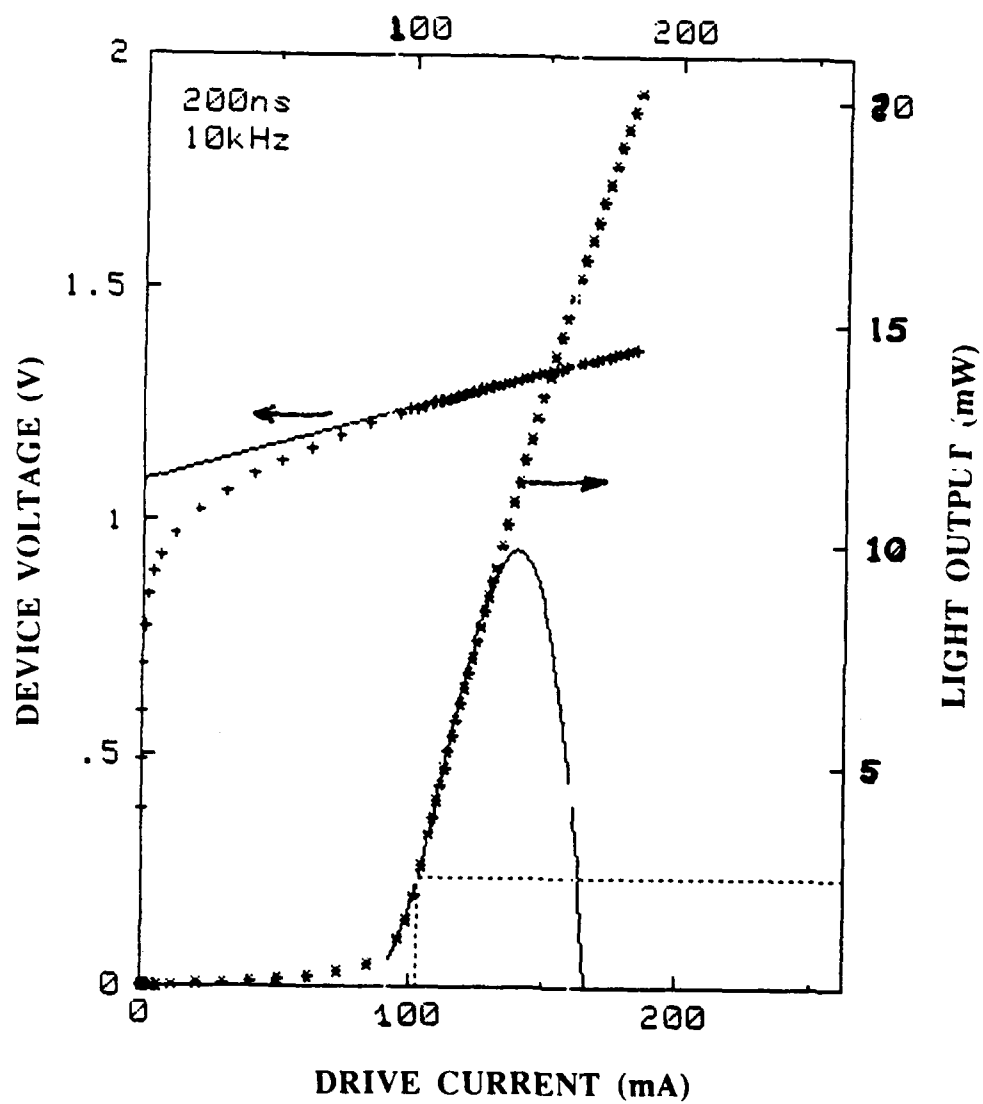
Fig. 33: Device voltage and light output vs. drive current for Siemens laser LB-195-106-10, before AR coating.
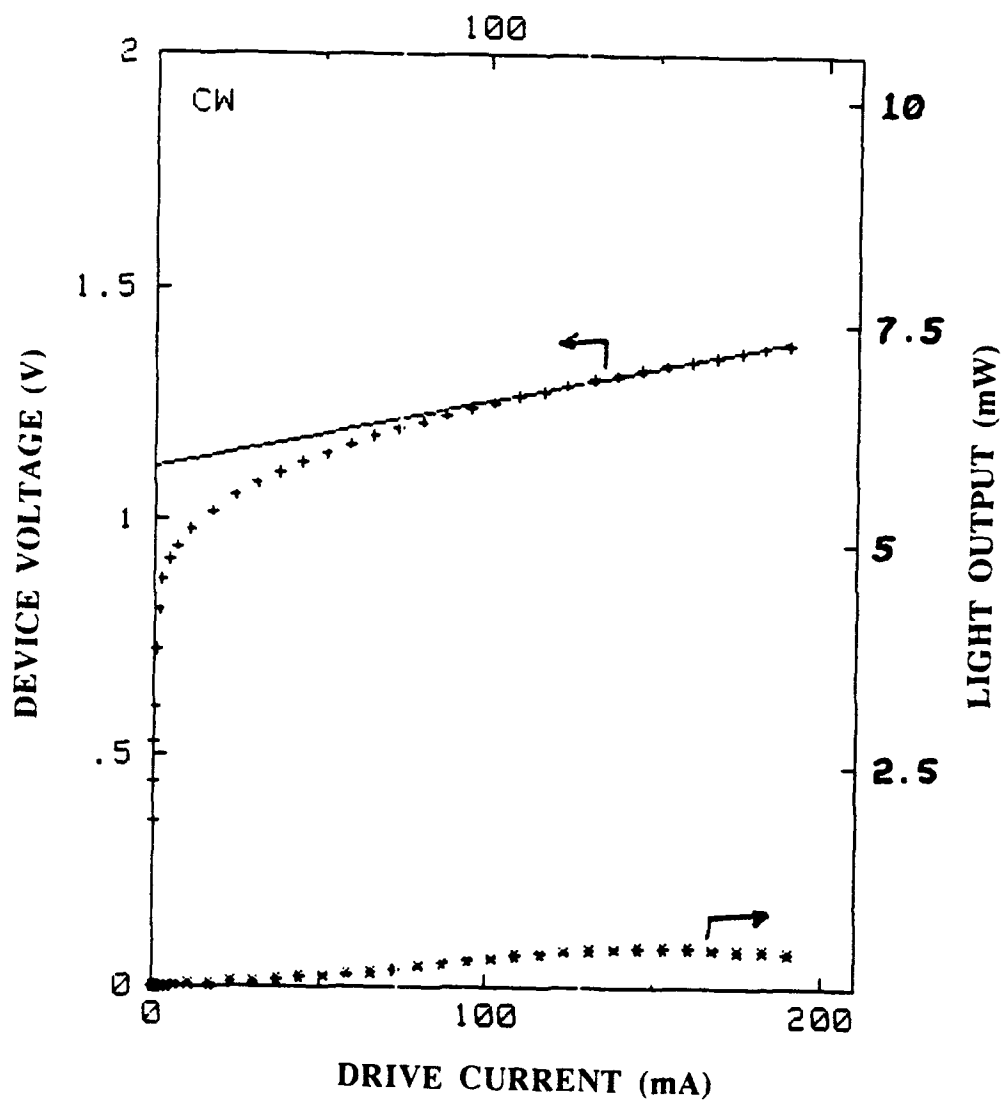
Fig. 34: Device voltage and light output vs. drive current for Siemens laser LB-195-106-10, after AR coating.
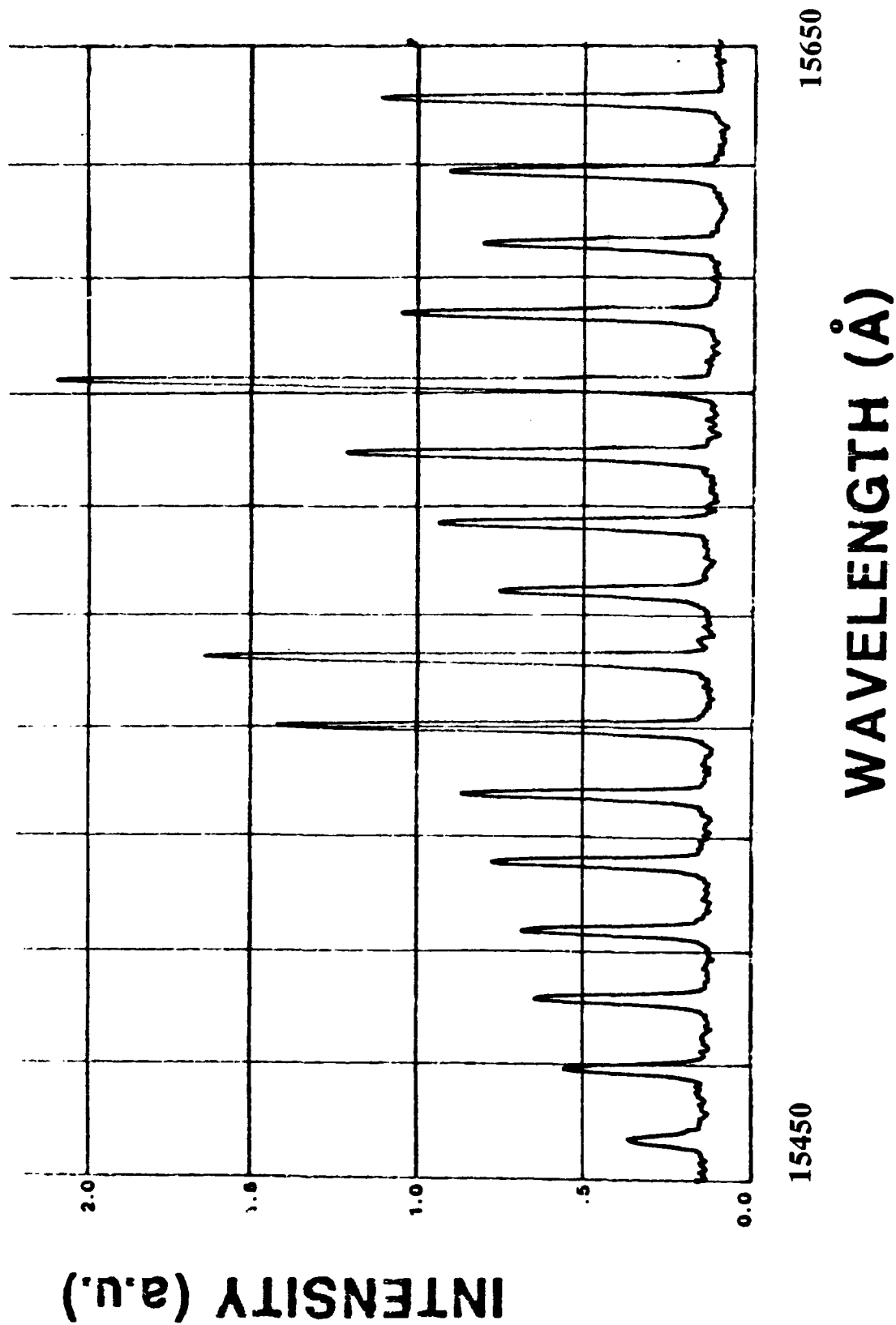
Fig. 35: Longitudinal mode spectrum of laser W-2808 at I-80 mA; $\lambda = 1559.5$ nm for peak wavelength; threshold current = 55mA.

112
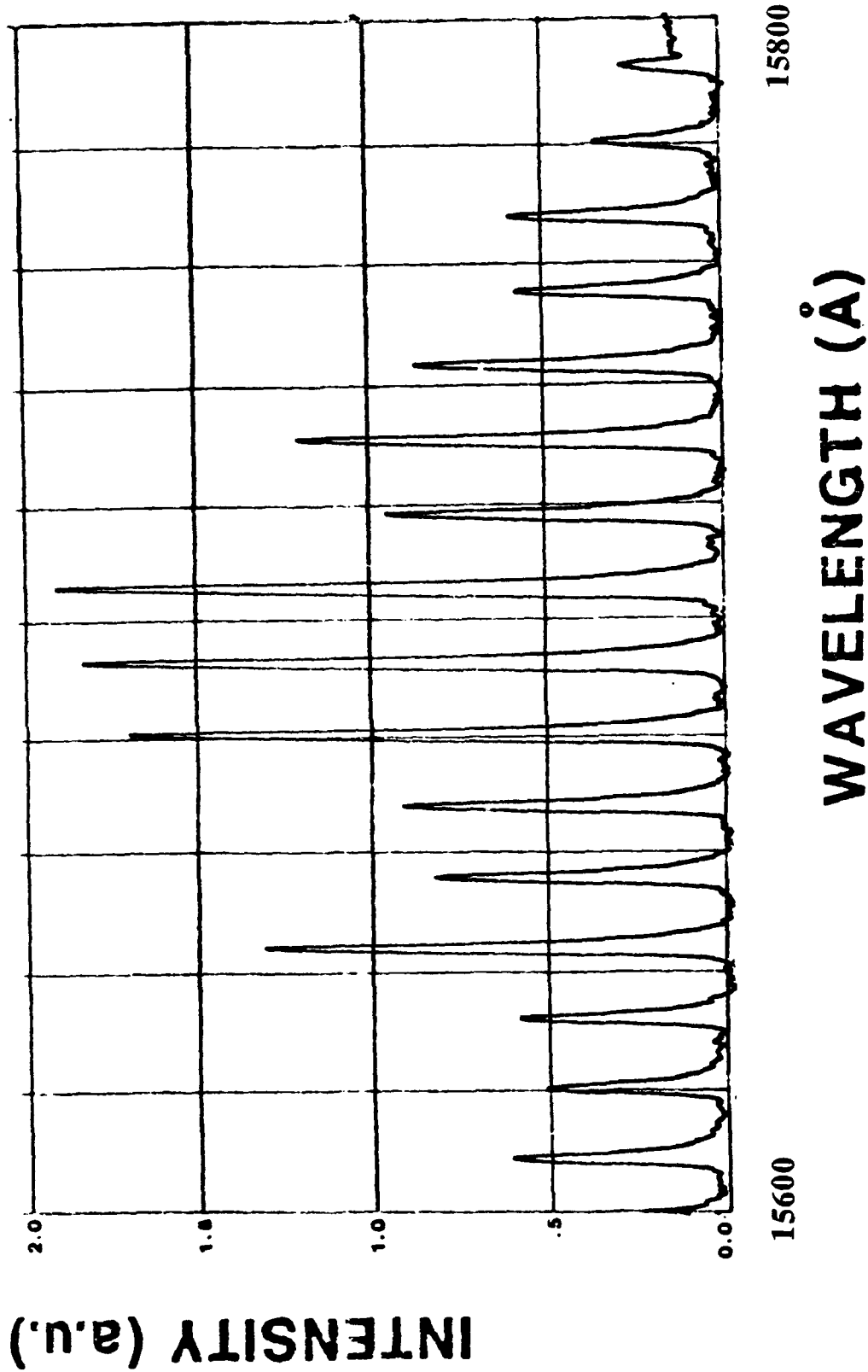
Fig. 36: Longitudinal mode spectrum of laser W-2809 at I-70 mA; λ = 1570.5 nm for peak wavelength; threshold current = 50 mA.
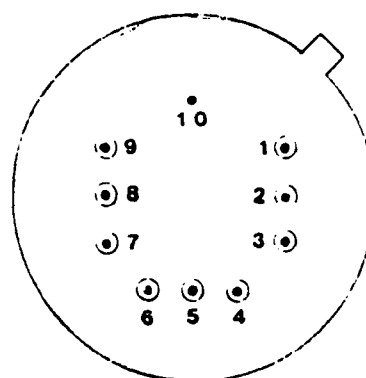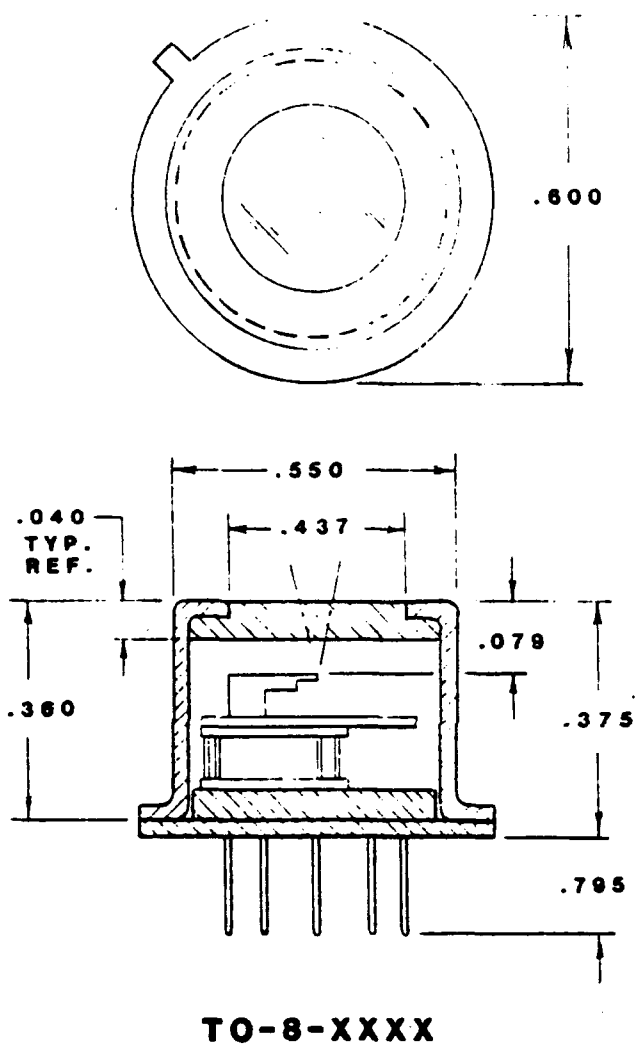
PIN CONFIGURATION		
1	COOLER (+)
2	THERMISTOR
3	DC BIAS INPUT
*4	PHOTODETECTOR CATHODE
*5	PHOTODETECTOR ANODE
6	LASER ANODE
7	LASER CATHODE
8	COOLER (-)
9	RF INPUT
10	GROUND

TO-8-XXXX

* PINS REVERSED ON
1.3 & 1.5 LASERS

OPTIONS:

1. NO COOLER

2. REMOVABLE WINDOW CAP

3. SPECIAL WINDOW CAP

Fig. 37:   Schematic showing mounting of laser on TO-8 package and pin configuration

114

RF INPUT
(PIN #9)

GROUND

COOLER ⊕ (PIN #1)

THERMISTOR

.40 TYP.

.10 TYP.

COOLER ⊖

LASER CATHODE

LASER ANODE

DC BIAS INPUT

.20
TYP.

PHOTODETECTOR **
ANODE

PHOTODETECTOR **
CATHODE
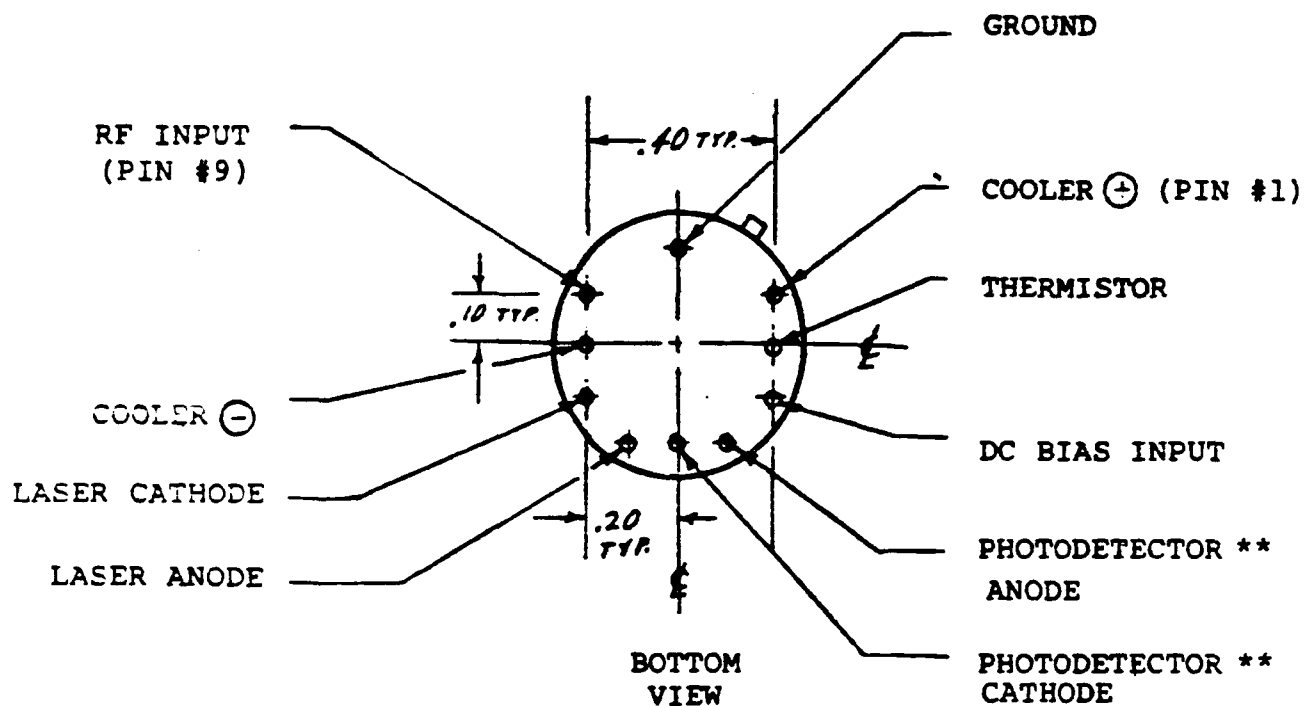
BOTTOM
VIEW

LASER HEAD PIN CONFIGURATION

MODEL TO-8

Fig. 38: Bottom view of pin configuration of TO-8 package

115
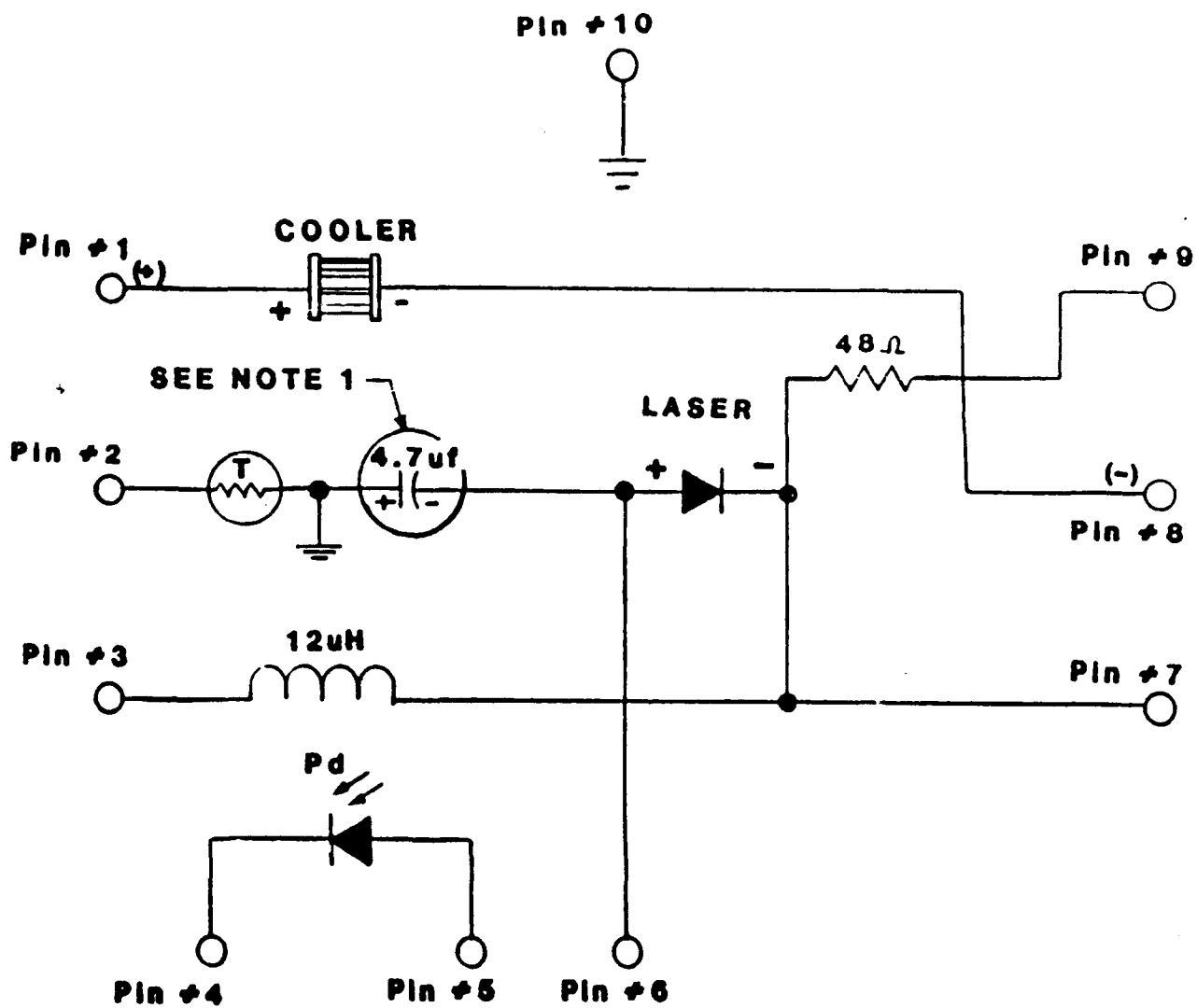
Fig. 39: Circuit diagram showing connection of pins in the TO-8 package

116

GENERAL OPTRONICS CORP.

THERMISTOR: FENWAL FA-41U1
SOLID LINE: NOMINAL R vs T
BROKEN LINES: UPPER AND LOWER LIMITS
MAXIMUM DELTA T=+/-3.7 @ 70 DEGREES C
MINIMUM DELTA T=+/-2.3 @ 25 DEGREES C
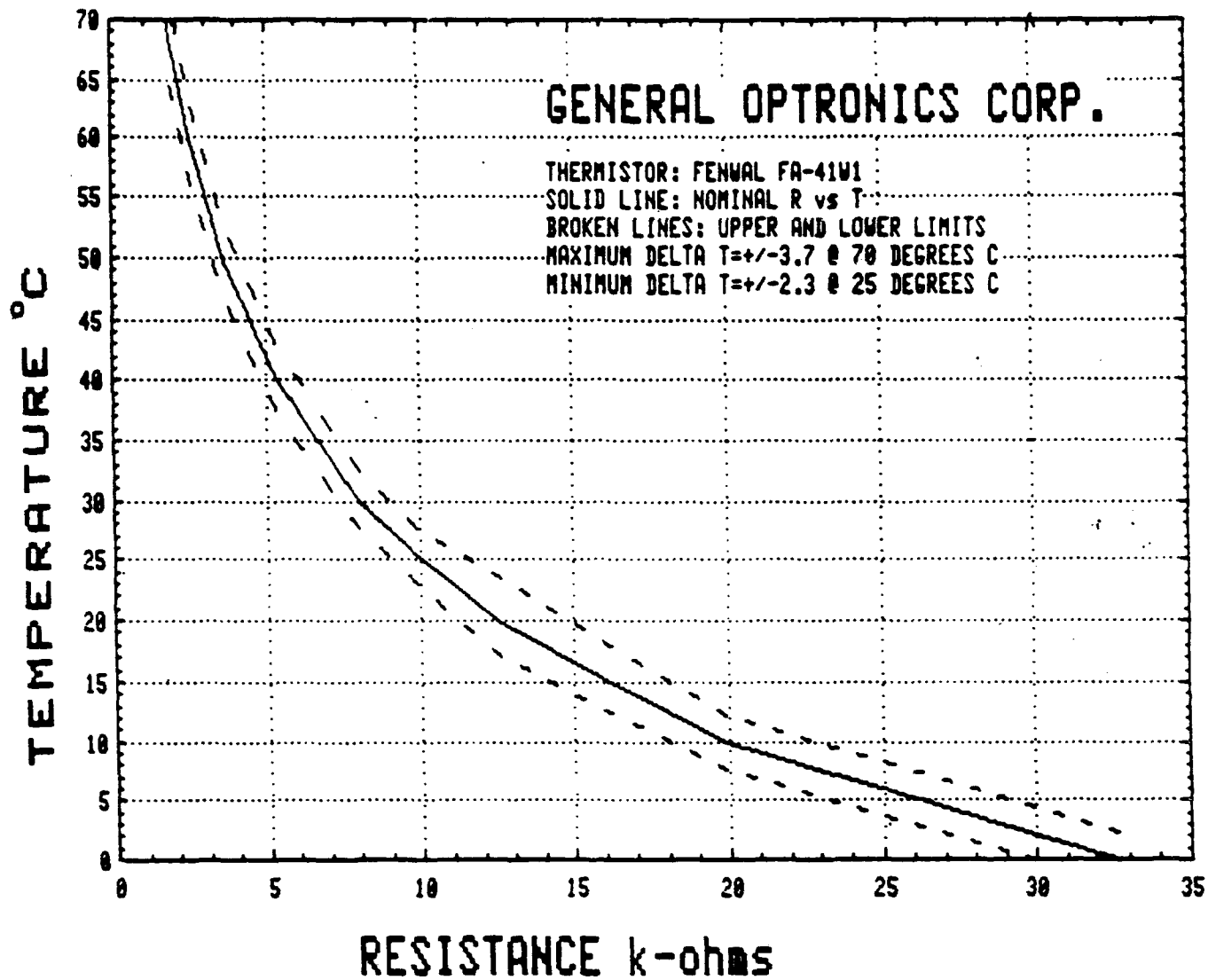
Fig. 40: Temperature vs. resistance of thermistor used in the TO-8 laser package
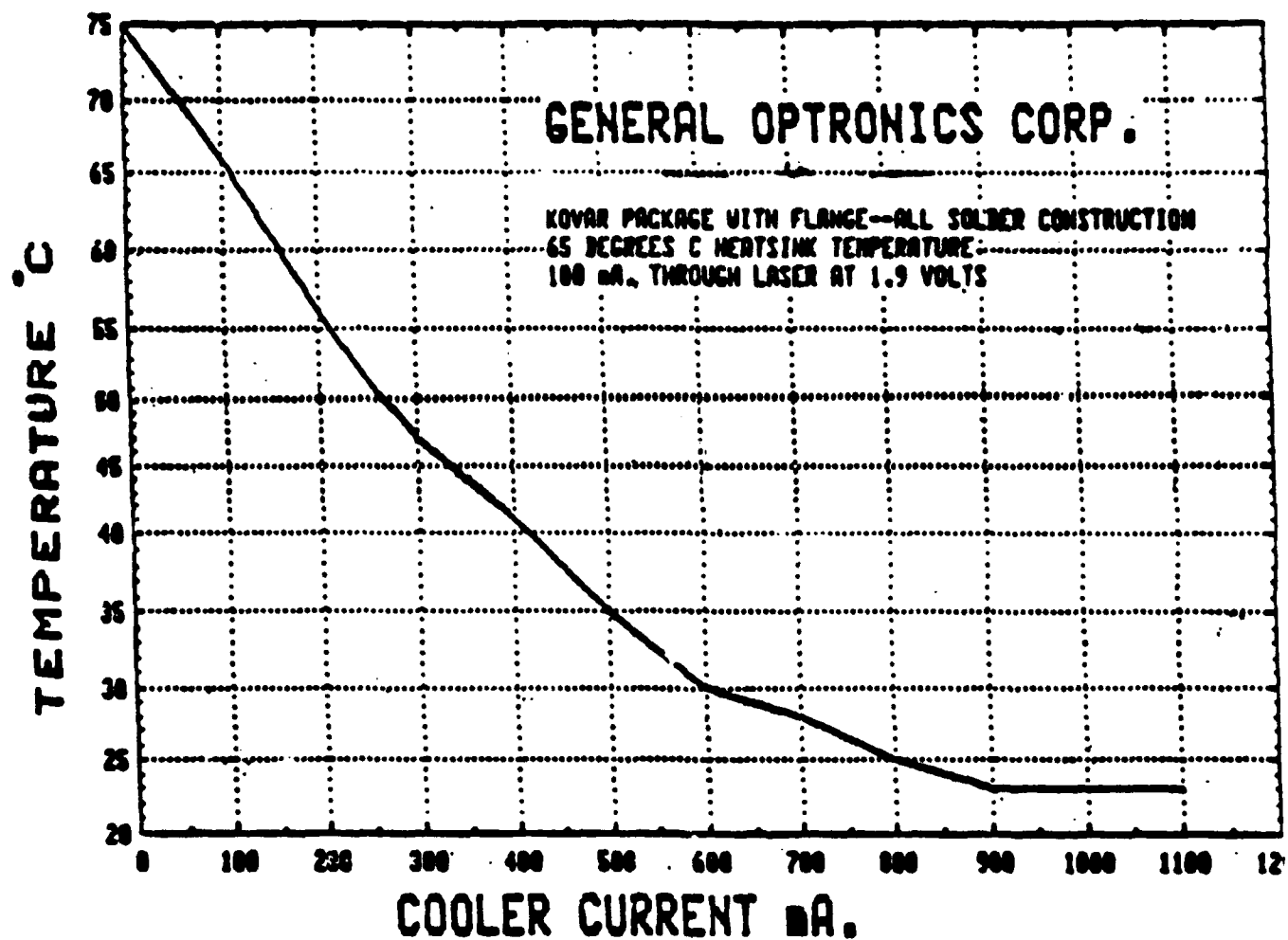
Fig. 41: Temperature vs. cooler current of thermoelectric cooler used in the TO-8 laser package
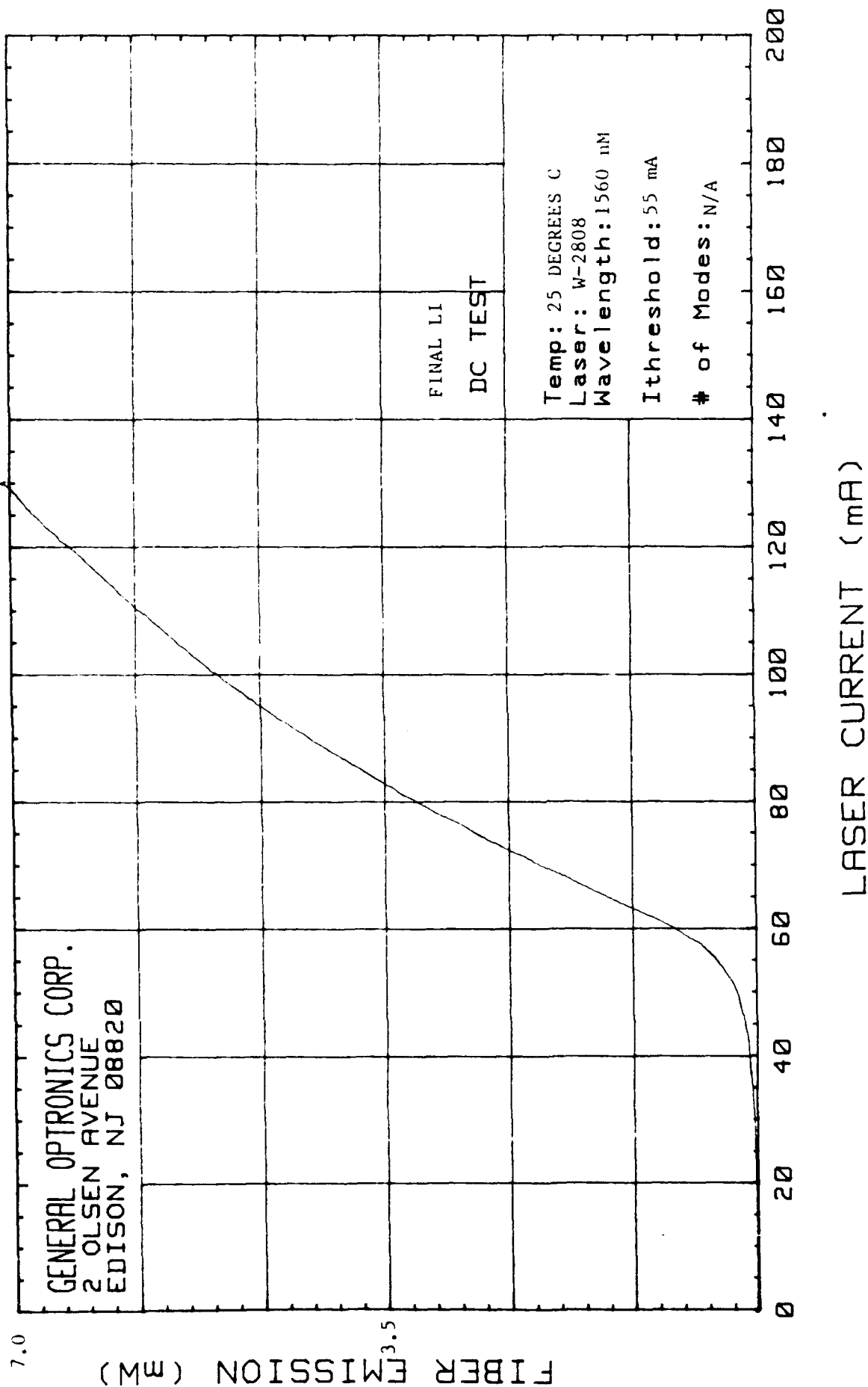
Fig. 42: Output power vs. drive laser current after mounting in TO-8 package for laser W-2808 at T=25°C
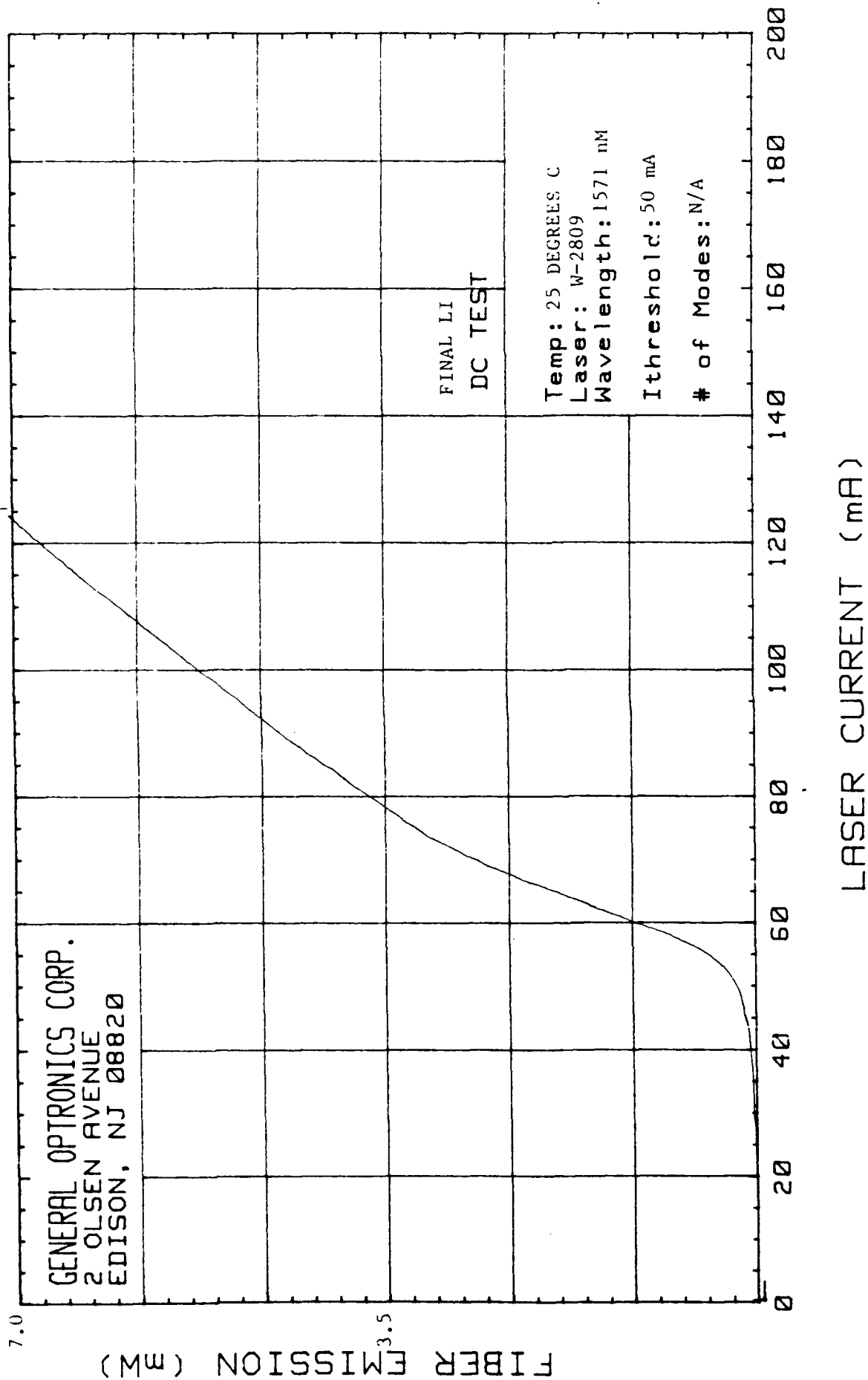
Fig. 43: Output power vs. drive laser current after mounting in TO-8 package for laser W-2809 at T=25°C

120

(xii)   The graded-idex rod lens was obtained from Nippon Sheet Glass Company and its characteristics were as follows:

Diameter: 1.8 mm

Na = 0.6   Both facets were AR coated at 1.3 μm (this is not optimum as our lasers operate at 1.57 μm and 1.56 μm)

Pitch: One-quarter so that a collimated beam is obtained as required before striking the diffraction grating.

(xiii)   The tapered single-mode fiber was obtained from contacts at the Dupont Company. These are only experimental fibers and are old and hence brittle. Handling them required considerable care. Many broke as well. Much further research is needed to obtain optimum designs for coupling and low reflectance.

Measurements carried out in our laboratory, FOCL (Fiber Optical Communications Lab.)

We were fortunate to have been loaned two optical spectrum analyzers by Advantest and Anritsu Corporations. These are fairly expensive pieces of equipment (~$35,000 each) and made our task reasonably easy.

I. Temperature and bias current effects on mode spectrum

This was done with no feedback to the cavity. The temperature was kept constant at 23°C with the temperature controller and the bias current was 80 mA and 55.7 mA. The mode spectrum is shown in figs. 44 and 45. At 80 mA we obtained many modes, as also supplied by the manufacturer. Hence it is important not to bias the laser substantially above threshold to get one longitudinal mode. The next two mode spectrum obtained, shown in figs. 46 and 47 were

Fig. 44: Measured spectrum at temp. & current indicated (Laser W-2809)

122
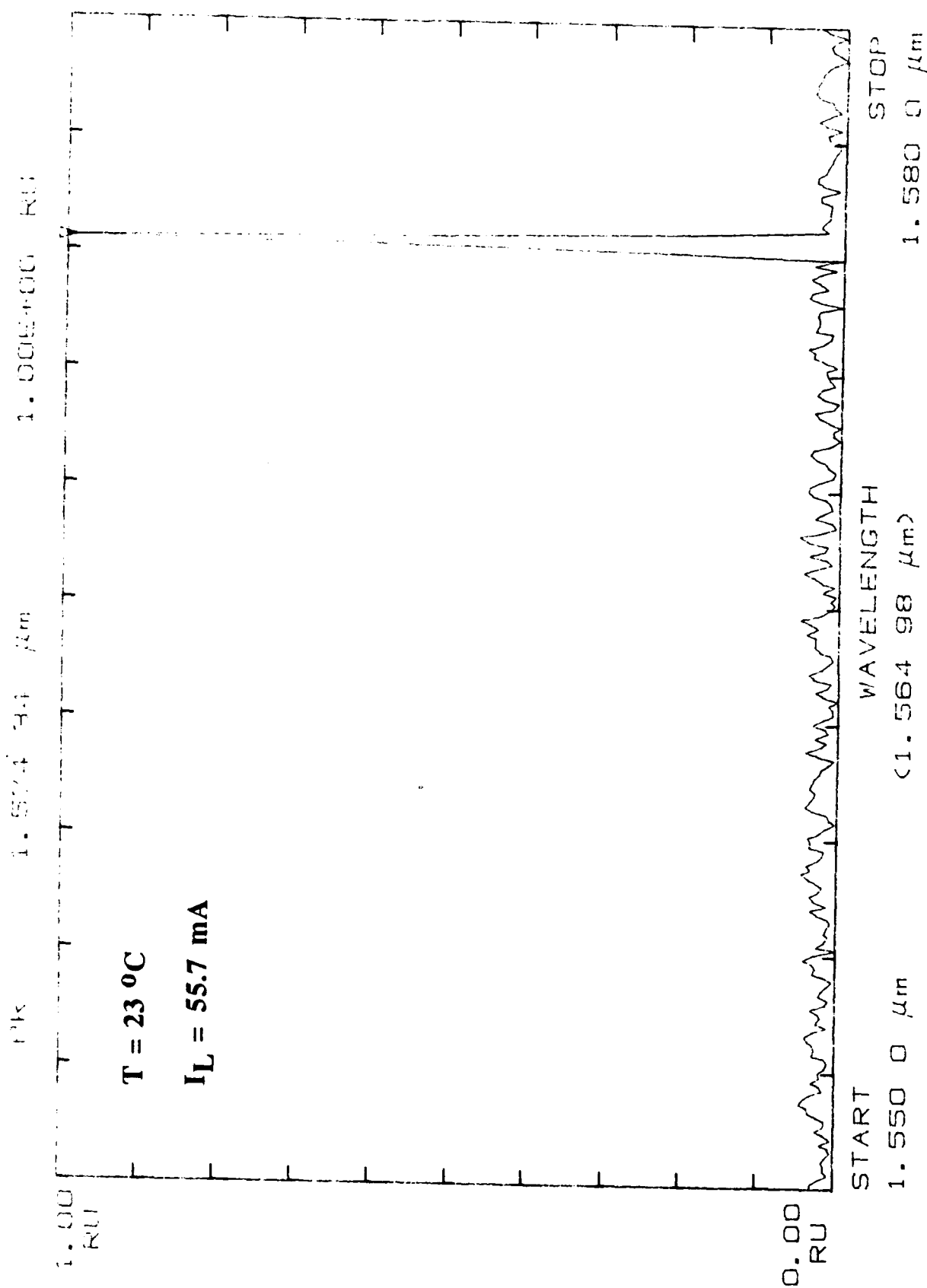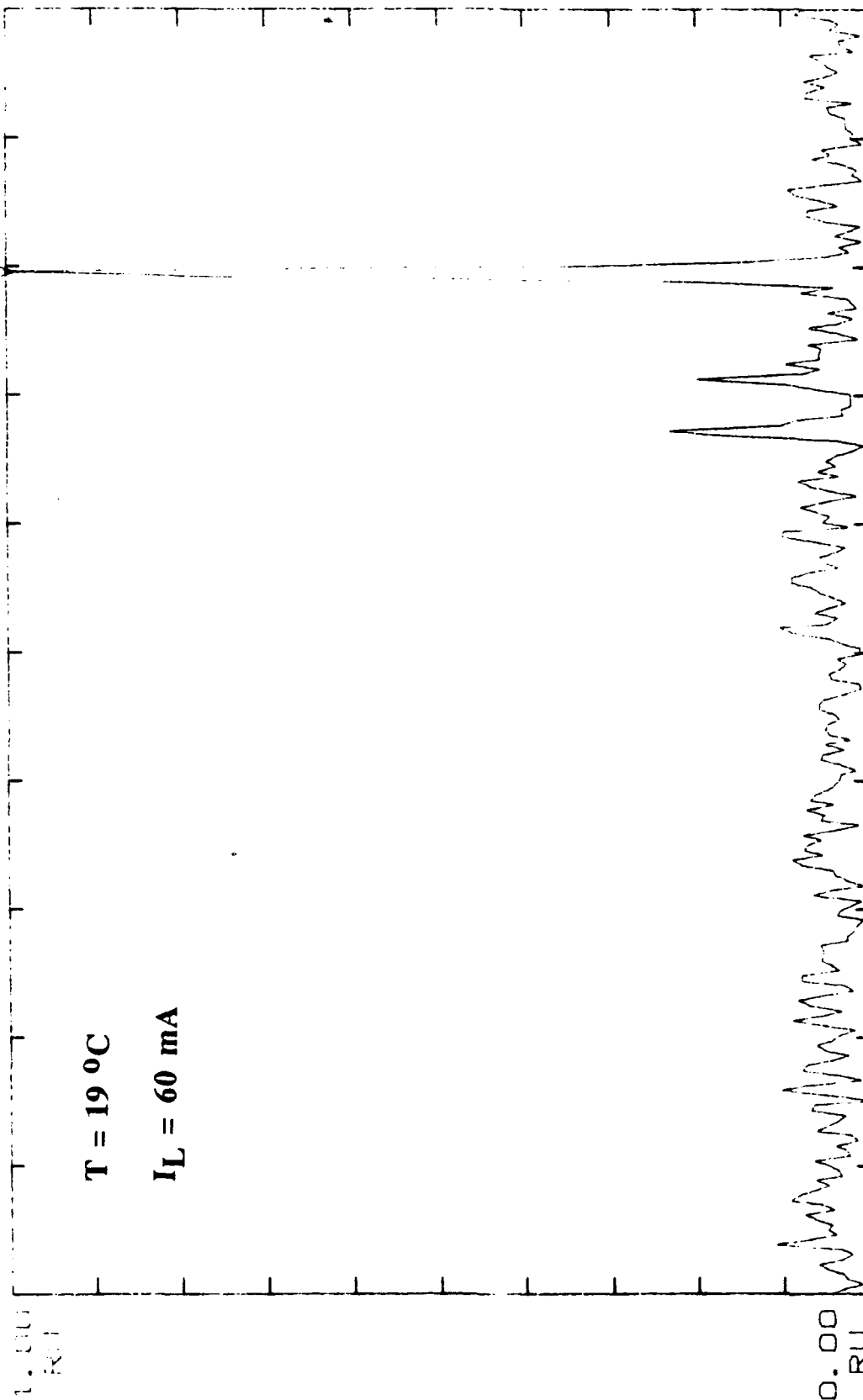
Fig. 45: Measured spectrum at temp. & current indicated (Laser W-2809)

Fig. 46: Measured spectrum at temp. & current indicated (Laser W-2809)

Fig. 47: Measured spectrum at temp. & current indicated (Laser W-2809)

at different temperatures, 19° and 10°C while keepting the bias current constant at 60 mA. The peak wavelength shifts as is well known.

The mode spectrum shown in figs. 48 thru 51 were obtained from different combinations of temperature and bias current indicated and further illustrate the frequency tuning behavior with these two parameters.

II. Power Measurements

The following measurements were done with the FP-ECSL.

(i)   Output power from uncoated facet without, and then with, optical feedback.

(ii)   Output power from the AR coated facet.

The results are shown in fig. 52 and are typical of what has been obtained in other laboratories as well.

III. Output Mode Spectrum with External Cavity

These were obtained with the Anritsu Optical Spectrum Analyzer on a total scan of 2 nm (0.2 nm/div) and are shown in fig. 53. Curve A is with feedback and Curve B is without feedback. The greater power in curve A with feedback is clearly distinguishable. The linewidth in both cases is resolution limited to ~0.2 nm, which means it is <24 GHz in both cases. The linewidths in solitary laser is < 1 GHz and that with external cavity is <100 kHz, but the spectrum analyzer cannot resolve this. One longitudinal mode is clearly seen. Our result is very similar to that obtained at British Telecom and presented at the 14th ECOC'88 in Brighton, U.K. in September 88. They used the same spectrum analyzer and their result is shown in fig. 54. Again only one longitudional mode is observed. The side mode supression ratio they obtained is >35 dB because their AR coated facet reflectivity is very low (<0.3%). Our figure is 12.8 dB as our facet reflectivity is ~4%, since we used the W-2809 laser. This was obtained from the spectrum shown in fig. 55.
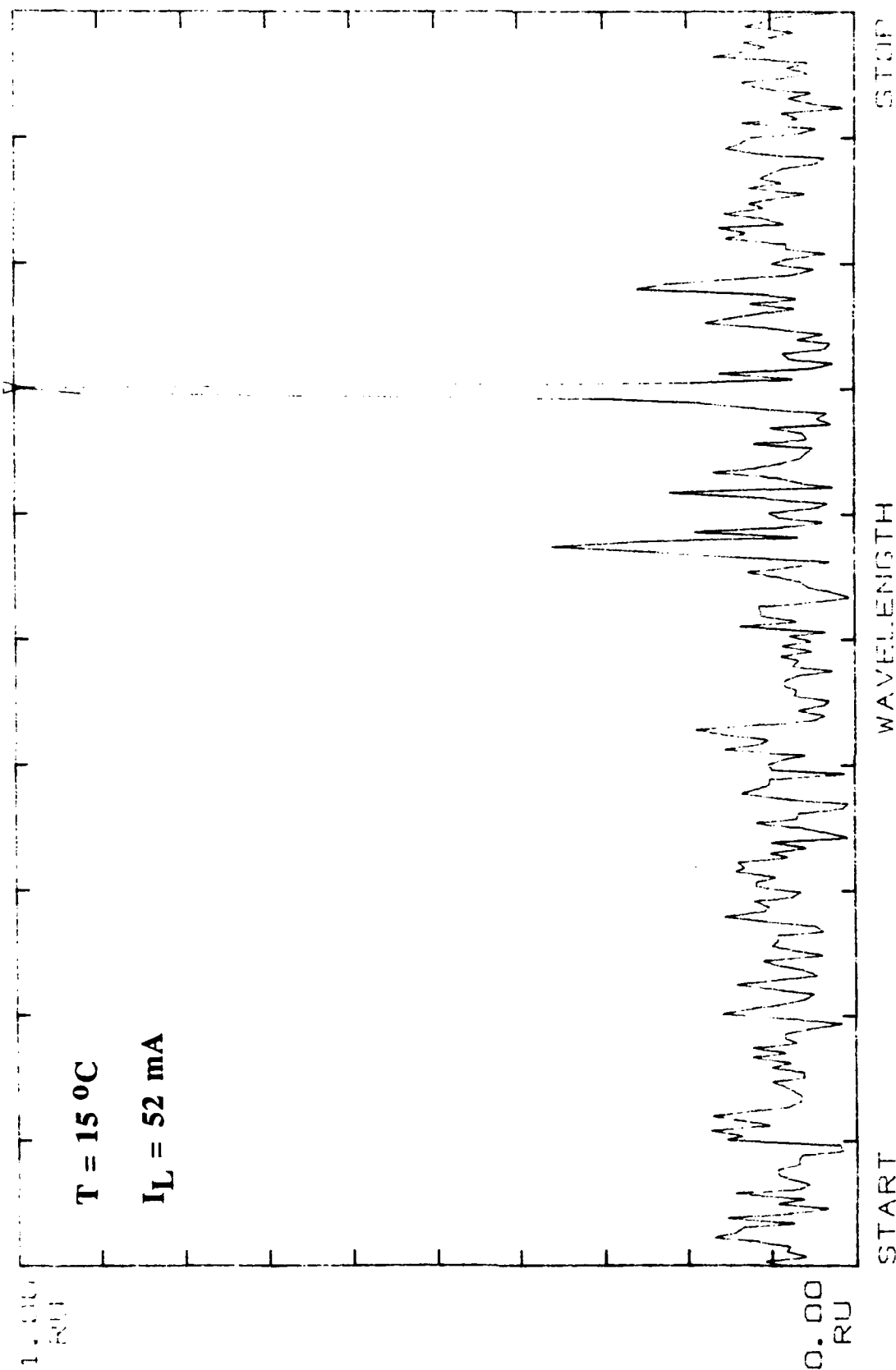
Fig. 48: Measured spectrum at temp. & current indicated (Laser W-2809)

** TQ8346 OPTICAL SPECTRUM ANALYZER **
SPECTRUM

T = 15 °C

I_L = 52 mA
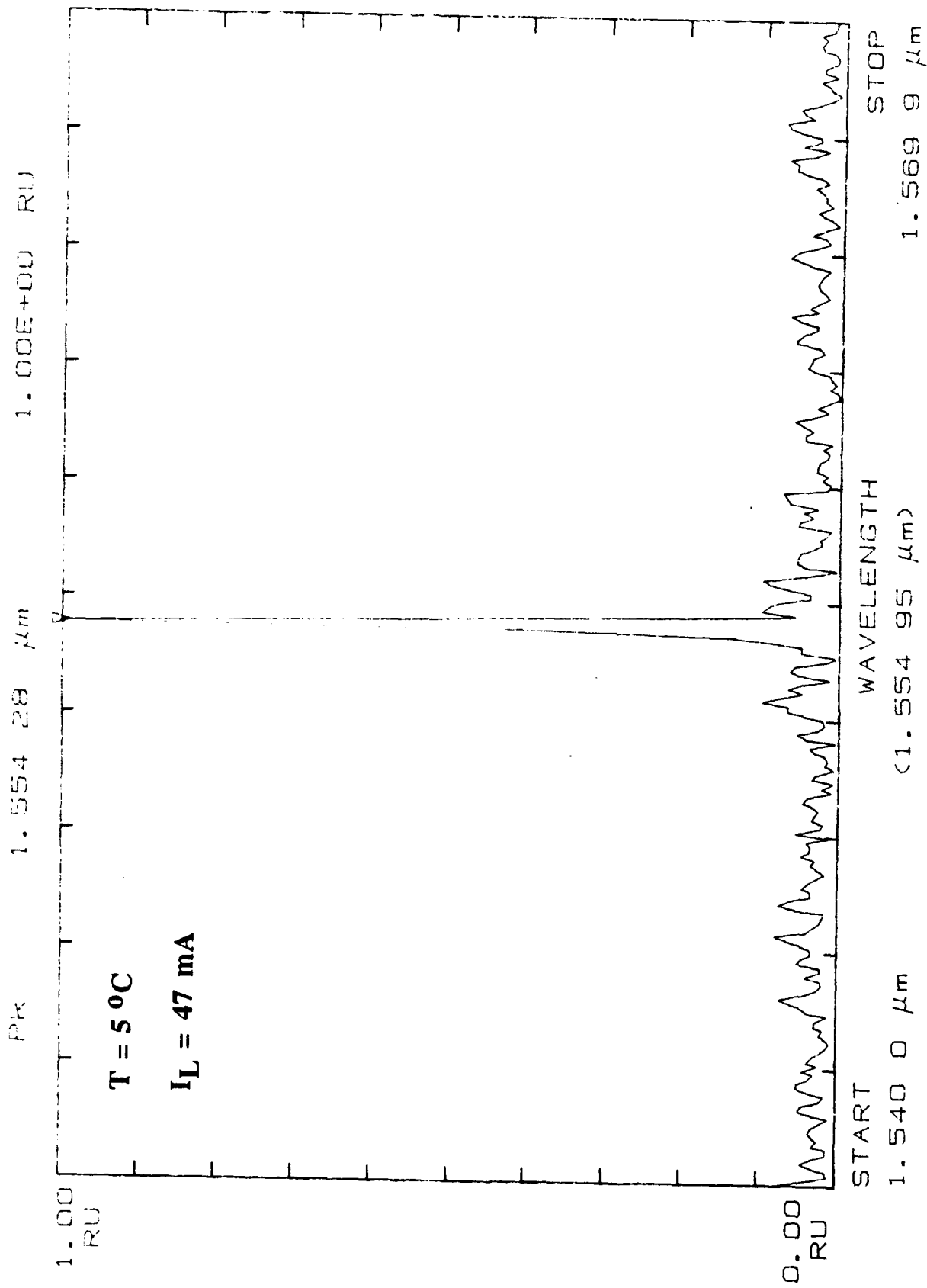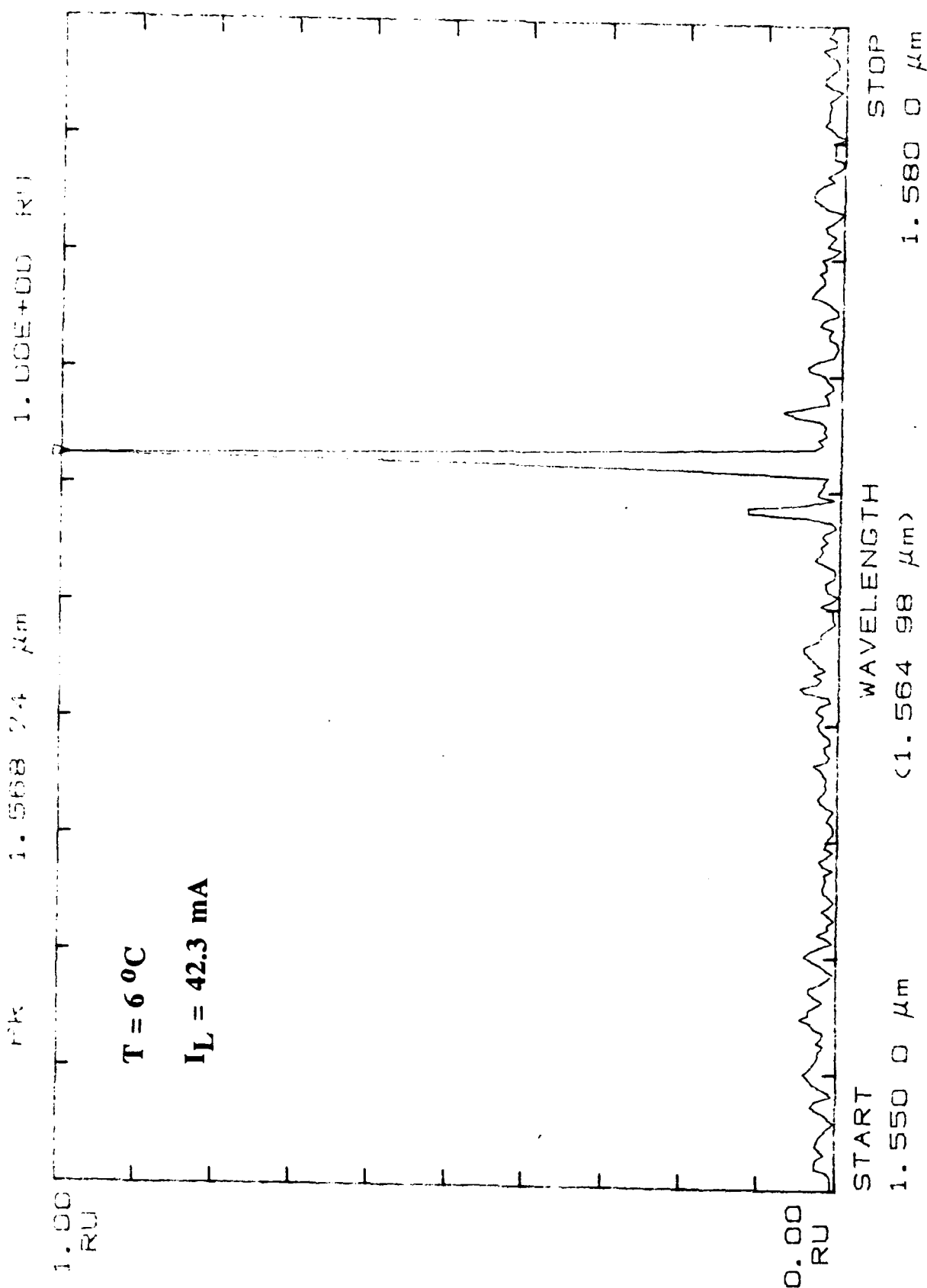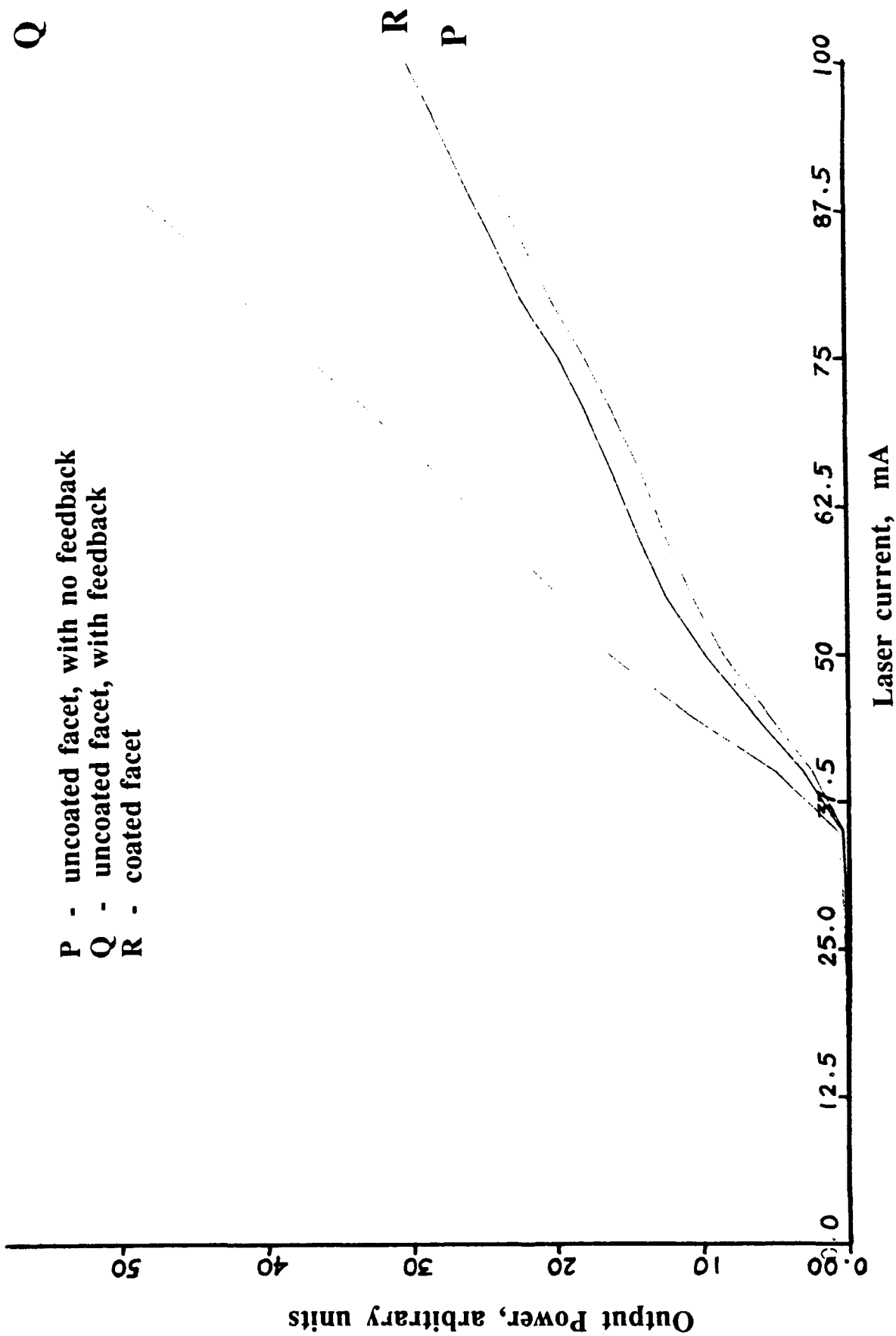
START
1.550 0 μm

WAVELENGTH
(1.564 98 μm)

STOP
1.580 0 μm

Fig. 49: Measured spectrum at temp. & current indicated (Laser W-2809)

Fig. 50: Measured spectrum at temp. & current indicated (Laser W-2809)

Fig. 51: Measured spectrum at temp. & current indicated (Laser W-2809)

Fig. 52: Out put power vs. laser drive current from the laser facets, as indicated.

P - uncoated facet, with no feedback
Q - uncoated facet, with feedback
R - coated facet

131
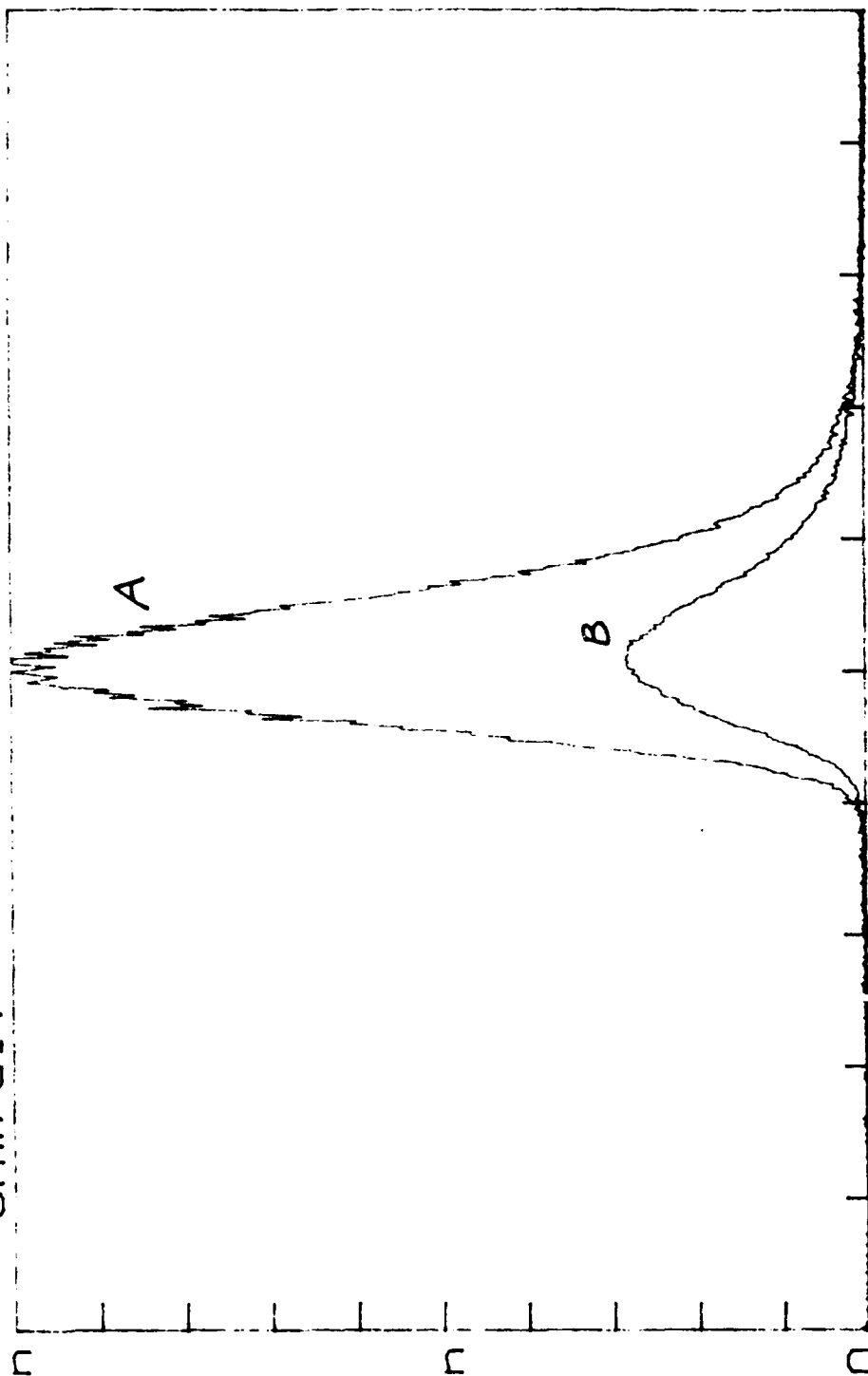
Fig. 53; Output mode spectrum of laser W-2809;
A - with feedback
B - without feedback
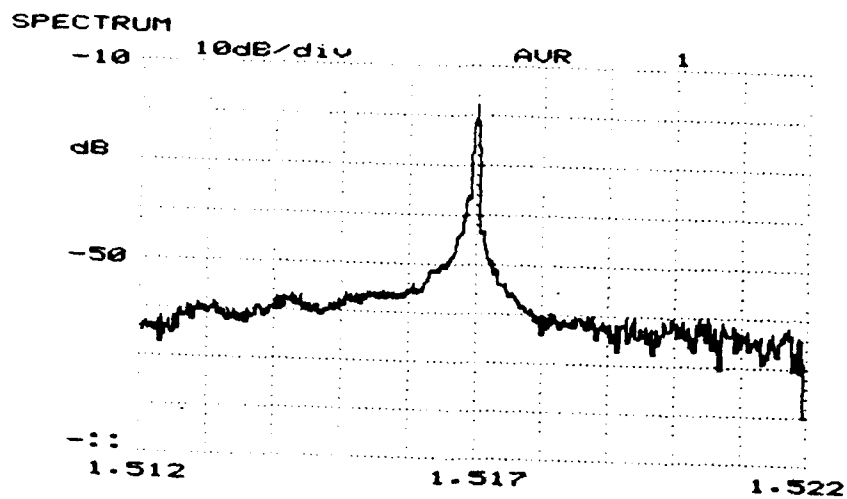
Fig. 54: Output mode spectrum obtained by BTRL with FP-ECSL using an air cavity with bulk collimating lens. (Ref: ECOC 88, UK.)

Anti-reflection coated facet reflectively is < 0.3%.

External cavity length is ~ 3 cm.

Diffraction grating has 1200 lines per mm.

Side mode suppression ratio is >35 dBs.

Separation of the laser modes is 0.7 nm, or ~ 80 GHz.
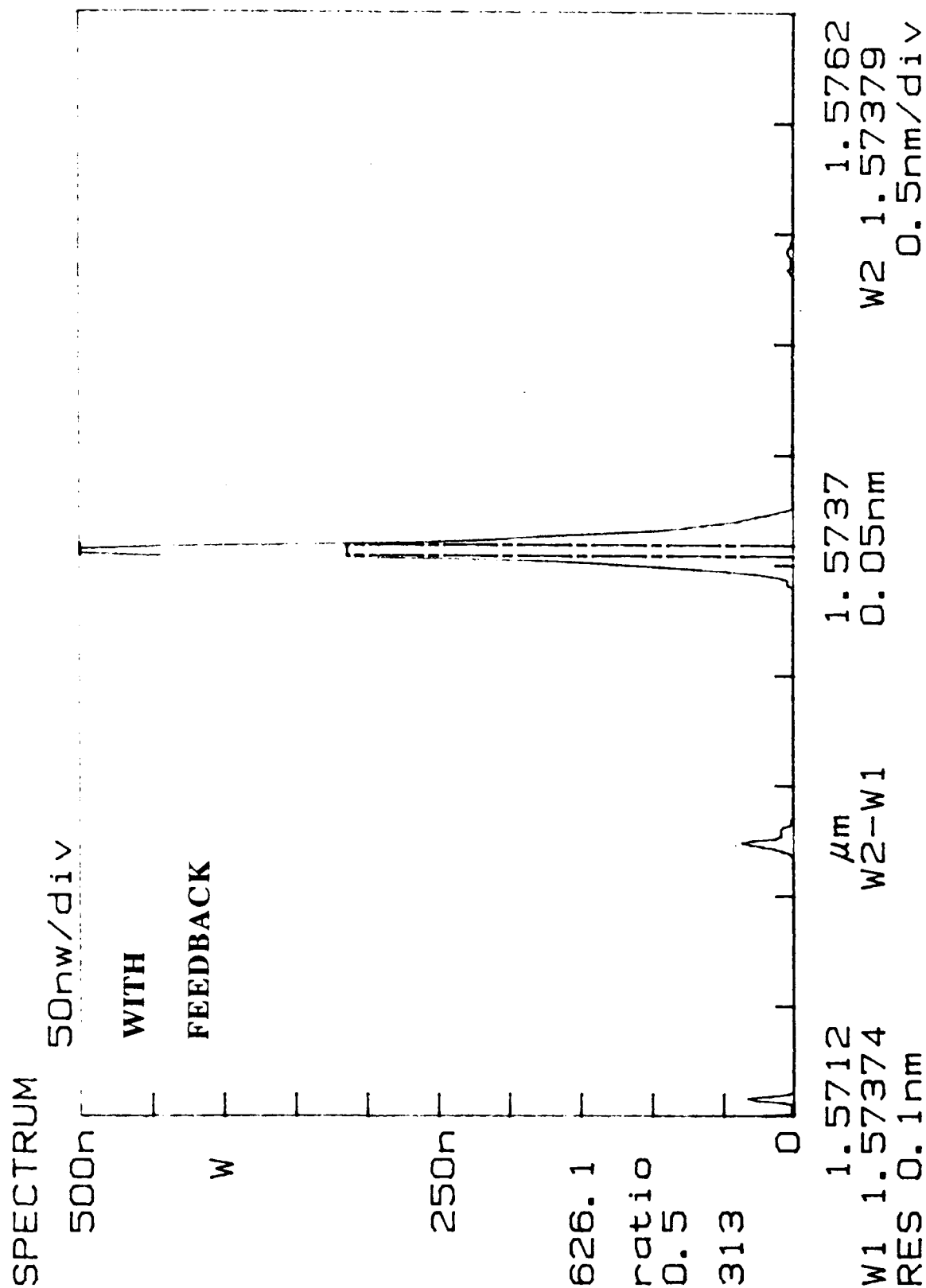
Separation of the ECSL modes is ~ 5 GHz.

Fig. 55: Output mode spectrum of laser W-2809 with optimized feedback. Resolution is 0.1 nm; Resolution limited FWHM is 0.05 nm.

## IV   Linewidth Measurement Considerations

We were loaned the Advantest Q73321 spectral linewidth testset with a 20 kHz resolution, so that we could resolve the linewidth in our FP-ECSL. Unfortunately, we had this unit for 2 days only and due to problems in optimum alignment of the external cavity at that time, we could not measure the linewidth accurately. A one-month, no cost extension was denied. We got a gift of 11 kilometers of single-mode fiber from Corning only very recently but need 4-6 weeks to set-up the delayed self-heterodyne as done in the above test.
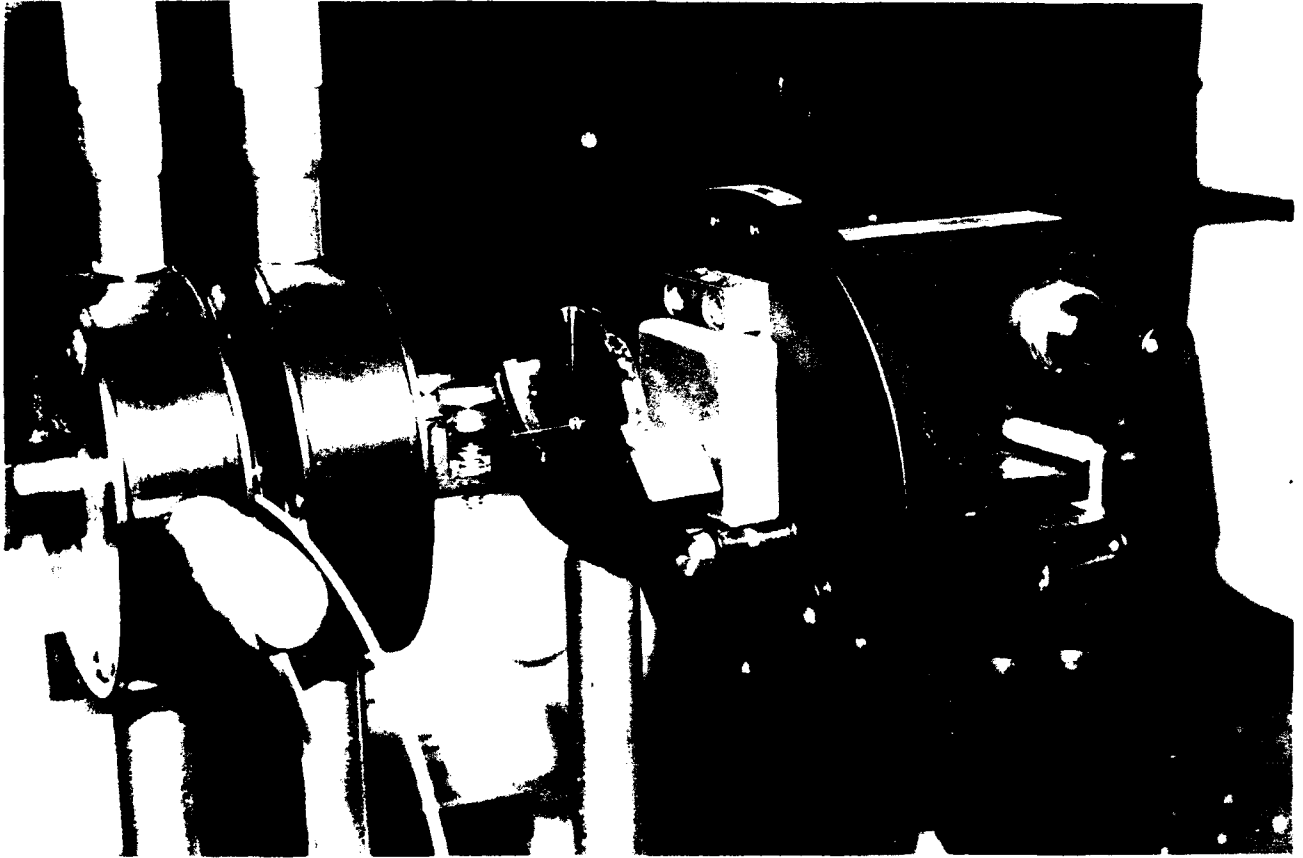
The overall view of the · P-ECSL is shown in the photographs, in fig. 56, and two close-up views are shown in figs. 57 and 58.
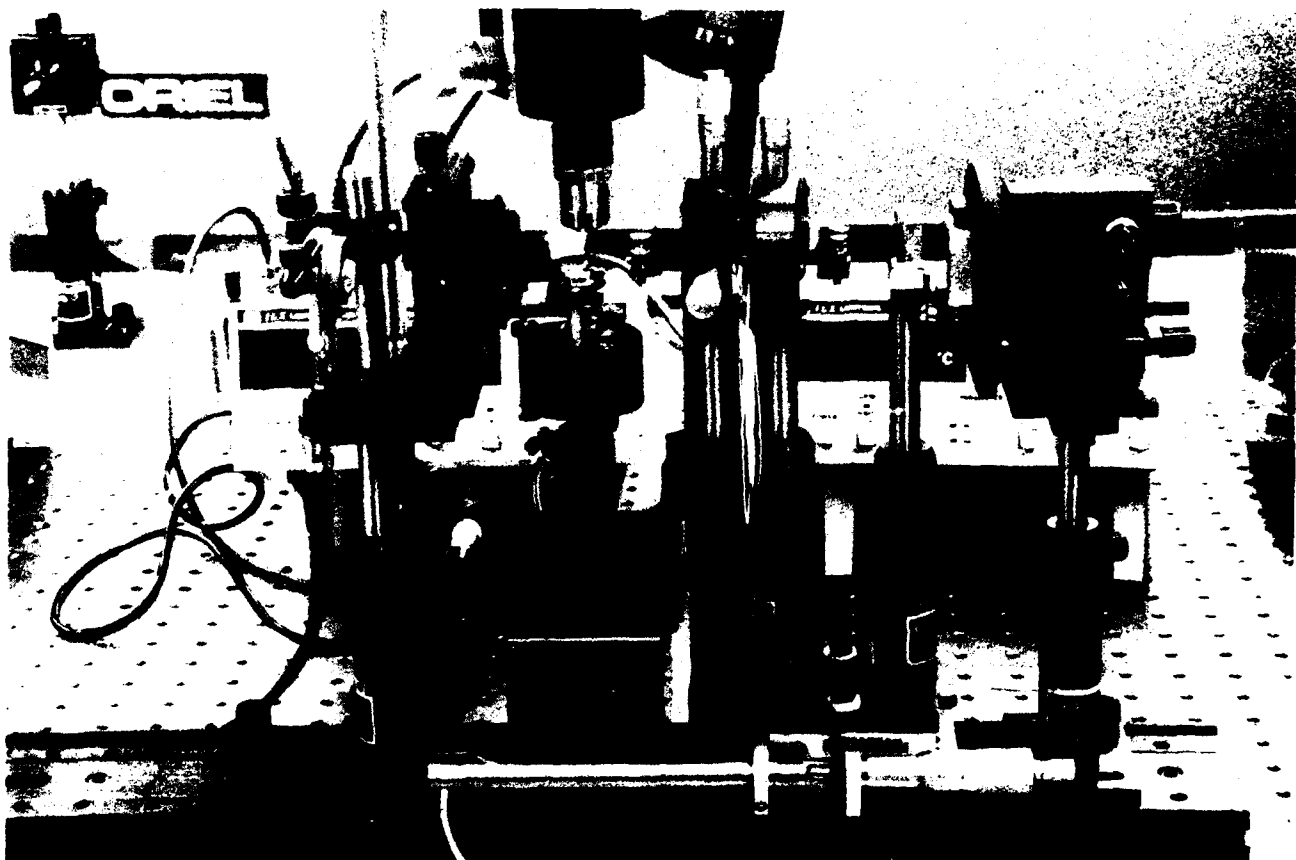
Fig. 56: Overall view of our novel FP-ECSL with single-mode
extended cavity and bulk diffraction grating end
reflector.
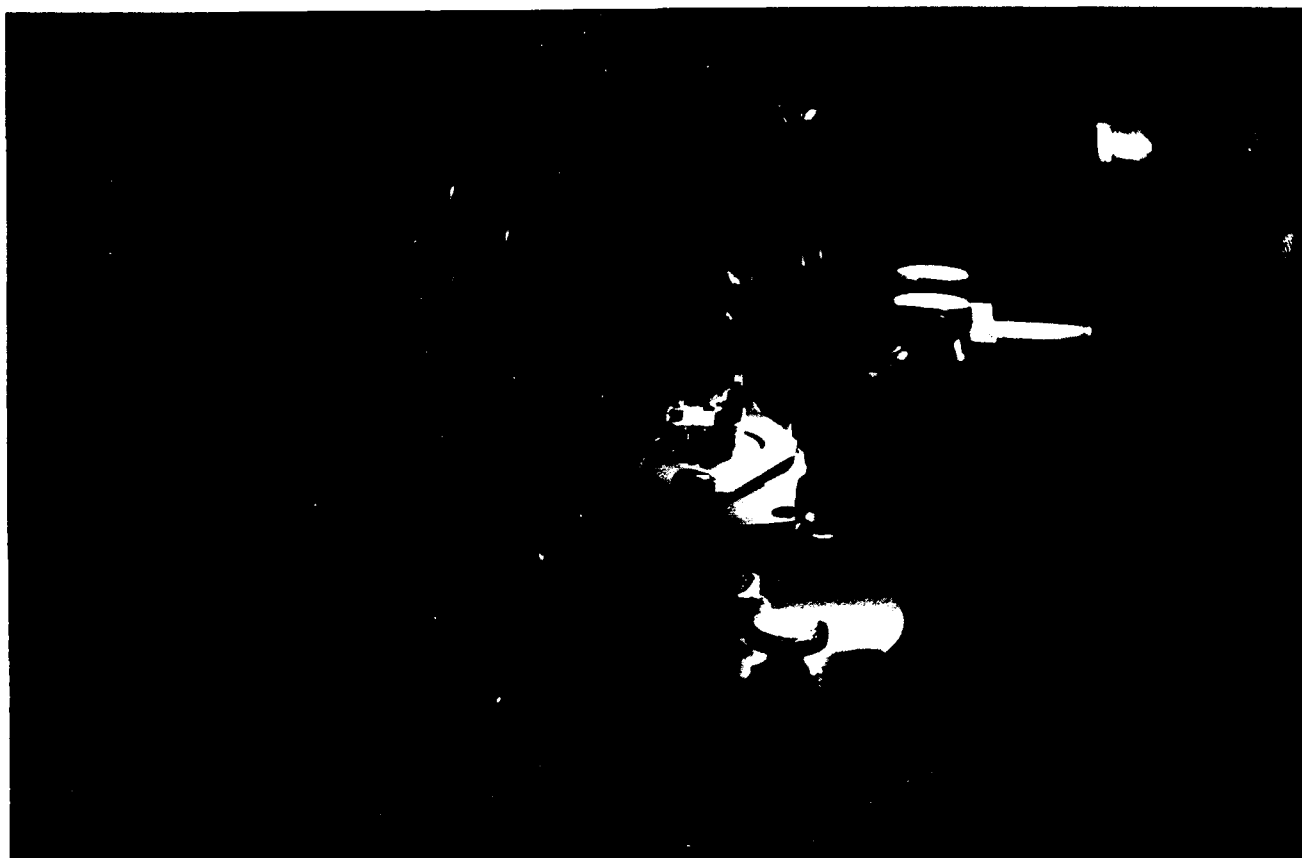
Fig. 57: Close-up view of laser and tapered single-mode fiber.

Fig. 58: Close-up view showing fiber, grin-rod lens and bulk diffraction grating end reflector.

REFERENCES

I. **EXTERNAL CAVITY STRUCTURES USING DFB SEMICONDUCTOR LASERS WITH STRONG FEEDBACK (DFB-ESCL)**

1. Chraplyvy, A. R., et. al., "Simple narrow linewidth 1.5 μm InGaAsP DFB external cavity", Electron. Lett., vol. 9, pp. 88-89 (1986).

2. Lee, T. P., Menocal, S. G., "Measured dynamic linewidth properties of a 1.5 μm DFB-GRIN-rod coupled-cavity laser under direct high-frequency modulation", Electron. Lett., vol. 21, no. 22, pp. 1046-1048 (1985).

3. Lee, T. P., Menocal, S. G., Matsumura, H., "Characteristics of linewidth narrowing of a 1.5 μm DFB laser with a short GRIN-rod external coupled cavity", ibid., vol. 21, no. 15, pp. 655-656 (1985).

4. Menocal, S. G., Lee, T. P., Leblanc, H.P., and Vodhanel, R. S., "A compact single frequency laser with a 1 MHz linewidth and ± 10 MHz frequency stability", Proceedings of SPIE Conference, vol. 273, pp. 60-65 (1986).

5. Park, C.A., "Optical sources for coherent systems", Proceedings of Conference EFOC/LAN 87, pp. 35-38.

6. Liou, K.Y., et. al., "Linewidth characteristics of fiber-extended cavity DFB lasers", Appl. Phys. Lett., vol. 48, no. 16, pp. 1039-1041 (1986).

7. Onaka, H., Miyata, H., Suyama, M. and Kuwahara, "A compact and stable distributed-feedback laser diode module with a fiber external cavity", CLEO/88, paper TUC4, Anaheim, California, Apr. 25-29 (1988).

8. Kikuchi, K., Ohoshi, T., "Simple formula giving spectrum-narrowing ratio of semiconductor laser output obtained by optical feedback", Electron. Lett., vol. 18, no. 1, pp. 10-11 (1982).

II. **FREQUENCY TUNABILITY OF DFB AND DBR LASERS**

9. G. P. Agrawal, N.K. Dutta, "Long wavelength Semiconductor Lasers", Van Nostrand Reinhold Company Inc., 1986.

10. S. Murata, I. Mito, K. Kobayashi, "Frequency modulation and spectral characteristics for a 1.5 μm phase-tunable DFB laser", Electron. Lett., vol 23, no. 1, pp. 12-14 (Jan. 1987).

11. H. Olesen, X. Pan, B. Tromberg, "Theoretical analysis of tuning properties for a phase-tunable DFB laser", to be published.

12. S. Murata, I. Mito, K. Kobayashi, "Over 5.8 nm continuous wavelength tuning of 1.5 μm wavelength tunable DBR laser", OFC/IOOC 87, paper WC3.

13. X Pan, "A theoretical model of multi-electrode DFB lasers", to be published.

14. Y. Kotaki, M. Matsuda, M. Yano, H. Ishikawa, H. Imaia, "1.55 μm wavelength tunable FBH-DBR laser", Electronics Letters, vol. 23, no. 7, pp. 325-327 (1987).

15. H. Imai, Y. Kotaki, M. Matsuda, Y. Kuwahara, H. Ishikawa, "Wavelength tunable laser with wide tuning range", CLEO 88, paper MB1.

16. B. Broberg, S. Nillson, "Widely tunable integrated Bragg laser", CLEO 88, paper MB2

17. S. Murata, I. Mito, K. Kobayashi, "Over 720 GHz (5.8 nm) frequency tuning by a 1.5 μm DBR laser with phase and Bragg wavelength control regions", Electronics Letters, vol. 23, no. 8, pp. 403-405 (1987).

18. N. K. Dutta, A. B. Piccirilli, T. Cella, R. L. Brown, "Electronically tunable distributed feedback lasers", Applied Physics Letters, vol. 48, no. 22, pp. 1501-1503 (1986).

III. FABRY-PEROT LASER AND BULK DIFFRACTION GRATING

19. R. Wyatt et al., "Tunable narrow line external cavity lasers for coherent optical systems", Br. Tele. Tech. J., vol. 3, pp 5-12, 1985.

20. R. Wyatt et. al., "Spectral linewidth of external cavity semiconductor lasers with strong frequency selective feedback", Electron. Lett., vol. 21, pp. 658-659, 1985.

21. M. R. Mathews et. al., "Packaged frequency-stable tunable 20 kHz linewidth 1.5 μm In GaAsP external cavity laser", Electron. Lett., vol. 21, pp. 113-114, 1985.

22. R. Wyatt et al., "10 kHz linewidth 1.5 μm InGaAsP external cavity laser with 55 nm tuning range", Electron. Lett., vol. 19, pp. 110-112, 1983.

23. N.A. Olsson and J. P. van der Ziel, "Performance characteristics of 1.5 μm external cavity semiconductor lasers for coherent optical communication", J. Lightwave Tech., vol. LT-5, pp. 509-515, 1987.

24. C. Y. Kuo and J. P. van der Ziel, "Linewidth reduction of 1.5 μm grating loaded external cavity semiconductor laser by geometric reconfiguration", Appl. Phys. Lett., vol. 48, pp. 885-887, 1986.

IV FABRY-PEROT LASER AND FIBER/PRISM DIFFRACTION GRATINGS

25. E. Brinkmeyer et al., "Fiber Bragg reflector for mode selection and line-narrowing of injection lasers", Electron. Lett., vol. 22, pp. 134-135, 1986.

26. C. A. Park et al., "Single-mode behavior of a multimode 1.55 μm laser with a fiber grating external cavity", Electron. Lett., vol. 22, pp. 1132-1133, 1986.

27. M. S. Whalen et al. "Tunable fiber-extended cavity laser", Electron. Lett., vol. 23, pp. 313-314, 1987.

28. J. Wittmann et al., "Narrow-linewidth laser with a prism grating/Grin rod lens combination serving as external cavity", Electron. Lett., vol. 23, pp. 524-525, 1987.

MANUSCRIPT 1

Tunability Aspects of DFB External Cavity Lasers

Tunability Aspects of DFB External Cavity Semiconductor Lasers

Harish R. D. Sunak & Clark P. Engert
Fiber Optical Communications Laboratory
Department of Electrical Engineering
University of Rhode Island
Kingston, RI 02881-0805

1   Introduction

The possibility of wavelength division multiplexing transmission with coherent detection techniques has prompted the need for a narrow-linewidth, tunable optical source. These types of systems offer the ability to transmit many channels simultaneously with narrow channel spacings depending upon the data rates transmitted. For a phase shift keying modulation system the required linewidth is on the order of between 0.1 and 0.5 percent of the channel bandwidth. Since solitary semiconductor lasers do not provide such a narrow-linewidth, the addition of passive external cavities is one way to reduce the linewidth.

Previous research on the addition of passive external cavities, which utilize the high feedback regime, to DFB semiconductor lasers has been most promising. These types of structures produced optical sources with reduction of the linewidth by a factor of a 1000 and increased stabilization from reflected feedback to -20 dB[1]. Even for relatively low data rates(∼100 Mbits/s), the linewidth from such a device is satisfied for the heterodyne detection, phase shift keying transmission system. However, these types of devices lack the ability to be electrically fine tuned.

Thus far, research into the tunability of solitary DFB semiconductors has produced a phase tunable DFB(PT-DFB). These type of solitary lasers show continuous tuning regions of 1.2 nm(150 GHz)[2]. This types of tuning provides a

142

fast, stable electrically generated means of tuning the optical source. So a natural evolution is to integrate the two types of systems to provide a narrow-linewidth, frequency stable, tunable optical source. Such a system based on PT-DFB semiconductor lasers offers an electrical means of tuning.This is a great advantage of this type of system over a Fabry-Perot laser based external cavity structure which rely on mechanically adjusting the diffraction grating to provide tuning. However, the increase in mechanical stability of DFB based external cavities leads to a much smaller tuning range. Thus far tuning characteristics for a PT-DFB based external cavity laser utilizing the high feedback regime have not been characterized.

2   Theoretical Considerations

The type of laser structure analyzed is illustrated in figure 1. In order to operate in the high feedback regime, r_2 must have an antireflection coating and f_2 must have a high reflection coating. Generally to be operating in the high feedback regime, power feedbacks greater than 10% are needed.[3]

Since the amount of feedback needed to insure good stability is relatively high, the model that will be used will incorporate the feedback from the external cavity and the phase region into the facet reflectivities of normal DFB lasers. This type of analysis has been suggested by A.R.Chraplyvy *et. al.*[4] Our analysis starts with the threshold condition for an ordinary DFB laser which is given by[5]

$$\left(\frac{r_a - r}{1 - rr_a}\right)\left(\frac{r_b - r}{1 - rr_b}\right) exp\left(2i\gamma L\right) = 1 \tag{1}$$

where $r_{a,b}$ are the *effective* facet reflectivities, L is the length of the active region, γ is the complex wave number, and r is the effective distributed reflectivity from the grating. The effective reflectivity caused by the grating is given by $r = -\frac{\kappa}{\gamma+\Delta\beta}$.The complex wave number is given by, $\gamma = \pm\left(\Delta\beta^2 - \kappa^2\right)^{\frac{1}{2}}$, where κ is the coupling coefficient and $\Delta\beta$ is the difference between the mode propagation constant and the Bragg condition. By dividing up the $\Delta\beta$ into the real and imaginary components one obtains the customary detuning parameter,δ, and power gain,$\frac{\alpha}{2}$.

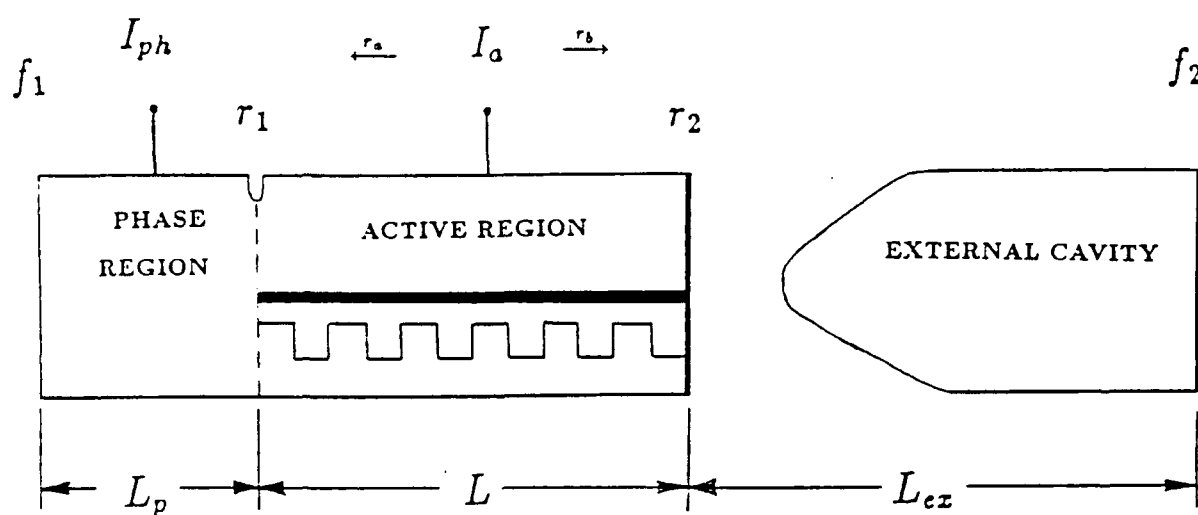Since the reflectivities are not truly defined only at the edge of the active region,

Figure 1: Schematic diagram for the PT-DFB based external cavity laser with parameters appropriately labeled.

then we can find the general reflecting term of the external cavity and phase region by[6]

$$r_{a,b} = \frac{r_{1,2} + \left[\eta^2\left(1 - r_{1,2}^2\right) - r_{1,2}\right] f_{1,2} \exp\left(-j2\gamma_{p,ex}L_{p,ex}\right)}{1 - r_{1,2}f_{1,2}\exp\left(-j2\gamma_{p,ex}L_{p,ex}\right)} \qquad (2)$$

where the phase region is signified by p, the external region is signified by ex, and the first index corresponds to the phase region and the second corresponds to the external region. It is assumed as in ref.[6] that the reflectivities, coupling, and transmission coefficients are equal whether seen from the inside of the laser cavity or the external cavity interface. Also it is assumed that forward and backward transmission coefficients are equal, multipling together to give the $\left(1 - r_{1,2}^2\right)$ term.

For the external feedback reflectivity we assume that the feedback is in-phase and so the reflectivity from the external cavity is given by,

$$r_b = \frac{r_2 + \left[\eta^2(1 - r_2) - r_2\right] f_2}{1 - r_2 f_2} \qquad (3)$$

where appropriate terms can be see in fig 1. We also assumed the loss in the external cavity is constant and this loss will be absorbed in the coupling term, since both terms will remain constant during tuning.

For the phase region, assuming that the coupling efficiency is one and the r_1 reflectivity is zero, then the reflectivity seen by the active region caused by the phase region is given by

$$r_a = f_1 \exp\left(-j2\gamma_p L_p\right) \qquad (4)$$

where γ_p is the complex wave number. Unlike the external cavity region, the losses and index of refraction will change in the phase region because the number of carriers will change with changes in the pumping current of the phase region. The wave number is split up into the appropriate components to reflect this[6],

$$\gamma_p = \left(\frac{2\Pi}{\lambda}n + \Gamma\frac{\Delta n}{\Delta N_p}\right) + j\left(\frac{2\Pi}{\lambda}\bar{\alpha}_p + \Gamma\frac{\Delta\bar{\alpha}_p}{\Delta N_p}\right) \qquad (5)$$

where n is the index of refraction, N_p is the carrier density injected into the phase region, λ is the wavelength of the propagating wave, $\bar{\alpha}_p$ represents the material loss

in the phase region, and Γ is the confinement factor of the injected current to the waveguide section in the phase region.

The number of carriers in the phase region is related to the phase pumping current(I_p) by recombination mechanisms given by,

$$I_p = e \times vol_{wg} \times N_p \left(A + BN_p + CN_p^2 \right) \tag{6}$$

where vol_{wg} is the volume of the waveguide in the phase region and e is the charge of a carrier. The constants A,B, and C take into account recombination mechanisms. For the 1.3 μm bandgap phase region, values of 1.0 $\times 18^8$/s, 4.0$\times 10^{-17} m^3$/s, and 6.6 $\times 10^{-41} m^6$/s, respectively were used for the constants.

We now solve the transcendental equation in eq.1 utilizing the above equations to solve for the normalized detuning parameter $\left(\bar{\delta} = \delta L \right)$ and normalized mode loss ($\bar{\alpha} = \alpha L$) as a function of the injected current. Taking into account the gain wavelength profile, we determine which mode has the lowest threshold current and consider this mode to lase. We assumed that the wavelength gain profile is a linear function of the current density. Our analysis does not take into account the hysteresis effect and, therefore, the maximum tuning range will be greater than our theoretical predictions.[2,7] We also assumed the gain decreased quadratically from its peak value to give the gain(g) at the mode wavelength, λ, by[6,7]

$$g = a \left(N - N_0 \right) \left[1 - \left(\lambda - \lambda_p \right)^2 \right] \tag{7}$$

where N_0 is the transparent carrier density and a is a multiplication constant. The value used for a is 2.5 $\times 10^{-20}$ m^{-2}. The wavelength peak, λ_p, is given by[7],

$$\lambda_p = \lambda_{p0} - \frac{d\lambda_p}{dN} \left(N - N_0 \right) \tag{8}$$

where $\frac{d\lambda_p}{dN}$ is determined from the 1.3 μm wavelength gain profile to be 5.44 $\times$ 10^{-32} m^4. [8] Utilizing the results from ref. [9], we can determine the wavelength transparency value (λ_{p0}) to be 1.643 μm and the transparency carrier density to be 8.0$\times 10^{23}$m^{-3}. The resultant wavelength gain profile can be seen in fig 2.
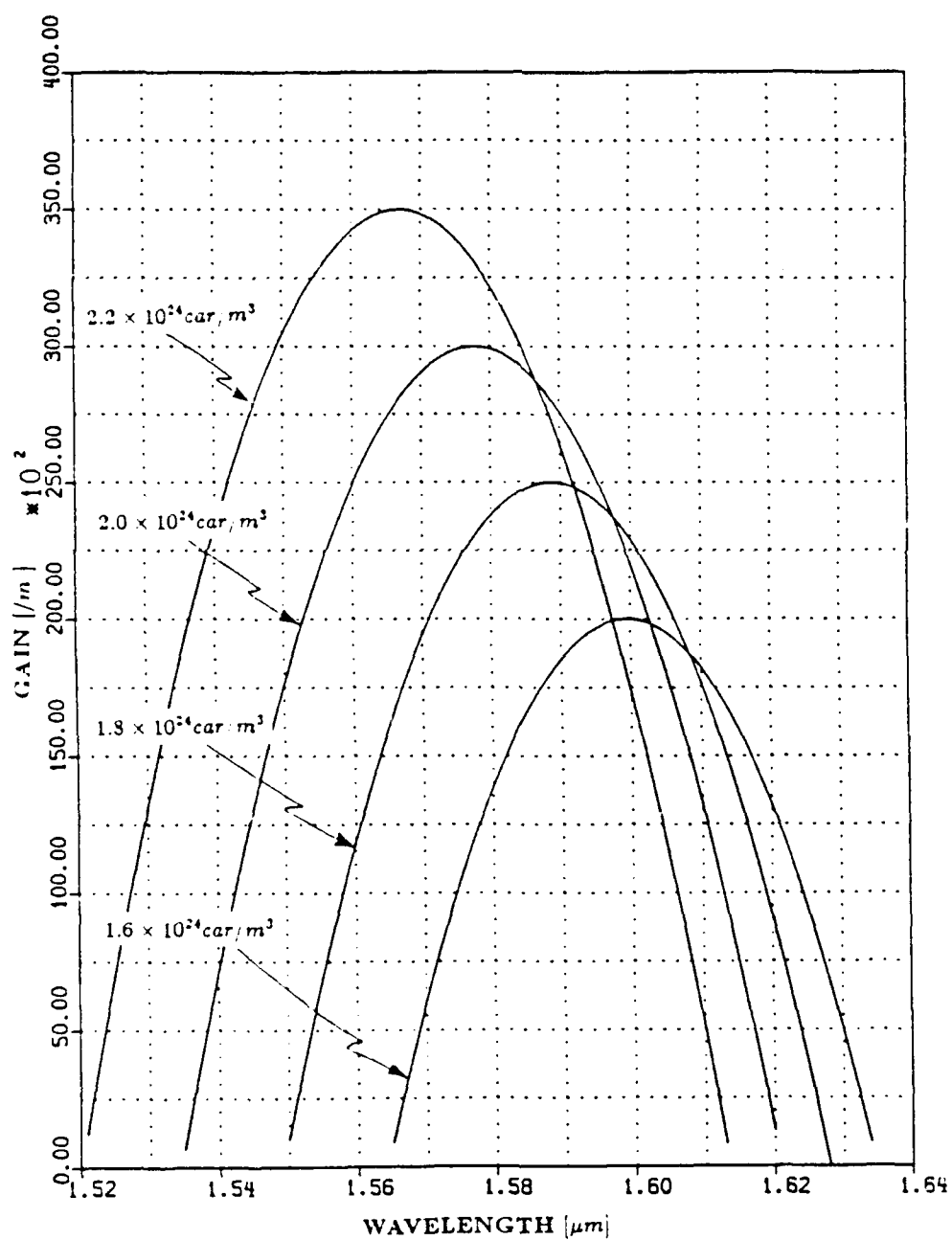
Figure 2: Wavelength gain profile model used to describe the gain curve for 1.55 μm bandgap InGaAsP material.

147

By finding the mode which exhibits the lowest threshoid carrier density, we can determine the lasing frequency change from.

$$\Delta f = \frac{\Delta \bar{\delta} c}{2 \Pi n L} \tag{9}$$

where c is the speed of light, and $\Delta \bar{\delta}$ is the change in the normalized detuning parameter from the initial condition($I_p = 0$).

3   Design Parameters

The tuning range of a PT-DFB based external laser structure pictured in figure 1 is analyzed. The solitary laser is assumed to have a 1.55 μm InGaAsP active region and a 1.3 μm InGaAsP phase region of variable length. In our analysis the change of the refractive index and the material loss are taken to be $\frac{\Delta n}{\Delta N_p} = -4.2 \times 10^{-27}$ m^3 and $\frac{\Delta \alpha}{\Delta N_p} = 1.8 \times 10^{-21}$ m^2.[5] The initial material loss is taken to be $\overline{\alpha_{ph}} = 20$ cm^{-1}. The front facet is not coated and has an amplitude reflectivity of 0.5656. The power feedback from the external cavity is 10% for a reflectivity of 0.3162. The relationship for the carrier density from the injected current in the active region has been determined with $A = 1 \times 10^8$/s, $B = 8 \times 10^{-17}$ m^3/s, and $C = 4 \times 10^{-41}$ m^6/s.[5] We assumed the waveguide section had thickness of 0.23 μm and a thickness of 1.2 μm while the length was left as a variable. The length, width, and thickness of the active region of the DFB are taken to be 300, 1.5, and 0.1 μm, respectively. The confinement factor of the lateral and transverse fields in the active region is taken to be 0.4. Whereas, the confinement value of the injected current in the phase region to the waveguide section was taken to be 0.27.

The first design parameter which will be considered is the placement of the Bragg condition with respect to the wavelength profile gain curve in fig. 2. All device parameters are understood to be the same as above and the normalized coupling coefficient is 1.5. The length of the phase region is chosen to be 200 μm to illustrate all the possible lasing modes. The Bragg wavelength must be placed such that over the variable gain change during tuning the lasing mode will occur on or near the gain peak. This critierion is set so that the lasing mode is

determined from the DFB grating and not the gain peak profile. By doing this, Fabry-Perot(FP) modes will not lase and good mode selectivity is produced. In our analysis, the threshold gain varied from a minimum of 240 cm^{-1} to a maximum of 280 cm^{-1}. As a consequence from fig 2, we see that the wavelengths of the gain peaks, for these respective threshold gains, are from 1.591 μm to 1.583 μm. Therefore, the Bragg wavelength should be located around these wavelengths if FP modes are not to lase.

The Bragg wavelength of 1.58 μm, proved to be the optimum value when considering the gain profile and its lasing characteristics can be seen in fig 3 for a length of 200 μm; our results predict that the maximum continuous frequency tuning is 50 GHz from the 1.6 mA to 14 mA region with a normalized coupling coefficient of 1.5. In this region, in which the lasing is taking place on the shorter wavelength side of the Bragg wavelength, the frequency tuning is approximately linear at the end of the tuning range. Initially, the tuning rate was 11.79 GHz/mA, and, at the end of the tuning, the rate fell to 2.752 GHz/mA. The approximate linear tuning range was 25 GHz wide, which is ideally the kind of tuning desired, with a tuning rate of 4.0 GHz/mA $\pm$ 1.5 GHz/mA.

The next design parameter which is analyzed to determine its effect on tuning is the normalized coupling coefficient. Generally speaking, the κL value should be as close to 1.25 as possible so as not to introduce spacial hole burning which increases the linewidth.[10] The power associated with the nearest side mode which is given by the side mode suppression ratio(SMSR) must also be considered. The κL value was varied between 1.0 and 2.0 to determine the effects on tuning with all other parameters constant. From our results, the maximum tuning range for $\kappa L = 1$ is 51 GHz, however, FP modes lased which makes use of this coupling coefficient useless. At the highest coupling coefficient of $\kappa L = 2$, the maximum tuning range was 40 GHz from the -393 GHz to -353 GHz frequency range. Although the high coupling gives greater SMSR, as can be seen in fig 4, the increased mode selectivity factor was only increased by an average increase in the threshold current of 0.05 mA, while the continuous tuning decreased by 15 GHz. Thus from these results the optimum value for the normalized coupling coefficient was 1.5.
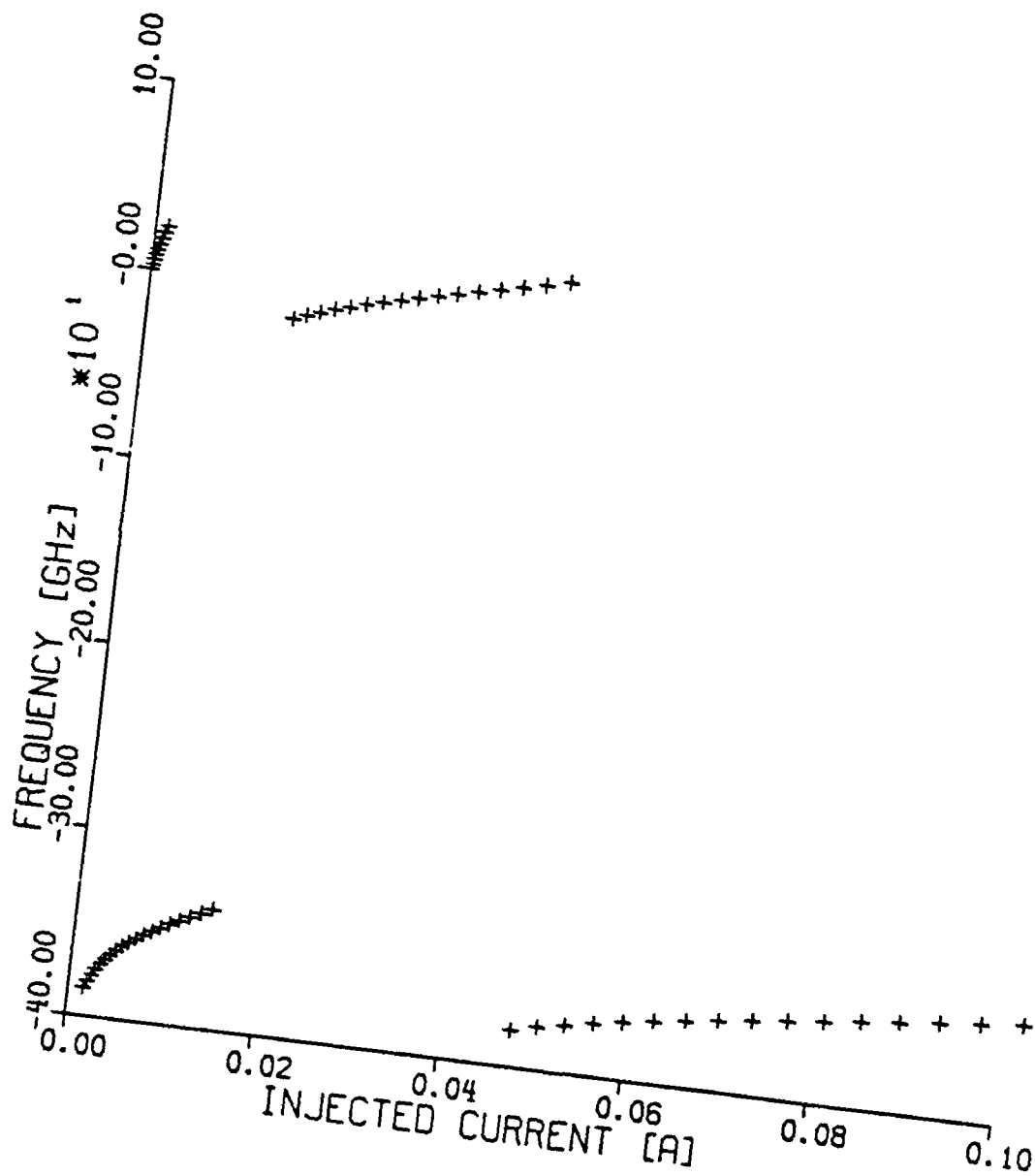
Figure 3: Lasing frequency versus injected current in the phase region for a Bragg wavelength of 1.58 μm and a phase region length of 200 μm.
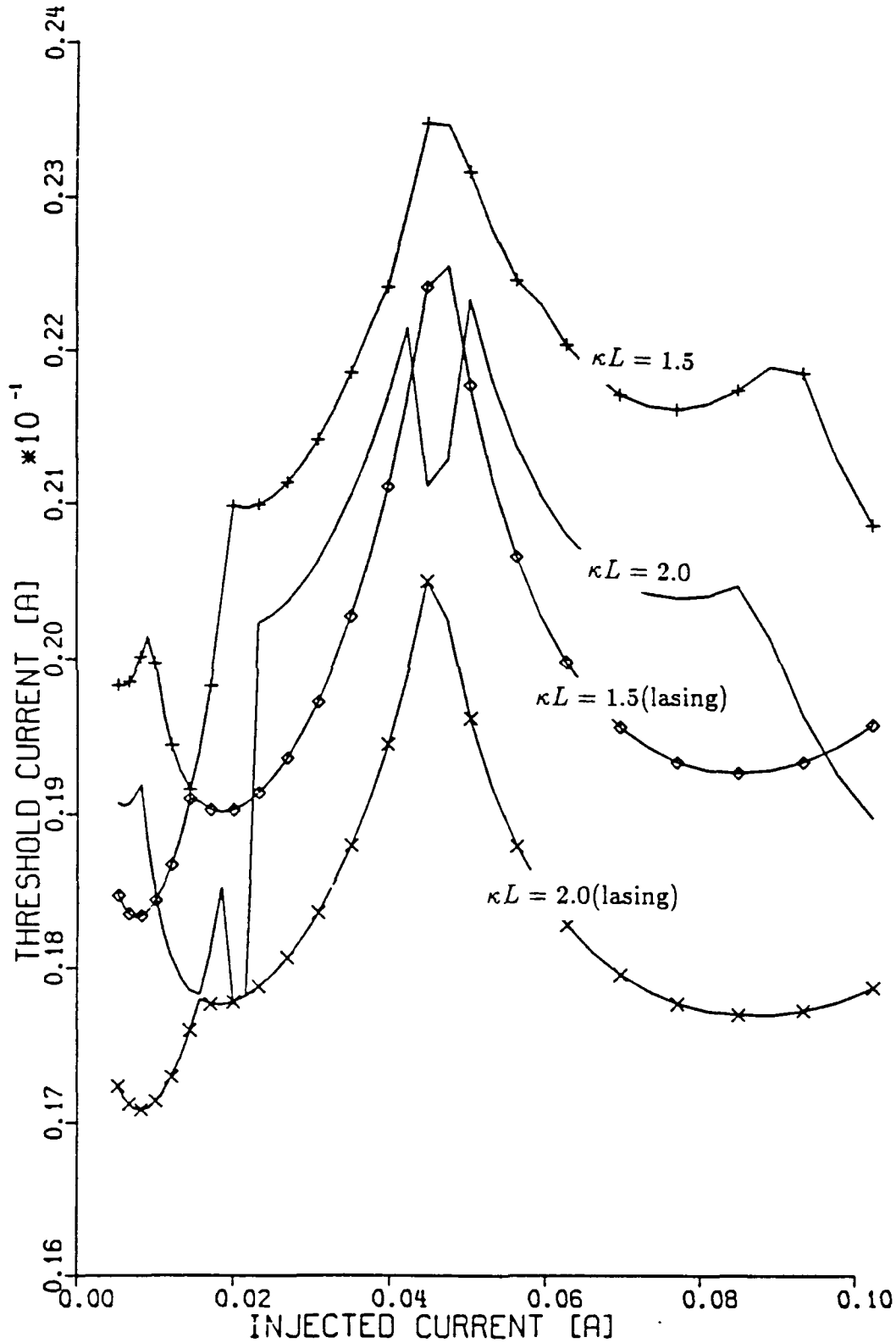
150

Figure 4: Threshold current characteristics for the lasing mode and the next side mode versus injected current in the phase region for κL values 1.5 and 2.

From previous results(fig 3) we see that for a phase length of 200 μm lasing jumps back and forth and back again. Ideally, considering limitations on cleaving techniques, we want only two complete modes to lase only once, because there is no need for repetition. Since an exact length within a few percent of the lasing wavelength can not be made, an initial random phase fluctuation is introduced in each laser chip. One could either lower the injected current or reduce the phase length to get rid of the repetitious modes. Since decreasing the injected current does not lead to increasing the production yield, we looked at reducing the length of the phase region. We took the maximum injected current level which is limited by the isolation resistance and recombination mechanisms to be 100 mA. We varied the phase region length between 50 and 200 μm and observed the effects on tuning. The optimum tuning length was 100 μm which gave us two complete mode jumps we were looking. A synopsis of results for various Bragg wavelengths and normalized coupling coefficients can be seen in fig 1 for a phase region length of 100 μm. The optimum conditions determined by the same methods above yielded a κL value of 1.5 and a Bragg wavelength of 1.58 μm. At these optimum parameters, we observed a higher tuning range of 55 GHz than at the 200 μm phase length as can be seen in fig 5. This is due to the lesser losses occurring for the injected current with a smaller phase region length as can be seen is eq. 4 and eq. 5. Also the tuning rate was lower starting off at 6.49 GHz/mA and ending at 0.81 GHz/mA at 2.4 mA and 40 mA, respectively.

The last mode on the high end of the tuning current region appears to have a very linear continuous tuning. This has an initial tuning rate of 0.645 GHz/mA and a final tuning rate of 0.352 GHz/mA over a continuous tuning range of 25.5 GHz, which was limited by the 100 mA of maximum injected current to the phase region. Although, operation in this tuning region appears very attractive, there are limitations caused by high losses and isolation resistance between the phase region and active region.

The next parameter analyzed is the effect caused by introducing phase fluctuations at the grating edge as mentioned previously. As we can see in fig 6, varying

Bragg Wavelength (μm)	Tuning Range (GHz)
1.57	58
1.575	58
1.58	55
1.585	51
1.59	50

Normalized Coupling Coefficient	Continuous Tuning Range (GHz)
1.0	53
1.25	59
1.5	55
1.75	50
2.0	47

Table 1: Results for a phase region of 100 μm; *i* - variation of Bragg Wavelength($\kappa L = 1.5$), *ii* - variation of $\kappa L(\lambda_{Bragg} = 1.58\mu$m).
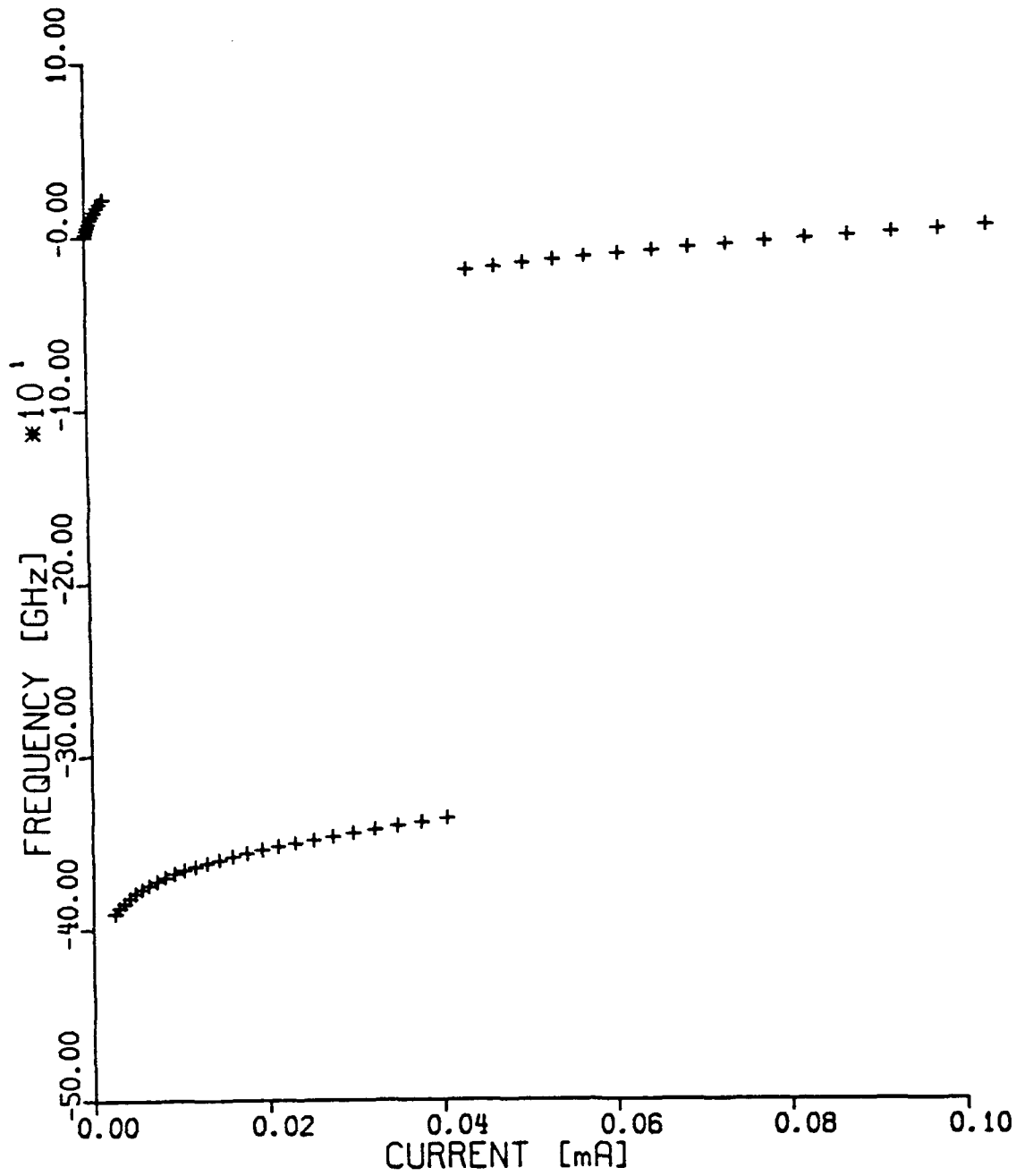
Figure 5: Frequency tuning characteristics with a Bragg wavelength of 1.58μm, phase length of 100 μm, and κL of 1.5.

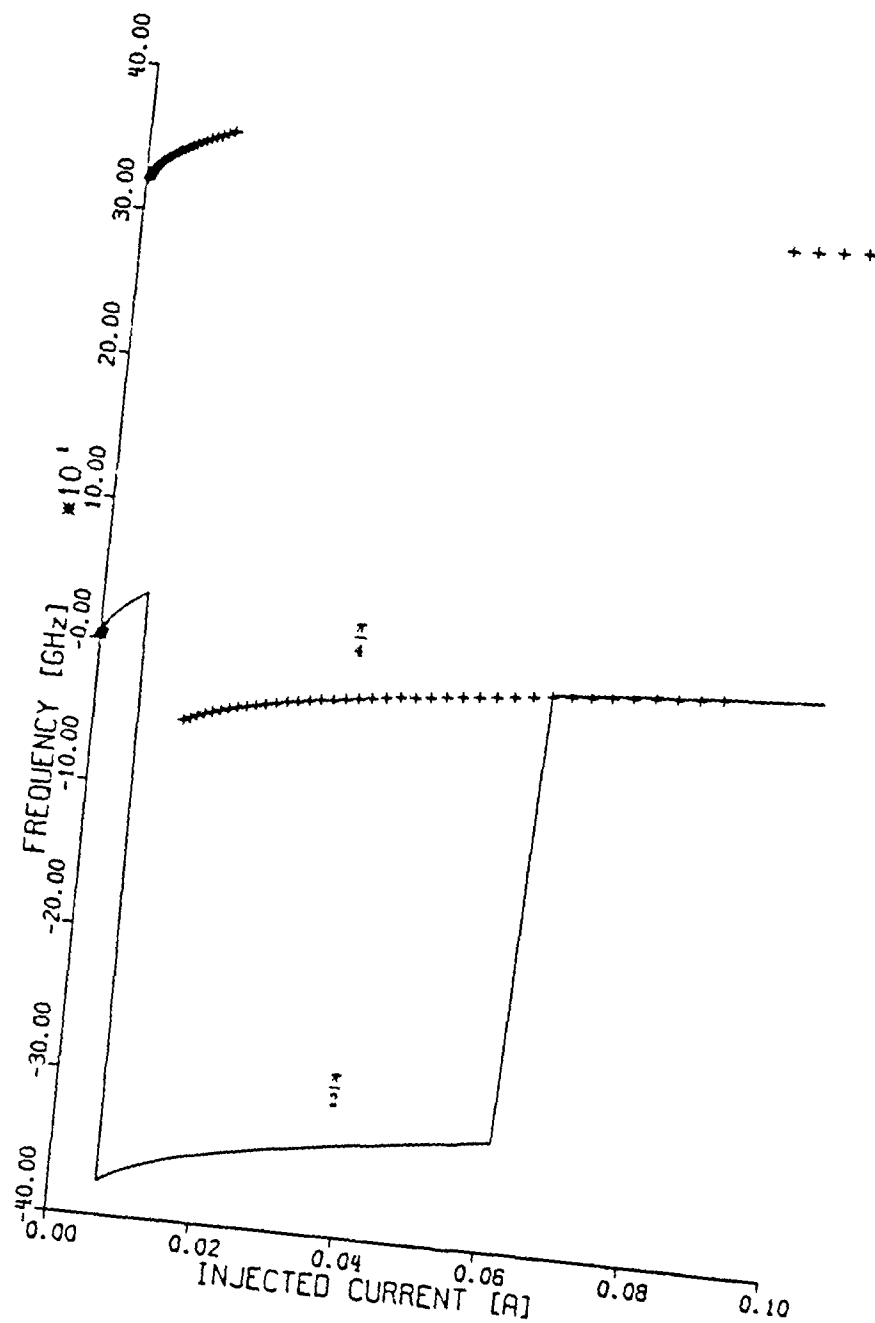Figure 6: Lasing frequency characteristics with a random angle of $\frac{\pi}{4}$ and $\frac{\pi}{2}$ introduced at r_1.

155

the initial phase only rotates the tuning region frequencies with respect to the injected current. As the initial phase fluctuated, the maximum continuous tuning region rotated toward the middle current range and the maximum tuning region became more linear. For random phase fluctuations with a length of 100 μm and an initial phase fluctuation of $\frac{\pi}{4}$, the tuning rate started at 3.73 GHz/mA and ended at 0.696 GHz/mA in the current range from 7.2 mA to 60 mA. This had a near linear continuous tuning range of 29.5 GHz for the linear region given by 0.77 GHz/mA$\pm$0.28GHz/mA. For the random phase of $\frac{\pi}{2}$ the rate was 1.14 GHz/mA at the current of 12.9 mA and 0.45 GHz/mA at the current of 85.6 mA. The maximum continuous tuning range remained the same at 55 GHz with random phases introduced.

4   Conclusions

From our results for the type of structure analyzed one can see that the normalized coefficient and phase region length play the biggest determination in the tuning range. To obtain a wide tuning range a normalized coupling coefficient of 1.5 or better is needed to provide good mode selectivity bearing in mind that the linewidth is reduced by over coupling the laser cavity. If accurate data on gain curves and variable gains are not accessible, then the use of a higher normalized coupling coefficient is needed. Phase lengths must be of the order of 100 μm are needed to produce a linear tuning region of approximately 28 GHz.

5   References

1. K.Y. Liou *et.al.*,"Linewidth characteristics of fiber-extended cavity DFB laser", *Appl. Phys. Lett.*, vol.48, pp.1039-1041, 1986.

2. S. Murata, I. Mito, and K. Kobayashi,"Frequency modulation and spectral characteristics for a 1.5 μm phase tunable DFB", *Electron. Lett.*, vol.23, pp.12-13, 1987.

3. R.W. Tkach and A.R. Chraplyvy,"Regimes of feedback effects in distributed feedback lasers", *J. of Lightwave Tech.*, vol.Lt-4, pp.1655-1661, 1986.

4. A.R. Charplyvy *et. al.*,"Simple-narrow-linewidth 1.5 μm InGaAsP DFB external cavity lasers", *Electron. Lett.*, vol.22, pp.88-89, 1986.

5. G.P. Agrawal and N.K. Dutta, *Long-Wavelength Semiconductor Lasers*, Van Nostrand Reinhold Company Inc., New York, New York, 1986.

6. H. Olesen, X. Pan and B. Tromberg,"Theoretical analysis of tuning properties for a phase-tunable DFB laser", to be published in *IEEE J. Quantum Electron.*, 1988.

7. B. Tromberg, H. Olessen, X. Pan, S. Saito,"Transmission line description of optical feedback and injection locking Fabry-Perot and DFB lasers", *IEEE J. of Quantum Electron.*, vol.QE-23, pp.1875-1889, 1987.

8. N.K. Dutta,"Calculated absorption, emission and gain in $In_{.72}Ga_{.28}As_{.6}P_{.4}$", *J. of Appl. Phys.*, vol.51, pp.6095-6099, 1980.

9. S. Tsuji *et. al.*,"Low threshold operation of 1.5 μm DFB laser diodes", *J. of Lightwave Tech.*, vol.Lt-5, pp.822, 1987.

10. S. Soda *et. al.*, *Electron. Lett.*, vol.22, pp.1047, 1986.

MANUSCRIPT 2

Linewidth considerations for DFB External Cavity Lasers

Linewidth Considerations for DFB External Cavity Semiconductor Lasers

Harish R. D. Sunak & Clark P. Engert
Fiber Optical Communications Laboratory
Department of Electrical Engineering
University of Rhode Island
Kingston, RI 02881-0805

1 Introduction

Coherent fiber optical communication systems(COFOCS) have a much better sensitivity and increased channel selectivity over direct-detection intensity modulation(DD-IM) communication systems. Multichannel systems have been proposed which would exploit the low-loss window of silica-based fibers. However, presently solitary semiconductor lasers do not possess the narrow linewidth requirement for COFOCS which utilize the most stringent encoding schemes that offer the best performance improvement. To decrease the linewidth of solitary DFB lasers, external cavities have been added to increase the lifetime of the photons in the cavity.[1,2] By utilizing the strong feedback regime when the power feedback is greater than 10%,[3] these optical sources reduce the solitary linewidth and have greater insensitivity to reflected feedback. One structure utilizing a single mode fiber as an external cavity had a reduction of the solitary linewidth by 1000 fold and was insensitive to a -20dB reflective feedback.[1]

Our work will characterize the critical parameters which will determine the reduction in the linewidth. By starting with the solitary linewidth we will develop into the external cavity linewidth. While doing this we will keep in mind the three different architectures generally used; DFB + GRIN-rod, DFB + Mirror Cavity,

and DFB + Single-Mode Fiber. An example of the type of structure being analyzed is seen in fig 1.

2 Theoretical Consideration

2.1 Solitary Linewidth

We start with the linewidth of the solitary DFB laser which can be derived from the Shawlow-Townes expression and taking into account the linewidth broadening we get,[4]

$$\Delta\nu = \frac{n_{sp}v_g^2 h\nu\alpha_m\left(\alpha_m + \alpha_{int}\right)}{8\pi P_o}\left(1 + \alpha^2\right) \tag{10}$$

where v_g is the group velocity, $h\nu$ is the energy of the photon emitted, α_{int} is the sum of all the internal losses, n_{sp} is the spontaneous emission factor, P_o is the output power from the facet, α_m is the cavity loss, and α is the linewidth enhancement factor. These parameters will be developed more to give a complete understanding of the linewidth parameter.

The spontaneous emission factor is given by

$$n_{sp} = \frac{1}{1 - exp(\frac{h\nu - eV}{kT})} \tag{11}$$

where eV is the quasi-Fermi level seperation, T is the absolute temperature and k is Boltzmann's constant. The mode loss can be determined from the threshold equation for a DFB laser given by [5]

$$\left(\frac{r_a - r}{1 - rr_a}\right)\left(\frac{r_b - r}{1 - rr_b}\right)exp\left(2i\gamma L\right) = 1 \tag{12}$$

where r is the effective DFB reflection coefficient, $r_{a,b}$ are the effective reflectivities of the facets which take into account the losses of the phase and external cavity, γ is the complex wave number, L is the active region length of the DFB. The propagation factor in the active cavity region is given by

$$\gamma = \pm \left[\Delta \beta^2 + \kappa^2 \right]^{\frac{1}{2}} \tag{13}$$

where $\Delta \beta$ is the difference between the mode propagation constant and the Bragg wavelength, and κ is the value of the coupling coefficient. The $\Delta \beta$ can also be expressed in terms of its real and imaginary parts given by the detuning parameter, δ, and the mode loss, $\frac{\alpha_m}{2}$. The linewidth enhancement factor, α, is the ratio of the change of the real part of the refractive index to the imaginary part of the refractive index during relaxation oscillations.

The effective reflectivity in its most general form is given by [6]

$$r_{a,b} = \frac{r_{1,2} + \left[\eta^2 \left(1 - r_{1,2}^2 \right) - r_{1,2}^2 \right] f_{1,2} \exp \left(-j 2 \gamma_{p,ex} L_{p,ex} \right)}{1 - r_{1,2} f_{1,2} \exp \left(-j 2 \gamma_{p,ex} L_{p,ex} \right)} \tag{14}$$

where the phase region is signified by p, the external region is signified by ex, and the first indices corresponds to the phase region and the second corresponds to the external region. It is assumed as in ref.[6] that the reflectivities, coupling, and transmission coefficients are equal whether seen from the inside of the laser cavity or the external cavity interface. It is also assumed that forward and backward transmission coefficients are equal multipling together to give the $\left(1 - r_{1,2}^2 \right)$ term.

A numerical calculation of the linewidth for a typical solitary DFB laser linewidth of length 250 μm operating at 1.55 μm is as follows. For an output power of 2 mW, n_{sp} of 1.7, $\alpha_m = 60$ cm^{-1}, $\alpha_{int} = 44$ cm^{-1}, α of 5.4, and v_g of 0.75×10^{10} cm s^{-1} we get a value of 45.47 MHz for the solitary laser linewidth.[7]

2.2 External Cavity

With the addition of an external cavity in the high feedback regime, the linewidth of the structure is reduced. In essence, with the addition of the external passive cavity, the laser structure can be considered as an extended cavity laser with the DFB acting as the active region. By adding a passive cavity one increases the number of photons in the cavity and decreases the spontaneous emission rate according to the ratio of the total cavity power to the power in the semiconductor cavity or its inverse, respectively.

From [8] the linewidth with the addition of an external cavity laser for a FP laser is given by,

$$\Delta\nu = \frac{n_{sp}v_g \left[\frac{\alpha_{int}L - \ln r_a |r_b(w)|}{L} \right]}{4\pi P_o} WF\left(1 + \alpha^2\right) \qquad (15)$$

where,

$$W = \frac{v_g h\nu}{L} \ln\left(r_a \mid r_b(w)\mid\right)^{-1} \times \left[1 + \frac{r_a}{\mid r_b(w)\mid}\frac{1 - \mid r_b(w)\mid^2}{1 - r_a^2}\right]^{-1} \qquad (16)$$

and,

$$F = \left[1 + \frac{1}{\tau_{in}}Re\left(j\frac{1}{r_b(w)}\right) - \frac{\alpha}{\tau_{in}}Im\left(j\frac{1}{r_b(w)}\frac{dr_b(w)}{dw}\right)\right]^{-2} \qquad (17)$$

where τ_{in} is the round-trip time according to the group velocity, v_g, or the reciprocal mode spacing of the solitary laser. W represents the ratio of output power, P_o, to the photon number in the cavity and F gives the effective frequency dependence on the feedback. Recognizing that the $\frac{1}{L}\ln\left(r_a \mid r_b(w)\mid\right)^{-1}$ is the mirror loss of a FP laser with the rear facet of r_b, we can relate the mirror loss to the mirror loss of the DFB laser. From which we get

$$\Delta\nu = \frac{v_g n_{sp}}{4\pi P_o}\left(\alpha_{int} + \alpha_m\right)WF\left(1 + \alpha^2\right)^{-1} \qquad (18)$$

where,

$$W = v_g h\nu\alpha_m \times \left[1 + \frac{r_a}{\mid r_b(w)\mid}\frac{1 - \mid r_b(w)\mid^2}{1 - r_a^2}\right]^{-1} \qquad (19)$$

and F remains the same as before, and α_m is the mirror loss of a DFB with a rear facet r_b and τ_{in} corresponds to the mode spacing of the DFB with r_b as the back facet.

With the rear facet of the semiconductor cavity zero, the reduction in the solitary linewidth is given by [8]

$$\Delta\nu = \Delta\nu_{sol}\left(1 + \frac{\tau_{ex}}{\tau_{in}}\right)^{-2} \qquad (20)$$

where $\Delta\nu_{sol}$ is the solitary laser linewidth with its rear facet equal to the effective feedback of the external cavity, τ_{in} is the reciprocal mode spacings and τ_{ex} is the round trip time in the external cavity($\tau_{ex} = 2L_{ex}n_{ex}/v_{gex}$). The reciprocal mode spacing for a DFB can be determined from the threshold condition for a DFB. The difference between the lasing mode and its nearest side mode can be expressed in terms of the normalized detuning parameter. From which the time a photon spends in a DFB laser is equal to

$$\tau_{in} = \frac{2\pi L n}{c \mid \Delta\overline{\delta_{l,sm}} \mid} \tag{21}$$

where c is the speed of light, n is the refractive index in the laser cavity, L is the length of the active region and $\Delta\overline{\delta_{l,sm}}$ is the difference between the normalized detuning parameter($\overline{\delta} = \delta L$).

3 Design Parameters

The first parameter which will be analyzed is the criterion for a power feedback of 10% which is needed to operate in the high feedback regime. Equation 14 gives the effective amplitude reflectivity feedback in terms of the rear facet, r_2, η, the coupling efficiency, and the cavity facet reflectivity. Since r_2 must be small, so that the device operates as an extended cavity laser, we set this value to an empirically used value of 0.0707. The coupling efficiency is varied for the different typesw of cavities used. Therefore, we found the minimum value for f_2 which would give the 10% power feedback required. Our results are shown in fig. 7 in which the coupling efficiency is varied and the value of f_2 is determined. From this picture, a coupling efficiency of at least 27% is needed to operate in the high feedback regime. From this diagram, one can determine the facet reflectivity needed for the type of external cavity structure used.

The next parameter, the linewidth reduction, is dependent upon the operation point of the DFB laser which changes with tuning. Fig 8 shows the frequency tuning of the structure versus injected current into the phase region. As tuning

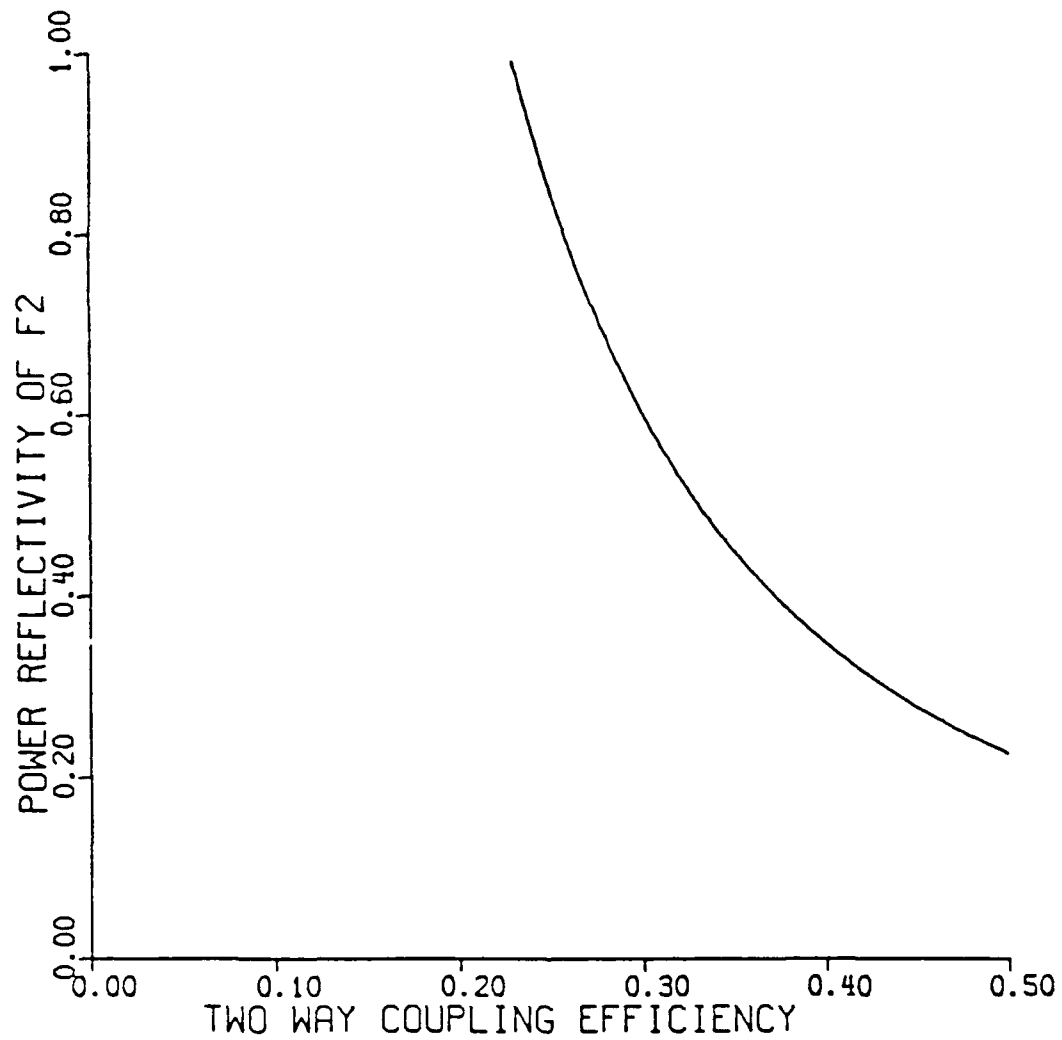Figure 7: Minimum value needed for facet reflectivity versus the two-way coupling efficiency, η^2.

takes place the operation point of the DFB laser changes and this causes the amount of reduction of the solitary linewidth to change. Fig 9 illustrates the threshold current of the lasing mode. This figure gives us an approximation of the solitary laser linewidth versus tuning since the threshold current is proportional to the sum of the mode loss and the internal loss. From figure 3, we can see, in the maximum continuous tuning range(3.7mA-40 mA), the threshold changes from 19.7 to 18.8 mA which corresponds to a decrease of 13.5% in the losses. Thus we expect the solitary linewidth would also change by about a factor of about 20% over the tuning range. The reduction change with tuning for various normalized coupling coefficients(κL) can be seen in figure 4. Previously the κL value of 1.5 was found to be optimum for tuning. For this value the linewidth reduction changes from 5231 to 4600 for an external fiber cavity of 5.5 cm. Thus we must chose the external cavity length with the minimum reduction factor of 4600 over the maximum tuning range.

The effect coupling has on the laser linewidth reduction can also be seen in fig 10. The higher the coupling coefficient, the less the linewidth reduction of the solitary linewidth. Physically, the greater the κL value tends to store more power in the laser cavity, thereby reducing the ratio of the total structure power to semiconductor power stored.

From equation 20 we see as the external cavity gets longer the solitary linewidth reduction factor gets larger. In our analysis, there is not a linewidth floor , however, experimentally[9] and theoretically[10] a floor exists on the absolute linewidth in the range of 10 to 20 kHz. Since requirements for practical systems of PSK homodyne detection systems at bit rates of 140 Mbits/s or greater do not need such a narrow linewidth, our analysis is correct. In fig 11 we have plotted the linewidth reduction for external cavities of different index of refractions corresponding to an air cavity and a single-mode fiber cavity or GRIN-rod cavity. We see that the reduction is much less for fiber or Grin-rod cavities. Since GRIN-rod cavities only come in lengths of maximum 4 mm, the maximum reduction for a GRIN-rod cavity is 34. Comparatively, a thousand fold reduction in the linewidth for an air cavity would require a length of 38 mm while for a single-mode fiber cavity the length
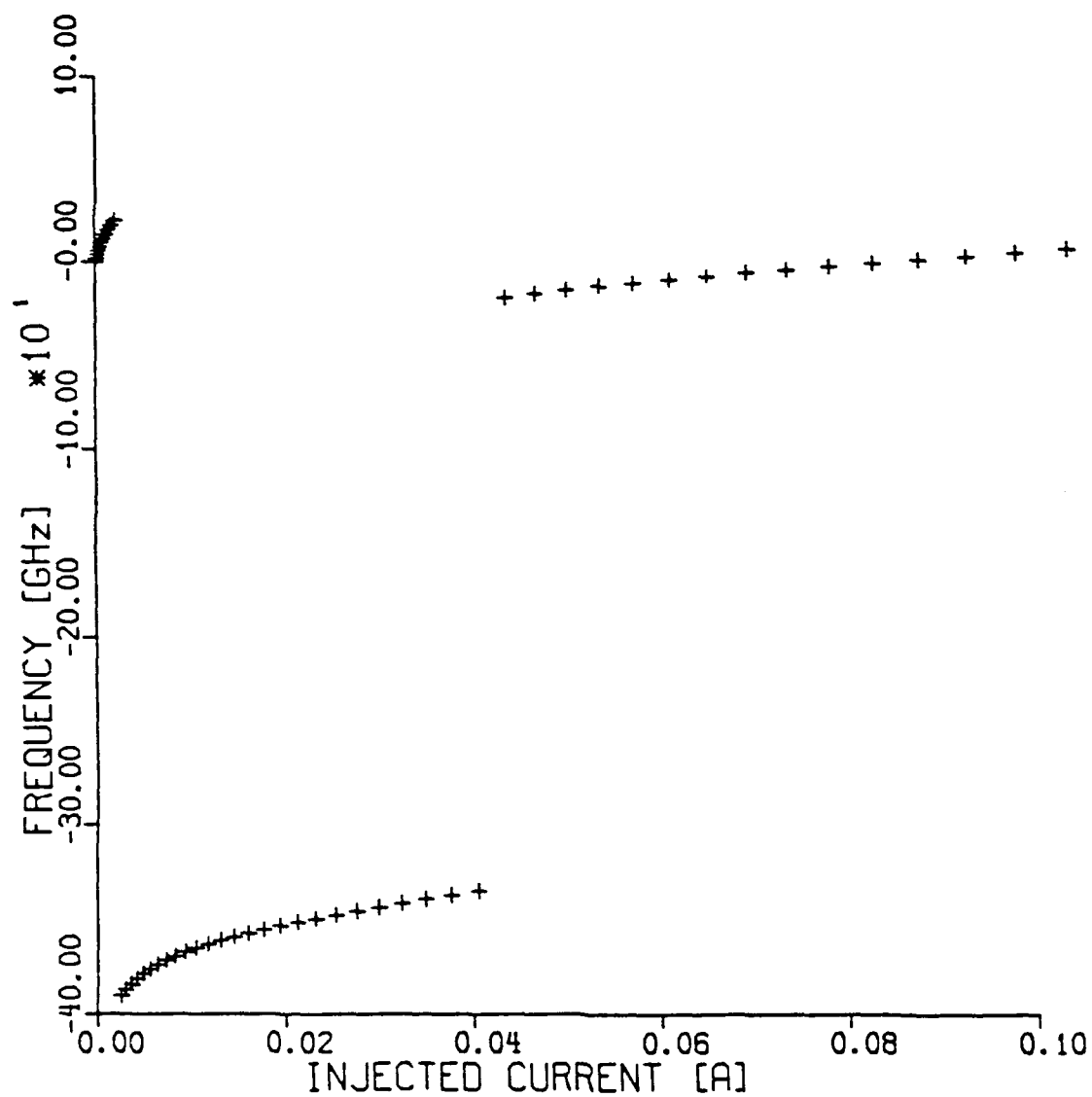
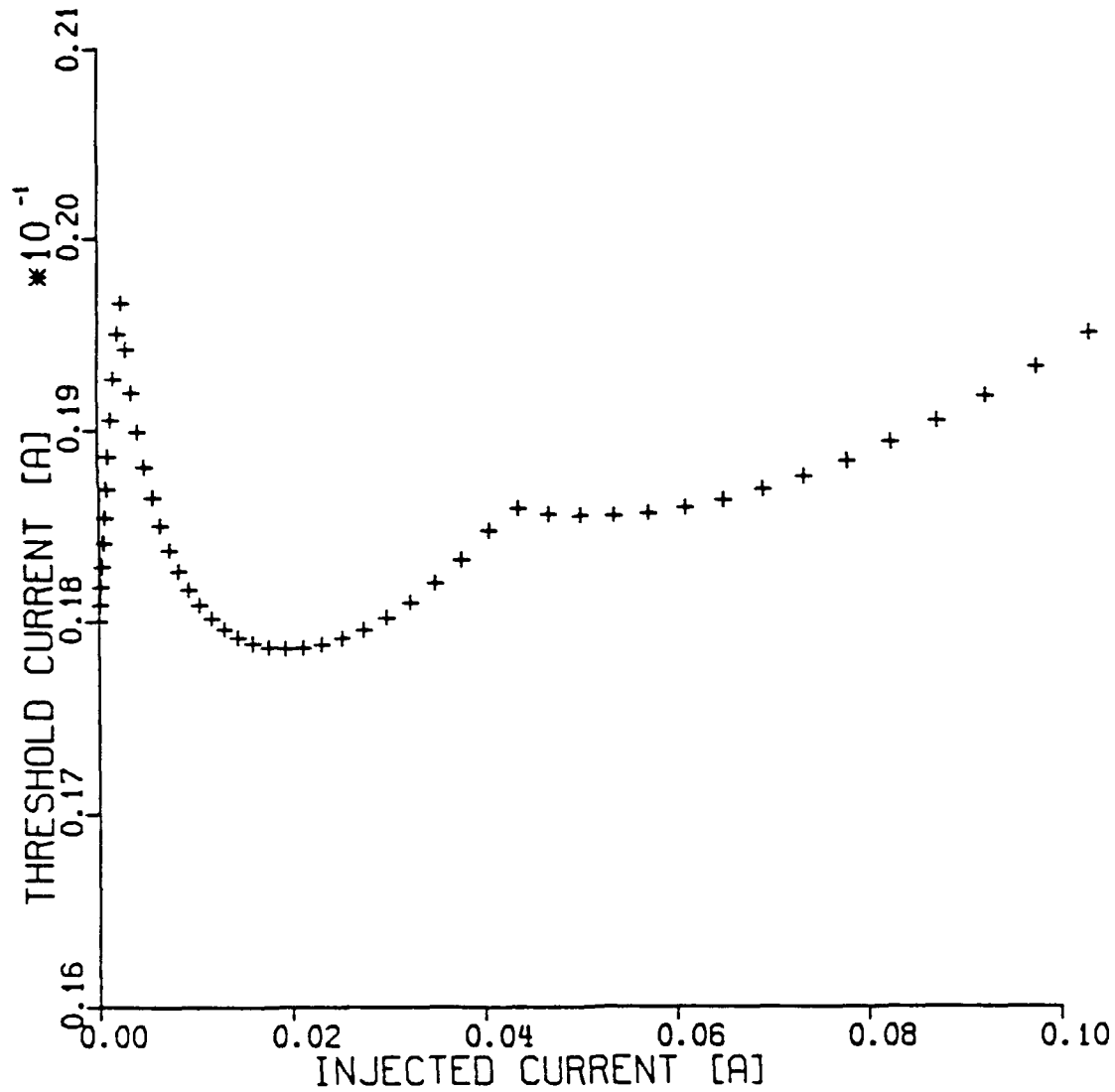Figure 8: Frequency plot versus injected current into the phase region for a 100 μm long phase region with a κL of 2 and λ_{Bragg} of 1.58 μm.

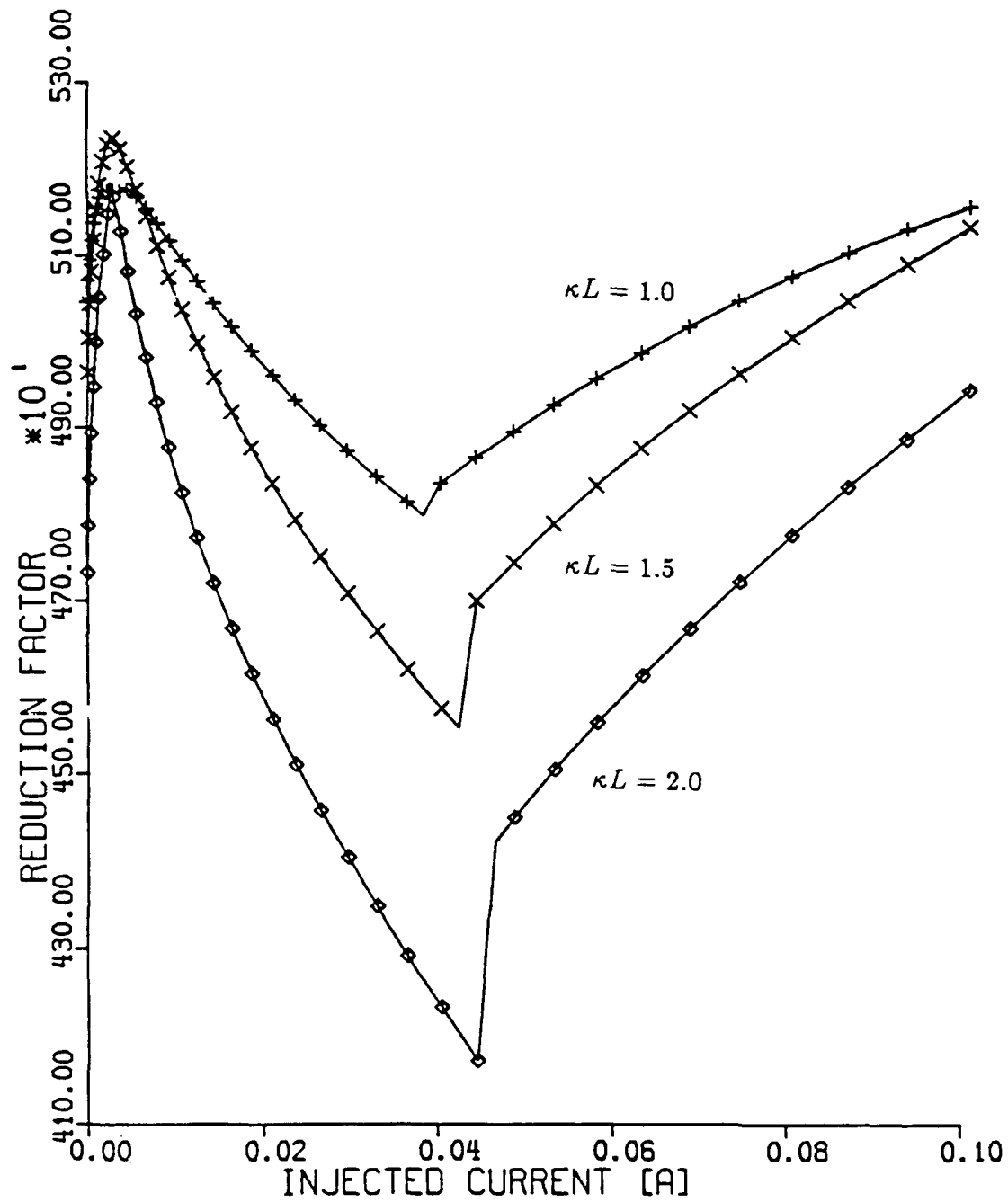Figure 9: Threshold current of the lasing mode verus injected current in the phase region.

Figure 10: Reduction factor for different normalized coupling coeficients.
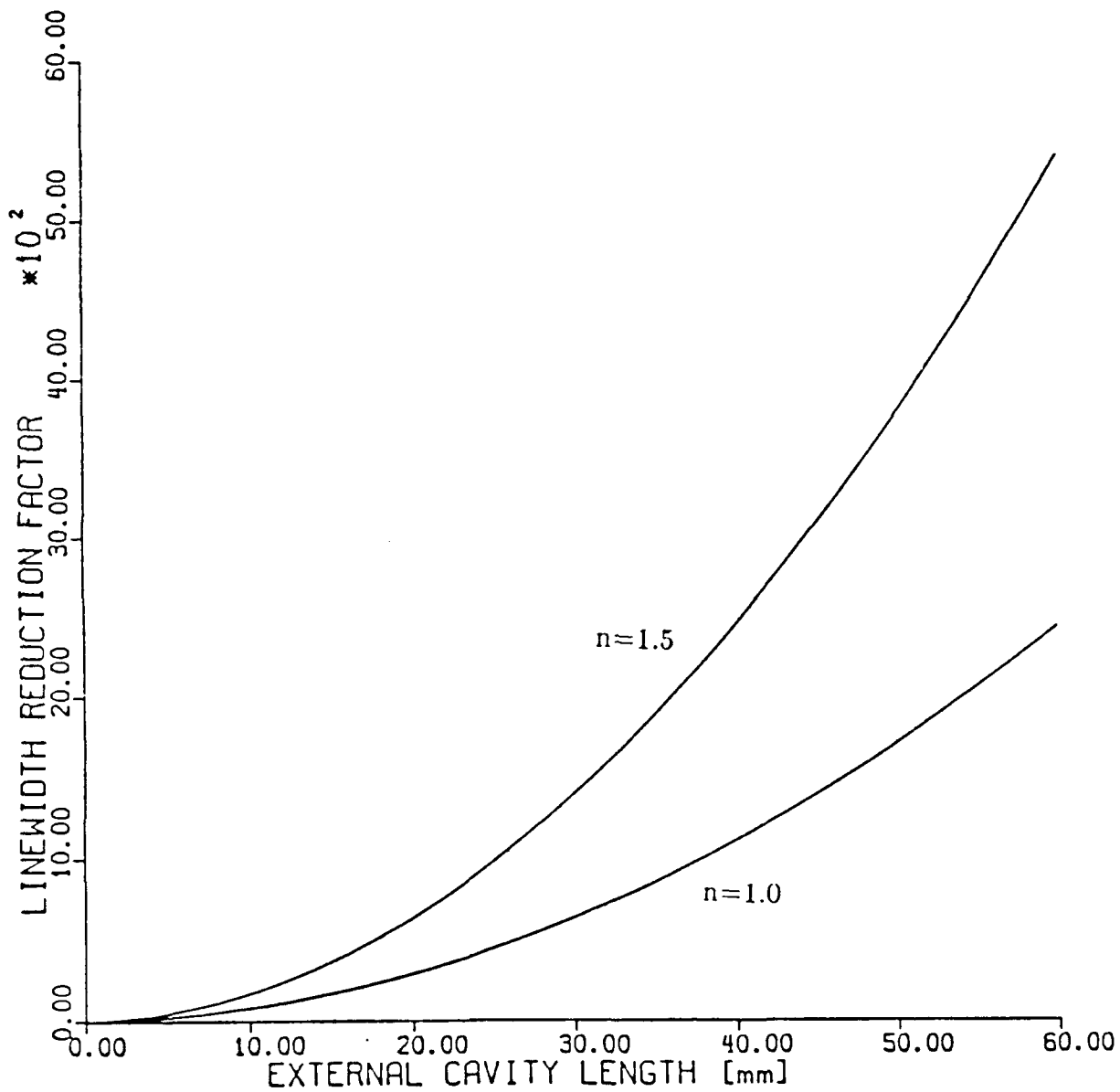
Figure 11: Length versus reduction for external cavities of different index of refraction. The reduction factor plotted is the minimum of the maximum continuous tuning region.

169

DFB-ECSL FOR COFOCS

BIT RATE=140 MBITS/SEC

Modulation	Demodulation	Linewidth	Structure	Optimum Length[mm]
ASK FSK	Heterodyne with envelope Detection	14 MHz to 70 MHz	*Solitary DFB*[†] GRIN-rod	4.0
DPSK	Heterodyne with delay time demodulation	420 kHz to 700 kHz	*Fiber Cavity* Mirror Cavity	8.5 - 7.0 12.5 - 9.5
PSK	Heterodyne	420 kHz to 700 kHz	*Fiber Cavity* Mirror Cavity	14.5 - 7.0 22.0 - 9.5
PSK	Homodyne	70 kHz to 140 kHz	*Fiber Cavity* Mirror Cavity	21.5 - 7.0 32.0 - 9.5

†Most practical structure is shown in italics.

Table 2: Summary of length requirements for the different structures used with different modulation schemes.

DFB-ECSL FOR COFOCS

BIT RATE=565 MBITS/SEC

Modulation	Demodulation	Linewidth	Structure	Optimum Length[mm]
ASK FSK	Heterodyne with envelope Detection	56 MHz to 282 MHz	*Solitary DFB*	
DPSK	Heterodyne with delay time demodulation	1.7 MHz to 2.83 MHz	*GRIN-rod* Fiber Cavity Mirror Cavity	4.0 3.5 - 3.0 5.5 - 4.0
PSK	Heterodyne	565 kHz to 2.83 MHz	*Fiber Cavity* Mirror Cavity	7.0 - 3.0 10.5 - 4.0
PSK	Homodyne	282 kHz to 565 kHz	*Fiber Cavity* Mirror Cavity	10.5 - 7.0 15.5 - 10.5

†Most practical structure is shown in italics.

Table 3: Summary of length requirements for the different structures used with different modulation schemes.

171

DFB-ECSL FOR COFOCS

BIT RATE=1.2 GBITS/SEC

Modulation	Demodulation	Linewidth	Structure	Optimum Length[mm]
ASK FSK	Heterodyne with envelope Detection	120 MHz to 600 MHz	*Solitary DFB*	
DPSK	Heterodyne with delay time demodulation	3.6 MHz to 6.0 MHz	*GRIN-rod* Fiber Cavity Mirror Cavity	4.0 2.5 - 1.5 3.5 - 2.5
PSK	Heterodyne	1.2 MHz to 6.0 MHz	*Fiber Cavity* Mirror Cavity	4.5 - 1.5 7.0 - 2.5
PSK	Homodyne	600 kHz to 1.2 MHz	*Fiber Cavity* Mirror Cavity	7.0 - 4.5 10.5 - 7.0

†Most practical structure is shown in italics.

Table 4: Summary of length requirements for the different structures used with different modulation schemes.

DFB-ECSL FOR COFOCS

BIT RATE=2.4 MBITS/SEC

Modulation	Demodulation	Linewidth	Structure	Optimum Length[mm]
ASK FSK	Heterodyne with envelope Detection	240 MHz to 1.2 GHz	*Solitary DFB*	
DPSK	Heterodyne with delay time demodulation	7.2 MHz to 12.0 MHz	*GRIN-rod*	4.0
PSK	Heterodyne	2.4 MHz to 12.0 MHz	*GRIN-rod* Fiber Cavity Mirror Cavity	4.0 1.0 - 3.0 4.5 - 1.5
PSK	Homodyne	1.2 MHz to 2.4 MHz	*Fiber Cavity* Mirror Cavity	4.5 - 3.0 6.5 - 4.5

†Most practical structure is shown in italics.

Table 5: Summary of length requirements for the different structures used with different modulation schemes.

required need only be 26 mm.

Different modulation schemes and detection schemes require different linewidth at their appropriate bit rates. In tables 2 to 5 we have listed the required lengths for the respective structure. In these tables, the solitary linewidth of the DFB is assumed to be 50 MHz. Also, the preferred structure is labeled based on the length of the cavity. When reductions from the solitary linewidth are less than 34, the most practical structure is a GRIN-rod cavity due to the small size of the cavity. Above this value, the practical structure is the fiber cavity. It requires shorter lengths than the mirror cavity and is less susceptible to perturbations in the air of the cavity.

4   Conclusions

From our results, we can see that a two way coupling efficiency of at least 0.25 is needed to operate in the high feedback regime. The greater the coupling efficiency, the less the requirement on the rear facet reflectivity needed. Also, the length of the external cavity is very critical in the determination of the absolute linewidth of the laser. For reductions in the solitary linewidth of 34 or less, the GRIN-rod cavity is the most practical. For reductions in the solitary linewidth greater than 34, the single-mode fiber cavity is the most practical. The length of the external cavity required depends greatly on the solitary linewidth and the linewidth required from the system which depends upon the bit rate, modulation system and the error-free transmission rate required.

5   References

1. K.Y. Liou *et. al.*,"Linewidth characteristics of fiber-extended cavity DFB lasers",*Appl. Phys. Lett.*, vol.48, pp.1039-1041, 1986.

2. A.R. Charplyvy *te. al.*,"Simple-narrow-linewidth 1.5 μm InGaAsP DFB external cavity lasers",*Electron. Lett.*, vol."?, pp.88-89, 1986.

3. R.W. Tkach and A.R. Chraplyvy,"Regimes of feedback effects in distributed feedback lasers".*J. of Lightwave Tech.*, vol.Lt-4, pp.1655-1661, 1986.

4. K. Keisuke *et. al.*,"Analysis of the Spectral Linewidth of Distributed Feedback Laser Diodes",*J. of Light. Technol.*, vol.LT-3, pp.1048-1055, 1985.

5. G.P. Agrawal and N.K. Dutta,*Long-Wavelength Semiconductor Lasers*, Van Nostrand Reinhold Company Inc., New York, New York, 1986.

6. H. Olesen, X. Pan and B. Tromberg,"Theoretical analysis of tuning properties for a phase-tunable DFB laser", to be published in *IEEE J. Quantum Electron.*, 1988.

7. C.H. Henry and R.F. Kazarinov,"Instabilities of Semiconductor Lasers Due to Optical Feedback from Distant Reflectors",*IEEE J. Quantum Electron.*, vol.QE-22, pp. 294-301, 1986.

8. E. Patzak *et. al.*,"Semiconductor Laser Linewidth in Optical Feedback Configurations",*Electron. Lett.*, vol.19, pp.110-112, 1983.

9. R. Wyatt and W.J. Devlin,"10 kHz Linewidth 1.5 μm InGaAsP External Cavity Laser with 55 nm Tuning Range",*Electron. Lett.*, pp.110-112, 1983.

10. A.P. Bogatov and P.G. Eliseev, "Theory of the Single-Mode Emission Spectrum of Semiconductor Laser",*Proc. of the 11th IEEE International Semiconductor Laser Conf.*, Boston,MA, Aug.29-Sept.1, pp.202-203, 1988.

MANUSCRIPT 3

Linewidth Calculations in
Tunable External Cavity Fabry-
Perot Semiconductor Lasers
with strong frequency-selective
feedback for coherent lightwave
systems

Linewidth Calculations in Tunable External Cavity Fabry- Perot Semiconductor Lasers with Strong Frequency-Selective Feedback for Coherent Lightwave Systems

I. Introduction

Significant research is being carried out in the world on various aspects of coherent fiber optical communication systems (COFOCS), devices and systems, because they offer two distinct advantages: (i) increased sensitivity (5-20 dB) and (ii) increased selectivity (100 MHz instead of 100 GHz) over direct-detection intensity modulation optical communications systems used these days. Semiconductor lasers are preferred as practical sources for COFOCS since they have the potential to be packaged robustly. For coherent optical communication systems, semiconductor lasers need to have fairly narrow linewidths ($\Delta\nu$). The exact requirement depends on the modulation format used (ASK, FSK, DPSK or PSK). Linewidths typically in the tens of kHz to tens of MHz are required for data rate in the hundreds of MHz range. Another important required feature in the coherent source is tunability, especially in the local oscillator to select the various channels transmitted simultaneously through the single-mode fiber. To obtain these features, various types of external cavity structures are being developed. These include C^3 [1], GRECC [2], fiber-external cavity [3], external mirror [4], bulk diffraction grating [5]-[6], fiber diffraction grating [7] etc. Linewidth reduction from the solitary laser linewidth is obtained in all these structures. These external cavity semiconductor lasers (ECSL) are based on the fact that the characteristics of the laser diode are affected by optical feedback. Among all the reported structures, ECSL with strong feedback, i.e., frequency selective feedback from a bulk diffraction grating, appears to be the most promising in terms of narrow linewidth and tunability. Wyatt et al. [5] have obtained the narrowest linewidth ($\sim$ 1 kHz) and the widest tuning range ($\sim$ 135 nm or $\sim$ 16000 GHz) with this arrangement.

The important design parameters of the ECSL which affect the linewidth are: optical

feedback ratio, reflectivity of the laser facet nearer to the feedback component, frequency detuning of the optical feedback, and the external cavity length. We have previously reported. only in abstract form, the dependence of $\Delta\nu$ on these parameters [8], and obtained good agreement with published experimental results. We now give more details of the analysis with further details of the optimum cavity length for minimum linewidth.

II. Theoretical Development

The configuration shown in Fig. 1 will be considered in this paper. r_1, r_2 and r_3 are the amplitude reflectivities of the diode facets and grating reflector respectively. t_2 is the transmissivity. n is the refractive index in active region of the solitary laser. τ_{in} and τ_{ex} are the round trip time in the solitary laser and external cavity respectively. κ is the cavity coupling coefficient between two cavities. The effective reflectivity r_{eff} can be written as

$$r_{eff} = \frac{r_2 + r_3(r_2^2 + \kappa^2 t_2^2)\exp(-j\delta)}{1 + r_2 r_3 \exp(-j\delta)} = r_e e^{j\phi}, \tag{1}$$

where $\delta = 4\pi L_{ex}/\lambda_i$ is a phase detuning. λ_i is the tunable wavelength due to diffraction grating.

In the analysis of a coupled optical resonator, the amplitude of the single longitudinal Fabry-Perot cavity mode becomes a dynamic variable. The change of the mode amplitude is governed by the field equation follows as [9]

$$\frac{d}{dt}E(t) = (\frac{\Delta G}{2} - iw)E(t) + kE(t - \tau_{in}), \tag{2}$$

where ΔG is the deviation from the threshold value in $\sec^{-1}$, and w is the frequency of the mode, k is the feedback coupling coefficient.

From this field equation, we may obtain [10]-[13] the spectral linewidth $\Delta\nu_{ex}$ for the ECSL with strong feedback as

$$\Delta\nu_{ex} = \Delta\nu_0 \cdot \left(\frac{L_0}{L_{eff}}\right)^2, \tag{3}$$

178

where $\Delta \nu_s$ is the solitary laser linewidth with $r_2 = r_e$ in equation (1) and L_{eff} is the effective external cavity length and is given by [10],[13]

$$L_{eff} = L_0 \left(1 + \frac{1}{\tau'_{in}} \frac{d}{dw} [\varphi(w) + \alpha r_e(w)] \right),$$ (4)

where τ'_{in} is the round trip time with group velocity. We may express L_{eff} for $\delta = 0$ and $\kappa = 1$ as

$$L_{eff} = L_0 \left(1 + \frac{\tau_{ex}}{\tau'_{in}} \frac{r_3(1 - r_2^2)}{r_3(1 + r_2^2) + r_2(1 + r_3^2)} \right),$$ (5)

Henry [14] has derived the linewidth of a solitary laser as

$$\Delta \nu_s = \frac{v_g^2 h \nu g_0 n_{sp} \alpha_0}{8 \pi P} (1 + \alpha^2),$$ (6)

where v_g is the group velocity, $h\nu$ is the bandgap energy, g_0 is the threshold gain, α_0 is the mirror loss, n_{sp} is the spontaneous emission factor, α is the linewidth enhancement factor, P is the output power.

When an ECSL is assembled, some parameters in equation (6) change their values. These are ν, g_0, n_{sp}, α_0, and P. The value of α will change if the optical feedback is coherent, because the increased stimulated emission rate due to feedback is proportional to the feedback intensity as long as it is coherent; whereas the spontaneous rate is independent of coherent feedback. These changes in parameter values are important and obviously affects the linewidth. Substituting equation (6) into (3) we can obtain

$$\Delta \nu_{ex} = \Delta \nu_s \cdot M \cdot \left(\frac{L_0}{L_{eff}} \right)^2,$$ (7)

where M represents changes in the parameter values and is given by

$$M = \frac{2 g_t(w) \alpha_m(w) f_c}{g_0 \alpha_0} \left(1 + \frac{r_1}{r_e} \frac{1 - r_e^2}{1 - r_1^2} \right)^{-1},$$ (8)

where $g_t(w)$ and $\alpha_m(w)$ are the threshold gain and mirror loss in compound cavity laser, and f_c is a correction factor considering the AR coating [12].

179

Before we state the expression for $g_t(w)$ in equation (8), we need to consider the nonlinear gain effect due to strong optical feedback. This nonlinear gain results mainly from both spectral and spatial hole burning. There is a gain reduction in the Fabry-Perot modes due to hole burning [13]. In other words, there is an induced absorption $\delta\alpha$, which is responsible for the side mode suppression [15]. Thus $g_t(w)$ can be written as

$$g_t(w) = \alpha_l + \delta\alpha + \alpha_m(w), \tag{9}$$

where α_l is the medium loss in the active region and $\alpha_m(w)$ is given by

$$\alpha_m(w) = \frac{1}{L_0} \ln \frac{1}{r_1 r_e}. \tag{10}$$

Even though equation (3) predicts that the linewidth is a linear function of L_{ex}^{-2}, this relationship does not hold for long external cavity lengths. Kuo and Ziel [16] have observed this dependence in the linewidth reduction of ECSL with strong feedback, as long as L_{ex} is less than ~ 7 cm. Clearly, the cavity Q factor increased with the addition of the external reflector. This enhancement of the Q factor is responsible for the reduction in spectral linewidth. However, the maximum value of the Q factor in an ECSL operating in the single mode regime is limited by the excitation of satellite modes and dispersive mode coupling [17]. The maximum value of L_{eff} in equation (7) for the minimum linewidth can be written as [17]

$$L_{max} = L_0 \left(1 + \frac{\kappa}{2\pi\tau_{in}} \frac{1}{\Delta\nu_s} \right). \tag{11}$$

If we put $\kappa = 0.5$, $L_0 = 250$ μm, $\Delta\nu_s = 20$ MHz, $M = 4$, we find that the minimum achievable linewidth $\Delta\nu_{ex}$ is 180 Hz. When $\Delta\nu_s = 100$ MHz for a solitary 1.55 μm laser with 1mW output, the minimum $\Delta\nu_{ex}$ calculated gives 5.6 kHz. Olsson and Ziel [6] obtained $\Delta\nu_{ex} = 7.4$ kHz with $L_{ex} = 18$ cm. Thus the theoretical prediction of equation (11) gives excellent agreement with experimental data. Therefore, the minimum or limiting value of $\Delta\nu_{ex}$ depends on the solitary laser linewidth. Fig. 2 shows the minimum $\Delta\nu_{ex}$ as a function of $\Delta\nu_s$. When $\Delta\nu_s$ is greater than about 1 GHz, we shall consider the spectral bandwidth

of the optical feedback [18]. In this paper we ignore the coherence pumping effect due to the narrow band feedback (<1 GHz).

III. Numerical results

It is well known that very small optical feedback ($\sim 10^{-6}$) affects the dynamic characteristics of semiconductor lasers. We initiated the numerical calculations with very small optical feedback to simulate this phenomena. As shown in Fig. 3, there is a linewidth fluctuation with very small values of R_3. This figure is in good agreement with the phenomena. This also implies that the linewidth equations derived in the previous sections work for the weak feedback regime. We shall examine the effects of four critical parameters: r_2, r_3, L_{ex}, and frequency detuning.

The frequency detuning can be defined as [5]

$$\phi = \frac{\delta w}{\Delta w} \times 360, \tag{12}$$

where δw is the frequency detuning from the spontaneous emission peak in the gain spectrum, and Δw is the internal mode spacing of the semiconductor laser. Fig. 4 shows the dependence of the lorentzian linewidth, normalized to 1 mW, on the detuning angle (ϕ) from the exact resonance condition. We have shown detuning both for $-\phi$ and $+\phi$ ($-\phi$ means external cavity mode is on the longer wavelength side of Fabry-Perot longitudinal mode). Hence the direction of the detuning is of critical importance. Also, for $-\phi$ tuning, a minimum linewidth of 110 Hz exists at $\phi = -154°$ for the cavity parameters indicated, but, if not controlled effectively, can result in large broadening at $\phi = -188°$ and $-314°$ with linewidths of 63 kHz and 100 MHz respectively. The unstability for small angles of $+\phi$ is clearly observed as commented in Ref [5]. Fig. 5 shows the linewidth fluctuation dependence on the detuning angle with the reflectivity of the AR coated facet as a parameter. This figure indicates that R_2 needs to be much less than about 0.5 % for the linewidth stability regardless of feedback detuning.

Fig. 6 shows the linewidth dependence on R_2 with R_3 as a parameter, for fixed values of L_{ex}=10 cm and ϕ=0. We can conclude that it is more important to have very low values of R_2 (<5 %) than high values of R_3 (>10 %). This is further confirmed in Fig. 7 where we show the dependence of the linewidth on R_3 with R_2 as a parameter. As we can observe, the linewidth increases substantially for very low values of R_3, <1 %. Small changes in the cavity parameters, in this low feedback region, due to external perturbations or internal frequency beating, causes instability. For instance, the internal field in the gain medium with frequency w_0 will interact with an injected optical field. When the feedback has a relatively wide frequency bandwidth, induced polarization occurs, which contains combination frequencies $w_i \pm$ n$(w_0 - w_i)$, where n=1,2,3,... The different polarizations at these beat frequencies in turn result in a change of the carrier density in the compound cavity modes. This change seems to be enough to cause linewidth instability. Thus, we need to have R_3 greater than $\sim$ 10 % for the stable operation. Fig. 8 is different version of Fig. 7. Fig. 8 also shows the dependence of the linewidth on R_3 by considering spectral density. As we can see, the lorentzian linewidth becomes narrower with stronger optical feedback.

Fig. 9 illustrates the linewidth as a function of the external cavity length with R_3 as a parameter and fixed values of R_2=4 % and ϕ=0. The linewidth is a linear function of L_{ex}^{-2} and the slope of the curve depends on R_2, R_3. The smaller the optical feedback, the more susceptible the linewidth is with the variation of the length of the external cavity. The dashed line is the minimum achievable linewidth, $\Delta\nu_{ex}$=5.6 kHz for $\Delta\nu_s$=100 MHz, from the equation (11). From this figure we obtain the optimum length of external cavity, L_{ex}= 22 cm, 18.6 cm, 17.2 cm for R_3= 0.1, 0.3, 0.5 respectively. This consideration of optimum length of external cavity is of critical importance in the design of ECSL.

IV. Discussion and conclusions

When we formulate effective reflectivity, we ignore the polarization of lasing field.

182

However, the reflectivity depends strongly on the polarization of the field. It has been observed that the degree of polarization decreases with detuned feedback, while it increases with the tuned feedback [19]. But the dependence of reflectivity on polarization in diffraction grating is the subject of further study.

The stability of ECSL with strong feedback mainly depends on that of the internal Fabry-Perot mode. The internal mode instability due to loss modulation and mode hopping causes the fluctuation in frequency and amplitude of the lasing field. The stability in both frequency and amplitude is very susceptabe to the environmental factors such as temperature and pressure. Small variations of these parameters cause a change in the cavity length, refractive index, threshold current and gain spectrum, etc. For instance, temperature variation causes the shift of the gain peak at 5 A/$^\circ$C and internal mode at 0.8 A/$^\circ$C [20].

In summary, we have shown that the linewidth of strong feedback ECSL is strongly dependent on R_2, R_3, L_{ex}, and frequency detuning of the feedback. Also, control and direction of frequency detuning is important; otherwise $\Delta\nu_{ex}$ can increase drastically. Linewidth less than 10 kHz and having very small fluctuations can be obtained with $R_2 \approx 0.5$ % and high R_3 (>30 %). From the minimum values of $\Delta\nu_{ex}$ we can easily obtain the optimum length of external cavity. Therefore we may design relatively short strong feedback ECSL with stability.

Reference

1. T. P. Lee, C. A. Burrus and D. P. Wilt,"Measured spectral linewidth of variable-gap cleaved-coupled-cavity lasers", *Electron. Lett.*, vol. 21, pp 53-54, 1985

2. K. Y. Lieu and C. A. Burrus,"Spectral linewidth of a GRECC laser with added external cavity", *Electron. Lett.*, vol. 21, pp 353-354, 1985

3. K. Y. Lieu, Y. K. Jhee, C. A. Burrus, K. L. Hall and P. J. Anthony,"Narrow linewidth fiber-external cavity injection laser", *Electron. Lett.*, vol. 21, pp 933-934, 1985

4. R. Lang and K. Kobayashi,"External optical feedback effects on semiconductor injection laser properties", *IEEE J. Quantum Electron.*, vol. QE-16, pp. 347-355, 1980

5. R. Wyatt, K. H. Cameron and M. R. Matthews,"Tunable narrow line external cavity lasers for coherent optical systems", *Br. Tele. Tech. J.*, vol. 3, pp 5-12, 1985

6. N. A. Olsson and J. P. van der Ziel,"Performance characteristics of 1.5 μm exteranl cavity semiconductor lasers for coherent optical communication", *J. Lightwave Tech.*, vol. LT-5, pp. 509-515, 1987

7. C. A. Park, C. J. Rowe, J. Buss, D. C. J. Reid, A. Carter and I. Bennion,"Single-mode behavior of a multimode 1.55 μm laser with a fiber grating external cavity", *Electron. Lett.*, vol. 22, pp 1132-1133, 1986

8. I. W. Oh and H. R. D. Sunak,"Linewidth calculations in tunable semiconductor external cavity lasers for coherent optical communication systems", *Tech. Digest*, Series vol 3, OFC/IOOC'87, pp 157

9. R. Lang and K. Kobayashi,"External optical feedback effects on semiconductor injection laser properties", *IEEE J. Quantum Electron.*, vol. QE-16, pp. pp 347-355, 1980

10. E. Patzak, A. Sugimura, S. Sato, T. Mukai and H. Olessen,"Semiconductor laser linewidth in optical feedback configurations", *Electron. Lett.*, vol. 19, pp 1026-1027, 1983

11. B. Tromborg, J. H. Osmundsen and H. Olesen,"Stability analysis semiconductor laser in an external cavity", *IEEE J. Quantum Electron.*, vol. QE-20, pp. pp 1023-1032, 1984

12. C. H. Henry,"Theory of spontaneous emission noise in open resonators and its appication to lasers and optical amplifiers", *J. Lightwave Tech.*, vol. LT-4, 288-297, 1986

13. R. K. Kazarinov and C. H. Henry,"The relation of line narrowing and chirp reduction resulting from the coupling of a semiconductor lasers to a passive resonator," *IEEE J. Quantum Electron.*, vol. QE-23, pp 1401-1409, 1987

14. C. H. Henry,"Theory of the linewidth of semiconductor lasers", *IEEE J. Quantum Electron.*, vol. QE-18, pp 259-264, 1982

15. A. P. Bogatov, P. G. Eliseev, O. A. Kobildzhanov and V. R. Madgazin,"Suppression and spectral splitting of amplitude noise due to mode beatings in a single-frequency injection laser", *IEEE J. Quantum Electron.*, vol. QE-23, pp 1064-1070, 1987

16. C. Y. Kuo and J. P. van der Ziel,"Linewidth reduction of 1.5 μm grating loaded external cavity semiconductor laser by geometric reconfiguration", *Appl. Phys. Lett.*, vol. 48, pp 885-887, 1986

17. R. A. Suris and A. A. Tager,"Emission spectrum of a semiconductor laser with an external resonator", *Sov. J. Quantum Electron.*, vol. 16, pp. 1373-1380, 1987

18. I. W. Oh and H. R. D. Sunak,"The dependence of feedback bandwidth on the spectral linewidth in external cavity semiconductor lasers for coherent lightwave communication systems", *SPIE Proc.*, vol. 841, pp 328-333, 1987

19. C. Y. Kuo, private communication

20. L. A. Coldren and T. L. Koch ,"External cavity laser design", *J. Lightwave Tech.*, vol. LT-2, 1045-1050, 1984
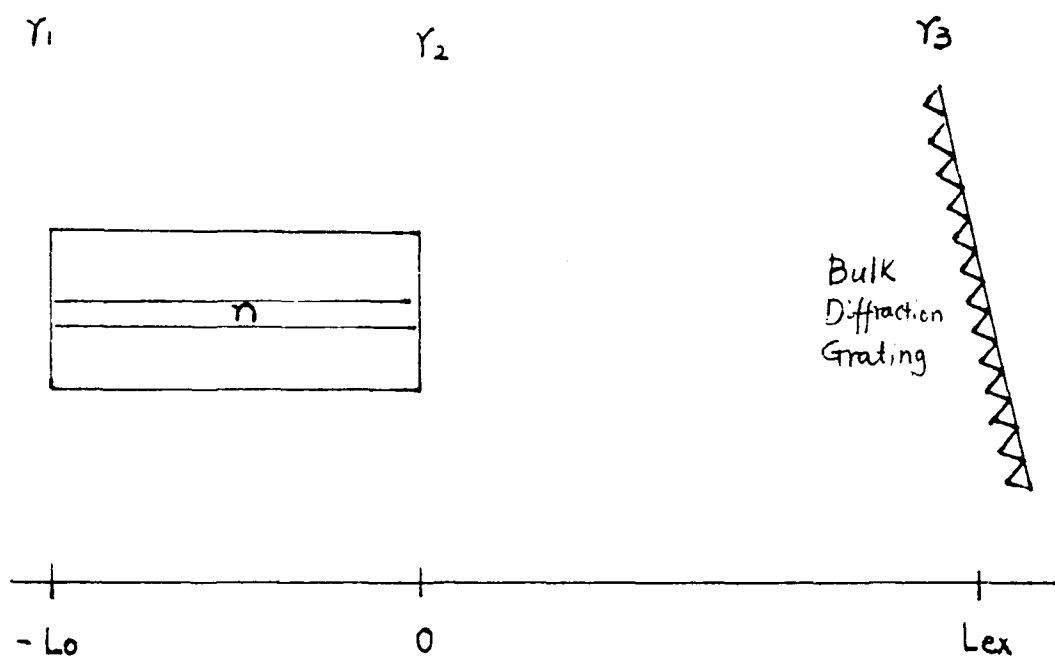
Fig. 1 : The configuration of the FP-ECSL with strong feedback.

Fig. 2 : The minimum (limiting) linewidth in FP-ECSL as a function of solitary laser linewidth (κ-the cavity coupling coefficiency is the parameter).
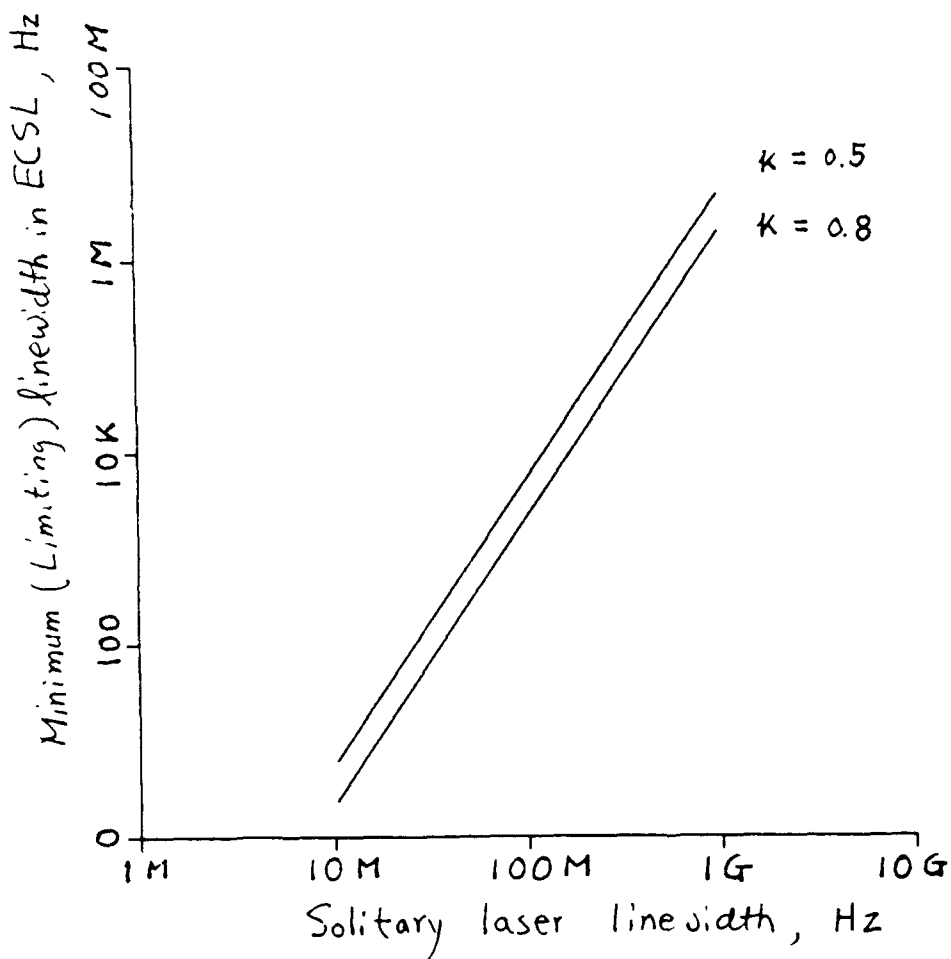
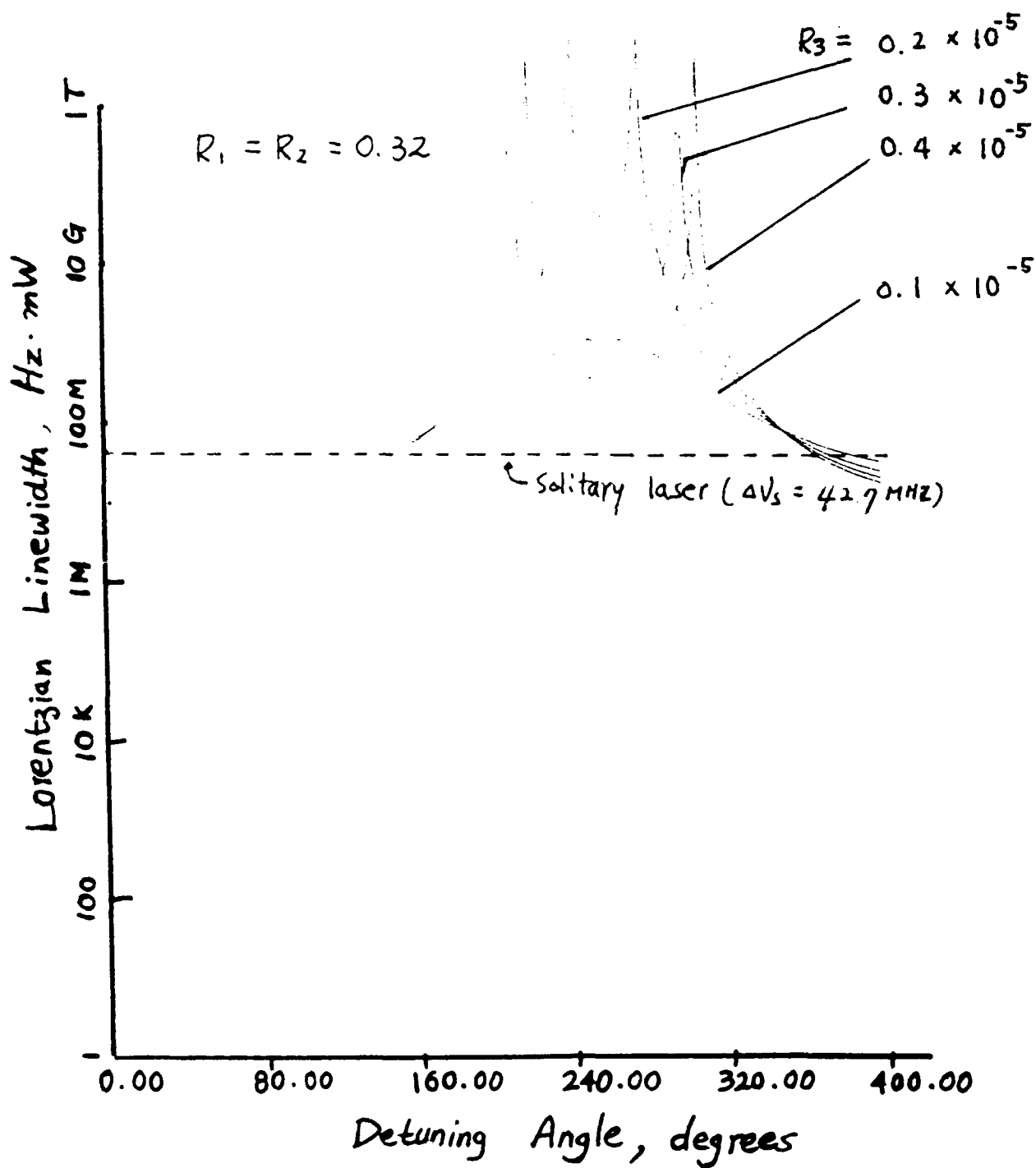Fig. 3 : Linewidth fluctuation due to small levels of optical feedback (weak feedback).

$R_1 = R_2 = 0.32$

$R_3 = 0.2 \times 10^{-5}$

0.3×10^{-5}

0.4×10^{-5}

0.1×10^{-5}

solitary laser ($\Delta\nu_s = 42.7$ MHz)

Lorentzian Linewidth, Hz·mW

Detuning Angle, degrees

Fig. 4 : Theoretical linewidth vs detuning angle (ϕ) for $-\phi$ and $-\phi$ indicated: R_1=0.32, R_2=0.09, R_3=0.25, L_{ex}=10 cm.
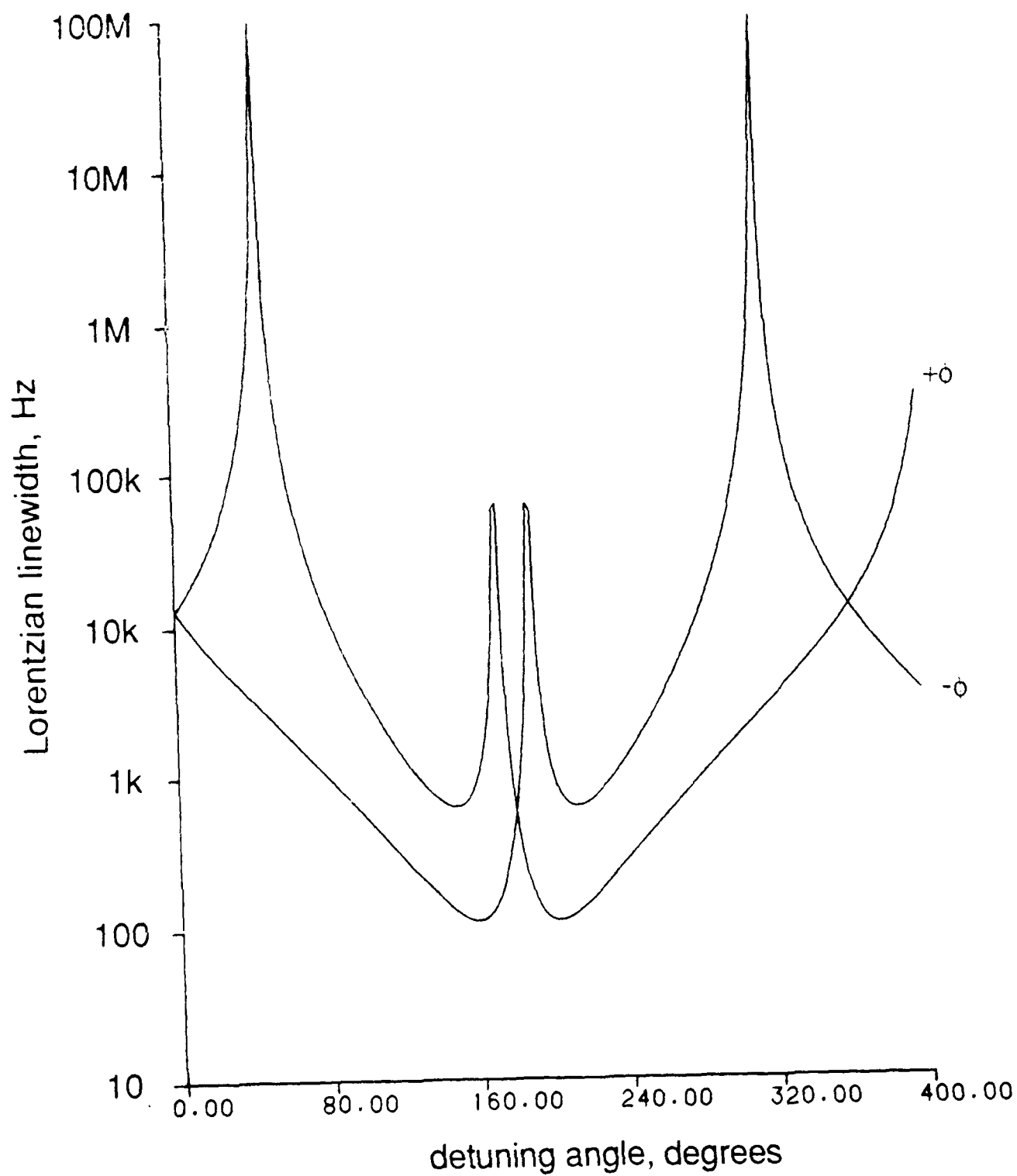
Fig. 5 : Linewidth variation as a function of detuning angle with R_2 as parameter (R_3=0.15, L_{ex}=10 cm).
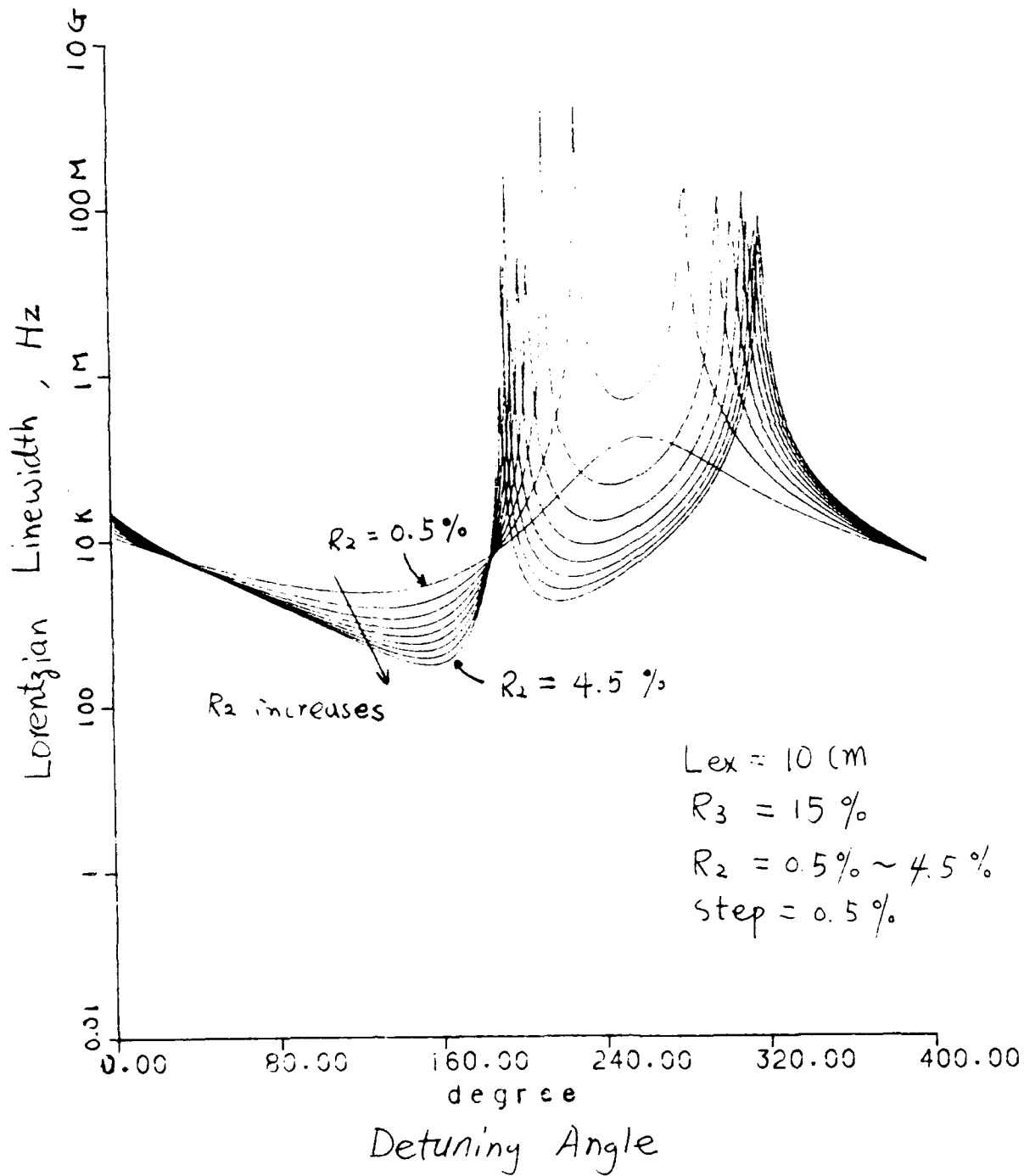
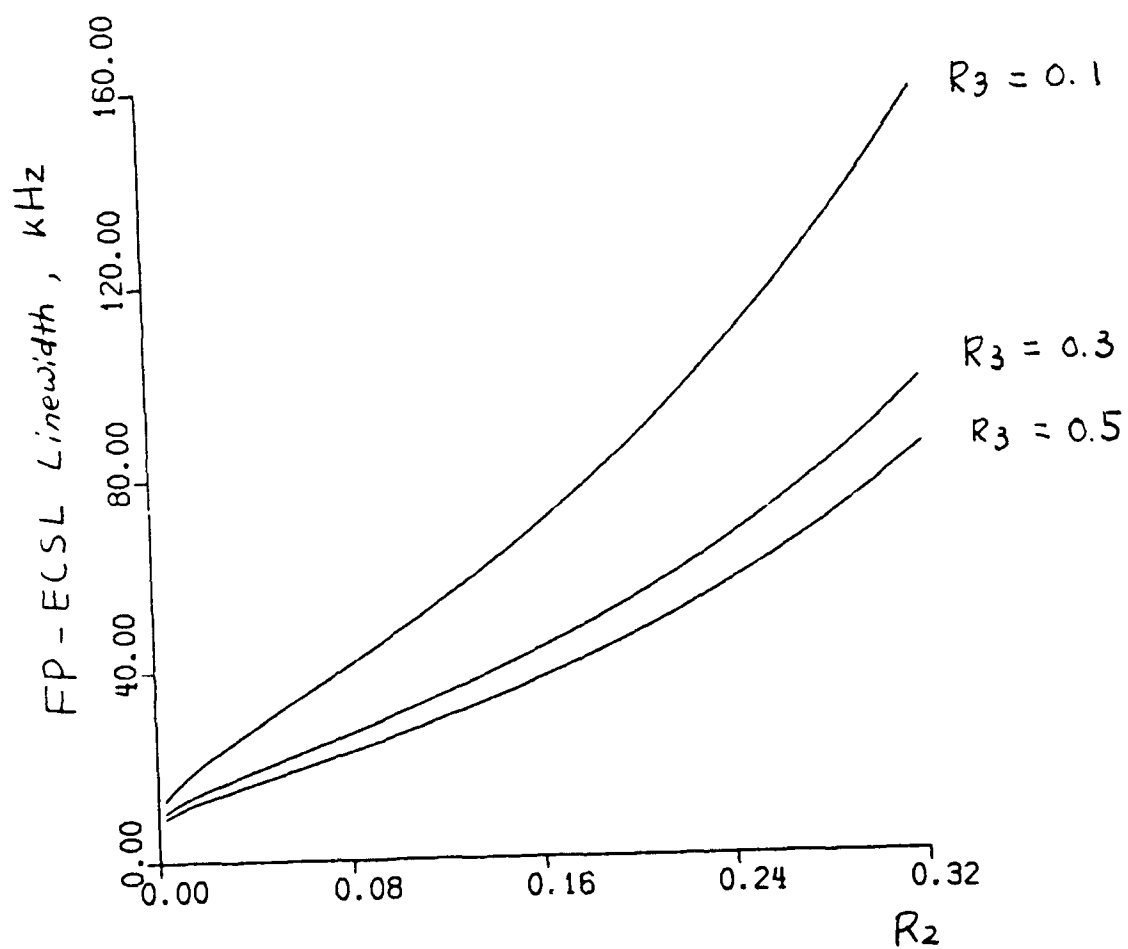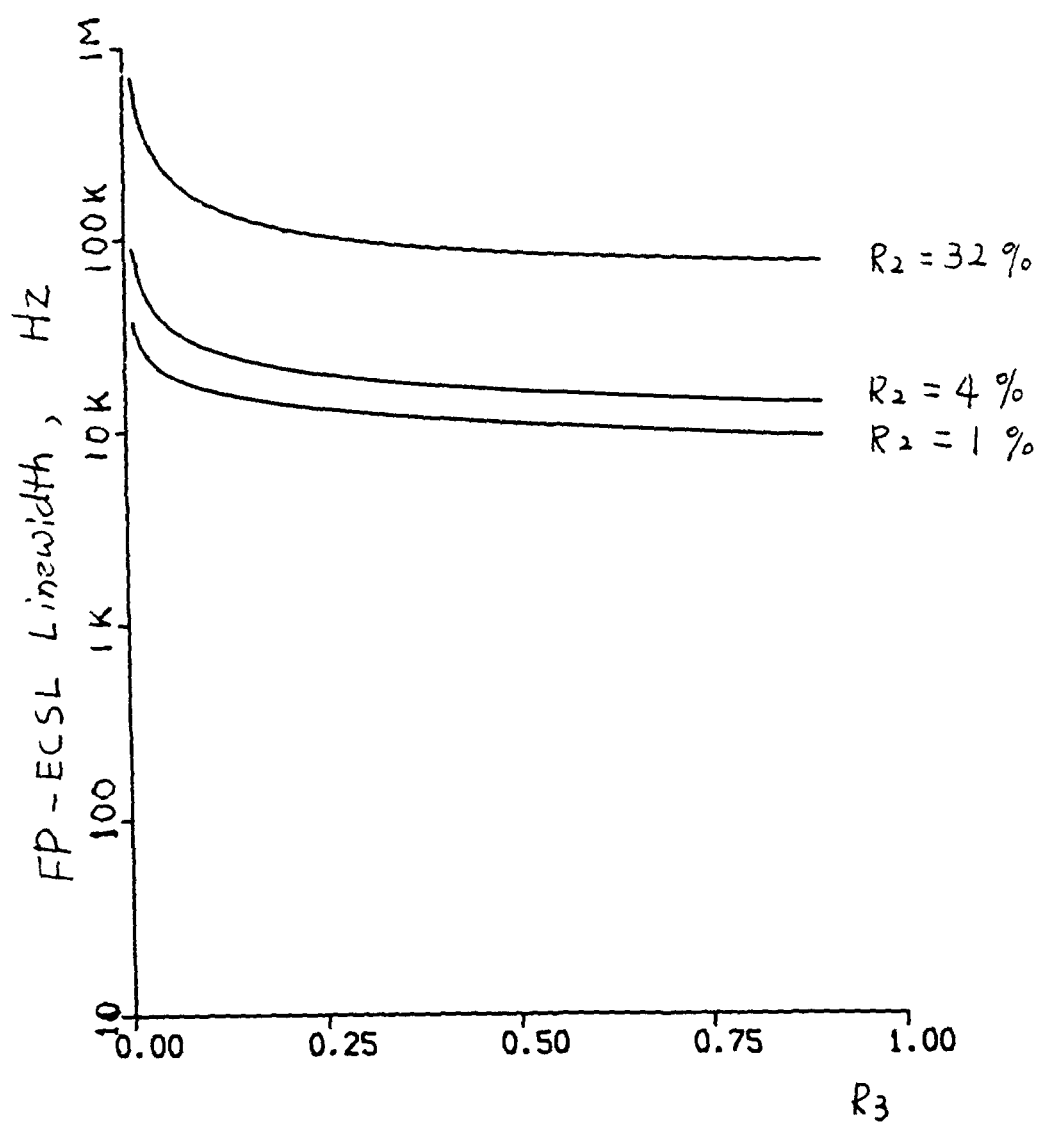Fig. 6 : Linewidth variation as a function of R_2 with R_3 as parameter ($\phi=0$, $L_{ex}=10$ cm).

Fig. 7 : Linewidth dependence on R_3 for various values
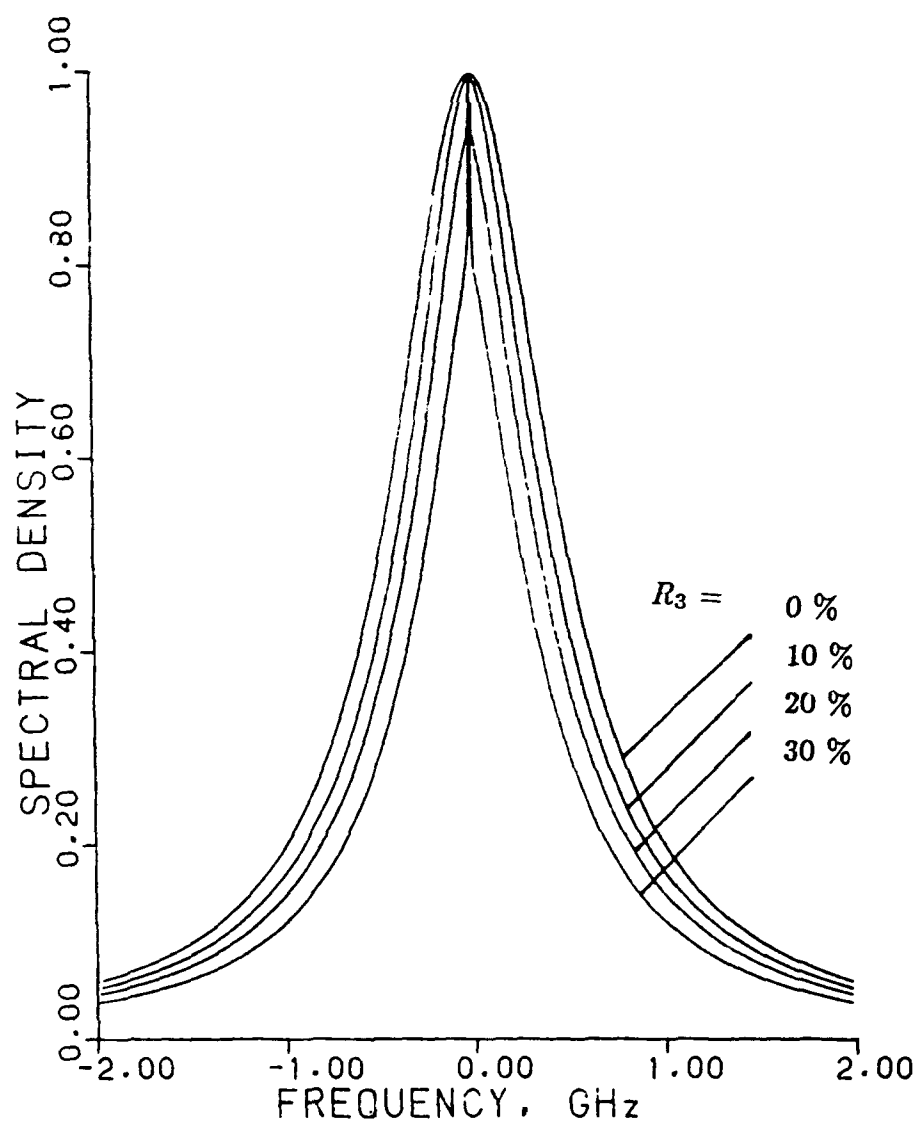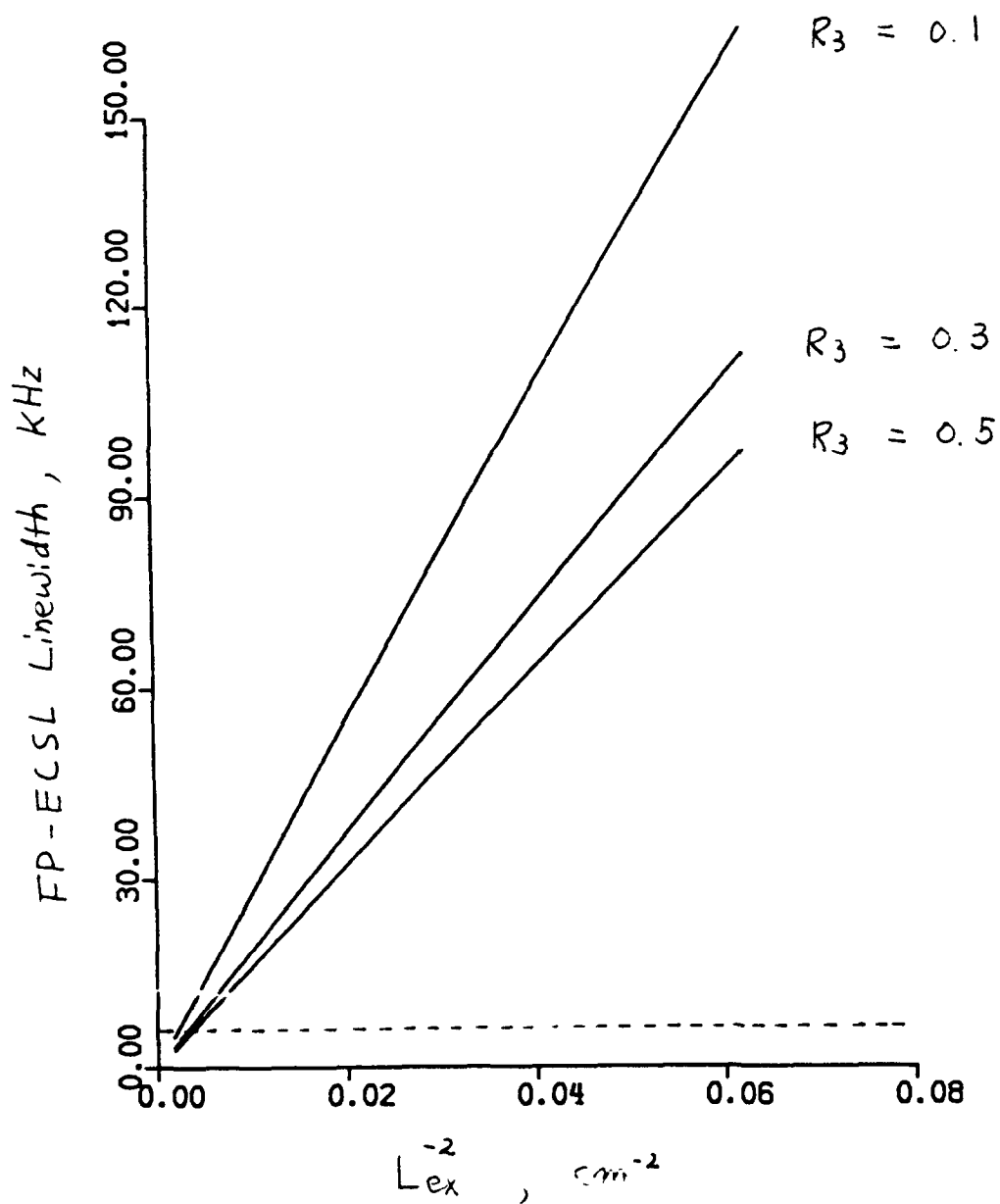of R_2 ($\phi=0$, $L_{ex}=10$ cm).

Fig. 8 : Spectral density of lorentzian lineshape as a function of R_3

Fig. 9 : Linewidth dependence on the external cavity length with R_3 as parameter ($\phi=0$, $R_2=0.04$).

MANUSCRIPT 4

Linewidth calculations in External Cavity Fabry-Perot Semiconductor Lasers with strong frequency-selectivity feedback for coherent lightwave systems.

Linewidth Calculations in External Cavity
Fabry- Perot Semiconductor Lasers with Strong
Frequency-Selective Feedback for Coherent Lightwave Systems

Harish R. D. Sunak

Il-Whan Oh

Department of Electrical Engineering

Fiber Optical Communication Laboratory

University of Rhode Island

Kingston, RI 02881-0805

Abstract

Linewidth calculations in external cavity semiconductor lasers (ECSL) are presented. The important design parameters of the ECSL which affect the linewidth are: optical feedback ratio, reflectivity of the laser facet nearer to the feedback component, frequency detuning of the optical feedback, the external cavity length, and feedback bandwidth. By analizing the effects of these parameters on the linewidth, we can identify their optimum values for the stable operation of the external cavity laser.

Significant research is being carried out in the world on various aspects of coherent fiber optical communications (COFOCS), the devices and systems. Semiconductor lasers are preferred as practical sources for COFOCS since they have the potential to be packaged robustly. For coherent optical communication systems, semiconductor lasers need to have fairly narrow linewidths ($\Delta\nu$). Linewidths typically in the tens of kHz to tens of MHz are required for data rate in the hundreds of MHz range. Another important required feature in the coherent source is tunability, especially in the local oscillator to select the various channels transmitted simultaneously through the single-mode fiber. To obtain these features, various types of external cavity structures are being developed. The external cavity semiconductor lasers (ECSL) are based on the fact that the characteristics of the laser diode are affected by the optical feedback. Among all the reported structures, ECSL with strong feedback, i.e., frequency selective feedback from a bulk diffraction grating, appears to be the most promising in terms of narrow linewidth and tunability.[1,2] Wyatt et al. have obtained narrow linewidth ($\sim$ 1 kHz) and the wide tuning range ($\sim$ 135 nm or $\sim$ 16000 GHz) with this arrangement.[1]

The important design parameters of the ECSL which affect the linewidth are: optical feedback ratio, reflectivity of the laser facet nearer to the feedback component, frequency detuning of the optical feedback, the external cavity length, and feedback bandwidth. We have previously reported, only in abstract form, the dependence of $\Delta\nu$ on these parameters[3], and obtained good agreement with published experimental results. We now give more details of the analysis with further details of the optimum cavity length for minimum linewidth.

The configuration shown in Fig. 1 (a) will be considered in this paper. r_1, r_2 and r_3 are the amplitude reflectivities of the diode facets and the grating reflector respectively. t_2 is the transmissivity. n is the refractive index in the active region of the solitary laser. τ_{ex} is the round trip time in the external cavity. κ is the intensity coupling coefficient between the two cavities. The effective reflectivity r_{eff} can be written as

$$r_{eff} = \frac{r_2 + r_3(r_2^2 + \kappa t_2^2)\exp(-j\delta)}{1 + r_2 r_3 \exp(-j\delta)} = r_e \exp(j\phi), \tag{1}$$

where $\delta = 4\pi L_{ex}/\lambda_i$ is a phase detuning. λ_i is the tunable wavelength due to the diffraction grating.

In the analysis of a coupled optical resonator, the amplitude of the single longitudinal Fabry-Perot cavity mode becomes a dynamic variable. The change of the mode amplitude is governed by the field equation follows as[4]

$$\left(1 + \frac{1}{\tau'_{in}} \frac{d}{dw}[\phi(w) + \alpha \ln r_e(w)]\right) \frac{d}{dt} E(t) = \frac{\Delta G}{2}(1 - i\alpha) E(t), \qquad (2)$$

where ΔG is the deviation from the threshold value in $\sec^{-1}$, and w is the angular frequency of the mode, α is the linewidth enhancement factor, and τ'_{in} is the round trip time with group velocity.

From this field equation, we can obtain the spectral linewidth $\Delta\nu_{ex}$ for the ECSL with strong feedback as[4-7]

$$\Delta\nu_{ex} = \Delta\nu_0 \cdot \left(\frac{L_0}{L_{eff}}\right)^2, \qquad (3)$$

where $\Delta\nu_0$ is the solitary laser linewidth with $r_2 = r_e$ in equation (1) and L_{eff} is the effective external cavity length and is given by[4,7]

$$L_{eff} = L_0 \left(1 + \frac{1}{\tau'_{in}} \frac{d}{dw}[\phi(w) + \alpha \ln r_e(w)]\right). \qquad (4)$$

We can express L_{eff} for $\delta=0$ and $\kappa=1$ as

$$L_{eff} = L_0 \left(1 + \frac{\tau_{ex}}{\tau'_{in}} \frac{r_3(1 - r_2^2)}{r_3(1 + r_2^2) + r_2(1 + r_3^2)}\right). \qquad (5)$$

Henry has derived the linewidth of a solitary laser as[6]

$$\Delta\nu_s = \frac{v_g^2 h\nu g_0 N_{sp} \alpha_0}{8\pi P_0}(1 + \alpha^2), \qquad (6)$$

where v_g is the group velocity, $h\nu$ is the bandgap energy, g_0 is the threshold gain, α_0 is the mirror loss, P_0 is the output power, and $N_{sp} = Kn_{sp}$. k is the gain guiding factor representing the astigmatism of the diode radiation, and n_{sp} is a factor representing the incomplete inversion of the population.

When an ECSL is assembled, some parameters in equation (6) change their values. These are ν, g_0, N_{sp}, α_0, and P. These changes in parameter values are

important and obviously affects the linewidth. Substituting equation (6) into (3) we obtain

$$\Delta \nu_{ex} = \Delta \nu_s \cdot M \cdot \left(\frac{L_0}{L_{eff}} \right)^2, \tag{7}$$

where M represents changes in the parameter values and is given by

$$M = \frac{2 g_t(w) \alpha_m(w) P_0 f_c}{g_0 \alpha_0 P(w)} \left(1 + \frac{r_1}{r_e} \frac{1 - r_e^2}{1 - r_1^2} \right)^{-1}, \tag{8}$$

where $g_t(w)$ and $\alpha_m(w)$ are the threshold gain and mirror loss in the compound cavity laser, $P(w)$ is the output power with feedback, and f_c is a correction factor considering the AR coating.[6]

Even though equation (3) predicts that the linewidth is a linear function of L_{ex}^{-2}, this relationship does not hold for long external cavity lengths. Kuo and Ziel have observed this dependence in the linewidth reduction of ECSL with strong feedback, as long as L_{ex} is less than ~ 7 cm.[8] Clearly, the cavity Q factor increased with the addition of the external reflector. This enhancement of the Q factor is responsible for the reduction in spectral linewidth. However, the maximum value of the Q factor in an ECSL operating in the single mode regime is limited by the excitation of satellite modes. Thus, the maximum value of L_{eff} in equation (7) can be written as[9]

$$L_{max} = L_0 \left(1 + \frac{\kappa}{2 \pi \tau_{in}} \frac{1}{\Delta \nu_s} \right). \tag{9}$$

If we put $\kappa = 0.25$, $L_0 = 250$ μm, $\Delta \nu_s = 100$ MHz, $M = 4$, we find that the minimum achievable linewidth $\Delta \nu_{ex}$ is 5.6 kHz. Olsson and Ziel obtained $\Delta \nu_{ex} = 7.4$ kHz with $L_{ex} = 18$ cm.[2] Thus the theoretical prediction of equation (9) gives good agreement with experimental data. Therefore, the minimum or limiting value of $\Delta \nu_{ex}$ depends on the solitary laser linewidth. Fig. 1 (b) shows the minimum $\Delta \nu_{ex}$ as a function of $\Delta \nu_s$. When $\Delta \nu_s$ is greater than about 1 GHz, we shall consider the spectral bandwidth of the optical feedback.

Fig. 2 (a) shows the linewidth dependence on r_2^2 with r_3^2 as a parameter, for fixed values of $L_{ex} = 10$ cm and $\phi = 0$. We can conclude that it is more important to have very low values of r_2^2 (<5 %) than high values of r_3^2 (>10 %). This is further confirmed in Fig. 2 (b) where we show the dependence of the linewidth on r_3^2 with r_2^2 as a parameter. As we can observe, the linewidth increases substantially for very

199

low values of r_3^2, <1 %. Small changes in the cavity parameters, in this low feedback region, due to external perturbations or internal frequency beating, causes instability. Thus we need to have r_3^2 greater than ~ 10 % for the stable operation.

Fig. 3 illustrates the linewidth as a function of the external cavity length with r_3^2 as a parameter and fixed values of r_2^2=4 % and φ=0. The linewidth is a linear function of L_{ex}^{-2} and the slope of the curve depends on r_2^2, r_3^2. The smaller the optical feedback, the more susceptible the linewidth is with the variation of the length of the external cavity. The dashed line is the minimum achievable linewidth, $\Delta\nu_{ex}$=5.6 kHz for $\Delta\nu_s$=100 MHz, from the equation (9). From this figure we obtain the optimum length of external cavity, L_{ex}= 22 cm, 18.6 cm, 17.2 cm for r_3^2= 0.1, 0.3, 0.5 respectively. This consideration of the optimum length of the external cavity is of critical importance in the design of ECSL.

When we consider the effect of the feedback bandwidth on the spectral linewidth, it is convenient to obtain the effective reflectivity of the two diode facets. We can write the effective reflectivity as

$$r_{eff} = r_2 + \frac{r_1(1 - r_2^2)\kappa \exp(g'l)\exp(j\delta)}{1 - r_1 r_2 \exp(g'l)\exp(j\delta)}, \qquad (10)$$

where δ=$4\pi l n/\lambda_i$ is a phase detuning, and $g' = g - \alpha_l$ with gain g and medium loss α_l. From the threshold condition $r_e \cdot r_3 = 1$, we can obtain that

$$ax^2 + bx + c = 0, \qquad (11)$$

where $a, b,$ and c are constants, and $x = r_1 r_2 \exp(g'l)$. The wavelength dependent r_3 for the first grating order is given by[10]

$$r_3(\lambda) = r_0 \exp\left(-\left(\frac{N_{eff}}{4}\right)^2 (k_i\lambda - 2\pi)^2\right), \qquad (12)$$

where r_0 is a constant, k_i is the propagation constant for injection wavelength λ_i, N_{eff} is the effective number of illuminated lines of the grating. By solving the eqn. (11) for the threshold gain g, we obtain the output spectrum of the Fabry-Perot resonator. Fig. 4 shows the output spectrum of the laser diode as a Fabry-Perot resonator model. We can observe that the spectrum becomes narrower as

the feedback bandwidth decreases. In this figure, we use $N_{eff}=1500$, 2500, 3500. corresponding values of the FWHM bandwidth $\Delta\nu_f$ are 136 GHz, 82 GHz, and 58 GHz respectively. If $\Delta\nu_f$ is in the range 200 ~ 400 GHz, the dependence on the linewidth can be ignored. When we take the spontaneous emission into account, the line shape of the output spectrum of the laser diode can be considered as a lorentzian.

When we formulated the effective reflectivity, we ignored the change of the polarization in the feedback field. However the reflectivity depends strongly on the polarization of the field. It has been observed that the degree of polarization decreases with detuned feedback, while it increases with the tuned feedback.[11] The dependence of reflectivity on the input polarization to the diffraction grating is being investigated.

In summary, we have shown that the linewidth of strong feedback ECSL is strongly dependent on r_2^2, r_3^2, L_{ex}, frequency detuning of the feedback and feedback bandwidth. Also, control and direction of frequency detuning is important; otherwise $\Delta\nu_{ex}$ can increase drastically. Linewidth less than 10 kHz and having very small fluctuations can be obtained with $r_2^2 \approx 0.5$ % and high R_3 (>20 %). From the minimum values of $\Delta\nu_{ex}$ we can calculate the optimum length of external cavity. Therefore we can design relatively short strong feedback ECSL ($< 5cm$) with good stability.

References

1. R. Wyatt, K. H. Cameron and M. R. Matthews, *Br. Tele. Tech. J.*, **3**, 5(1985)

2. N. A. Olsson and J. P. van der Ziel, *J. Lightwave Tech.*, **LT-5**, 509(1987)

3. i. W. Oh and H. R. D. Sunak, *Tech. Digest Series*, **3**, OFC/IOOC'87, 157(1987)

4. E. Patzak et al., *Electron. Lett*, **19**, 1026(1983)

5. B. Tromborg et al., *IEEE J. Quantum Electron.*, **QE-20**, 1023(1984)

6. C. H. Henry, *J. Lightwave Tech.*, **LT-4**, 288(1986)

7. R. Kazarinov and C. H. Henry, *IEEE J. Quantum Electron.*, **QE-23**, 1401(1987)

8. C. Y. Kuo and J. P. van der Ziel, *Appl. Phys. Lett.*, **48**, 885(1986)

9. R. A. Suris and A. A. Tager, *Sov. J. Quantum Electron.*, **16**, 1373(1987)

10. B. Tromborg et al., *IEEE J. Quantum Electron.*, **QE-23**, 1875(1987)

11. C. Y. Kuo, private communication

Figure Captions

Fig. 1 (a) Schematic of strong feedback ECSL.

(b) The minimum (limiting) linewidth in ECSL as a function of solitary laser linewidth (κ-the intensity coupling coefficient is the parameter).
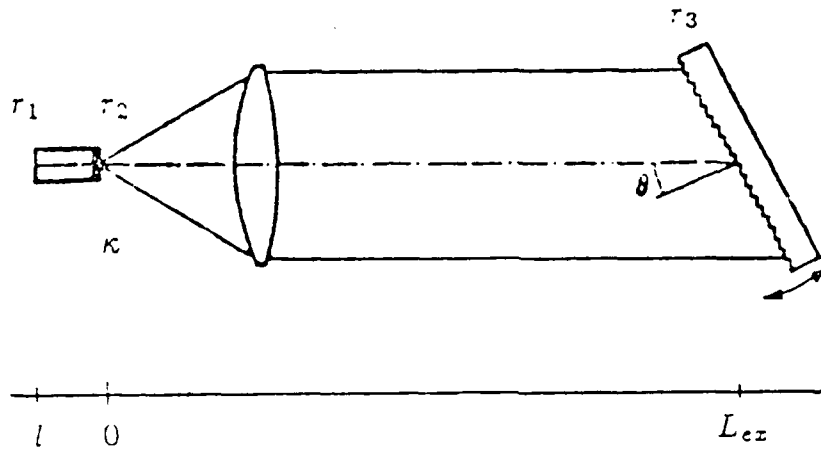
Fig. 2 (a) Linewidth variation as a function of r_2^2 with r_3^2 as parameter (ϕ=0, L_{ex}=10 cm).

(b) Linewidth dependence on r_3^2 for various values of r_2^2 (ϕ=0, L_{ex}=10 cm).

Fig. 3 Linewidth dependence on the external cavity length with r_3^2 as parameter (ϕ=0, r_2^2=0.04).

Fig. 4 Output spectrum of the laser diode as a Fabry-Perot resonator; detuning ϕ is defined as $\phi = 360 \times \Delta\lambda/\delta\lambda$. ($\Delta\lambda$: resonant frequence change from FP cavity mode, $\delta\lambda$: the free spectral range.)
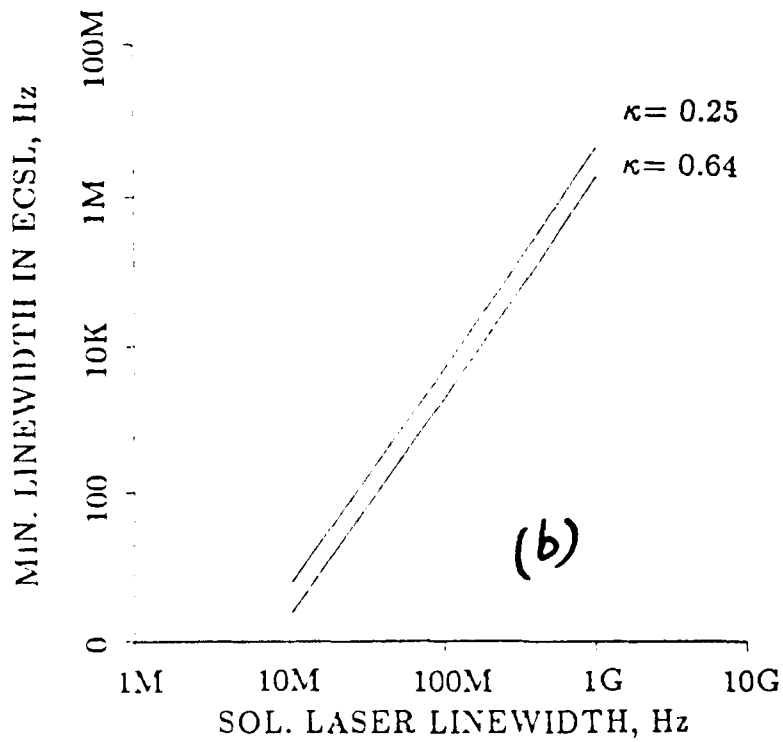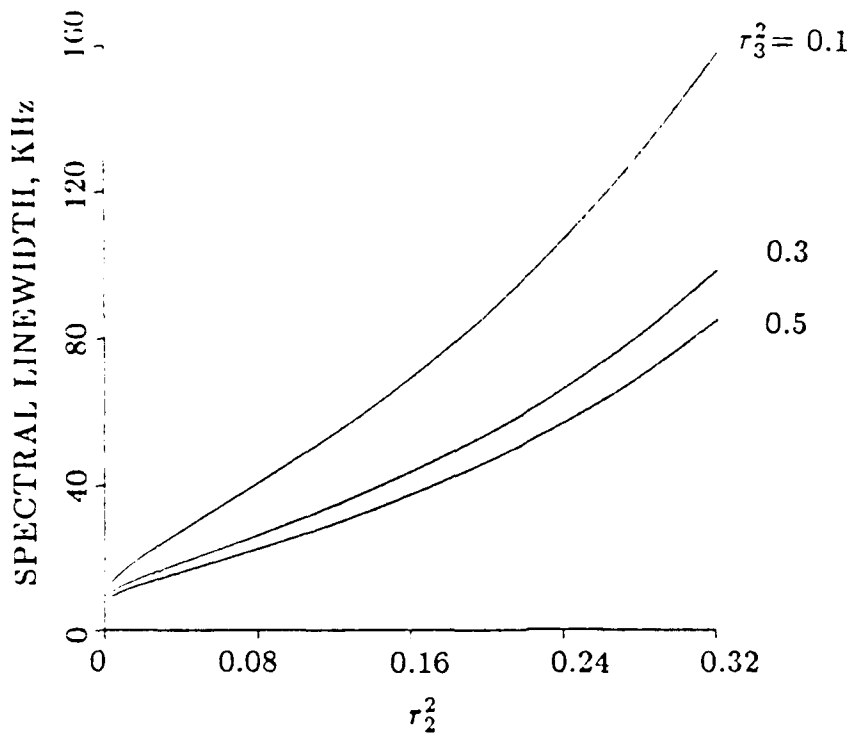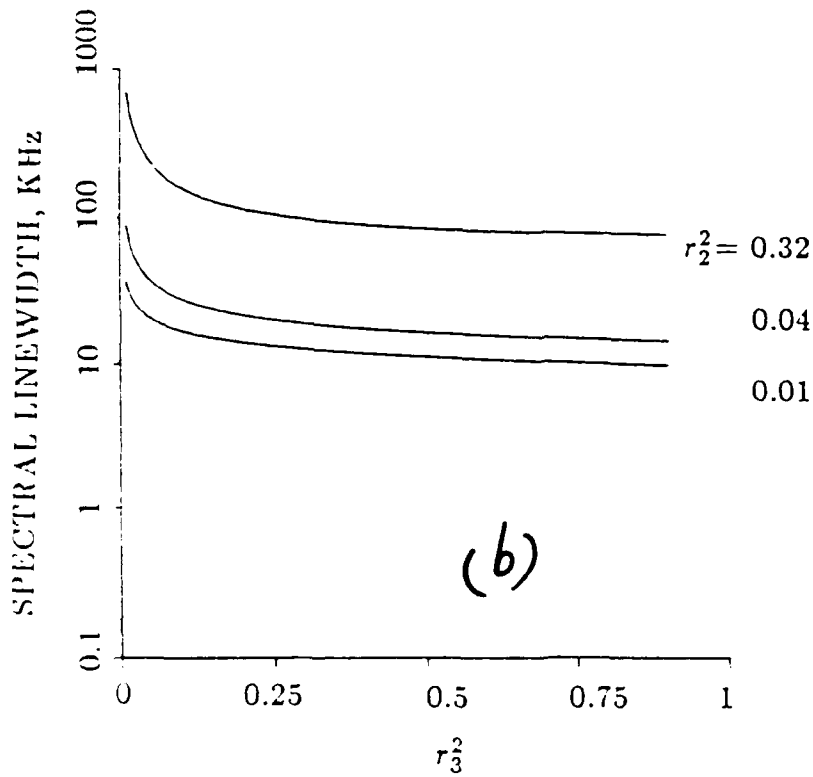
Fig. 1

(a)

(b)

$\kappa = 0.25$

$\kappa = 0.64$

MIN. LINEWIDTH IN ECSL, Hz

100M

1M

10K

100

0

SOL. LASER LINEWIDTH, Hz

1M   10M   100M   1G   10G

Fig. 2

(a)

(b)

205

Fig. 3

SPECTRAL LINEWIDTH, KHz

$r_3^2 = 0.1$

0.3

0.5

$1/L_{ex}^2$, cm^{-2}

Fig. 4

Figure showing output power vs detuning curves, with axis labels OUTPUT POWER, mW (vertical) ranging from 0.00 to 2.50, and DETUNING (horizontal) ranging from -90.00 to 90.00. Curves labeled $\Delta\nu_f = $ 58 GHz, 82 GHz, and 136 GHz.
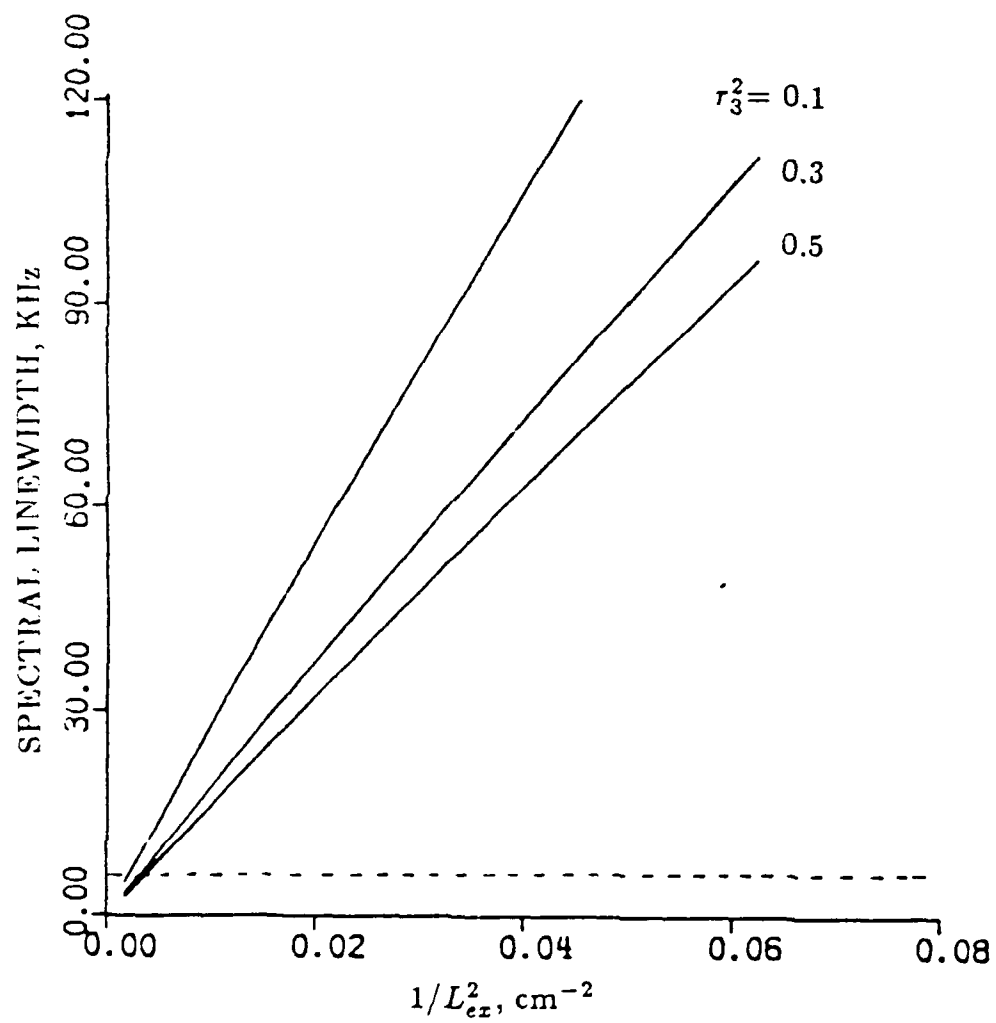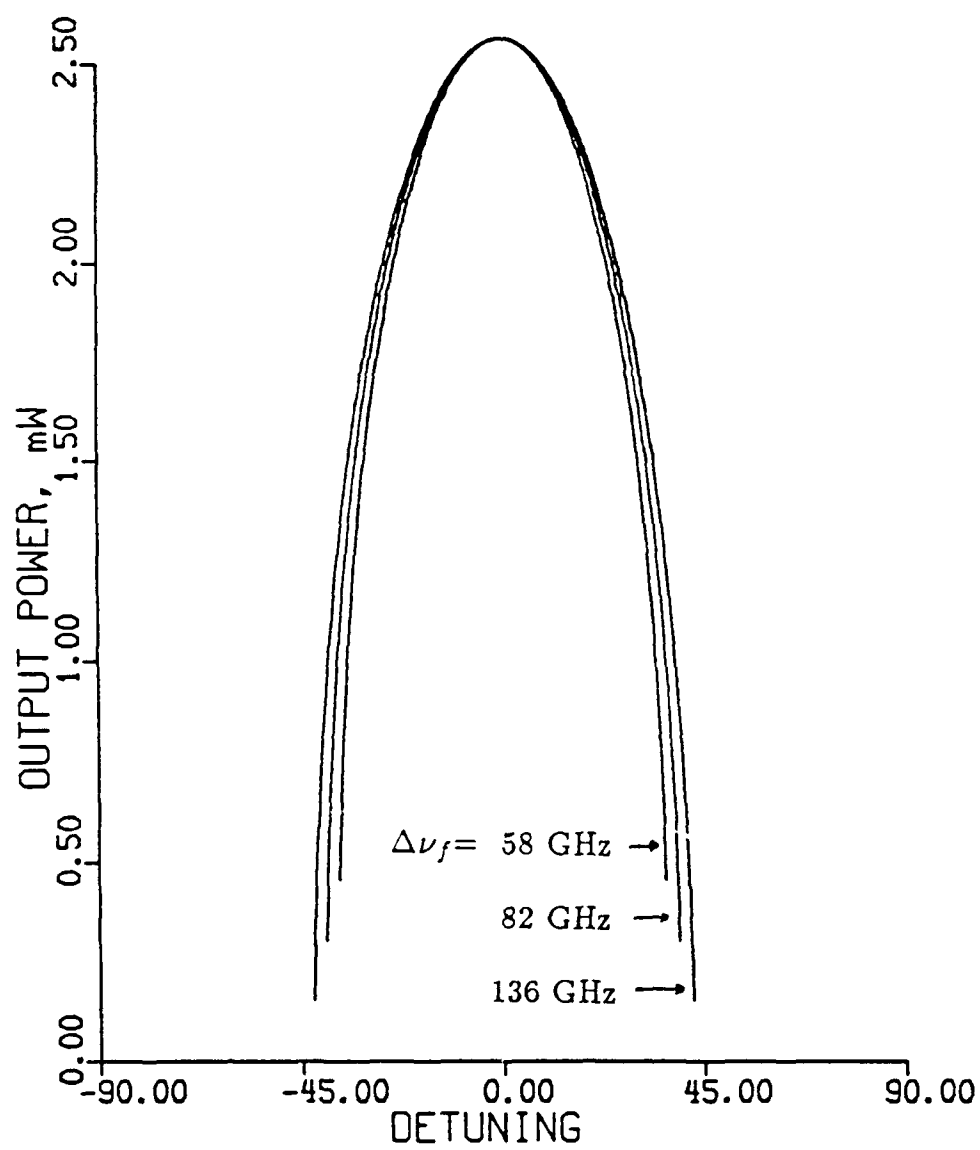
<u>MANUSCRIPT 5</u>

Frequency Tuning Characteristics of External Cavity Fabry-Perot Semiconductor Lasers with strong feedback for coherent lightwave systems.

Frequency Tuning Characteristics of External Cavity Fabry-Perot Semiconductor Lasers with Strong Feedback for Coherent Lightwave Systems

Harish R. D. Sunak

Il-Whan Oh

Department of Electrical Engineering
Fiber Optical Communication Laboratory
University of Rhode Island
Kingston, RI 02881-0805

Abstract

We have theoretically studied the tuning characteristics of strong feedback external cavity semiconductor lasers. It is shown that the gain change mechanism induced by the strong optical feedback in the Fabry-Perot cavity is responsible for spectral tuning in this structure. The Fabry-Perot resonator with an external cavity can support wide detuning frequencies with varying threshold gain. The threshold gain decreases as the diffraction grating is tuned toward longer wavelengths. The resulting bistable region increases with higher optical feedback.

INTRODUCTION: For coherent optical communication systems, semiconductor lasers need to have fairly narrow linewidths. Linewidths typically in the tens of kHz to tens of MHz are required for data rate in the hundreds of MHz range. Another important required feature in the coherent source is tunability, especially in the local oscillator to select the various channels transmitted simultaneously through the single-mode fiber. To obtain these features, various types of external cavity semiconductor lasers (ECSL) have been developed. Among the reported structures, strong feedback ECSL, i.e., frequency selective feedback from a bulk diffraction grating, appears to be the most promising in terms of narrow linewidth and tunability[1]. The wide tunability range which this structure can offer will ultimately turn out to be the most important advantage we get from frequency multiplexed coherent lightwave systems.

The important physical insights behind spectral tuning in strong feedback ECSL can be explained in terms of self-injection locking. The gain change mechanism with injection locking allows the lasing field to follow the injected feedback field by a reduction in gain[2]. As a result of gain reduction, the resonance frequency of the Fabry-Perot (FP) cavity is shifted towards lower frequencies. In Reference [3], the tuning mechanism in this structure was explained by the change in the refractive index only. In this letter we show that the spectral tuning of a strong feedback ECSL can be achieved by the gain change mechanism due to self-injection locking.

The configuration shown in Fig. 1 (a) will be considered in this paper. r_1, r_2 and r_3 are the amplitude reflectivities of the two diode facets and grating reflector respectively. κ_1 is the intensity coupling efficiency into the FP cavity from the external cavity. κ_2 is the intensity coupling efficiency into the external cavity from FP cavity, considering phase front distortion. n is the refractive index of the active medium. E_0 and E_i are the lasing field and injected feedback field respectively. λ_0 and λ_i are the wavelengths of FP cavity and external cavity respectively. Fig. 1 (b) shows the effective reflectivity r_e of FP facets which depends on phase detuning.

THEORY: We can write the effective reflectivity r_e in Fig. 1(b) as

$$r_e = r_2 + \frac{r_1(1 - r_2^2)\sqrt{\kappa_1\kappa_2}\exp(g'l)\exp(j\delta)}{1 - r_1 r_2 \exp(g'l)\exp(j\delta)}, \tag{1}$$

where $\delta = 4\pi l n$, λ_i is a phase detuning, and $g' = g - \alpha_l$ with gain g and medium loss α_l. From the threshold condition $r_e \cdot r_3 = 1$, we can show that

$$ax^2 + bx + c = 0, \tag{2}$$

where

$$x = r_1 r_2 \exp(g'l), \quad a = r_3^2 (p - r_2)^2 - 1$$

$$b = \left(2r_2 r_3^2 (p - r_2) + 2\right)\cos\delta, \quad c = (r_2 r_3)^2 - 1$$

$$p = (1 - r_2^2)\sqrt{\kappa_1 \kappa_2}/r_2, \kappa_1 = \epsilon_0 + \epsilon_1 \cos\delta_i.$$

In the above expression ϵ_0 and ϵ_1 represent the coupling change due to L_{ex} variation, and $\delta_i = 4\pi L_{ex}/\lambda_i$. The wavelength dependent r_3 for the first grating order is given by[4]

$$r_3(\lambda) = r_0 \exp\left(-\left(\frac{N_{eff}}{4}\right)^2 (k_i \lambda - 2\pi)^2\right), \tag{3}$$

where r_0 is a constant, k_i is the propagation constant for injection wavelength λ_i, N_{eff} is the effective number of illuminated lines of the grating. The threshold gain g_{th} of the FP resonator can be obtained by

$$g_{th} = \alpha_l + \frac{1}{l}\ln(\frac{x}{r_1 r_2}), \tag{4}$$

The angular frequency shift Δw and gain change Δg in the FP resonator due to optical feedback are given by[2]

$$\Delta w = -w_1(\alpha\cos\phi + \sin\phi), \tag{5}$$

$$\Delta g = -\beta l^{-1}\cos\phi, \tag{6}$$

where $w_1 = \delta\nu \cdot \beta$ with the free spectral range $\delta\nu$, α is the linewidth enhancement factor, ϕ is the phase change in the lasing field due to injected feedback field, and β which may be written as

$$\beta = \frac{\sqrt{\kappa_1 \kappa_2}(1 - r_2^2)r_3}{1 + r_2 r_3}$$

The phase difference $\Delta\psi$ between lasing field and injected field is given by[5]

$$\Delta\psi = \sin^{-1}(\frac{\Delta w}{2\pi\beta \cdot \delta\nu}). \tag{7}$$

211

For small $\Delta\psi$ we obtain from equations (5) and (7)

$$\Delta\psi = \frac{1}{2\pi}(\alpha \cos\phi + \sin\phi). \tag{8}$$

The constant phase ψ_0 in the lasing field (neglecting phase noise) varies due to resonant frequency shift and gain change as shown in equations (5) and (6). Thus, the phase ψ in the FP resonator can be written as

$$\psi = \psi_0 + \Delta\psi + \frac{4\pi l}{\lambda_i}\frac{\partial n}{\partial N}\frac{\partial N}{\partial g}(g - \Delta g), \tag{9}$$

where N is the carrier density. We assumed $\partial n/\partial N$ to be -0.7×10^{-20} from Reference [6], and $\partial g/\partial N$ to be 10^{-16} from the linear gain relation ($g = a'N + b'$). We note that Δg is negative due to the fact that $\partial n/\partial N$ is negative and $\Delta\psi_0$ is proportional to Δg. The small variation in Δg will cause a change in the refractive index which will be given by

$$n = n_0 + \frac{\partial n}{\partial g}\Delta g, \tag{10}$$

where, n_0 is the refractive index in FP cavity without optical feedback.

So far we considered only one FP cavity mode. The overall tuning behavior through the whole spectral gain range can be obtained with the same procedure shown above. The difference will be in the peak gains of the FP modes, which can be written as

$$g_m = (1 - d \cdot m^2) \cdot (a'N + b'), \tag{11}$$

where d is a constant and m is a mode number $(0, \pm 1, \pm 2, \cdots)$.

RESULTS AND DISCUSSIONS: Fig. 2 shows threshold gain in the FP cavity as a function of the phase detuning with r_0 as a parameter. The solitary FP cavity allows those frequencies satisfying the condition of standing waves to oscillate. However, if we provide an external cavity with strong optical feedback, the FP cavity can allow detuned wavelengths to oscillate. We can observe that the higher the feedback, the wider is the frequency detuning allowed in the FP resonator. For example, the active medium of the FP resonator can support up to $\pm 40°$, $\pm 56°$, and $\pm 70°$ of detuning for $r_0^2 = 0.1$, 0.2, and 0.3 respectively; where detuning angle, ϕ_d is defined as $\phi_d = 360 \times \Delta\lambda/\delta\lambda$, where $\Delta\lambda$ is the resonant frequency change from FP cavity

212

mode, and $\delta\lambda$ is the free spectral range. Also, we can observe that the larger the detuning, the higher is the gain required to achieve the oscillation.

Fig. 3 shows the threshold gain as a function of the phase detuning in degrees with $\Delta\lambda$, the resonant frequency shift of FP resonator, as parameter. The curve in this figure shows the threshold gain with $r_2^2 = 0.03$, $r_0^2 = 0.1$ similar to Fig. 2. The straight lines are obtained from equations (9) and (10). Since self-injection locking is possible within the range of $\phi = 0°$ to $-90°$ after Ref. [2], the linear variation shifted as $\Delta\lambda$ increases as shown in Fig. 3. The threshold gain, at the point where the curve and the straight line meet, becomes smaller as $\Delta\lambda$ increases. Therefore, when the diffraction grating is tuned to longer wavelengths, the output power increases. This fact has been well observed experimentally in refs. [3] and [7]. When the tuning occurs towards shorter wavelengths, the output power experiences bistable operation. The bistable output is shown in the inset. We observe that the bistable region increases with the optical feedback. Thus, the tuning direction of the diffraction grating is important for proper frequency tuning. We note that small change of the constant phase ψ_0 in eqn. (9) causes the shift in the straight lines. Also, we can show that the continuous tuning range between the FP modes increases with the value β in eqn. (6).

CONCLUSION: We present a theoretical analysis of the spectral tuning characteristics of ECSL with strong feedback. The gain change mechanism in the active medium of the FP resonator is responsible for the spectral tuning of this structure. We have shown that the threshold gain decreases as the diffraction grating is tuned towards longer wavelengths and the bistable region increases with higher optical feedback. It is suggested that an AR coating with small r_2^2 (< 1 %) and high optical feedback ($r_3^2 > 20$ %) are required for a wider continous tuning range and stable operation.

References

1. R. Wyatt, K. H. Cameron and M. R. Matthews,"Tunable narrow line external cavity lasers for coherent optical systems", *Br. Tele. Tech. J.*, 1985, **3**, pp 5-12

2. C. H. Henry, N. A. Olsson and N. K. Dutta,"Locking range and stability of injection locked 1.54 um InGaAsP semiconductor lasers", *IEEE J. Quantum Electron.*, 1985, **QE-21**, pp 1152-1156

3. V. Yu. Bazhenov et al.,"Bistable operation and spectral tuning of injection laser with external dispersive cavity", *IEE Proc.*, 1982, **129 I**, pp. 77-82

4. B. Tromborg, H. Olesen, X. Pan and S. Saito,"Transmission line description of optical feedback and injection locking for Fabry-Perot and DFB lasers", *IEEE J. Quantum Electron.*, 1987, **QE-23**, pp. 1875-1889

5. W. W. Chow,"Phase locking of lasers by an injected signal", *Optics Lett.*, 1982, **7**, pp. 417-419

6. J. Manning, R. Olshansky and C. B. Su,"The carrier-induced index change in AlGaAs and 1.3 μm InGaAsP diode laser", *IEEE J. Quantum Electron.*, 1983. **QE-19**, pp. 1525-1530

7. N. A. Olsson and J. P. van der Ziel,"Performance characteristics of 1.5 μm exteranl cavity semiconductor lasers for coherent optical communication", *J. Lightwave Tech.*, 1987, **LT-5**, pp. 509-515
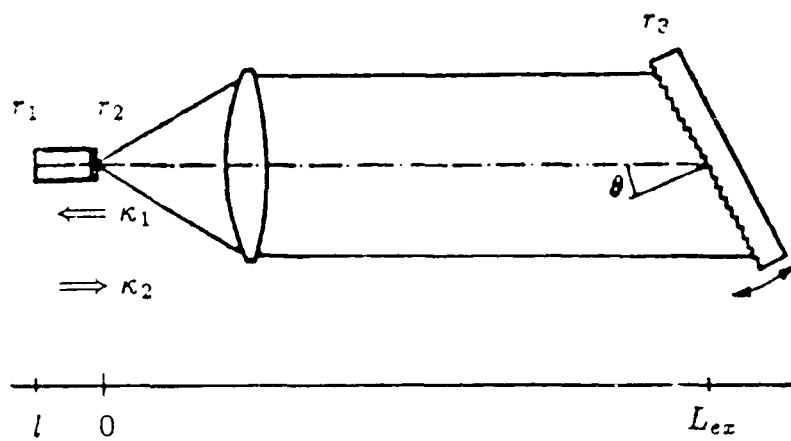
Figure Captions
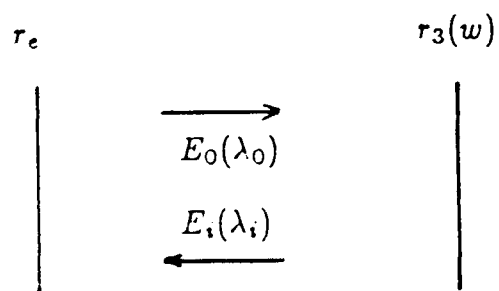
Fig. 1 (a) Schematic of strong feedback ECSL.

   (b) Effective reflectivity of FP resonator.

Fig. 2 Threshold gain of FP resonator with external cavity as a function of detuning with r_0^2 as parameter ($r_2^2=0.03$, $\kappa_1=0.2$, $\kappa_2=0.8$, $N_{eff}=1600$, $\alpha=5$).

Fig. 3 Threshold gain dependence on wavelength variation ($r_0^2=0.1$, the other parameters are the same as in Fig. 2). Inset shows that the bistability depends on the tuning direction of diffraction grating.
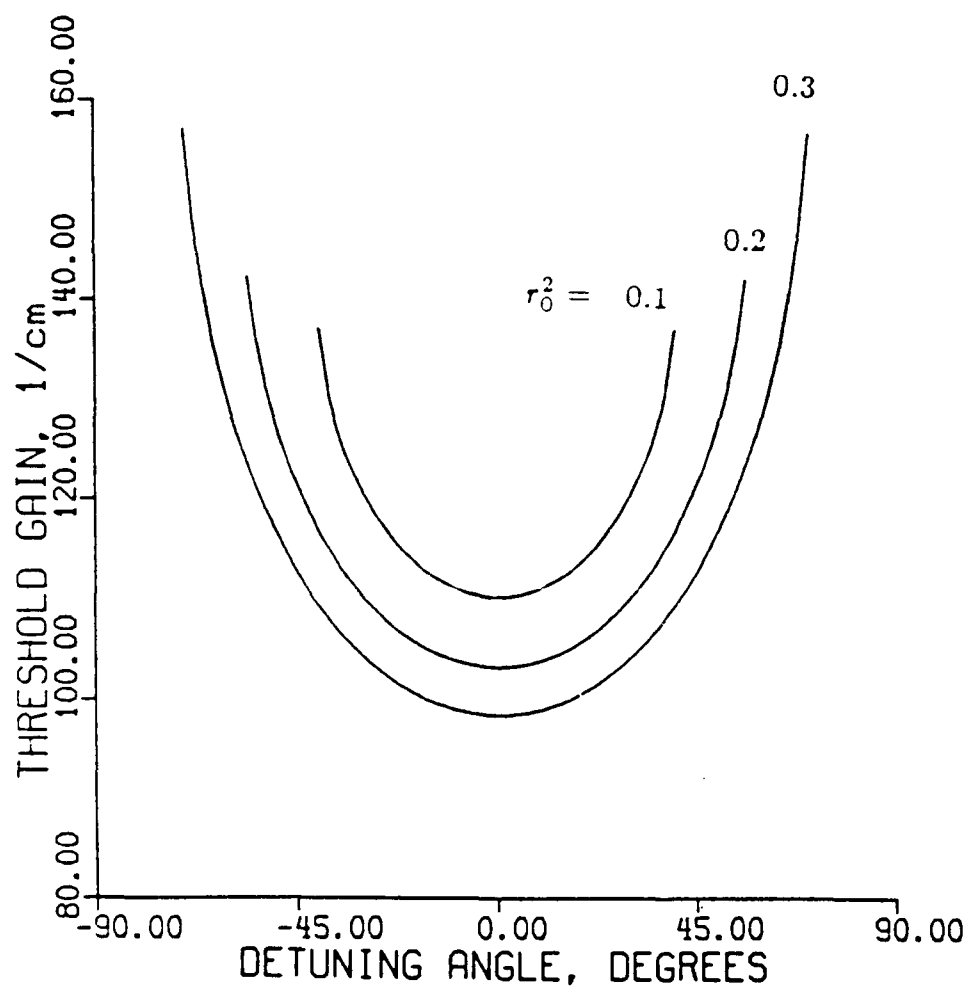
(a)

r_e $r_3(w)$
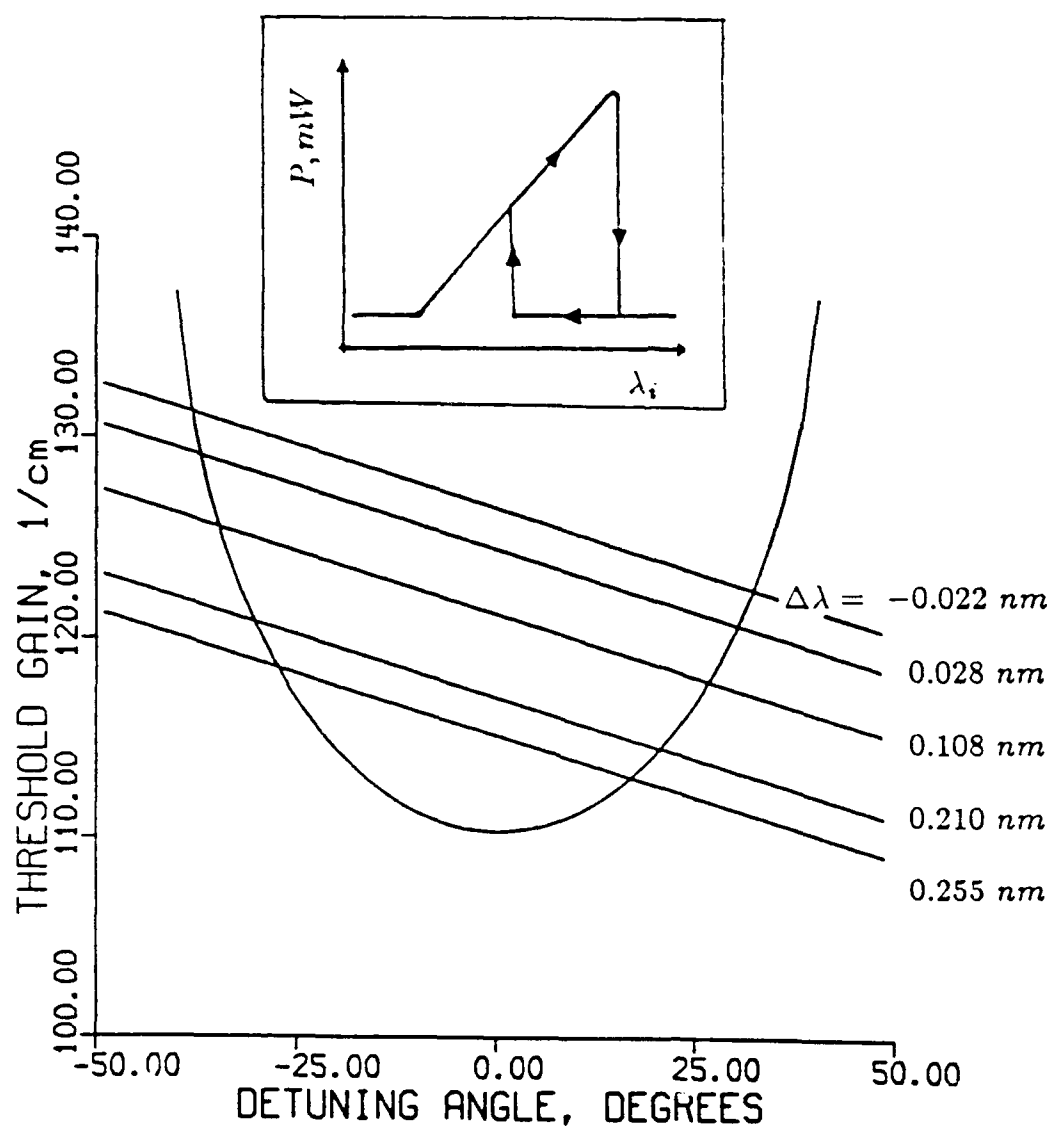
$\overrightarrow{E_0(\lambda_0)}$

$E_i(\lambda_i)$

(b)

FIG 1

FIG 2

FIG 3

218